CONTENTS

Bella Syakina, Radiaeh Mohd Nor, and M. Edi Armanto. Elucidating indigenous farmers' avoidance of deep peatlands for food crop farming in South Sumatra province, Indonesia 3

Katherine Karamanoli, Athanasios Papaioannou, and Theano Samara. Soil fertility and plant nutrition of *Pinus pinaster* and *Pinus radiata* reforestations in Halkidiki, Northern Greece 16

Hari Sutikno, Syarifuddin Kadir, Hafizianor, and Yusanto Nugroho. Plant adaptability and species diversity after coal mining reclamation in South Borneo 28

Zainal Abidin, Muhammad Irfan Affandi, Adia Nugraha, and Dewi Lengkana. Analysis of water consumption in community based water service surrounding Wan Abdul Rachman Forest Park, Lampung province..... 38

Svitlana A. Sytnyk, Viktoriia M. Lovynska, Kyrylo K. Holoborodko, Natalia K. Vasylieva, Yurii I. Gritsan, Iryna M. Loza, Oleksandr Ye. Pakhomov, Liudmila P. Golodok, and Hynek Roubik. Chlorophyll fluorescence characteristics in *Robinia pseudoacacia* L. under conditions of urban forest ecosystems in Dnipro city..... 50

Svetoslav Anev. Light acclimation of European beech (*Fagus sylvatica* L.) saplings after canopy destruction 66

Salwaa Ainayya, Awanda Sifa Maharani, Sri Sunarti, Arif Nirsatmanto, and Ganis Lukmandaru. Kraft pulping of 3-year-old *Acacia* hybrid (*A. mangium* × *A. auriculiformis)* clonal wood..... 79

Teodora Lyubomirova, Nasko Iliev, and Ivan Iliev. Grafting of *Syringa vulgaris* L. cultivars 93

Muhammad Irfan Affandi, Alifia Hasyimi, and Fembriarti Erry Prasmatiwi. Financial analysis of cat's eye resin business in West Coast Regency, Lampung province, Indonesia 107

Yuriy O. Rumiankov, Olga Porokhniava, Volodymyr Hrabovyi, Hryhoriy I. Muzyka, Tetyana Kopylova, Volodymyr Vitenko, Iryna Pushka, and Vasyl Zayachuk. Preservation and optimisation of 'Dubynka' historical planting of National dendrological park 'Sofiyivka' 120

Zlatomir Dimitrov, Radka Koleva, Toma Tonchev, and Hristo Nikolov. Utilisation of multitemporal SAR data for mapping and statistical analysis of ice and snow breakage of mountainous mixed forest in Bulgaria with Sentinel-1..... 139

Liubov Ishchuk, Volodymyr Hrabovyj, Halyna Ishchuk, Inna Didenko, Tatiana Kovalchuk, and Svetlana Kurka. Comparative characteristics of the leaf surface ultrastructure of plants of genus *Populus* L. 160

Kameliya Petrova. Assessment of aboveground litterfall under the beech forest canopy in Vitinya permanent sample plot 173

Rida Oktorida Khastini, Iing Dwi Lestari, Indah Juwita Sari, and Fajrin Indah. Nurunnisa Record of root endophytic fungi associated with Pteridophytes from Gunung Tukung Gede Nature Reserve, Indonesia 183

Renhart Jemi, Nuwa, and Lamboris Rianto Sitorus. Oleoresin *Baeckea frutescens* L. activity against *Pleurotus ostreatus* (Jacq. ex Fr.) P.Kumm. 197

FORESTRY IDEAS, 2024, vol. 30, No 1 (67): 3–15

Elucidating indigenous farmers' avoidance of deep peatlands for food crop farming in South Sumatra province, Indonesia

Bella Syakina[1*], Radiaeh Mohd Nor[1], and M. Edi Armanto[2]

[1]Centre for Global Sustainability Studies, University Sains Malaysia, 11800 Penang, Malaysia.
[2]Faculty of Agriculture, Sriwijaya University, South Sumatra 30820, Indonesia.
[*]E-mail: bellasyakina@student.usm.my

Received: 25 October 2023 / Accepted: 03 January 2024 / Available online: 15 January 2024

Open Access: This article is licensed under a Creative Commons Attribution 4.0 International License.

Abstract

Most peatlands in Indonesia have been drained for plantation industries (Oil palm, Acacia) and agricultural purposes in a broad sense. Theoretically, peatlands are extremely sensitive to hydrological changes. The research aimed to elucidate the fact that indigenous farmers avoid deep peatlands for food crop farming. This qualitative and quantitative research has been conducted from 2020 to 2023 in South Sumatra province. It used a field survey method and the data were collected by using a purposive sampling method. There are two main reasons farmers to avoid deep peatlands for cultivating food crops, namely instinctive and latent challenges. The first ones are temporary and technical, so farmers are able to overcome these challenges with a scientific and technological approach. Latent ones are very difficult or impossible to repair and tend to cause the destruction and extinction of peatlands. The government should stop granting concession permits and make deep and very deep peatlands into conservation areas, because of their impact on the environment. Approaches are recommended for sustainable peatland management, namely decentralisation, conservative, protective, and optimal approaches.

Key words: farmers, income, instinctive challenges, latent challenges, rice production, suitability.

Introduction

Peatlands are receiving serious attention as the issue of global climate change and global warming becomes stronger (Zuhdi 2019). They are natural ecosystems of high value because they have biodiversity, regulate the climate, and are a source of livelihood for millions of residents around the location (Zuhdi et al. 2019, Zhang et al. 2022). Damage to peatlands due to human activities such as agricultural expansion and drainage construction, peat mining, together with extreme climate manifestations have contributed to the degradation of around 65 million ha of peatlands in the world (Armanto et al. 2023a; 2023b). The emissions resulting from this damage are very significant and reach around 3 Gt CO_2 per year, or around 5 % of the global carbon balance (Junedi 2017, Holidi 2019). The problem of clearing peatlands, exces-

sive drainage, and frequent fires are the main factors contributing to Greenhouse Gas Emissions, such as CO_2, methane (CH_4), and nitrogen oxide (N_2O), which will become a time bomb for the sustainability of our life (Armanto et al. 2022).

Peatlands in South Sumatra are about 1.01 million ha and mostly found in the Eastern Part (Armanto 2019a, 2019b; Holidi et al. 2019). About 44 % of those peatlands are located in non-forest areas, 42 % in production forests (He et al. 2023), oil palm and acacia plantations, and the rest (14 %) found in protected forests (wildlife reserves and national parks). At present time most peatlands have been drained for oil palm plantation (Armanto and Wildayana 2022, 2023), oil palm and acacia plantations and agricultural purposes in a broad sense (Alikhani et al. 2021).

The peatlands cultivation has changed groundwater levels, namely groundwater depletion, drainage systems, swamp forest logging and land clearing by burning (Wildayana and Armanto 2018a, 2018b). Farmers cultivating food crop farming (especially rice) in peatlands always pay serious attention to the depth of peatlands because in very deep ones (Yan et al. 2023), besides it is difficult and less fertile to cultivate rice, so it produced low rice yield and low income of farmers (Byg et al. 2023, Wildayana and Armanto 2018c, 2018d, 2021). Furthermore, this research is important because it provides information about indigenous farmers avoid deep peatlands for food crop farming (Wildayana et al. 2019, 2018).

This research aims to understand indigenous knowledge why farmers avoid the deep peatlands. It focuses on explaining scientifically why deep peatlands are avoided by indigenous farmers while the government gives concession permission to private companies such as oil palm and acacia plantations.

Materials and Methods

Research location

The research was carried out from 2020 to 2023 and was conducted in South Sumatra province, Indonesia which is geographically located between 1–4° South latitude and 102–106° East longitude (Fig. 1).

According to the Decree of the Ministry of Environment and Forestry of Indonesia Republic, Nr. SK.129/MENLHK/SETJEN/PKL.0/2/2017 concerning Determination of the PHU Map, total area of observed PHU was 995,756 ha (PMRA 2022). General descriptions of observed PHU are given in Table 1.

Table 1. General descriptions of observed peatland hydrological units.

Parameters	Merang-Ngirawan	Saleh-Sugihan	Sugihan-Lumpur	Burnai-Sibumbung
Area, ha	82,021	190,230	636,828	86,679
Burnt area 2019, ha	8513	29,167	39,786	10,134
Restoration types	Canal blocking and livelihood revitalisation	Canal blocking	DPG and canal backfilling	3-R and DPG
Targeted restoration area, ha	Muara Medak, 33,104	All villages in PHU, 4766	All villages in PHU, 228,378	All villages in PHU, 39,445

Note: DPG – Peat care village program; 3-R – rewetting; revegetation and revitalisation. Source: Field and laboratory data analysis (2023).

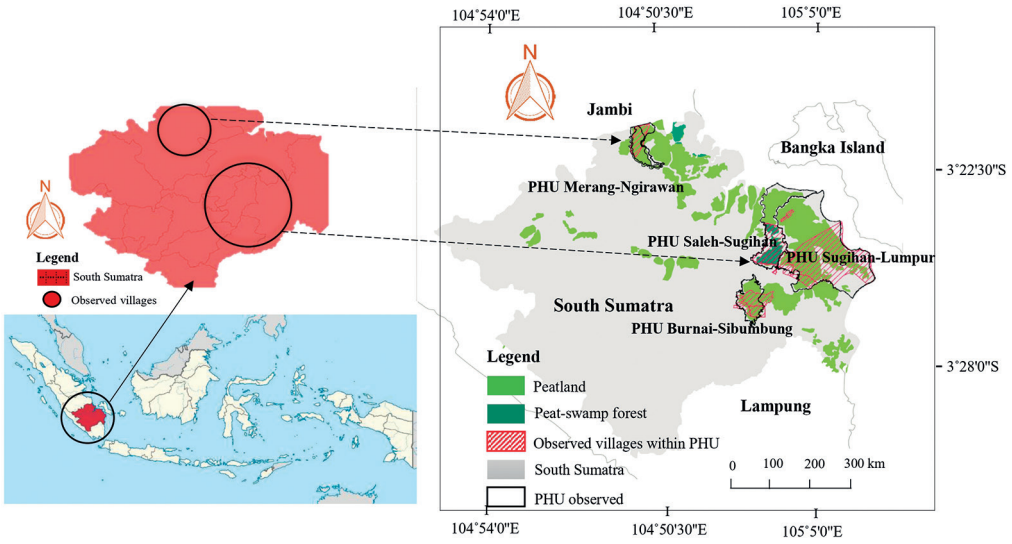


Fig. 1. Research location in South Sumatra province, Indonesia.
Note: PHU is Peat Hydrological Unit.

Study population

The number of respondents interviewed was 525 households (15 % of the total population of 3500 households of peatlands), and 2–3 villages were selected for each PHU, so the number of selected villages was 12. Data of respondents were collected by using a purposive random sampling method, questionnaires, and snowball sampling techniques (Table 2).

Informant criteria

The interview scopes were on questions about elucidating indigenous farmers avoid deep peatlands for food crop farming. Data and information were taken also from related stakeholders, namely government, concession owners, NGOs as

Table 2. General descriptions of selected respondents.

Plots and size	Districts (villages)	Population (household)	Sample (respondent)
Merang-Ngirawan (82,021 ha)	Musi Banyuasin (Merang-kepayang, Muara medak)	770	116
Saleh-Sugihan (190,230 ha)	Banyuasin (Banyu biru, Simpang heran)	910	137
Sugihan-Lumpur (636,828 ha)	OKI (Simpang tiga sakti, Riding)	945	142
Burnai-Sibumbung (86,679 ha)	OKI (Kedaton, Menang raya)	875	131
Total		3500	525

Source: Field and laboratory data analysis (2023).

well as indigenous farmers.

Research instrument

This research is a combination of qualitative and quantitative methods. This research used a field survey method and the data were collected by using a purposive sampling method. Composite soil samples were taken purposively at depths of 5–20 cm and 30–50 cm, then analysed in the laboratory for bulk density and organic C. The complete research objects and parameters as well as measurement methods are summarised in Table 3.

Data analysis

All data collected were processed on the basis of measured parameters and analysed, tabulated, elaborated descriptively, and then analysed statistically by using SPSS program version 21. The land suitability method was carried out following the Ministry of Agriculture Regulation concerning Guidelines for Land Suitability for Agricultural Commodities No. 79/Permentan/OT.140/8/2013. The pace at which the depth of peatlands varies year over year is the basis for the data projections for 2050 (PMRA 2022). The results for projections for 2050 were derived from the data.

Rice production and income of farmers was calculated at the MDG price of IDR 4500 kg^{-1}. The Indonesian Rupiah (IDR) exchange rate is: 1 IDR = $6.0842 \cdot 10^{-5}$ € and 1 € = 16,436 IDR (average for November 2023). Revenue was obtained from multiplying rice production by the selling price, while the average income of farmers is the difference between revenue and production costs. Rice production was measured using Square method 5×5 m and income of farmers was calculated using farm analyses with formula (1).

$$I = TR - TC, \quad (1)$$

where: I is income, IDR million·ha^{-1}·yr^{-1}; TR is total revenue, IDR million·ha^{-1}·yr^{-1}; TC is total cost, IDR million·ha^{-1}·yr^{-1}.

Table 3. Research object, parameter and methods of measurements.

Object	Parameters	Methods	Total samples
Farmers	Legality and ownership, %	Questionnaire	525
	Age, year	Questionnaire	525
Peatlands	Plot area of farmers, ha	Questionnaire	525
	Peat maturity (scale)	Squeeze method	80
	Bulk density, g·cm^{-3}	Ring sample	э
	Organic C, %	Walkey and Black	40
	Area percentage, %	Questionnaire	525
	Peat depths, m	Boring	80
	Soil acidity, pH value	pH meter	80
	Soil fertility (scale)	Certainty factor method	40
	Inundation depth, m	piezometer	40
	Aluminium and iron, ppm	Spectrophotometer	80
Rice	Production, t MDG·ha^{-1}·yr^{-1}	Square method 5×5 m	16

Note: MDG is milled dry grain.

Results and Discussion

Characteristics of farmers' activities

Plot area of farmers (generally > 84 %) had plots on average < 5 ha, only a small number of farmers had > 5 ha, meaning most farmers only fulfilled their own family needs (subsistence farming). Distance describes how far the plots are from the main road to the district capital, the average is 36 km away from the main road. It is relatively close, making easier for rural communities to transport. Roads play a very important role in facilitating village development; alleviating poverty through increasing production and prices of agricultural products; and reducing agricultural input costs. Therefore, the expansion of rice fields increased markedly in areas close to markets and roads, but the road construction can cause degradation of the peatlands.

Legality and ownership (explaining the plot locations), it turns out that > 95 % of the rice fields were located in PHU area. This was not in accordance with the spatial plan because all PHU areas may not be converted into agricultural and plantation areas. Ownership explains how rice fields owners get plots, around 61 % of rice fields plot ownership was obtained through market buying and selling transactions.

Age of the plot owners at the conversion time was around 40 years with an average length of education of 12 years (Senior High School). They have been involved in trading (average 26 years); or domiciled as a civil servant (25 years), and commercial plantations (35 years). It is noteworthy that very few subsistence farmers were doing rice field farming (only 13 years).

Expansion of rice fields began in the 1980s. This expansion has brought many changes to the physical landscape or ecosystem and created rural socio-economic changes. The changes started with the transmigration program, but over time, farmers expanded rice fields and faced various intrinsic challenges and latent challenges of peatlands, so farmers avoided deep peatlands for food crop farming (rice fields).

Our interviewed results explained that in the end they realised peatlands were not suitable for rice fields, so that in the 1960s native farmers became less motivated to farm on them. However, starting in the 2000s, large companies operating in the plantation industries expanded the area of oil palm plantations to > 10,000 ha. Finally, the government formed a foundation of the Nucleus Estate System (NES), where the plantation industries are responsible for processing and distributing Fresh Fruit Bunches (FFB). Farmers act as plasma under the supervision of the plantation industries and do not manage their oil palm directly. Instead, farmers are coordinated in a production organisation called Village Unit Cooperative (VUC) that functions as a partially integrated management system. As a result, in the field, there is often a communication gap between the parties involved and FFB financial transparency, and one of the main challenges is the lack of technical assistance received by plasma farmers. Differences of opinion between the two parties sometimes drag on and last for 20 years. Finally, farmers have difficulties in replanting of their oil palm trees.

Since plantation industries have entered PHU sites, farmers have been encouraged to own peatlands even though they were aware that these peatlands are not suitable for rice fields due to latent challenges. The goal of farmers is to con-

trol the peatlands and oil palm after knowing the economic potential of FFB. Farmers gained knowledge from experience as workers in the plantation industries or as part of core partnerships between companies and farmers. Hence, they were trying to sell their peatlands although their peatlands are located in conservation areas (depths of peatlands more than 3 m).

Characteristics of peatlands

Results determining peatland suitability for agriculture – peatland maturity, bulk density (BD), carbon content and peatland depths, are presented in Table 4.

BD values varied between 0.11–0.29 $g \cdot cm^{-3}$ depending on weathering level. The more mature of peatlands is observed, the BD values will increase. Fibric maturity has average BD lower than 0.11 $g \cdot cm^{-3}$, but hemic and sapric maturity has average BD values more than 0.20 $g \cdot cm^{-3}$ because of the influence of compaction. The average BD of fibric is significantly different from the average BD of hemic and sapric. Increase BD is due to compaction and increased peatlands degradation.

The carbon contained in peatland is known as organic C content in peatlands of 43–54 %. It is closely related to peatlands maturity. With the increasing maturity, organic C content decreases and is significantly different between organic C in fibric, compared to organic C in hemic and sapric. It diversity ranges from 54.27 ±2.24 % for fibric; about 49.32 ±3.78 % for hemic, around 43.78 ±8.76 % for sapric and significantly different among the values.

Table 4 shows that the highest peat maturity is hemic (close to 50 %), followed by sapric maturity and the lowest is fibric maturity, 36.26 % and 17.86 % respectively. The large area of hemic maturity is caused by land clearing, drainage and repeated fires, so that the peatlands become well decomposed.

It is explained in Figure 2 that from 1990 to 2050, very deep and deep peatlands show a downward trend, because of massive forest and land fires, intensive drainage and illegal logging systems getting out of control. On the contrary, shallow peatland shows an upward trend, started with the lowest percentage in the beginning of the year and will become the highest in the year 2050, which is around 5 % and 60 % of each. Furthermore, although the peatlands medium also shows a downward trend, it is predicted that in 2050 it will remain just slightly below 40 %, about 10 % higher than in 2020.

Very deep peatlands (> 3 m) with a fibric to hemic maturity were found in dome area and are largely avoided by farmers for food crop farming because they are less fertile and have no agricultural potency and recommended as for a conser-

Table 4. Distribution and characteristics of peatlands maturity.

Peat maturity	BD, $g \cdot cm^{-3}$	Organic C, %	Area, %
Fibric	0.11 ±0.12[a]	54.27 ±2.24[a]	17.86
Hemic	0.21 ±0.17[b]	49.32 ±3.78[b]	45.88
Sapric	0.29 ±0.28[c]	43.78 ±8.76[c]	36.26
Total			100.00

Note: BD is bulk density. Means in one column and followed by the same lower case are not significantly different at the 5% test level.

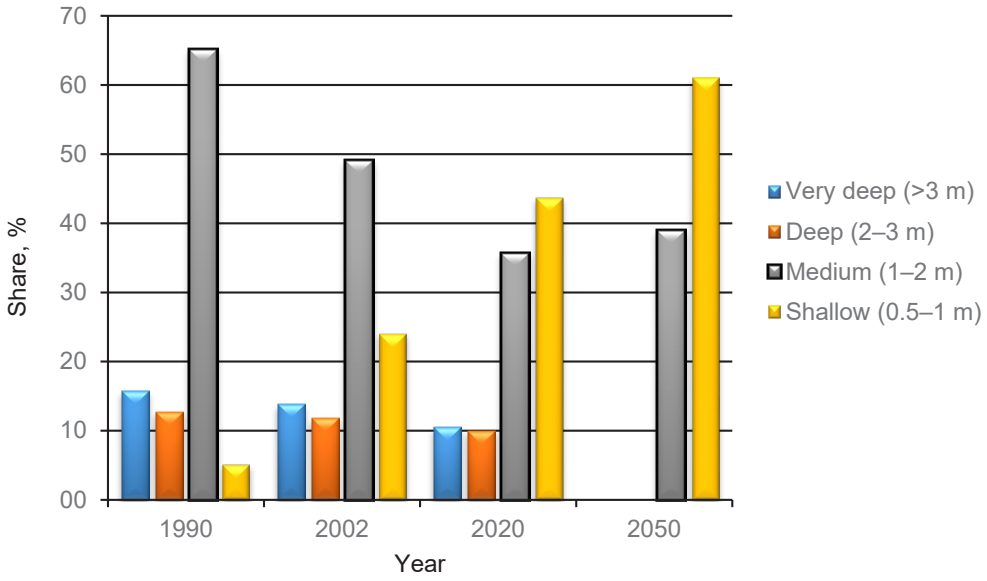


Fig. 2. Estimated depths of peatlands in the research area 1990–2050.
Source: It was interpreted from Landsat images (1990, 2002, 2020) and the field survey (2023). It was estimated on the basis of PMRA (2022) and the field survey (2023).

vation area. In general, these peatlands have a very inhibited drainage, rapid permeability, and has a very deep cross-section of the soil.

Deep peatlands (2–3 m) have experienced the fate of almost the same as very deep peatlands. It is estimated that deep peatlands would disappear in 2050 because the Government has permitted large private companies to cultivate Oil palm and Acacia. The peatlands become objects of forest and land fires, intensive drainage and illegal logging systems that are going increasingly uncontrolled. Deep peatlands with fibric to hemic maturity were commonly found in dome areas.

Medium peatlands (1–2 m) with hemic to sapric maturity were commonly found on the sides or edges of the peatlands dome. These peatlands generally have potential for food crop farming. Indigenous farmers have cultivated food crops, vegetables, and fruits in these peatlands.

Shallow peatlands (0.5–1 m) continued to increase from year to year remarkably compared to other peatlands. In 1990 the peatlands had an area of around 5.27 %, and its increase occurred due to excessive peatlands clearing by logging, drainage, and fires. In 2002, the extent was 24.24 % and around 43.77 % in 2020 and estimated to expand to 61.07 % in 2050.

Suitability of peatlands for food crop farming

Instinctive challenges of peatlands are predominantly temporary, technical or economic, so they are easier to overcome with science and technology approaches. Various instinctive challenges were identified, namely release of toxic metals, eutrophication of surface water, disruption of hydrological balance, waterlogging,

drought, local fisheries, release of organic pollutants, changes in salt and freshwater systems, changes in groundwater supply, and air pollution. Especially for food crop farming (rice fields), instinctive challenges can be overcome with land suitability methods.

Peatlands can be classified into four land capability classes, namely class S1 (very suitable), S2 (suitable), S3 (marginally suitable), and N (not suitable) according to the Ministry of Agriculture Regulation concerning Guidelines for Land Suitability for Agricultural Commodities No. 79/Permentan/OT.140/8/2013. Figure 3 illustrates the potential of peatlands for food crop farming. Data on food crop farming in peatlands indicates a 63 % less potential, which is notably significantly different from a high potential of only 1 %. Then, it shows that low potential and medium potential, declared 20 % and 16 % respectively.

There is a relationship between land suitability class and rice cultivation production. This relationship is expressed in the form of a description as follows:

1) High potential if land suitability for rice cultivation was in the range of 75 % classified as suitable and < 25 % as marginally suitable. Rice production ranges from 8–10 t MDG·ha^{-1}·year^{-1}.

2) Medium potential if land suitability for rice cultivation consisted of 25–50 % classified as suitable and 50–75 % as marginally suitable. Rice production ranges from 5–7 t MDG·ha^{-1}·year^{-1}.

3) Low potential if land suitability for rice cultivation was indicated as 50–75 % classified as marginally suitable and 25–50 % as unsuitable). Rice production ranges from 2–4 t MDG·ha^{-1}·year^{-1}.

4) Less potential if land suitability class for rice cultivation showed > 75 % classified as permanently not suitable and < 25 % as marginally suitable. Rice production ranges from less than 1 t MDG·ha^{-1}·year^{-1}.

The results presented in Figure 3 show, that 63 % of the research area belonged to less potential, meaning there is no opportunity for rice cultivation because there are a lot of latent challenges and very difficult to reclaim or require high costs and rice production is not optimal. Limiting factors of peatland suitability for rice cultivation are given in Table 5. It was relevant with work of Armanto et al. (2013).

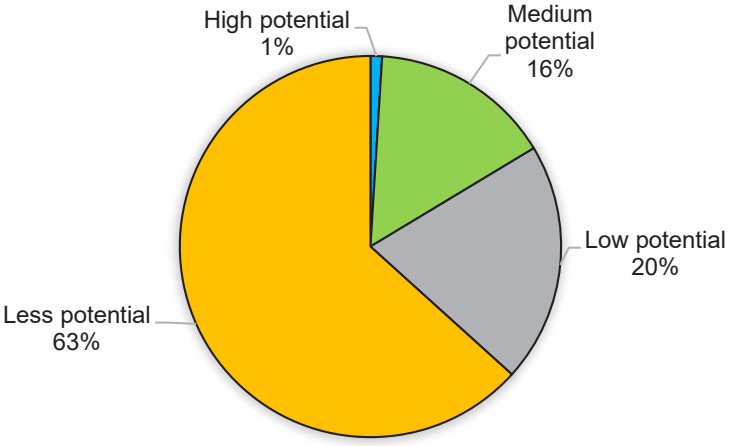


Fig. 3. Potency of peatlands for rice cultivation.

Source: Land suitability is based on topographic maps of South Sumatra (scale 1:50,000), Landsat imaginary analyses (2022), soil maps, field observations and laboratory analyses (2023).

Suitability class N means that the land shows dominant la-

Table 5. Limiting factors of peatland suitability for rice cultivation.

Class	Subclass*	Limiting factors
N	N	Latent limiting factors
S3	S3-anfx	Soil acidity, soil fertility, stagnant water, Al, Fe toxicity
S2	S2-nfx	Soil fertility, stagnant water and Al, Fe toxicity
S2	S2-anfx	Soil acidity, soil fertility, stagnant water and Al, Fe toxicity

Note: * a – very high soil acidity and difficult to be managed; n – very low to low soil fertility; f – flood, frequency and duration, flood water depth and water flow should be considered in order to determine this limitation; x – salinity, high salt content which limits crop growth. Source: Results of field observation, laboratory and image analyses (2023).

tent limiting factors. Land suitabilityS3 indicates that there are factors limiting plant growth, including soil acidity, soil fertility, stagnant water, Al, Fe toxicity. Land suitability class 2 indicating there are limiting factors including soil fertility, stagnant water and Al, Fe toxicity.

The results of field and laboratory analysis showed that even though peatlands provide low suitability for rice cultivation, there are still few opportunities to increase actual suitability to potential suitability based on agricultural science and technology by providing soil ameliorant materials and other actions needed (Table 6). For example, the actual land suitability class (S3-anfx) can be increased to potential land suitability (S2-af) by providing actions including lime, macro- and microfertilizers, water blocking leading to peatlands, not burning biomass, not leaching Na and H elements, and keeping peatlands always wet. However, the actual land suitability of S3-nfx and S3-nx can change to potential land suitability of S3-fx and S3-x only by changing the limiting factors but cannot change the land suitability class order, because the factors determining the land suitability class order are very dominant.

Rice production and income of farmers

Rice was developed by indigenous farmers for their own food (subsistence farming) because it is relatively easy to cultivate and its price was stable compared to other food crops and are capable of providing rice production ranging from 2.50–6.50 t MDG ha^{-1}·$year^{-1}$. The average rice production cost was IDR 5.5 million ha^{-1}·$year^{-1}$.

Table 7 shows differences in rice production and income of farmers based on peat depth. The deeper the peatlands

Table 6. Efforts to increase land capability for rice cultivation.

Actual*	Potential	Efforts to increase actual suitability to potential suitability
S3-anfx	S2-af	Lime, macro- and microfertilizers, water blocking leading to peatlands, not burning biomass, not leaching Na and H elements, and keeping peatlands always wet
S2-anfx	S2-af	
S3-nfx	S3-fx	
S3-nx	S3-x	

Note: * a – very acidic and difficult to be managed; n – very low to low fertility; f – flood, frequency, duration, flood depth and water flow should be considered in order to determine this limitation; x – salinity, high salt content. Source: Results of field observation, laboratory and image analyses (2023).

Table 7. Rice productivity and income of farmers in peatlands.

Peat depths	Average rice production, t MDG·ha^{-1}·year^{-1}	Income of farmers, IDR million·ha^{-1}·year^{-1}
Very deep	< 2.12 ±0.15^{a}	3.49 ±0.24^{a}
Deep	3.20 ±0.26^{b}	8.88 ±0.31^{b}
Medium	4.10 ±0.24^{c}	12.79 ±0.34^{c}
Shallow	4.45 ±0.20^{d}	19.10 ±0.32^{d}

Note: Values in the same column and indicated by the same superscript are not significantly different at the test level of 5%; MDG is milled dry grain.

were identified, the lower rice production was because the more limiting factors for rice growth were found, such as low soil fertility; unregulated water conditions; less able to support rice growth; pest and disease attacks; lack of soil nutrients; technical difficulties in the rice cultivation due to access difficulty to very deep and deep peatlands.

Rice production and income of farmers were significantly different for each peatland depth. Income of farmers was obtained from the t-test, so it was concluded that H0 was rejected, meaning there were differences in income among them based on different peatland depths. Peatlands with shallow depths could provide the highest rice production and income of farmers (around 4.45 t MDG·ha^{-1}·year^{-1} and IDR 19.10 million·ha^{-1}·year^{-1}) and were significantly different from very deep, deep and medium peatlands.

Latent challenges and land uses of peatlands

All coercive actions against peatlands have triggered the presence of latent challenges in peatlands, for example biodiversity loss (habitat, genetics, genes) especially for native flora and fauna; loss of production functions (peat, water, crop cultivation); and loss of social and environmental functions. Latent challenges are generally hidden and lie beneath what we perceive as obvious, deep, long-standing, and ongoing, but they still emerge in a variety of ways. They are very difficult or impossible to reclaim and tend to lead to the destruction and disappearance of peatlands.

Latent challenges were only possible done by strong investors, plantation industries and large speculators who were capable of converting peatlands to oil palm and acacia plantations on a large scale. Farmers were unable to face this latent challenge because it was repeated, global, and had huge impacts on the environment. Even if it continues to grow and is less attended, it is possible that peatlands will disappear in 2050 as represented in Figure 2. It illustrates that the area of deep peatlands is decreasing from year to year, on the other hand, the area of shallow peatlands is becoming more and more widespread over time. This indicates that deep peatlands will be destroyed and disappeared.

Conclusions

Peatlands fall into land suitability classes of N (permanently not suitable) and S3 (marginally suitable), if peatlands are forced for rice cultivation, then rice cultivation cannot be carried out

optimally. There are two main reasons farmers avoid deep peatlands for cultivating food crops, namely instinctive challenges and latent challenges.

Instinctive challenges are dominantly temporary, technical or economic, non-repetitive, local, and have less impact on the environment, so that they are easier to overcome with a scientific and technological approach and farmers are able to face these instinctive challenges. Efforts needed to overcome the instinctive challenges, namely installing water blocking to irrigate peatlands (rewetting), liming, not burning peatlands, and fertilizing. Based on their potential, there are four potential groups of peatlands, namely high potential; medium potential; low potential; and less potential.

Latent challenges are very difficult or impossible to repair and tend to lead to the destruction and extinction of peatlands. Latent challenges are only possible for strong investors, plantation industries and large speculators capable of converting peatlands to oil palm and acacia plantations on a large scale. The government should stop granting business permits (concessions) and make deep and very deep peat lands for conservation areas, not reserved for large private companies for Oil palm and Acacia plantations because of their environmental impact, especially due to the logging process, over drainage and land clearing by burning is global, regional and local. Four approaches are recommended for sustainable peatland management, namely decentralisation approach; conservative approach; protective approach, and optimal approach.

It is suggested to the Government to carry out coordination at any level involving stakeholders, government and indigenous farmers in carrying out peatlands restoration. Peatlands are not permitted to be opened for any purpose without having adequate technology and knowledge regarding the two characteristics of peatlands, namely instinctive challenges and latent challenges. Apart from that, it is necessary to involve indigenous farmers in the use of peatlands.

Acknowledgements

On this valuable opportunity, the authors would like to express their thanks to all support systems, supervisor, and the indigenous farmers on the research plots who have greatly helped carry out this research both in the field and in the laboratory.

References

Alikhani S., Nummi P., Ojala A. 2021. Urban wetlands: A Review on Ecological and Cultural Values. Water 13(22): 1–47. http://dx.doi.org/10.3390/w13223301

Armanto M.E. 2019a. Improving Rice Yield and Income of Farmers by Managing the Soil Organic Carbon in South Sumatra Landscape, Indonesia. Iraqi Journal of Agricultural Sciences 50(2): 653–661. https://doi.org/10.36103/ijas.v2i50.665

Armanto M.E. 2019b. Comparison of Chemical Properties of Peats under Different Land Uses in South Sumatra, Indonesia. Journal of Ecological Engineering 20(5): 184–192. https://doi.org/10.12911/22998993/105440

Armanto M.E., Adzemi M.A., Wildayana E., Imanudin M.S. 2013. Land Evaluation for Paddy Cultivation in the Reclaimed Tidal Lowland in Delta Saleh, South Sumatra, Indonesia. Journal of Sustainability Science and Management 8(1): 32–42. http://jssm.umt.edu.my/files/2013/07/4w.pdf

Armanto M.E., Hermawan A., Imanudin

M.S., Wildayana E., Sukardi, Triana A.N. 2023a. Biomass and Soil Nutrients Turnover Affected by Different Peat Vegetation. Journal of Wetlands Environmental Management 11(1): 31–42. http://dx.doi.org/10.20527/jwem.v11. i1.292

Armanto M.E., Wildayana E. 2022. Accessibility Impact to Government Programs on the Household Income Contribution at the Various Livelihood Sources of Farmers. Agriekonomika Journal 11(1): 62–75. https://doi.org/10.21107/agriekonomika.v11i1.13191

Armanto M.E., Wildayana E. 2023. Predictive Mapping for Soil pH and Phosphate based on Kriging Interpolation. International Conference on Sustainable Environment, Agriculture and Tourism (ICOSEAT), Advances in Biological Sciences Research 26: 254–262. https://doi.org/10.2991/978-94-6463-086-2_33

Armanto M.E., Wildayana E., Syakina B. 2023b. Deciphering the Anthropogenic Challenges of Peat Swamp Forest Degradation to Improve Awareness and Emphasis on Restoration in South Sumatra. Forestry Ideas 29(2): 207–215. https://forestry-ideas.info/issues/issues_Index.php?-journalFilter=73

Armanto M.E., Zuhdi M., Setiabudidaya D., Ngudiantoro, Wildayana E., Hermawan A., Imanudin M.S. 2022. Deciphering Spatial Variability and Kriging Mapping for Soil pH and Groundwater Levels. Journal of Suboptimal Lands 11(2): 187–196. http://www.jlsuboptimal.unsri.ac.id/index.php/jlso/article/view/577/526

Byg A., Novo P., Kyle C. 2023. Caring for Cinderella – Perceptions and Experiences of Peatland Restoration in Scotland. People Nature 5(2): 302–312. https://doi.org/10.1002/pan3.10141

He N., Yan P., Liu C., Xu L., Li M., Van Meerbeek K., Zhou G., Zhou G., Liu S., Zhou X., Li S., Niu S., Han X., Buckley T.N., Sack L., Yu G. 2023. Predicting Ecosystem Productivity Based on Plant Community Traits. Trends in Plant Science 28(1): 43–53. https://doi.org/10.1016/j.tplants.2022.08.015

Holidi, Armanto M.E., Damiri N., Putranto D.D.A. 2019. Characteristics of Selected Peatland Uses and Soil Moistures based on TVDI. Journal of Ecological Engineering 20(4): 194–200. https://doi.org/10.12911/22998993/102987

Holidi 2019. The Level of Drought and Fire Risk in Various Types of Peat Landuses. PhD thesis, Sriwijaya University, Indonesia. 108 p. (in Indonesian).

Junedi H. 2017. Water Management on Oil Palm Plantation in Peatland Areas. Sriwijaya University, PhD thesis. Indonesia. 154 p. (in Indonesian).

PMRA (Peat and Mangrove Restoration Agency) 2022. Performance Report of Peat and Mangrove Restoration Agency [Laporan Kinerja. Badan Restorasi Gambut dan Mangrove 2022]. 113 p. (in Indonesian). https://brgm.go.id/publikasi/

Wildayana E., Armanto M.E. 2018a. Lebak Swamp Typology and Rice Production Potency in South Sumatra. Agriekonomika 7(1): 30–36. https://doi.org/10.21107/agriekonomika.v7i1.2513

Wildayana E., Armanto M.E. 2018b. Dynamics of Landuse Changes and General Perception of Farmers on South Sumatra Wetlands. Bulgarian Journal of Agricultural Science 24(2): 180–188. http://www.agrojournal.org/24/02-02.html

Wildayana E., Armanto M.E. 2018c. Formulating Popular Policies for Peat Restoration based on Livelihoods of Local Farmers. Journal of Sustainable Development 11(3): 85–95. https://doi.org/10.5539/JSD.V11N3P85

Wildayana E., Armanto M.E. 2018d. Utilizing non-timber extraction of swamp forests over time for rural livelihoods. Journal of Sustainable Development 11(2): 52–62. https://doi.org/10.5539/jsd.v11n2p52

Wildayana E., Armanto M.E. 2021. Empowering Indigenous Farmers with Fish Farming on South Sumatra Peatlands. HABITAT 32(1): 1–10. https://Doi.Org/10.21776/Ub.Habitat.2021.032.1.1

Wildayana E., Armanto M.E., Zahri I., Adriani D., Syakina B. 2019. Socio Economic Factors Causing Rapid Peatlands Degra-

dation in South Sumatra. Sriwijaya Journal of Environment 3(3): 87–95. http://dx.doi.org/10.22135/sje.2018.3.3.87-95

Wildayana E., Armanto M.E., Zulkifli I., Radiatmoko I. A., Umar S. A., Syakina B., Oktavia, R., Sari E. 2018. Surviving Strategies of Rural Livelihoods in South Sumatra Farming System, Indonesia. E3S Web of Conferences 68, 02001. 9 p. https://doi.org/10.1051/e3sconf/20186802001

Yan P., Fernández-Martínez M., Van Meerbeek K., Yu, G., Migliavacca M., He N. 2023. The Essential Role of Biodiversity in the Key Axes of Ecosystem Function. Global Change Biology 29(16): 4569–4585. https://doi.org/10.1111/gcb.16666

Zhang L., Song J., Hua X., Li X., Ma D., Ding M. 2022. Smallholder rice Farming Practices Across Livelihood Strategies: A Case Study of the Poyang Lake Plain, China. Journal of Rural Studies 89: 199–207. https://doi.org/10.1016/J.Jrurstud.2021.12.001

Zuhdi M., Armanto M.E., Setiabudidaya D., Ngudiantoro N., Sungkono S. 2019. Exploring peat thickness variability using VLF method. Journal of Ecological Engineering 20(5): 142–148. https://doi.org/10.12911/22998993/105361

Zuhdi M. 2019. Spatial Modelling of Peat Thickness based on Electromagnetic Waves. PhD thesis, Sriwijaya University, Indonesia. 116 p. (in Indonesian).

FORESTRY IDEAS, 2024, vol. 30, No 1 (67): 16–27

Soil fertility and plant nutrition of *Pinus pinaster* and *Pinus radiata* reforestations in Halkidiki, Northern Greece

Katherine Karamanoli[1*], Athanasios Papaioannou[2], and Theano Samara[1]

[1]Forest Research Institute, Hellenic Agricultural Organization 'Demeter', Vasilika – Thessaloniki, Greece. [*]E-mail: karamanoli@fri.gr

[2]Laboratory of Forest Soils, Department of Forestry and Natural Environment, School of Agriculture, Forestry and Natural Environment, Aristotle University of Thessaloniki, Finikas – Thessaloniki, Greece.

Received: 31 January 2023 / Accepted: 03 January 2024 / Available online: 15 January 2024

Open Access: This article is licensed under a Creative Commons Attribution 4.0 International License.

Abstract

Pinus pinaster Aiton (maritime pine) and *Pinus radiata* D.Don (radiata pine) are both coniferous species not native in Greece, which were artificially installed in Halkidiki, Northern Greece, since the early 1970s. The research was performed to estimate the soil conditions of both conifers in two different areas, where the reforestation has been successful. The best site quality stands were selected, having particularly deep soil. Samples of soil, litter and needles were taken for both species from 16 different sample plots in two sites: Stratoni and Sithonia. From the results, higher concentrations of most soil nutrients, as well as better absorption of P and N by trees, were found in Stratoni for both conifers. Tree dimensions for both conifers are greater in Stratoni, corresponding to the higher nutrient content and an observed higher humidity. The concentrations of nutrients in soil, litter and foliage for each conifer species were assessed according to the literature.

Key words: conifers, litter, maritime pine, Mediterranean ecosystems, Monterrey pine, needles, soil nutrient content.

Introduction

Soil fertility plays a decisive role controlling the growth of plants in forest ecosystems, but forests also have a greater influence on the soil conditions than most of other plant ecosystem types (Binkley and Giardina 1998). Moreover, soil fertility plays a key role in influencing the establishment and growth of artificial forests. Viewpoints about soil fertility vary widely, so many researchers have suggested that attention should be shifted towards another concept: soil quality (Patzel et al. 2000).

Studies on litter decomposition are very important for understanding the way a forest ecosystem functions. Litter decomposition controls the nutrient release rate and the availability of soil nutrients to plants (Kurz et al. 2000). Only a small pro-

portion of nutrients used by plants (S, Ca, Mg, K) comes from releases of minerals from soil. The largest proportion comes from the mineralization by micro-organisms of the soil organic matter, including the organic material fallen from the trees through litterfall (Swift et al. 1979). Furthermore, nutrients in foliage influence the dynamics of tree nutrition, affecting carbon assimilation and wood yield (Sheriff et al. 1986).

Pinus pinaster Aiton and *Pinus radiata* D.Don are both fast-growing conifers, suitable for wood production (Alía et al. 1997). *P. pinaster* is a native Mediterranean conifer plant, used in afforestation mainly in Southwestern Europe, but also in Africa, New Zealand and Australia (Ferreira-Santos et al. 2020). The Mediterranean Basin is also considered a typical habitat for *P. radiata*, a native South American conifer, but with up to 93 % successful reforestations in many Mediterranean areas around the world (Richardson and Rundel 1998, Hermoso et al. 2007, Arias-Rodil et al. 2015). *P. pinaster* and *P. radiata* were both artificially reforested in Halkidiki, Northern Greece, mainly in the early 1970s (Varelides and Kritikos 1994). Both seemed to fail, as extensive reforestations were destroyed by drought (Papamichos and Alifragkis 1980), chlorosis in young plants occurred (Nakos 1978), both conifers showed a low life expectancy, compared to endemic pine species, such as *P. brutia* and *P.nigra* (Zagas and Ganatsas 2001).

The H:D ratio is used to quantify the risk of storm damage, using classic or modern models (Ogana et al. 2020). According to Sudmeyer et al. (2004), *P. pinaster* and *P. radiata* have similar root lateral extent and the greatest root density within 0.5 m of the soil surface.

Regarding soil nutrient content, Knicker et al. (2005) found concentrations of N between 0.07 and 0.11 % in topsoil (0–20 cm) of a natural *P. pinaster* forest in Spain. Martins et al. (2009) found total N 0.47 % and P 2.06 $mg \cdot 100^{-1}$ in topsoil of *P. pinaster* on sandy soils in Galicia, Northwestern Spain. Respectively, Hopmans and Elms (2009) found the following concentrations: N 0.7 %, P 0.57 $g \cdot kg^{-1}$, K 0.79 $g \cdot kg^{-1}$, Ca 6.95 $g \cdot kg^{-1}$, Fe 1.946 $mg \cdot kg^{-1}$, Mn 382 $mg \cdot kg^{-1}$, Zn 13.7 $mg \cdot kg^{-1}$ and Cu 3 $mg \cdot kg^{-1}$ in litter of an Australian *P. radiata* plantation on podzolized sands. In addition, Turner and Lambert (1988) found N 0.48 %, P 0.63 $mg \cdot g^{-1}$ in litter, N 0.09 %, P 0.12 $mg \cdot gr^{-1}$ and N 0.05 %, P 0.105 $mg \cdot gr^{-1}$ at two soil depths (0–7.5 cm and 30–37 cm), respectively, in Australian *P. radiata* plantations. Among the mineral nutrients, soil nitrogen status is deliberated as being the primary regulating factor, while phosphorous is usually considered as a limiting nutrient because of the low quantity in circulation in major forests (Devi and Yadava 2007, Krishna and Mahesh 2017).

Regarding nutrient content in foliage, Butcher (1977) found the following concentrations: N 0.8 %, P 0.71 $mg \cdot g^{-1}$, K 6.02 $mg \cdot g^{-1}$, Ca 1.5 $mg \cdot g^{-1}$, Mg 1.94 $mg \cdot g^{-1}$, Mn 18.13 $mg \cdot kg^{-1}$ and Zn 25.67 $mg \cdot kg^{-1}$ in needles of *P. pinaster* plantations in Australia. Respectively, Romanyà and Vallejo (2004) found N 1.62–1.73 %, P 1.17–1.57 $mg \cdot g^{-1}$ K 8.08–6.76 $mg \cdot g^{-1}$ and Mg 1.16–2.02 $mg \cdot g^{-1}$ in foliage of *P. radiata* plantations in Spain. Moreover, Hopmans and Elms (2009) found N 1.29 %, P 1.32 $mg \cdot g^{-1}$, K 7.31 $mg \cdot g^{-1}$, Ca 6.8 $mg \cdot g^{-1}$, Mg 2.03 $mg \cdot g^{-1}$, Fe 83 $mg \cdot kg^{-1}$, Mn 534 $mg \cdot kg^{-1}$, Zn 16.2 $mg \cdot kg^{-1}$ and Cu 2.76 $mg \cdot kg^{-1}$ in foliage of *P. radiata* plantations in Australia. Merino and Edeso (1999) found N 1.48 %, P 2.02 $mg \cdot g^{-1}$, Mg

1.21 mg·g^{-1} and Ca 6.41 mg·g^{-1} in the foliage of *P. radiata* after intense soil treatment in Northern Spain.

Temperature, precipitation and chemical content of litter strongly control rates of litter decomposition, influencing the recycling of nutrients and thus ecosystem fertility (Aerts et al. 1997, Brant et al. 2006, Smyth et al. 2015). The most favourable microclimate found especially in Stratoni, due to humidity, has been pointed out by Greek forest researchers (Chatzistathis 1980).

The aim of this study is to estimate soil conditions and the differences in nutrient content between two forest sites in Stratoni and Sithonia, where both conifers managed to survive and grow.

Material and Methods

Study area

The study areas are in Stratoni at the Northeast of Halkidiki and at the peninsula of Sithonia at the South of Halkidiki. Both study areas include reforestations of both *Pinus pinaster* and *Pinus radiata* (Fig. 1). The distance between sites is more than 50 km. The elevation of sampling plots ranges from 450 to 545 m in Sithonia and from 0 to 280 m in Stratoni. Although the climate is mainly temperate and mild, it is locally influenced by topography. The dry period lasts 1.5–2.5 months, rendering the area vulnerable to fire. Average annual precipitation is 795 mm, mean annual temperature is 9.85 °C and daily mean temperature ranges from 2.1 to 21.6 °C in the study areas.

According to the ISSS Working Group RB (1998a, 1998b), the soils are Eutric Cambisols, containing shallow and moderately deep soils, developed under typical Mediterranean vegetation. Forest soil has formed on gneiss parent material in reforestations of Stratoni; correspondingly, the forest soil has formed on granite – argillic schist in reforestations of Sithonia. Pine reforestations were carried out since the early 1970s according to Greek Forest Services. Native vegetation is dominated by oaks, such as mainly kermes oak (*Q. coccifera* L.), holm oak (*Q. ilex* L.), plane trees (*Platanus orientalis* L.) or evergreen

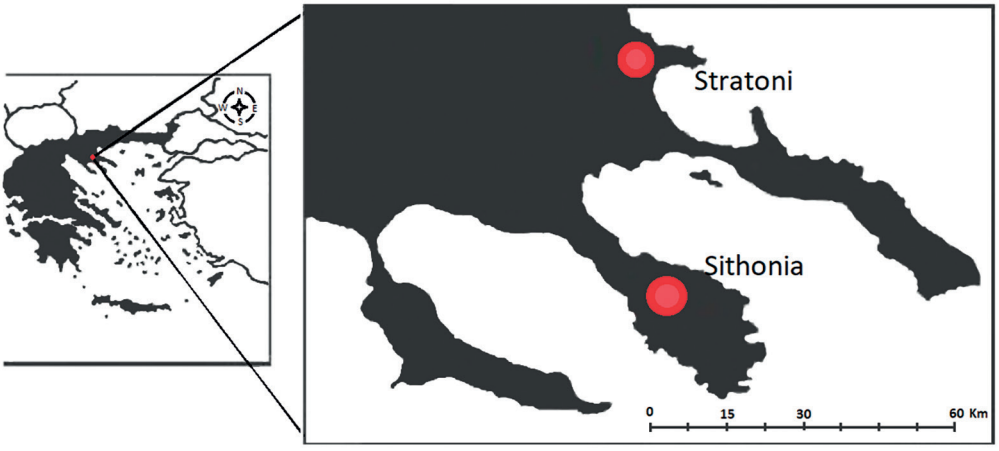


Fig. 1. The study area.

shrubs, such as tree heath (*Erica arborea* L.), strawberry tree (*Arbutus unedo* L.), Greek strawberry tree (*Arbutus andrachne* L.), rock rose (*Cistus* sp.), black alder (*Alnus glutinosa* L.), mastic tree (*Pistacia lentiscus* L.), green olive tree (*Phyllirea latifolia* L.) and turpentine tree (*Pistacia terebinthus* L.).

Sixteen sample plots were chosen, eight for both conifer species, each covering an area of 314 m^2. All sample plots were located within a pure and undisturbed *Pinus pinaster* and *Pinus radiata* plantations. The sample plots were selected by random systematic sampling for both conifers, keeping a distance of more than 2 km from each other, in order to represent different forest microenvironments. Sample plots from Stratoni were located between 24°03'39'' E latitude, 40°43'42'' N longitude and 23°54'22'' E latitude, 40°46'31'' N longitude, while sample plots from Sithonia are located between 23°58'32'' E latitude, 40°09'14'' N longitude and 24°03'44'' E latitude, 40°20'39'' N longitude. The elevation of sample plots ranges from 0 to 120 m in Stratoni and from 425 to 545 m in Sithonia. The average slope is 7–10 %, while the dominant aspect is oriented northeast.

At both Stratoni and Sithonia, eight sample plots were selected, four for *Pinus pinaster* and four for *Pinus radiata*. Sample plots were chosen according to the field- based survey data from the Greek Forestry Services. At each sample plot the breast height diameter and the height of all healthy trees was measured to assess the growth of both conifers and the differences between the two areas. The measurements of breast height diameter were carried out using a calliper and a diameter tape (accuracy 1 cm). Height measurements were carried out using a Blume-Leiss and a Haga altimeter (accuracy 0.1 m). Forked trees (in $h < 1.3$ m) were measured as two different trees. Field measurements were implemented in the middle of the growing period (July-August) (Dobbertin et al. 2013).

Methods

A square metallic frame with dimensions of 25×25 cm was used for the sampling of litter. Litter's samples were randomly selected in five sites per plot, separately for each organic horizon (pine needles and twigs, partially decomposed layer or well decomposed humus). The litter within the square area was transferred into labelled plastic bags. Pine needle samples, one per each sampling plot, were also selected. About one hundred and sixty litter samples and sixteen pine needles samples were transported to the Forest Soil Laboratory of Aristotle University. The collected samples were dried in an oven at 74 °C for 48 h, next the samples were weighed, grounded and prepared for analyses. Soil samples were taken from depths of 0–10, 10–20, 20–40 and 40–60 cm from two different soil profiles per sample plot. About one hundred and twenty soil samples were transferred into labelled plastic bags and transported to the laboratory. Then all soil samples were air-dried, weighed, grounded, passed through a 2 mm sieve and prepared for analyses.

Litter's and needles' chemical analyses were performed in pulverized and homogenized material. Total nitrogen (N) was estimated using Kjeldahl digestion method (Stevenson 1982). The nutrients Ca, Mg, K, Na, Fe, Mn, Zn και Cu were measured using an atomic absorption spectrophotometer (PerkinElmer, Inc., USA) in a mixed solution of HNO_3, $HClO_4$ and H_2SO_4 (5:1:0.5) (Allen et al. 1986). Phosphorus

was determined using the molybdate blue colorimetric method.

Soil N was determined using Kjeldahl digestion method (Stevenson 1982). Extractable P was also measured using the blue of ammonium sulphoparamolybdate method (Olsen and Sommers 1982). Exchangeable cations, such as Ca, Mg, and K were determined using the CH_3COONH_4 1N solution of pH 7 (Grant 1982). The micronutrients Fe, Mn, Zn and Cu were determined using the diethylenetriaminepentaacetic acid solution of pH 7.3 (Lindsay and Norvell 1978). All extracted cations Ca, Mg, K, Fe, Mn, Zn and Cu were measured using an atomic absorption spectrophotometer.

Statistical analysis

All statistical analyses were performed using the SPSS statistics software (Version 20 2014). The uncorrelated t-test is used to calculate whether the averages of two groups from different samples differ significantly from each other (Howitt and Cramer 2001). Therefore, t-tests were used to assess the significance of differences between concentrations of nutrients from the two areas. Nine dependent variables were selected for regression analysis: N (%); P, Mg, Ca, K ($mg \cdot g^{-1}$); Cu, Fe, Zn, Mn (ppm). Independent sample t-tests were used to compare means of variables (concentrations of nutrients) for soil, litter and needles from Stratoni and Sithonia, as well as to compare the dimensions of trees in both areas. In addition, *p*-values from the two-tailed probability computed using the t-distribution were compared to an alpha level of 0.05 (SAS 2008).

Results

Tree dimension measurements

The maximum total tree height was found above 20 m for both conifer species, while the maximum breast height diameter was found above 43 cm for *Pinus pinaster* and above 33 cm for *P. radiata* on the sample plots of Stratoni. Correspondingly, the maximum total tree height was found above 16 m for both conifer species, while the maximum breast height diameter was found above 26 cm for *P. pinaster* and above 22 cm for *P. radiata* on the sample plots of Sithonia.

Dendrometric variables

Table 1 shows the dendrometric variables on sampling plots, including average height (H), average breast height diameter (D), H:D ratio and tree density.

There are significant differences between the two areas in most variables. Higher values in average height and average breast height diameter are presented

Table 1. Dendrometric variables (mean ± s.d.) for *Pinus pinaster* and *Pinus radiata* in both areas.

Species	Area	H, m	D, cm	H:D	Density, ha^{-1}
Pinus pinaster	Stratoni	**19.75 ±4.81**	**44.20 ±13.13**	**0.47 ±0.11**	1210
	Sithonia	**18.05 ±2.85**	**27.64 ±4.75**	**0.66 ±0.07**	1019
Pinus radiata	Stratoni	**21.15 ±2.19**	**33.28 ±3.69**	0.64 ±0.05	1015
	Sithonia	**17.25 ±1.74**	**24.70 ±1.83**	0.69 ±0.05	981

Note: Values in bold indicate a significant difference between different areas.

in Stratoni, especially for *Pinus pinaster*. The H:D ratio is higher in Sithonia, especially for *P. radiata*. Therefore, the larger number of trees per hectare is found in Stratoni for *P. pinaster*, while the smaller one is found in Sithonia for *P. radiata* (Table 1).

Chemical composition in needles, litter and soil

Chemical composition of *Pinus pinaster*

Concentrations of most measured nutrients are higher in Stratoni. Specifically, concentrations of i) N, P, Mg, Cu, and Fe in needles, ii) P, Mg, Fe and Mn in litter and iii) P, Ca, K, and Zn in soil at most soil depths have higher values in Stratoni.

Table 2 shows concentrations of nutrients in needles and litter for *P. pinaster* in both areas.

Table 3 shows concentrations of nutrients in soil according to soil depth for *P. pinaster* in both areas.

Chemical composition of *Pinus radiata*

Concentrations of N, P and Zn in needles, Mg, Fe and Zn in litter are higher in Stratoni. Overall, all macronutrient concentrations, but P at shallow soils, are higher in Stratoni, as well as concentrations of Ca, K and Zn at most soil depths.

Table 4 shows concentrations of nutrients in needles and litter for *P. radiata* in both areas.

Similarly Table 5 shows concentrations of nutrients in soil according to soil depth for *P. radiata* in both areas.

Soil chemical properties under *Pinus pinaster* stands

In both study areas the soil was acid (pH 4.02–5.36). Concentrations of most nutrients in soil show higher values in Stratoni, where P, Ca, K, and Zn are in higher concentrations. On the contrary, in Sithonia only Fe is in higher concentrations in soil. The different parent material between the two areas plays an important role. In litter,

Table 2. Nutrients (mean ±s.d.) in needles and litter for *Pinus pinaster* in Stratoni and Sithonia.

Elements	Needles		Litter	
	Stratoni	Sithonia	Stratoni	Sithonia
		Nutrients		
N, %	**1.11 ±0.45**	**0.73 ±0.02**	0.84 ±0.35	0.63 ±0.13
P, mg·g^{-1}	**0.79 ±0.13**	**0.61 ±0.15**	**0.47 ±0.15**	**0.32 ±0.09**
Ca, mg·g^{-1}	3.52 ±1.97	4.75 ±0.59	**4.83 ±0.28**	**6.04 ±0.96**
Mg, mg.g^{-1}	**2.72 ±0.50**	**2.03 ±0.47**	**3.27 ±1.22**	**1.94 ±0.28**
K, mg·g^{-1}	4.85 ±1.19	6.09 ±1.55	1.10 ± 0.34	1.33 ±0.17
		Micronutrients		
Cu, mg·kg^{-1}	**11.29 ±7.4**	**3.63 ±0.9**	24.33 ±8.1	23.26 ±7.6
Fe, mg·kg-^{1}	**962.36 ±353**	**310.44 ±57.1**	**3.071 ±628.0**	**2.070 ±153.8**
Zn, mg·kg-^{1}	38.12 ±9.28	34.79 ±6.91	**298.28 ±66.2**	**744.78 ±187.72**
Mn, mg·kg-^{1}	125.74 ±68.94	168.83 ±61,77	**101.80 ±10.8**	**60.47 ± 8.46**

Note: Values in bold indicate a significant difference between different areas.

Table 3. Nutrients (mean ±s.d.) in soil for *Pinus pinaster* in Stratoni and Sithonia.

Elements	Depth of soil layer							
	0–10 cm		10–20 cm		20–40 cm		40–60 cm	
	Stratoni	Sithonia	Stratoni	Sithonia	Stratoni	Sithonia	Stratoni	Sithonia
				Nutrients				
N, %	**0.22 ±0.07**	**0.13 ±0.07**	0.11 ±0.07	0.11 ±0.06	0.08 ±0.06	0.09 ±0.03	0.06 ±0.05	0.06 ±0.03
P, mg·100g^{-1}	**1.32 ±0.60**	**0.63 ±0.08**	**1.03 ±0.37**	**0.52 ±0.06**	**0.88 ±0.45**	**0.47 ±0.09**	**0.72 ±0.33**	**0.47 ±0.10**
Ca, cmole·kg^{-1}	**5.57 ±3.11**	**1.33 ±0.83**	**4.31 ±2.64**	**1.51 ±1.00**	**3.48 ±2.09**	**1.71 ±0.83**	**4.31 ±3.50**	**1.40 ±0.79**
Mg, cmole·kg^{-1}	**0.42 ±0.19**	**0.19 ±0.12**	0.21 ±0.09	0.15 ±0.08	0.15 ±0.09	0.19 ±0.09	0.11 ±0.05	0.12 ±0.05
K, cmole·kg^{-1}	**12.93 ±5.50**	**3.43 ±3.27**	**8.24 ±5.22**	**2.79 ±3.58**	6.27 ±4.88	3.07 ±1.57	**6.32 ±5.50**	**1.86 ±1.21**
				Micronutrients				
Cu, mg.kg^{-1}	2.18 ±0.99	3.10 ±2.60	2.40 ±1.29	2.75 ±1.61	2.01 ±0.84	4.00 ±2.32	2.03 ±0.78	1.96 ±0.84
Fe, mg·kg^{-1}	**32.14 ±11.14**	**42.55 ±5.47**	30.83 ±12.2	38.80 ±6.2	**26.99 ±0.89**	**39.7 ±7.53**	**23.78 ±6.9**	**34.2 ±4.29**
Zn, mg·kg^{-1}	**11.63 ±4.39**	**3.08 ±0.99**	**4.83 ±1.98**	**1.45 ±0.69**	**3.33 ±1.44**	**1.22 ±0.94**	**2.46 ±1.63**	**0.90 ±0.33**
Mn, mg·kg^{-1}	26.05 ±12.98	24.98 ±6.21	19.15 ±16.2	11.43 ±7.14	17.28 ±15.28	8.29 ±5.72	**13.9 ±12.3**	**6.41 ±5.62**

Note: Values in bold indicate a significant difference between different areas.

Table 4. Nutrients (mean ±s.d.) in needles and litter for *Pinus radiata* in Stratoni and Sithonia.

Elements	Needles		Litter	
	Stratoni	Sithonia	Stratoni	Sithonia
		Nutrients		
N, %	**1.66 ±0.84**	**0.85 ±0.052**	1.04 ±0.35	0.85 ±0.07
P, mg·g-^{1}	**0.97 ±0.11**	**0.58 ±0.03**	0.46 ±0.19	0.46 ±0.19
Ca, mg·g-^{1}	**3.12 ±1.06**	**5.84 ±2.62**	4.63 ±3.15	7.02 ±1.74
Mg, mg·g-^{1}	1.97 ±0.34	2.01 ±0.69	**2.92 ±0.69**	**2.09 ±0.48**
K, mg·g^{-1}	7.63 ±2.77	6.06 ±0.76	1.75 ±1.09	1.09 ±0.18
		Micronutrients		
Cu, mg·kg-^{1}	7.68 ±1.92	8.74 ±3.90	22.17 ±15.23	28.22 ±5.64
Fe, mg·kg-^{1}	1,334 ±1.33	487.05 ±342.14	**3,034 ±588.30**	**2,318 ±465.00**
Zn, mg·kg^{-1}	**84.62 ±65.62**	**30.81 ±10.53**	**140.22 ±90.74**	**57.59 ±10.50**
Mn, mg·kg^{-1}	210.12 ±110.00	253.58 ±120.24	512.14 ±456.48	826.14 ±245.87

Note: Values in bold indicate a significant difference between different areas.

Table 5. Nutrients (mean ±s.d.) in soil for *Pinus radiata* in Stratoni and Sithonia.

Elements	Depth of soil layer							
	0–10 cm		10–20 cm		20–40 cm		40–60 cm	
	Stratoni	Sithonia	Stratoni	Sithonia	Stratoni	Sithonia	Stratoni	Sithonia
				Nutrients				
N, %	**0.26 ±0.93**	**0.09 ±0.03**	0.14 ±0.10	0.08 ±0.01	0.09 ±0.07	0.06 ±0.02	**0.03 ±0.01**	**0.051 ±0.01**
P, mg·100g^{-1}	1.0 ±0.73	0.52 ±0.14	0.84 ±0.70	0.54 ±0.21	0.65 ±0.43	0.46 ±0.07	0.55 ±0.19	0.46 ±0.12
Ca, cmole·kg^{-1}	**3.34 ±2.46**	**1.20 ±0,26**	**2.72 ±2.06**	**1.08 ±0.52**	**2.60 ±1.64**	**1.14 ±0.36**	**3.47 ±1.90**	**0.96 ±0.49**
Mg, cmole·kg^{-1}	**0.33 ±0.08**	**0.20 ±0.08**	0.21 ±0.07	0.17 ±0.09	0.16 ±0.11	0.17 ±0.05	0.17 ±0.13	0.14 ±0.04
K, cmole·kg^{-1}	**9.35 ±6.13**	**2.68 ±1.11**	**6.66 ±4.78**	**2.01 ±1.36**	**5.03 ±3.64**	**1.74 ±0.74**	**6.13 ±3.95**	**1.38 ±0.55**
				Micronutrients				
Cu, mg.kg^{-1}	2.02 ±1.39	2.58 ±1.83	3.04 ±1.88	2.14 ±1.06	3.03 ±1.45	1.75 ±1.04	1,93 ±0.57	1.74 ±0.75
Fe, mg·kg^{-1}	33.14 ±9.32	42.94 ±8.94	32.90 ±8.26	38.61 ±10.22	26.85 ±5.97	28.50 ±10.04	21.04 ±7.05	27.84 ±7.67
Zn, mg·kg^{-1}	**7.66 ±3.75**	**1.70 ±0.80**	**4.47 ±3.62**	**0.95 ±0.30**	3.70 ±5.01	0.73 ±0.35	**4.64 ±3.85**	**0.75 ±0.10**
Mn, mg·kg^{-1}	21.54 ±15.63	16.83 ±8.30	21.83 ±17.62	10.83 ±10.02	20.32 ±19.35	6.66 ±5.97	12.29 ±11.52	4.95 ±4.10

Note: Values in bold indicate a significant difference between different areas.

higher concentrations of P, Mg Fe and Mn were found in Stratoni, while higher concentrations of Ca and Zn were found in Sithonia. Due to better growth of *P. pinaster* in Stratoni, greater amounts of organic residues are produced, so higher nutrients' concentrations in litter are observed. In needles, concentrations of N, P, Mg, Cu and Fe were found in higher concentrations in Stratoni.

Soil chemical properties under *Pinus radiata* stands

In both study areas the soil was also acid (pH 4.02–5.36). Concentrations of macronutrients at shallow soils, concerning extracted cations, also show higher values in Stratoni, where the soil has higher concentrations of N, Ca, Mg, and K. At a greater depth (>10 cm), higher Ca and K content is observed in Stratoni. Higher concentrations of Zn was also found in soil in Stratoni. Higher concentrations of Mg, Fe and Zn in litter and N, P and Zn in needles were found in Stratoni, but only higher concentrations of Ca in needles were found in Sithonia. Concentrations of most nutrients in litter and needles do not show statistically significant differences between the two areas, but there are significant differences in most nutrients between the two areas at shallow soils.

Discussion

Soil in both areas is deep, compared to most pine reforestations in Greece, concerning mainly semi-mountainous, semi-

arid, rather dry, warm areas. Tree dimensions for both conifers are obviously greater in Stratoni, presenting the best tree growth in Halkidiki. The H:D ratio shows greater wind stability in Stratoni for *P. pinaster*, but no differences between the two areas for *P. radiata*.

The amounts of Ca, Mg and K and micronutrients in soil are due to the parent material. Therefore, in Stratoni the greater quantity of Ca in soil is due to limestone rocks, which are common in the study areas. Moreover, greater amounts of Zn in Stratoni or Fe in Sithonia are also due to the parent material and soil impurities.

Higher concentrations of P in litter and soil were found in Stratoni for *Pinus pinaster*. Moreover, concentrations of N only at shallow soils of both conifers showed higher values in Stratoni. For *P. pinaster* the results showed equal or higher concentrations of N, but lower concentrations of P in soil in relation to natural forests in Spain. For *P. radiata*, results showed equal higher concentrations of most nutrients in soil, but lower concentrations of P in litter in relation to *Pinus radiata* plantations in Australia (Turner and Lambert 1988, Knicker et al. 2005, Hopmans and Elms 2009, Martins et al. 2009).

In Stratoni higher concentrations of N, P, Mg, Cu and Fe were found in foliage of *P. pinaster*, as well as higher concentrations of N, P and Zn were found in foliage of *P. radiata*. P and N-absorption by trees is an important growth factor for both coniferous species that seems to be better in Stratoni. Phosphorus and nitrogen concentrations in needles found in Sithonia for both conifers are below the reported marginal level and below the values commonly observed in other *Pinus pinaster* and *Pinus radiata* stands that are known to be nutrient limited. However, phosphorus concentrations in needles found in Stratoni for *P. radiata* were also below the critical levels according to the literature (Will 1985, Zas 2003, Zas and Serrada 2003, Warren et al. 2005, Martins et al. 2009).

The results show low phosphorus content in soil of both areas, mainly in Sithonia, that is an aggravating factor for the growth of both conifers.

Conclusions

All measured dendrometric variables for both conifers are greater in Stratoni. Comparing the two areas, the highest nutrient content in soil, litter and needles for both conifers was found in Stratoni. The greatest differences were observed at shallow soils (0–10 cm) for most nutrients. Consequently, Stratoni seems to be more suitable area for both conifers and this is clearer for *Pinus pinaster*. The phosphorus content in litter, foliage and soil at all depths is higher in Stratoni for *Pinus pinaster*, however, there is a phosphorus deficit concerning both areas. The results show that nutrient content in litter, soil and foliage found mainly in Stratoni, does not appear to be prohibitive for both conifers, but certainly, given a lack of phosphorus, has nothing to do with data from high-productivity forests. The results contribute to the planning of appropriate forest management for both areas, considering the prospect of preserving or replacing both conifer species.

References

Aerts R. 1997. Climate, Leaf Litter Chemistry and Leaf Litter Decomposition in Terrestrial Ecosystems: A Triangular Relationship. Oikos 79(3): 439–449. https://doi.

org/10.2307/3546886

Alía R., Moro J., Denis J.B. 1997. Performance of Pinus pinaster provenances in Spain: Interpretation of the genotype by environment interaction. Canadian Journal of Forest Research 27(10): 1548–1559. https://doi.org/10.1139/X97-122

Allen S.E., Grimshaw H.M., Rowland A.P. 1986. Chemical analysis. In: Moore P.D., Chapman S.B. (Eds), Methods in Plant Ecology. 2nd Ed. Oxford, London, Blackwell Scientific Publications: 285–344.

Arias-Rodil M., Diéguez-Aranda U., Rodríguez Puerta F., López-Sánchez C.A., Canga Líbano E., Cámara Obregón A., Castedo-Dorado F. 2015. Modelling and localizing a stem taper function for *Pinus radiata* in Spain. Canadian Journal of Forest Research 45(6): 647–658. https://doi.org/10.1139/cjfr-2014-0276

Bai Z., Li H., Yang X., Zhou B., Shi X., Wang B., Li D., Shen J., Chen Q., Qin W., Oenema O., Zhang F. 2013. The critical soil P levels for crop yield, soil fertility and environmental safety in different soil types. Plant Soil 372(1–2): 27–37. doi: 10.1007/s11104-013-1696-y

Binkley D., Giardina C. 1998. Why do tree species affect soils? The Warp and Woof of tree soil interactions. Biogeochemistry 42: 89–106. https://doi.org/10.1023/A:1005948126251

Brant J.B., Myrold D.D., Sulzman E.W. 2006. Root controls on soil microbial community structure in forest soils. Oecologia 148(4): 650–659. https://www.jstor.org/stable/20445954

Butcher T.B. 1977. Impact of moisture relationships on the management of *Pinus pinaster* Ait. Plantations in Western Australia. Forest Ecology and Management 1: 97–107. https://doi.org/10.1016/0378-1127(76)90014-1

Chatzistathis A. 1980. Causes for the inadequacy of reforestation under extreme ecological conditions in Halkidiki. The forest magazine 90(October–December): 59–66 (in Greek).

Devi A.S., Yadava P.S. 2007. Wood and leaf litter decomposition of Dipterocarpus tuberculatus Roxb. In a tropical deciduous forest of Manipur, North East India. Current Science 93(2): 243–246. http://www.jstor.org/stable/24099313

Dobbertin M., Neumann M., Schroeck H.-W. 2013. Chapter 10 – Tree Growth Measurements in Long-Term Forest Monitoring in Europe. Developments in Environmental Science 12: 183–204. https://doi.org/10.1016/B978-0-08-098222-9.00010-8

Ferreira-Santos P., Genisheva Z., Botelho C., Santos J., Ramos C., Teixeira J.A., A. Rocha C.M.R. 2020. Unravelling the Biological Potential of *Pinus pinaster* Bark Extracts. Antioxidants 9(4), 334. https://doi.org/10.3390/antiox9040334

Grant E.G. 1982. Exchangeable cations. In: Page A.L. (Ed.), Methods of Soil Analysis. Part 2. Chemical and Microbiological Properties. 2nd Ed. Madison, American Society of Agronomy, Soil Science Society of America: 159–164.

Hermoso E., Carballo J., Fernandez-Golfin J.I. 2007. Structural characterization of *Pinus radiata* D.Don timber from Pais Vasco (Spain) according to standard modifications. Maderas, Ciencia y Tecnologia 9(3): 223–232. http://dx.doi.org/10.4067/S0718-221X2007000300003

Hinsinger P. 2001. Bioavailability of soil inorganic P in the rhizosphere as affected by root-induced chemical changes:a review. Plant Soil 237(2): 173–195. doi: 10.1023/A:1013351617532

Hopmans P., Elms S.R. 2009. Changes in total carbon and nutrients is soil profiles and accumulation in biomass after 30-year rotation of *Pinus radiata* on podzolized sands: Impacts of intensive harvesting on soil resources. Forest Ecology and Management 258(10): 2183–2193. https://doi.org/10.1016/j.foreco.2009.02.010

Howitt D., Cramer D. 2001. SPSS 10 Statistics for Windows. Athens, Cleidarithmos Publications. 288 p. (in Greek).

ISSS Working Group RB 1998a. World Reference Base for Soil Resources. Deckers J.A, Nachtergaele F.O, Spaargaren O.C. (Eds), Introduction. First edition. ISSS/ISRIC/FAO. Acco Leuven.

ISSS Working Group RB 1998b. World Reference Base for Soil Resources. Bridges E.M., Batjes N.H., Nachtergaele F.O (Eds), Atlas. First edition. ISSS/ISRIC/FAO. Acco Leuven.

Knicker H., Gonzalez-Vila F.J., Polvillo O., Gonzalez J.A., Almendros G. 2005. Fire-induced transformation of C- and N-forms in different organic soil fractions from a Dystric Cambisol under a Mediterranean pine forest (*Pinus pinaster*). Soil Biology & Biochemistry 37(4): 701–718 https://doi.org/10.1016/j.soilbio.2004.09.008

Krishna M.P., Mahesh M. 2017. Litter decomposition in forest ecosystems: a review. Energy, Ecology and Environment 2(4): 236–249. doi: 10.1007/S40974-017-0064-9

Kurz C., Couteaux M.M., Thiery J.M. 2000. Residence time and decomposition rate of *Pinus pinaster* needles. Soil Biology & Biochemistry 32(8–9): 1197–1206. https://doi.org/10.1016/S0038-0717(00)00036-5

Lindsay W.L., Norvell W.A. 1978. Development of a DTPA soil test for zinc, iron, manganese, and copper. Soil Science Society of America Journal 42(3): 421–428. https://doi.org/10.2136/sssaj1978.03615995004200030009x

Martins P., Sampedro L., Moreira X., Zas R. 2009. Nutritional status and genetic variation in the response to nutrient availability in *Pinus pinaster*. A multisite field study in Northwest Spain. Forest Ecology and Management 258(7): 1429–1436. https://doi.org/10.1016/j.foreco.2009.06.041

Merino A., Edeso J.M. 1999. Soil fertility rehabilitation in young *Pinus radiata* D.Don plantations from northern Spain after intensive site preparation. Forest Ecology and Management 116(1–3): 83–91. https://doi.org/10.1016/S0378-1127(98)00444-7

Nakos G. 1978. The problem of the chlorosis of *Pinus radiata*. Ministry of Agriculture, Directorate-General for Forests and Forest Environment. Athens Forest Research Foundation: 15–20 (in Greek).

Ogana F.N., Corral-Rivas S., Gorgoso-Varela J.J. 2020. Nonlinear mixed-effect height-diameter model for *Pinus pinaster* Ait. and *Pinus radiata* D.Don. CERNE 26(1): 150–161. https://doi.org/10.1590/01047760202026012695

Olsen S.R., Sommers L.E. 1982. Phosphorus. In: Page A.L. (Ed.), Methods of Soil Analysis. Part 2. Chemical and Microbiological Properties. 2nd ed. Madison, American Society of Agronomy, Soil Science Society of America: 403–427.

Papamichos N.Th., Alifragkis D.A. 1980. Damage of the reforestations of Polygyros, Halkidiki, from the drought. Scientific Yearbook Agriculture, and Forestry Faculty of A.U.Th., volume CG(4): 76–106 (in Greek).

Patzel N., Sticher H., Karlen D.L. 2000. Soil Fertility – Phenomenon and Concept. Journal of Plant Nutrition and Soil Science 163(2): 129–142. doi: 10.1002/(SICI)1522-2624(200004)163:2<129::AID-JPLN129>3.0.CO;2-D

Richardson D.M., Rundel P.W. 1998. Ecology and Biogeography of *Pinus*: An introduction. In: Richardson D.M. (Ed.), Ecology and Biogeography of *Pinus*. Cambridge Univercity Press, Cambridge: 3–46.

Romanyà J., Vallojo V.R. 2004. Productivity of *Pinus radiata* plantations in Spain response to climate and soil. Forest Ecology and Management 195(1–2): 177–189. https://doi.org/10.1016/j.foreco.2004.02.045

SAS 2008. SAS/STAT® 9.2 User's Guide. SAS Institute Inc., Cary, nC, USA.

Sheriff D.W., Nambiar E.K.S., Fife D.N. 1986. Relationships between nutrient status, carbon assimilation and water use efficiency in *Pinus radiata* (D. Don) needles. Tree Physiology 2(1-2-3): 73–88. https://doi.org/10.1093/treephys/2.1-2-3.73

Smyth C.E., Macey D., Trofymow J.A. 2015. Long-term litter decay in Canadian forests and the influence of soil microbial community and soil chemistry. Soil Biology & Biochemistry 80: 250–259. doi: 10.1016/j.soilbio.2014.09.027

Staaf H., Olsson B.A. 1994. Effects of slash removal and stump harvesting on soil water chemistry in a clearcutting in SW Sweden. Scandinavian Journal of Forest Research 9(1–4): 305–310. https://doi.org/10.1080/02827589409382844

Stevenson F.J. 1982. Nitrogen-organic forms.

In: Page A.L. (Ed.), Methods of Soil Analysis. Part 2. Chemical and Microbiological Properties. 2nd Ed. Madison, American Society of Agronomy, Soil Science Society of America: 625–641.

Sudmeyer R.A., Speijers J., Nicholas B.D. 2004. Root distribution of Pinus pinaster, P. radiata, Eucalyptus globulus and E. kochii and associated soil chemistry in agricultural land adjacent to tree lines. Tree physiology 24(12): 1333–1346. https://doi.org/10.1093/treephys/24.12.1333

Swift M.J., Heal O.W., Anderson J.M. 1979. Decomposition in Terrestrial Ecosystems. Studies in Ecology, vol. 5. Blackwell Scientistic Publications, Oxford. 372 p.

Turner J., Lambert M.J. 1988. Soil properties as affected by *Pinus radiata* plantations. New Zealand Journal of Forestry Science 18(1): 77–91.

Varelides C., Kritikos T. 1994. Effect of site preparation intensity and fertilization on *Pinus pinaster* survival and height growth on three sites in northern Greece. Forest Ecology and Management 73(1–3): 111–115. https://doi.org/10.1016/0378-1127(94)03495-I

Warren C.R., McGrath J.F., Adams M.A. 2005. Differential effects of N, P and K on photosynthesis and partitioning of N in Pinus pinaster needles. Annals of Forest Science 62(1): 1–8. https://doi.org/10.1051/forest:2004088

Will G.M. 1985. Nutrient deficiencies and fertiliser use in New Zealand exotic forests. Forest Research Institute, New Zealand Forest Service, Rotorua, New Zealand. FRI Bulletin No. 97. 53 p.

Zagas T.D., Ganatsas P.P. 2001. Results of a forest species trial in an Arboretum of North Greece. Silva Gandavensis 66. https://doi.org/10.21825/sg.v66i0.820

Zas R., Serrada R. 2003. Foliar nutrient status and nutritional relationship of young *Pinus radiata* D.Don plantations in northwest Spain. Elsevier. Forest Ecology and Management 174(1–3): 167–176. https://doi.org/10.1016/S0378-1127(02)00027-0

FORESTRY IDEAS, 2024, vol. 30, No 1 (67): 28–37

Plant adaptability and species diversity after coal mining reclamation in South Borneo

Hari Sutikno[1], Syarifuddin Kadir[2], Hafizianor[2], and Yusanto Nugroho[2*]

[1]Graduate School of Agriculture, Lambung Mangkurat University, Banjarmasin, Indonesia.
[2]Faculty of Forestry, Lambung Mangkurat University, Banjarbaru, Indonesia.
[*]E-mail: ynugrohoulm@gmail.com

Received: 19 October 2023 / Accepted: 04 January 2024 / Available online: 15 January 2024

Open Access: This article is licensed under a Creative Commons Attribution 4.0 International License.

Abstract

Reclamation is an important activity to support ecosystem recovery after mine closure. The success of this effort depends on plant adaptability to environmental pressure, primarily related to high-acidity soil. However, more information about plant adaptability in reclamation sites is needed, although it is required to determine the alternative species for supporting revegetation efforts. Our study investigated the adaptability of multiple tree species used for coal mining reclamation and assessed their essential role in enhancing biodiversity in the degraded ecosystem. An ecological survey was conducted using a transect line method with a sampling plot size of 20×20 m and an interval from each 50 m. This study found that seven species were used to support the reclamation efforts, i.e., *Aleurites moluccana*, *Archindendron pauciflorum*, *Artocarpus heterophyllus*, *A. integer*, *Durio zibethinus*, *Hevea brasiliensis*, and *Mangifera casturi*. The survival across species was 78.60−89.39 %, with a height of 64.75−133.94 cm and a diameter of 0.59−1.39 cm. The species diversity was low, with a richness of 0.98 and a heterogeneity of 0.84. These species also had an unbalanced distribution pattern with an evenness index of 0.43. These findings showed that the selected plant species had good adaptability to the environmental conditions of the reclamation site. Although their contribution to biodiversity improvement was still low, there was a positive contribution from these species to biodiversity recovery after the mine closure. Further investigation is still required to monitor the long-term benefits of these species on ecosystem recovery in the reclamation area.

Key words: biodiversity, degraded ecosystem, environmental pressure, mine closure, revegetation.

Introduction

Coal mining is one of Indonesia's most important industries contributing to the gross domestic product (Nugroho et al. 2022, Supandi et al. 2023). However, it also has negative impacts on the environment in the future. Coal mining exploitation using an open-cut system changes the landscape (Nugroho et al. 2021), increases runoff and erosion (Jiang et al. 2022), reduces biodiversity (Sasaki et al. 2015), and causes soil contamination (Mourinha et al. 2022). This circumstance

creates degraded land after mine closure (Worlanyo and Jiangfeng 2021). To minimize the impact, reclamation effort is necessary to support land recovery. It is conducted by closing mining holes, returning soil, and establishing vegetation (Buta et al. 2019). This effort is expected to accelerate vegetation succession and minimize land degradation in the following periods.

Nevertheless, coal mining reclamation takes work and time to implement. This effort has many challenges, primarily related to soil characteristics. After the mine closure, the soil had high acidity and contained heavy metals due to the impact of chemical contamination (Li et al. 2018). This stimulates the high mortality of plants during coal mining reclamation. Soil with high acidity causes Al toxicity, inhibiting root growth and development (Hajiboland et al. 2022). At the same time, the excessive content of heavy metals is also toxic for plants (Chibuike and Obiora 2014). Consequently, the plant cannot grow well and has a high mortality risk. To tackle these constraints, selecting adaptive plant species is necessary to support coal mining reclamation (Stojnić et al. 2021). It can be conducted by planting several species to evaluate their adaptability in the reclamation area.

Until now, many reclamation activities have been implemented by coal mining managers. One of them is PT Borneo Indobara (BIB), a coal mining enterprise that has a concession area in South Borneo. BIB has conducted reclamation effort in its site by establishing several plant species. Unfortunately, information about adaptive plant species for coal mining reclamation in this area is rarely published, although it is required as basis information to support mining reclamation in the future. On another side, the current challenge of coal mining reclamation in BIB is not only about revegetation but also should consider biodiversity conservation through reclamation. Coal mining exploration with open-pit systems causes biodiversity loss, especially for native species. These plants have low natural regeneration; thus, artificial regeneration is required to conserve them. In this context, the result of the reclamation can also accelerate biodiversity recovery, primarily related to local species from the reclamation area (Trimanto and Shofiah 2018). Considering these explanations, there are two critical questions related to the reclamation effort in this site:

1. What kind of alternative plant species can facilitate coal mining reclamation?
2. How is the contribution of these species in recovering biodiversity at the reclamation site?

In order to address those questions, this study aims to evaluate the adaptability of multiple tree species used for coal mining reclamation and to assess their essential role in improving biodiversity. Results will deliver sufficient information for BIB managers related to the list of adaptive plant species for reclamation and their contribution to biodiversity recovery in the land.

Material and Methods

Study area

This study was conducted in a coal mining reclamation site managed by PT Borneo Indobara with a size of 6 ha. This area is part of the Riam Kanan Watershed in Artain Village, Banjar District, South Borneo. The study site has geographic coordinates 114°55’−115°15’ E and 3°21’−3°40’ S. It is situated in the lowland with topography predominantly hilly areas. Annual rainfall

ranges from 2000 to 3000 mm·yr^{-1} over the last ten years. The highest rainfall is recorded in December, while the lowest is in May. Dry periods occur for five months, from June to October. The average daily temperature is 25 °C with a minimum of 19 °C and a maximum of 35 °C. The reclamation effort on this site was conducted in 2020 by planting several alternative species in an open area. These species were planted by a spacing of 3×3 m. However, species distribution was irregular and not arranged in zonation.

Data collection

A field survey was undertaken by a systematic sampling method with a sampling intensity of 5%. The entire sampling plot in this study reached 40 units. The shape of each plot was square, with a size of 20×20 m (Alam et al. 2022). The plot was distributed systematically with a distance between plots of 50 m (Sadono et al. 2020b). It was expected to cover the variation of vegetation from the reclamation area.

Several parameters were recorded from each plot, i.e. species name, number of species, plant height, and plant diameter. The plants' name was determined using the guidance of plant species identification in the tropics (Suyanto et al. 2022). Plant height was measured using a pole from aboveground to the top crown (Wirabuana et al. 2021a). The measurement of plant diameter was undertaken by a caliper at 30 cm from aboveground (Wirabuana et al. 2019). It was conducted since most plants in the reclamation site were still categorised into seedlings and saplings although it has been 3 years post-reclamation.

In parallel, soil samples were also collected in every sampling plot at a depth of 0−10 cm (Nugroho et al. 2022). These samples were composited and brought to the laboratory for quality analysis. Six attributes were used to quantify the soil quality, namely soil acidity (pH H_2O), soil organic carbon (SOC), total nitrogen (TN), total phosphorus (TP), total potassium (TK), and cation exchange capacity (CEC) (Alam et al. 2022). Soil pH was determined using a pH meter while SOC was quantified using the Walkley−Black method. TN was analysed using Kjeldahl method. The ammonium acetate NH_4OAc 1 M, pH 7.0 extraction was applied to determine TK while for TP, Bray method was used. The ammonium acetate method was used to quantify the CEC. Soil analysis protocols were conducted following Estefan et al. (2013).

Data analysis

Three indicators were used to evaluate the adaptability of plant species in the study site: survival rate, average height, and average diameter. The survival rate for each species was calculated as the ratio between actual plant density and the initial planting density and is stated in percentage units (Wirabuana et al. 2021a). Meanwhile, the average height and diameter were computed based on the arithmetic mean of plant dimensions from every species (Wirabuana et al. 2022). The equations (1, 2 and 3) for quantifying those parameters are presented below:

$$SR = \frac{AD}{ID} \cdot 100, \quad (1)$$

$$H = \frac{h_1 + h_2 + h_3 + ...}{n}, \quad (2)$$

$$D = \frac{d_1 + d_2 + d_3 + ...}{n}, \quad (3)$$

where: *SR* is survival rate, %; *AD* is actual

species density; *ID* is initial planting density; *n* is the number of species abundance; *H* indicates average plant height, m; *D* is average plant diameter, cm; $h_{1,2,3}$,… are the heights of plants, m; and $d_{1,2,3,}$… indicate diameters of plants, cm.

The important value index (IVI) was also calculated to assess the essential role of each species in improving biodiversity in the reclamation site. It is an indicator commonly used in ecological studies to understand the bargaining position of certain species in communities (Matatula et al. 2021). This parameter was computed by summing the relative density and frequency owned by certain species (Sadono et al. 2020a). Only two parameters were considered for counting IVI because the size of plant species was in seedling and sapling stage (Purwanto et al. 2022). Detail equations (4, 5 and 6) for quantifying IVI are expressed below:

$$RD = \frac{SD}{TPD} \cdot 100, \quad (4)$$

$$RF = \frac{SF}{TF} \cdot 100, \quad (5)$$

$$IVI = RD + RF, \quad (6)$$

where: *RD* is relative density, *SD* indicates species density, *TPD* shows total population density, *RF* is relative frequency, *SF* is species frequency, and *TF* is total frequency.

In addition, the diversity of vegetation resulting from reclamation activity was also evaluated using three parameters, i.e. richness, heterogeneity, and evenness (Suyanto et al. 2022). The information is important and required to assess the effectiveness of the reclamation effort to facilitate biodiversity recovery in the long term. Vegetation richness was calculated by Margalef Index (R_1) (Singh 2020), while the heterogeneity of vegetation was assessed by the Shannon-Wienner Index (*H'*) (Naidu and Kumar 2016). The evenness of vegetation was counted using Pielou-Evenness Index (*J*) (Wirabuana et al. 2021b). The detailed equations (7, 8 and 9) for calculating those indicators are shown below:

$$R1 = \frac{S-1}{\ln(N)}, \quad (7)$$

$$H' = -\sum \frac{n_i}{N} \cdot \ln \frac{n_i}{N}, \quad (8)$$

$$J = \frac{H'}{\ln(S)}, \quad (9)$$

where: *S* is the number of species, *N* represents the total plant population, n_i describes the sum of plants from each species.

Results and Discussion

Soil characteristics

Results found that the soil in this site had high acidity with pH = 4.69 (Table 1). It also had low nutrient content like N (0.13 %), P (11.38 mg·100 g^{-1}), and K (10.49 mg·100 g^{-1}). The circumstance was similar to the common post-mining area with low fertility and extreme acidity (Li et al. 2018). However, our study also noted that there were moderate concentrations of SOC (2.40 %) and CEC (24.13 cmolc(+)·kg^{-1}). The coal mining manager added compost as organic matter into the soil during the revegetation process. This effort aimed to provide a better soil condition for establishing plant species.

Organic matter naturally contains nutrients, primarily C as its main component (Alam et al. 2022). When decomposition occurs, these nutrients would release into the soil and increase plant nutrient availability (Nugroho et al. 2022). In the context

Table 1. Soil characteristics in the reclamation site

Soil parameters	Unit	min	max	Mean	Categories
pH H_2O	-	3.86	5.29	4.69	acid
C-organic	%	1.50	3.03	2.40	moderate
N-total	%	0.07	0.17	0.13	low
P_2O_5	mg·100 g^{-1}	3.43	22.45	11.38	low
K_2O	mg·100 g^{-1}	1.11	26.10	10.48	low
CEC	cmolc(+)· kg^{-1}	19.38	30.39	24.13	moderate

Note: soil attributes classification is determined based on Nandini and Narendra (2012).

of reclamation, adding organic matter can also decrease the absorption of heavy metals by plants since the materials form complex compound and made them immobile (Egli et al. 2010). Supplying organic matter into the soil can also improve soil structure and aggregation (Purwanto and Alam 2020). Therefore, this strategy generally used by mining managers as a site preparation before conducting revegetation.

Plant adaptability

Seven alternative plants supported mining reclamation in this site, i.e. *Artocarpus heterophyllus* Lam., *Artocarpus integer* Merr., *Aleurites moluccana* (L.) Willd., *Mangifera casturi* Kosterm., *Archidendron pauciflorum* (Benth.) I.C.Nielsen, *Durio zibethinus* L., and *Hevea brasiliensis* Müll.Arg. (Table 2). All species exhibited good adaptability with a higher than 70 % survival rate. This finding was relatively similar to another study about the survival rate of plants in the reclamation area by approximately 70−80 % (Adman et al. 2020).

Many studies reported that plant survival was the main challenge of coal mining reclamation since the environmental conditions in post-mining areas had many constraints to facilitate species establishment (Maiti et al. 2007, Kuter et al. 2014, Lestari et al. 2019). Besides having extreme acidity and containing heavy metals (Li et al. 2018), soil mining also had low nutrient availability (Forján et al. 2019). It stimulated plant stress that caused mortality. However, several plant species could survive in this condition. These species naturally could tolerate this environment, but they would result in lower growth performance (Kuter et al. 2014). It directly confirmed why the plant dimension in the study site was still small, although they had been planted for two years.

This study reported that the highest

Table 2. Characteristics of plant species used for supporting mining reclamation.

Species	Survival, %	Height, cm	Diameter, cm
Aleurites moluccana	82.25 ±3.47	81.67 ±7.03	0.80 ±0.13
Archindendron pauciflorum	79.87 ±1.08	133.94 ±17.28	1.39 ±0.17
Artocarpus heterophyllus	81.70 ±2.92	69.82 ±6.26	0.59 ±0.10
Artocarpus integer	89.39 ±10.61	66.00 ±7.02	0.73 ±0.12
Durio zibethinus	79.39 ±0.61	64.75 ±7.62	0.65 ±0.06
Hevea brasiliensis	78.60 ±0.04	70.76 ±1.63	0.69 ±0.02
Mangifera casturi	78.97 ±0.19	77.47 ±4.34	0.99 ±0.07

mean survival rate was recorded for *A. integer* (89.39 ±10.61 %), while the lowest was noted for *H. brasiliensis* (78.60 ±0.04 %). It indicated that *A. integer* was the most adaptive species in the study site. Other literature data also supported that this species could grow well in very acid soil with full sun conditions (Morris 1997). It was similar to the environment in the post-mining area, dominated by bare land with high soil acidity.

Interestingly, this study noted that *A. pauciflorum* demonstrated the highest mean in height and diameter by 133.94 ±17.28 cm and 1.39 ±0.17 cm, respectively. It is indicated that this plant species could absorb water and nutrients more efficiently than other species. Higher resource absorption in plants naturally optimises their metabolism process (Yang et al. 2015). Thus, the plant has a better opportunity to grow and generate more excellent dimensions.

Species diversity

A total of six families were identified from the seven plant species in the study site (Table 3), wherein most alternative species were from Moraceae (2). According to the IUCN status, most plants were classified as Least Concern, except for *M. casturi*, which was grouped into Extinct (Table 4). Surprisingly, this study recorded that *H. brasiliensis* became the most abundant species in the study site. It also had the highest important value index (132.36) since this species showed the first rank in relative density and relative frequency (Table 4). This finding indicated

Table 3. Family categories, IUCN status, and frequency appearance of selected species for mining reclamation.

Family	Species	IUCN status	Frequency
Euphorbiaceae	*Aleurites moluccana*	Least Concern	rare
Fabaceae	*Archindendron pauciflorum*	Least Concern	rare
Moraceae	*Artocarpus heterophyllus*	Least Concern	rare
Moraceae	*Artocarpus integer*	Least Concern	rare
Malvaceae	*Durio zibethinus*	Least Concern	rare
Euphorbiaceae	*Hevea brasiliensis*	Least Concern	abundant
Anacardiaceae	*Mangifera casturi*	Extinct	rare

Table 4. Relative density, relative frequency, and important value index of every plant species.

Species	RD	RF	IVI
Aleurites moluccana	1.32	4.00	5.32
Archindendron pauciflorum	3.75	12.00	15.75
Artocarpus heterophyllus	2.43	8.00	10.43
Artocarpus integer	0.66	1.33	2.00
Durio zibethinus	4.42	9.33	13.75
Hevea brasiliensis	79.03	53.33	132.36
Mangifera casturi	8.39	12.00	20.39
Grand total	100	100	200

Note: *RD* is relative density, *RF* is relative frequency, IVI is important value index.

that *H. brasiliensis* became the most important species for supporting biodiversity recovery in the reclamation site, although this species only occupied the last stage of survival rate (Table 2).

H. brasiliensis could become the most abundant species because it was commonly used by local people on this site. In this case, establishing this species would attract the community to participate in reclamation efforts. Nevertheless, this strategy also affected the vegetation structure in the reclamation site, mainly related to the diversity level. According to the results, vegetation diversity in this site was classified into a low level of richness, heterogeneity, and evenness (Table 5). It could happen since the vegetation resulted from artificial regeneration with a planting design (Nugroho et al. 2021). This statement was supported by the value of the evenness index, which was categorised into an unbalanced distribution (Hussain et al. 2012).

Nevertheless, the reclamation activity still had a positive outcome since it could improve the biodiversity of the plants after the mine closure. Several studies also noted that the biodiversity recovery in the reclamation area occurred step by step over a long-term period (Al-Reza et al. 2016, Pauletto et al. 2016, Lestari et al. 2019, Kuzevic et al. 2022). In this case, the presence of plant species could help a succession process and minimize the risk of degradation.

Table 5. Richness, heterogeneity, and evenness of vegetation communities in the reclamation site.

Parameter	Indices	Value	Categories
Richness	Margalef	0.98	Disturbed
Heterogeneity	Shannon-Wiener	0.84	Bad
Evenness	Pielou	0.43	Unbalanced

Note: the classification of value is determined based on Hussain et al. (2012).

Conclusion

All selected species indicated good adaptability to the environmental conditions in the reclamation site. However, *Artocarpus integer* showed the highest average survival rate than other alternative plant species. *A. integer* became the most adaptive species in the study site. This study revealed that *Hevea brasiliensis* contributed the highest to improving biodiversity in this location. Although the vegetation diversity was low, the reclamation effort showed a prospective outcome to facilitate biodiversity recovery after mine closure. As it is well known, coal mining exploration using open-pit systems has caused biodiversity loss and provided extreme environmental conditions after post-mining. Therefore, only a few species can survive in this condition. In this case, our outcome has delivered important information on what kind of adaptive species to support the reclamation effort in this site.

Acknowledgements

The authors deliver their appreciation to PT Borneo Indobara, which allowed and permitted this study in its concession site. Gratitude is also addressed to the anonymous surveyor team survey, who supported data collection.

References

Adman B., Nugroho A.W., Yassir I. 2020. The growth of local tree species in post-coal mining areas in East Kalimantan. Indonesian Journal of Forestry Research 7(2): 83–97. http://dx.doi.org/10.20886/ijfr.2020.7.2.83-97

Alam S., Ginting S., Hemon M.T., Leomo S., Kilowasid L.M.H., Karim J., Nugroho Y., Matatula J., Wirabuana P.Y.A.P. 2022. Influence of land cover types on soil quality and carbon storage in Moramo Education Estate, Southeast Sulawesi, Indonesia. Biodiversitas 23(9): 4371–4376. https://doi.org/10.13057/biodiv/d230901

Al-Reza D.D., Prasetyo L.B., Hermawan R. 2016. Biodiversity of plants and birds in reclamation area of PT Bukit Asam, Muara Enim, South Sumatera. Journal of Tropical Forest Management 22(3): 158–168. doi: 10.7226/jtfm.22.3.158

Buta M., Blaga G., Paulette L., Păcurar I., Roşca S., Borsai O., Grecu F., Sînziana P.E., Negruşier C. 2019. Soil Reclamation of Abandoned Mine Lands by Revegetation in Northwestern Part of Transylvania: A 40-Year Retrospective Study. Sustainability 11(12): 1–18. https://doi.org/10.3390/su11123393

Chibuike G.U., Obiora S.C. 2014. Heavy Metal Polluted Soils: Effect on Plants and Bioremediation Methods. Applied and Environmental Soil Science 1, 752708. 12 p. http://dx.doi.org/10.1155/2014/752708

Egli M., Sartori G., Mirabella A., Giaccai D., Favilli F., Scherrer D., Krebs R., Delbos E. 2010. The influence of weathering and organic matter on heavy metals lability in silicatic, Alpine soils. Science and Total Environment 408(4): 931–946. https://doi.org/10.1016/j.scitotenv.2009.10.005

Estefan G., Sommer R., Ryan J. 2013. Methods of soil, plant, and water analysis. International Center for Agriculture Research in the Dry Areas. Third edition, Beirut, Lebanon. 243 p.

Forján R., Rodríguez-Vila A., Covelo E.F. 2019. Increasing the Nutrient Content in a Mine Soil Through the Application of Technosol and Biochar and Grown with *Brassica juncea* L. Waste and Biomass Valorization 10: 103–119. https://doi.org/10.1007/s12649-017-0027-6

Hajiboland R., Panda C.K., Lastochkina O., Gavassi M.A., Habermann G., Pereira J.F. 2022. Aluminum Toxicity in Plants: Present and Future. Journal of Plant Growth Regulation 42: 3967–3999, 256772637. doi: 10.1007/s00344-022-10866-0

Hussain N.A., Ali A.H., Lazem L.F. 2012. Ecological indices of key biological groups in Southern Iraqi marshland during 2005–2007. Mesopotamian Journal of Marine Science 27(2): 112–125. https://doi.org/10.58629/mjms.v27i2.162

Jiang H., Fan G., Zhang D., Zhang S., Fan Y. 2022. Evaluation of eco-environmental quality for the coal-mining region using multi-source data. Scientific Reports 12(1), 6623. 19 p. doi: 10.1038/s41598-022-09795-5

Kuter N., Dilaver Z., Gül E. 2014. Determination of suitable plant species for reclamation at an abandoned coal mine area. International Journal of Mining, Reclamation and Environment 28(5): 268–276. https://doi.org/10.1080/17480930.2014.932940

Kuzevic S., Bobikova D., Kuzevicova Z. 2022. Land Cover and Vegetation Coverage Changes in the Mining Area – A Case Study from Slovakia. Sustainability 14(3), 1180. 14 p. https://doi.org/10.3390/su14031180

Lestari D.A., Fiqa A.P., Fauziah, Budiharta S. 2019. Growth evaluation of native tree species planted on post-coal mining reclamation site in East Kalimantan, Indonesia. Biodiversitas 20(1): 134–143. https://doi.org/10.13057/biodiv/d200116

Li F., Li X., Hou L., Shao A. 2018. Impact of the Coal Mining on the Spatial Distribution of Potentially Toxic Metals in Farmland Tillage Soil. Scientific Reports 8, 14925. 10 p. https://doi.org/10.1038/s41598-018-33132-4

Maiti S.K., Shee C., Ghose M.K. 2007. Selection of plant species for the reclamation of mine-degraded land in the Indian con-

text. Land Contamination and Reclamation 15(1): 55–65. doi: 10.2462/09670513.690

Matatula J., Afandi A.Y., Wirabuana P.Y.A.P. 2021. Short communication: A comparison of stand structure, species diversity, and aboveground biomass between natural and planted mangroves in Sikka, East Nusa Tenggara, Indonesia. Biodiversitas 22(3): 1098–1103. https://doi.org/10.13057/biodiv/d220303

Morris R. 1997. *Artocarpus integer*. Plants for a Future. https://pfaf.org/user/Plant.aspx?LatinName=Artocarpus_integer

Mourinha C., Palma P., Alexandre C., Cruz N., Rodrigues S.M., Alvarenga P. 2022. Potentially Toxic Elements' Contamination of Soils Affected by Mining Activities in the Portuguese Sector of the Iberian Pyrite Belt and Optional Remediation Actions: A Review. Environments 9(1), 11. 35 p. https://doi.org/10.3390/environments9010011

Naidu M.T., Kumar O.A. 2016. Tree diversity, stand structure, and community composition of tropical forests in Eastern Ghats of Andhra Pradesh, India. Journal of Asia-Pacific Biodiversity 9(3): 328–334. https://doi.org/10.1016/j.japb.2016.03.019

Nandini R., Narendra B.H. 2017. Critical land characteristics of former eruption of Mount Batur in Bangli District, Bali. Jurnal Penelitian Hutan Dan Konservasi Alam 9(3): 199–211 (in Indonesian). doi: 10.20886/jphka.2012.9.3.199-211

Nugroho Y., Supandi, Suyanto, Matatula J., Wirabuana P.Y.A.P. 2021. Influence of understorey diversity on wildlife at the coal mining reclamation area in south Kalimantan, Indonesia. Biodiversitas 22(9): 3736–3742. https://doi.org/10.13057/biodiv/d220917

Nugroho Y., Suyanto, Rudy G.S., Supandi, Saputra Y.H.E., Alam S., Matatula J., Wirabuana P.Y.A.P. 2022. A comparison of soil characteristics from four land covers around a coal mining concession area in South Kalimantan. Journal of Degraded and Mining Lands Management 10(1): 3883–3888. doi: 10.15243/jdmlm.2022.101.3883

Pauletto E.A., Stumpf L., Pinto L.F.S., da Silva T.S., Ambus J.V., Garcia G.F., Dutra Junior L.A., Scheunemann T., Albert R.P. 2016. Reclamation of a degraded coal-mining area with perennial cover crops. Revista Brasileira de Ciência do Solo 40, e0150482. https://doi.org/10.1590/18069657rbcs20150482

Purwanto B.H., Alam S. 2020. Impact of intensive agricultural management on carbon and nitrogen dynamics in the humid tropics. Soil Science and Plant Nutrition 66(1): 50–59. https://doi.org/10.1080/00380768.2019.1705182

Purwanto R.H., Mulyana B., Satria R.A., Yasin E.H.E., Putra I.S.R., Putra A.D. 2022. Spatial distribution of mangrove vegetation species, salinity, and mud thickness in mangrove forest in Pangarengan, Cirebon, Indonesia. Biodiversitas 23(3): 1383–1391. https://doi.org/10.13057/biodiv/d230324

Sadono R., Soeprijadi D., Susanti A., Wirabuana P.Y.A.P, Matatula J. 2020a. Short communication: Species composition and growth performance of mangrove forest at the coast of tanah merah, East Nusa Tenggara, Indonesia. Biodiversitas 21(12): 5800–5804. https://doi.org/10.13057/biodiv/d211242

Sadono R., Wardhana W., Wirabuana P.Y.A.P., Idris F. 2020b. Productivity evaluation of *Eucalyptus urophylla* plantation established in dryland ecosystems, East Nusa Tenggara. Journal of Degraded and Mining Lands Management 8(1): 2502–2458. https://doi.org/10.15243/jdmlm.2020.081.2461

Sasaki K., Lesbarreres D., Watson G., Litzgus J. 2015. Mining-caused changes to habitat structure affect amphibian and reptile population ecology more than metal pollution. Ecological Application 25(8): 2240–2254. https://doi.org/10.1890/14-1418.1

Singh J.K. 2020. Structural characteristics of mangrove forest in different coastal habitats of Gulf of Khambhat arid region of Gujarat, west coast of India. Heliyon 6(8): e04685. https://doi.org/10.1016/j.heliyon.2020.e04685

Stojnić S., Bojović M., Pilipović A., Or-

LOVIĆ S. 2021. Selecting tree species for reclamation of coal mine tailings based on physiological parameters. Topola 208: 27–38. doi: 10.5937/topola2108027s

SUPANDI S., SAPUTRA Y.H.E., NUGROHO Y., SUYANTO S., RUDY G.S., WIRABUANA P.Y.A.P. 2023. The influence of land cover variation on soil erosion vulnerability around coal mining concession areas in South Borneo. Journal of Degraded and Mining Lands Management 10(2): 4289–4295. https://doi.org/10.15243/jdmlm.2023.102.4289

SUYANTO, NUGROHO Y., HARAHAP M.M., KUSUMANINGRUM L., WIRABUANA P.Y.A.P. 2022. Spatial distribution of vegetation diversity, timber production, and carbon storage in secondary tropical rainforest at South Kalimantan, Indonesia. Biodiversitas 23(12): 6147–6154. https://doi.org/10.13057/biodiv/d231208

TRIMANTO T., SHOFIAH F. 2018. Exploration of Flora Diversity and Recommending Species for Reclamation of Coal Mining with Biodiversity Concept in Besiq Bermai Forest, East Borneo. Journal of Tropical Life Science 8(2): 97–107. https://doi.org/10.11594/jtls.08.02.02

WIRABUANA P.Y.A.P., ALAM S., MATATULA J., HARAHAP M.M., NUGROHO Y., IDRIS F., MEINATA A., SEKAR D.A. 2021a. The growth, aboveground biomass, crown development, and leaf characteristics of three eucalyptus species at the initial stage of planting in Jepara, Indonesia. Biodiversitas 22(5): 2859–2869. https://doi.org/10.13057/biodiv/d220550

WIRABUANA P.Y.A.P., HENDRATI R.L., BASKOROWATI L., SUSANTO M., MASHUDI M., BUDI S.S.H., SETIADI D., SUMARDI D., ALAM S. 2022. Growth performance, biomass accumulation, and energy production in age series of clonal teak plantation. Forest Science and Technology 18(2): 67–75. https://doi.org/10.1080/21580103.2022.2063952

WIRABUANA P.Y.A.P., SADONO R., JURNIARSO S. 2019. Fertilization Effects on Early Growth, Aboveground Biomass, Carbon Storage, and Leaf Characteristics of *Eucalyptus pellita* F.Muell. in South Sumatra. Journal of Tropical Forest Management 25(3): 154–163. https://doi.org/10.7226/jtfm.25.3.154

WIRABUANA P.Y.A.P., SETIAHADI R., SADONO R., LUKITO M., MARTONO D.S. 2021b. The influence of stand density and species diversity into timber production and carbon stock in community forest. Indonesian Journal of Forestry Research 8(1): 13–22. doi: 10.20886/info.2021.8.1.13-22

WORLANYO A.S., JIANGFENG L. 2021. Evaluating the environmental and economic impact of mining for post-mined land restoration and land-use: A review. Journal of Environmental Management 279, 111623. 16 p. https://doi.org/10.1016/j.jenvman.2020.111623

YANG M., TAN L., XU Y., ZHAO Y., CHENG F., YE S., JIANG W. 2015. Effect of low pH and aluminum toxicity on the photosynthetic characteristics of different fast-growing eucalyptus vegetatively propagated clones. PLoS One 10(6), e0130963. 15 p. https://doi.org/10.1371/journal.pone.0130963

FORESTRY IDEAS, 2024, vol. 30, No 1 (67): 38–49

Analysis of water consumption in community based water service surrounding Wan Abdul Rachman Forest Park, Lampung province

Zainal Abidin[1*], Muhammad Irfan Affandi[1], Adia Nugraha[1], and Dewi Lengkana[2]

[1]Department of Agribusiness, Faculty of Agriculture, University of Lampung, Jalan Soemantri Brodjonegoro 1, Bandar Lampung, 35145, Indonesia. *E-mail: zainal.abidin@fp.unila.ac.id
[2]Department of Science Education, Faculty of Teaching and Education, University of Lampung, Jalan Soemantri Brodjonegoro 1, Bandar Lampung, 35145, Indonesia.

Received: 13 October 2023 / Accepted: 02 February 2024 / Available online: 10 February 2024

Open Access: This article is licensed under a Creative Commons Attribution 4.0 International License.

Abstract

The issue of providing clean water services is fundamental and an important part of the strategy to improve community welfare. Clean water facilities are generally provided by the government, but others are developed and managed by village communities. This research aims to: (1) analyse the supply and consumption of clean water in communities around Wan Abdul Rahman Forest Park (WARFP), (2) identify factors that determine household clean water consumption. This research employs a case study method in a community-based clean water management model around WARFP, in Gedong Tataan Sub-District, Pesawaran District. This research involved 90 households receiving clean water services. To answer objective 1, data tabulation analysis was used. To answer objective 2 multiple linear regression analysis was used. The study suggests that the clean water received by the community is very abundant, as indicated by the supply of clean water that exceeds household needs. The result also shows that: (1) the average water consumption of people in the study area *per capita* per day is 189 L with the lowest consumption being 40 L and the highest average consumption being 708 L. There are 29 respondents (32 %) who consume clean water less than the Ministry of Public Works and Housing (MPWPH) standard which is 121 L *per capita* per day. (2) Factors that influence clean water consumption are water supply, and household revenues. Number of family member and education did not have strong influence on water consumption.

Key words: clean water, consumption, multiple linear regression.

Introduction

Sufficient consumption of clean water is a basic right of society. In Sustainable Development Goals (SDGs), access to clean water along with sanitation aspects for the entire community is listed in Goal 6. (UNDP 2015). Bearing in mind that the Indonesian Government is committed to the SDGs, it is therefore mandatory for the government to fulfil them. Access to safe, clean water is a prerequisite for creating

a sustainable society so that providing access to clean water service will assist achieving that commitment (Dong et al. 2018). Clean water services also have dimensions in the context of efforts to reduce poverty because affordable clean water really helps poor communities. World Bank considered that providing affordable clean water for poor people in rural areas is strategic. The development of clean water in rural areas will encourage inclusive development (The World Bank 2019). In areas around forests, water services are part of efforts to protect water sources because local communities will protect water sources that provide the basic needs. This community-based water service potentially could fill the gap of water needs in rural area considering a lack of government support for clean water services.

A study by Ministry of Public Works and Public Housing (MPWPH) in 2016 showed that the minimum water requirement for urban communities was 121 L per day *per capita*, while survey results showed that water consumption for urban communities was 144 L per day *per capita*. The largest portion of water consumption (45 %) is for bathing (MPWPH 2017). Yet similar study for rural community has not available.

According to Indonesian National Standard or SNI (2002), the need for clean water *per capita* per day for urban communities is ranging from 150 to 250 L and the water needs of rural communities is 100 L. The water needed is for bathing, washing, drinking, hygiene, and other purposes. However, not all rural areas have been reached by the government's investment in clean water due to budget limitations and technical obstacles. As a result, the level of accessibility of village communities to affordable clean water is still not optimal. According to report of Central Bureau of Statistics (BPS 2023), the proportion of Indonesian people with clean, healthy water was only 44.5 % in 2022. This achievement is still far from other ASEAN countries achieved which reached above 91 % in 2016 (ASEAN 2017).

The Indonesian government's efforts to accelerate access to clean water for the community by encouraging Program for Provisioning Community Based Clean Water and Sanitation (PCWCBS) did not achieve optimal results and in 2021 the program was halted. One of the efforts made by the community to meet water needs is to utilize springs located in or surrounding forest area. Models like this are found quite a lot in the forests of Bukit Barisan National Park, areas around the forests of West Lampung, Tanggamus, and Pesawaran Districts, Lampung province. Community-based water management is an effort, an independent community initiative to fulfil the family's basic needs, namely water, by utilizing the resources from the environment around them (Abidin 2011). It was further explained that models like this also receive support from the government or other institutions that care about clean water services. However, the characteristics of such models have similarities, namely: (1) using local resources, (2) community initiative, (3) the organization is not uniform (some have organizations, some do not), (4) rely on community's volunteer, (5) local participation, (6) water quality not monitored regularly.

Due to the low accessibility of village communities to clean water, community efforts to obtain clean water are generally not recorded in government data. Meanwhile, clean water services that are built independently are generally not recorded. Thus, there is a problem in the form of not identifying the role of community-based

water management in meeting clean water needs as well as community access to water resources and how clean water is managed by the community.

Research on clean water provision is generally for urban or semi-urban areas. In Sidoarjo, East Java, Marsono and Nirwisaya (2020) evaluated that 2 of the 13 PCWCBS groups developed by the government were no longer operating. Meanwhile, the biggest challenge is public doubts about water quality and limited-service networks. This research was carried out in urban areas with deep well water sources. Other research in China performed by Dong et al. (2018) also focused on urban or city area. In several other studies in Indonesia, the relationship between forests and water services is starting to receive a lot of attention with various analyses used such as water and environmental services in National Park of Meru Betiri, East Java (Webliana et al. 2023). Others include (Alam and Hajawa 2007, Abidin et al. 2023) to investigate water services as environmental services in Java and Lampung. However, study on analysing water consumption of community residing nearby forest is still rare which encourages team to investigate.

According to Regional Technical Implementation Unit (RTIU) of Wan Abdul Rahman Forest Park (WARFP) (RTIU WARFP 2009, 2020), the forest park area is divided into several management blocks including: (a) the plant collection block which is used for collecting native and non-native plants; (b) protection block as an area to protect flora, animals, forest management together with the community, and (c) utilization block where community surrounding area allow to get access to the forest and obtain benefit of resources as long as keeping the forest maintained. This research was carried out in the utilization blocks, namely Wiyono and Kebagusan villages, Gedung Tataan Sub-district, Pesawaran District. This research aims to analyse: (1) community consumption of clean water and (2) factors that influence water consumption.

Object and Methods

Study area

The research was carried out in utilization block of WARFP. The research locations were in 2 villages, namely Wiyono (5°23’48.3” S, 105°08’35.3” E) and Kebagusan (5°24’18.3” S, 105°07’32.4” E) Villages, Gedung Tataan Sub-District, Pesawaran District, Lampung Province. The research was purposely selected these villages considering that the source of clean water is accessed directly from the utilisation zone area and they can represent villages located around north part of WARFP.

The site is located around 25 km west of the capital of Lampung province, Bandar Lampung city. The population of Gedung Tataan District in 2021 was 107,371 with population growth at 2.16 %, far above the national average. Population density is quite high too, namely 1106.3 people per km^2 (BPS Pesawaran District 2022). In terms of gender, male population is higher than the male one with sex ration at 107, which means that for every 100 female residents there are 107 male residents (BPS Pesawaran District 2021).

Wiyono and Kebagusan villages directly border to WARFP and have relatively large population, i.e. 14,200. The people rely on water sources from WARFP area. Wiyono Village has an area of 7 km^2 or around 7 % of the area of Gedong Tataan district. Meanwhile, Kebagusan village has

an area of around 4 km^2 or 4.12 %. Each has 8 hamlets. Respondents in Wiyono village are in 3 hamlets, namely Hamlet 5, 3 and Dam C. Meanwhile for Kebagusan village, the study was carried out in 2 hamlets, namely Hamlet 4 and 5. The following is a map of the research area.

From the map (Fig. 1), it can be seen that WARFP is on upstream of both villages.

The research was carried out from May to August 2023, which are months when rainfall is very low. Even in June-August 2023, Lampung is in a dry month and starting the El Niño of 2023.

Respondents

Respondents are households that receive clean water services and live in two research villages. The sample size was determined using the approach Isaac and Michael (1995) by formula (1):

$$n = \frac{N \cdot Z^2 \cdot \sigma^2}{N \cdot u^2 + Z^2 \cdot \sigma^2}, \quad (1)$$

where: N – population of people received water services in two villages, i.e. 250 households; n – sample size; Z is Z value at 95% confident level, i.e. Z = 1.96; σ – assumed standard deviation at 0.25; u – error estimate at 5%, i.e. u = 0.05.

With formula (1), the sample/respondent size is 77 families. However, this research increased the size of respondents to 90 respondents, spread across three clean water management groups, namely: (1) 2 independent clean water management groups in Wiyono and Kebagusan villages and (2) 1 clean water

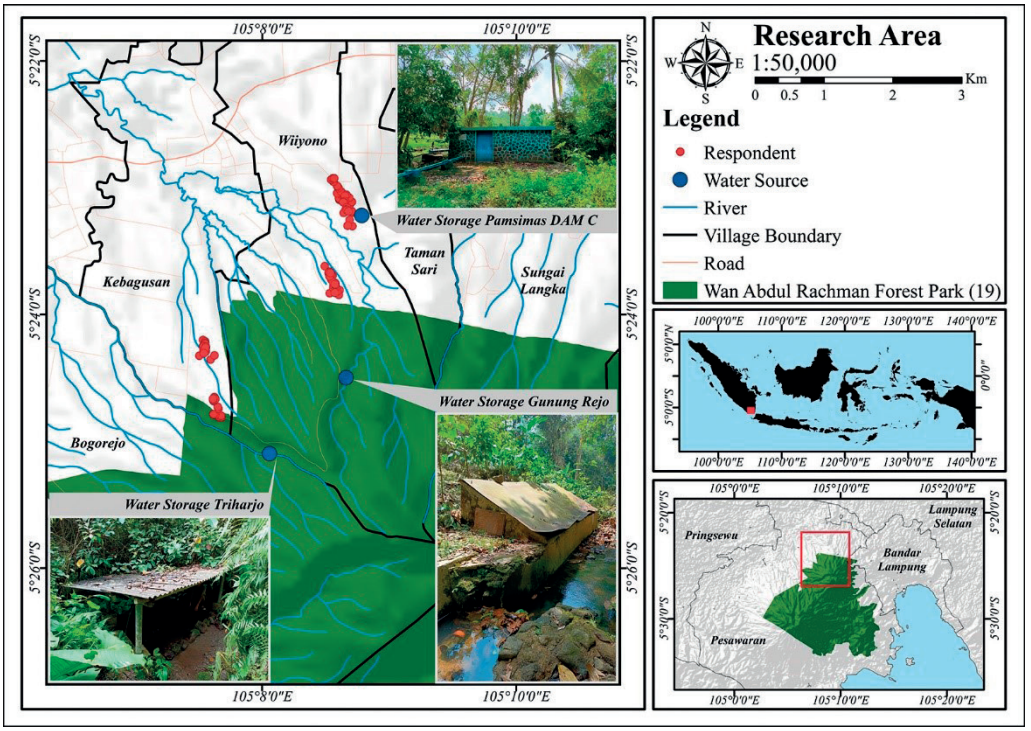


Fig. 1. Map of research site.

management group supported by Regional Company for Drinking Water (RCDW) in Dam C Hamlet of Wiyono village. Each group was represented by 30 households receiver of clean water, so in total there were 90 respondents. The use of disproportionate sampling is because assuming that respondents are relatively homogenous in terms of where they live, socio economic and social conditions.

Method of analysis

To answer objective No 1, the study employs descriptive analysis by tabulating and relating the data to benchmark data of SNI and the MPWPH. To answer objective 2, multiple linear regression analysis is used with the model equation (2) as follows (Baltagi 2008, Wooldridge 2013):

$$Y = \beta_o + \beta_1 \cdot X_1 + \ldots + \beta_n \cdot X_n + \mu, \qquad (2)$$

where: Y – average monthly water consumption, L per month; β_o – constant; β_o ... β_n – regression coefficient; μ – error term.

The variables were determined based on field observation and some researches relevant with this study. For example, a study by Fan et al. (2013) used correlation analysis for domestic consumption in rural area in China. The study suggested that water supply, age, educational attainment, household income, net family size, vegetable garden area, and solar water heater had strong correlation with water consumtion. Other relevant study done by Irianti et al. (2016), using regression analysis revealed some factors including family size, education, household wealth and some other variables inclined to use improved Drinking Water Supply (DWS). From previous studies combined with field observation, the study proposed the following independent variables, i.e.: X_1 = water supply per month, L per month; X_2 – education, year; X_3 – household revenue, IDR permonth; X_4 – Number of family member, person.

Results and Discussion

Characteristics of respondents

Characteristics of respondents described in this report include: (1) age, (2) education, (3) number of family members, (4) gender, and (5) family revenues. The distribution of respondents is presented in Table 1.

From the table above, the average age of respondents is 46 years with the youngest being 22 years and the oldest being 74. Therefore, the age difference is quite wide, reaching 53 years. The average age and media age is 46 years, indicating that respondents in the study location are still relatively of productive age. In terms of gender, 21 % respondent was female and 79 % was male.

In terms of education, there is also a wide difference between respondents with the highest education and those with the lowest level who have a difference of 13 years of education. The lowest level of education is only 3 years and the highest is 16 years (college completion). The average length of education is 9.3 years or the

Table 1. Characteristics of respondents.

Characteristics	Lowest	Highest	Average	Stdev	Median
Age, year	22	74	46.33	11.41	46.5
Education, year	3	16	9.27	2.92	9
Number of family members, person	3	6	4.5	0.73	5

equivalent of graduating from junior high school. Meanwhile, the median education is also equivalent to junior high school education, namely 9 years.

In terms of number of family members, the average number is 4.5 with the lowest being 3 people, namely a husband, a wife and a child. The highest is 6 with a median of 5 family members. So the it is the typical number of families in Indonesia, namely husband + wife + several children and siblings.

In terms of household revenue, the study results show that the average household revenues per year is IDR 28.9 million (Indonesian Rupiah; 1 IDR = 60,085,037·10^{12} € and 1 € = 16,645.3 IDR). This revenue comes from agriculture (on farm) worth IDR 14.5 million (50 %). Followed by revenues from off-farm, namely activities related to agriculture such as farm labour, processing of agricultural products, and agricultural-related commerce which contributes IDR 6 million per year (21 %). The third source of income is non-farm, namely IDR 8.4 million (19 %). Revenue from agriculture comes from various agricultural activities such as cocoa farming which contributes 53 % of on-farm revenue sources (Fig. 2).

Governance of water service

The concept of water governance is related to the conditions that enable management to function in managing water (FAO 2023). Rogers and Hall (2003) stated that water governance is related to a series of political, social, economic processes and administrative systems to develop and manage water resources and the delivery of water services to various community groups. Therefore, water governance is designed to ensure that water service could perform for today and future needs.

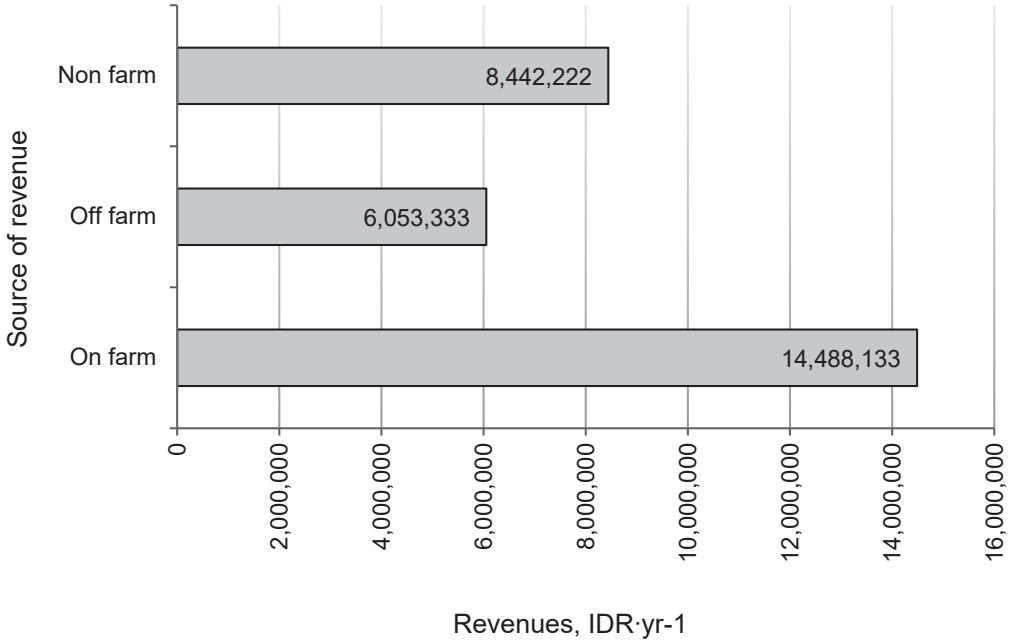


Fig. 2. Sources of household revenues.

In study site, sources of water are located in state property or public good, i.e. national park area. According to Mankiw (2018), public good property belongs to government or public and can be used for the benefit of people. The people in the study area are benefitting from public good of WARFP including the use of water resource. Since water is for public, not private, therefore the government do not apply environmental services fee. There are several reasons the government not to apply fee for environmental service: (1) it is not for commercial use, (2) beneficiaries are living nearby forest with less access to economy, (3) environmental service fee may lessen community participation, (4) installation of water is designed and funded by community with no government support.

Management of community based clean water service is done using community's volunteerism. According to Flood et al. (2005), volunteering is at the core and cannot be separated from service activities in both small and large organizations. Ideologically, volunteers play an important role in: (1) building society, (2) strengthening civil society, (3) developing equal relations between parties, (4) building public support, and (5) increasing public participation and accountability (Lingkar LSM 2023). In science and water research, volunteerism helps improve monitoring water and also data science collected by community (Church et al. 2019).

With volunteerism principle, (1) the price of clean water services is set not to make a profit, but only to cover operational costs, (2) officers do not receive a salary but rather want to help the community, and (3) no written rules prepared by the officers. With this principle, cost of getting water service is minimal and the commercial aspect of clean water is not applied, hence volunteerism improves the welfare of communities.

There are two models of water management in the study area. The following Table 2 is describing some characteristics of the two models, community based and community with RCDW.

Service fee is usually discussed and set by community. The fee was greatly influenced by how farming (coffee and cocoa) performed on that year. Therefore, performance of farming determines water service fee.

Cost of maintenance of community based with support RCWS is more expensive as this model require electricity to pump water to the households. While community-based model use gravitational system, no need for electricity.

Table 2. Characteristic of local community water service.

Characteristics	Community Based	Community with RCDW support
Organization	Not yet formalized	Not yet formalized
Method of determining service fee	Community discussion	Refer to RCDW rate
Maintenance	Voluntary	In cooperation with RCDW and community
Water distribution	Gravitation	Electric pump
Community participation	High	Medium
Maintenance fee	IDR 60,000 per year	IDR 120,000 per year
Sanction/penalty	Not available	Not available

Water consumption

According to SNI (2002) standard of using clean water *per capita* per day for urban communities is from 150 to 250 L and the water needs of rural communities is 100 L. The water needed is for bathing, washing, drinking, cleaning, etc. While according to MPWPH (2017), the minimum water requirement for urban communities is 121 L *per capita* per day, while survey results show that urban communities' water consumption is 144 L *per capita* per day. The biggest allocation of water use for family was for bathing, i.e. 45 % of daily water consumption. The study suggests that the average daily water consumption *per capita* of people is 189 L with the lowest consumption being 40 L and the highest being 708 L. The median amount of water consumption is 167 L *per capita* per day. There are around 26 % of respondent who use water less than 100 L *per capita* per day.

The data above shows that the water consumption of rural communities in the research location is partly below the SNI standard for clean water requirements and partly above the SNI. The number of respondents/communities who consume below the MPWPH's standard (121 L *per capita pe*r day) is quite high, that is 29 respondents (32 %). The causes of water consumption below the MPWPH's standard are: (1) lack of knowledge and (2) feeling that they already use enough water at home.

Meanwhile, the average daily water supply is 1994 L *per capita* per day. This figure shows that water supply exceeds average consumption. The minimum water discharge *per capita* is 240 L, which is above the consumption requirement. The median water discharge *per capita* is 1472 L. Meanwhile, the highest water discharge is 8100 L. From the data above, it appears that the water supply from WARFP exceeds household needs or consumption. This advantage is quite large and can be utilized by the community for other water uses.

The study shows that the majority of people (77 %) use excess water to irrigate fish ponds in their yards. The size of the fishpond varies with the smallest being 1.5×3×0.75 m up to 3×5×0.8 m.

Factors affecting water consumption

Factors affecting water consumption are estimated using multiple regression model (3) as stated in the followings:

$$Y = \beta_o + \beta_1 \cdot X_1 + \beta_2 \cdot X_2 + \beta_3 \cdot X_3 + \beta_4 \cdot X_4 + \mu, \quad (3)$$

where: Y – household water consumption; β_o – constant; $\beta_1, \beta_2, \beta_3$ and β_4 – regression coefficients; X_1 – water supply per month; X_2 – education; X_3 – household revenue; X_4 – number of family member; μ – error.

Definitions of variables are explained in the Table 3.

The computation of multiple regression is using Microsoft Excel for Mac. The summary of the result is as follows.

Result of ANOVA in the following table suggests that all variables affect consumption of water as indicated by F test with p value lower than 0.05 (Table 4).

For measuring effect of each independent variable to dependent variable, t-test is generated, and the result is as stated in Table 5. It suggests that 2 variables significantly affect monthly household water consumption. If other factors assume *ceteris paribus*, then revenue of family per month (negative) and water supply per month have significant effect to water consumption. This result is a bit different from other study: Motho et al. (2022) suggested that there was weak

Table 3. Definition of variables.

Variables	Definition	Measurement	Units
Household water consumption (Y)	Household water consumption for a month which consists of water for: 1. Bathing and toilet 2. Laundry 3. Dishes 4. Washing vehicles 5. Others	Compute households daily water consumption and converted to a month	L per household per month
Water supply per month (X_1)	Volume of water supply received by housholds per month	Supply of water to households on daily basis and converted to a month	L per household per month
Education (X_2)	Length of time respondent took formal school	Length of education time	Year
Household Revenue (X_3)	All revenues obtained by family in one month	Revenues from farm, off-farm, and nonfarm activities in a month	IDR per month per household
Number of family members (X_4)	Number of persons living in one family which consists of parents, children, and relatives.	Number of family members in a house	Person

Table 4. Anova of factors affecting water consumption.

Indicators	*df*	Sum of squares	Mean square	*F*-ratio	*p*-value
Regression	4	4,545,080,677	1,136,270,169	14.51	4.5057E-09
Residual	85	6,655,629,523	78,301,523.79		
Total	89	11,200,710,200			

Table 5. Effect of each independent variable to dependent variable.

Indicators	Coefficients	Standard Error	t-stat	*p*-value
Intercept	-1640.60874	6180.523438	-0.265448187	0.79130695
Water supply per month***	0.828849957	0.202189482	4.099372269	9.43778E-05
Education*	456.7721467	336.5558919	1.357195514	0.178312024
Revenue per month***	-0.39144947	0.099545671	-3.932360561	0.000171057
Number of family member*	1269.834862	1294.283178	0.981110536	0.329322558

Regression Statistics	
Multiple *R*	0.637012593
R Square	0.405785044
Adjusted *R* Square	0.377821987
Standard Error	8848.814824
Observations	90

Note: *** – highly significant, * – significant.

relationship between family income and demand for water. Other study in rural China by Fan et al. (2013) suggested that water supply, education, age, household income, net family size, vegetable area, and use of water heater have strong correlation with domestic water consumption.

According to the model (3) of the factors affecting water consumption, the following equation (4) is obtained:

$$Y = -1640.61 + 0.83 \cdot X_1^{***} + 456.77 \cdot X_2^{*} - -0.39 \cdot X_3 + 1269.83 \cdot X_4 + \mu \; . \quad (4)$$

However, the result suggests that there is negative influence of family revenue and water consumption, that is the higher the revenues, the less family are going to use water service. It is probably because family with more revenues could afford more expensive option that is deep well water pump. The deep well water is perceived more secure in terms of quality than pipe water from open-source spring.

The regression model did not show robust to estimate water consumption as it shows that R^2 is 0.40 indicating 40 % of independent variables could explain the model. Study by Fan et al. (2013) in China, using step wise regression model, also suggested that R^2 was not high, only around 20 %. This means there is still possible additional variables that can be included in the model or using different model in estimating water consumption.

Conclusion

This research provides important lessons about how communities meet basic needs, how to manage and maintain spring water sources, and how they use them for life in simple and inexpensive ways. Forest resources provide convenience because the springs come from maintained forests. The research results concluded that:

1. There are family has used water above national standard. However, 26 % family consumes water less than SNI and around 32 % family consumes less than average consumption of national water consumption.

2. Factors affecting water consumption significantly include water supply to family. Family revenues influence negatively to family water consumption. The more revenues family obtained, the less they consume pipe water consumption. Water supply for family has positive influence to the consumption of water. But, years of education and number of family members have less strong influence to water consumption.

3. More education in water consumption is advised especially for families that still use water less than national standard.

Acknowledgement

The team would like to express gratitude to Lembaga Penelitian Universitas Lampung for providing funding of this research.

References

Abidin Z. 2011. Economic Valuation of Community Based Clean Water Services in Sub-Watershed of Way Besai, West Lampung [Valuasi Ekonomi Jasa Air Bersih Berbasis Masyarakat di Sub-DAS Way Besai, Lampung Barat]. PhD thesis, Universitas Padjadjaran, Bandung, Jawa Barat. 274 p. (in Indonesian).

Abidin Z., Efendi I., Gultom D.T. 2023. Assessing Willingness to Pay for Improved Water Services from Forest Area in Bayas Jaya Village, Lampung Province. IOP Conference Series: Earth and Environmental Science 1145, 012013. doi:10.1088/1755-

1315/1145/1/012013

Alam S., Hajawa 2007. The Role of Forest Resources in the Economy and the Impact of Forest Rent Collection on Forest Sustainability in Gowa Regency [Peranan Sumberdaya Hutan Dalam Perekonomian Dan Dampak Pemungutan Rente Hutan Terhadap Kelestarian Hutan Di Kabupaten Gowa]. Perennial 3(2): 59–66 (in Indonesian). https://doi.org/10.24259/perennial.v3i2.173

ASEAN 2017. Theme 2: Social Progress in ASEAN. Jakarta. 46 p.

Baltagi B.H. 2008. Econometrics: Fourth Edition. Berlin, Germany, Springer-Berlin. 392 p.

BPS 2023. Proportion of households with access to basic services by province (Percent) [Proporsi rumah tangga dengan akses terhadap pelayanan dasar menurut provinsi (Persen)]. Central Bureau of Statistics [Badan Pusat Statistik] (in Indonesian). https://www.bps.go.id/id/statistics-table/2/MjAxNiMy/proporsi-rumah-tangga-dengan-akses-terhadap-pelayanan-dasar-menurut-provinsi.html

BPS Pesawaran Distric 2021. Gedong Tataan Sub-District in Numbers [Kecamatan Gedong Tataan dalam Angka]. Gedong Tataan, Central Bureau of Statistics of Pesavaran Distric [Gedong Tataan, BPS Kabupaten Pesawaran]. 103 p. (in Indonesian). https://www.scribd.com/document/510847667/Kabupaten-Pesawaran-Dalam-Angka-2021

BPS Pesawaran District 2022. Pesawaran District in Figures [Kabupaten Pesawaran Dalam Angka]. Central Bureau of Statistics of Pesawaran District [BPS Kabupaten Pesawaran]. 223 p. (in Indonesian). https://pesawarankab.bps.go.id/publication/2022/02/25/90fa9b40b202ad382886869a/kabupaten-pesawaran-dalam-angka-2022.html

Church S.P., Payne L.B., Peel S., Prokopy L.S. 2019. Beyond water data: benefits to volunteers and to local water from a citizen science program. Journal of Environmental Planning and Management, 62(2): 306–326. https://doi.org/10.1080/09640568.2017.1415869

Dong X., Du X., Zeng S., Bledsoe B.P. 2018. Benchmarking sustainability of urban water infrastructure systems in China. Journal of Cleaner Production 170(1): 330–338. https://doi.org/10.1016/j.jclepro.2017.09.048

Fan L., Liu G., Wang F., Geissen V., Ritsema C.J. 2013. Factors Affecting Domestic Water Consumption in Rural Households upon Access to Improved Water Supply: Insights from the Wei River Basin, China. Plos One 8(8): 1–8. https://doi.org/10.1371/journal.pone.0071977

FAO 2023. Water Governance. Retrieved from www.fao.org: https://www.fao.org/land-water/water/watergovernance/en/#:~:text=Water%20governance%20relates%20to%20the,institutions%3B%20and%20planning%2C%20decision%2D

Flood J.P., Jhonston M.E., Twynam G.D. 2005. Managing volunteers: Developing and implementing an effective programme. The 2005 Northeastern Recreation Research Symposium. Bolton Landing, USDA Forest Service. 425 p.

Irianti S., Prosetyoputra P., Sasimartoyo T.P. 2016. Determinants of household drinking-water source in Indonesia: An analysis of the 2007 Indonesian family life survey. Cogent Medicine 3(1), 1151143. 13 p. http://dx.doi.org/10.1080/2331205X.2016.1151143

Isaac S., Michael W.B. 1995. Handbook in Research and Evaluation: A Collection of Principles, Methods, and Strategies Useful in the Planning, Design, and Evaluation of Studies in Education and Behavioral Sciences. 6th Ed. Sandiego, EdITS. 262 p.

Lingkar LSM 2023. The Important Role of Volunteerism [Peran Penting Sebuah Kerelawanan]. NGO Circle [Lingkar LSM]. (in Indonesian). http://lingkarlsm.com/peran-penting-sebuah-kerelawanan/

Mankiw N.G. 2018. Principles of Economics. 8th Edition. Boston, Cengage Learning. 836 p.

Marsono B.D., Nirwisaya P.M. 2020. Evaluation of community-based water supply system in Krembung, Sidoarjo. INCRID.

IOP Conference Series: Earth and Environmental Science 623, 012043. 6 p. doi:10.1088/1755-1315/623/1/012043

Motho M., Kulawule O.D., Mothsolaphekho M.R., Mogomotsi P.K. 2022. Influence of household demographic and socio-economic factors on water demand in Ngamiland District, Botswana. Water Science 36(1): 48–59. https://doi.org/10.1080/23570008.2022.2048581

MPWPH (Ministry of Public Works and Public Housing) 2017. Urban Household Water Usage 144 Liters per Day [Pemakaian Air Rumah Tangga Perkotaan 144 Liter Perhari]. Ministry of Public Works and Public Housing of the Republic of Indonesia. (in Indonesian). https://pu.go.id/berita/pemakaian-air-rumah-tangga-perkotaan-144-liter-perhari#:~:text=Kebutuhan%20pokok%20minimal%20pemakaian%20air,bersih%20rumah%2C%20serta%20keperluan%20ibadah

Rogers P., Hall A.W. 2003. Effective Water Governance. TEC Background Papaers No. 7, Global Water Partnership, Technical Committee, Stockholm, Sweden. 44 p.

RTIU WARFP 2009. Book of Tahura Information [Buku Informasi Tahura]. Bandar Lampung: UPTD Taman Hutan Raya Wan Abdul Rachman. 37 p. (in Indonesian).

RTIU WARFP 2020. Profile of Tahura Wan Abdul Rachman [Profil Tahura Wan Abdul Rachman]. Dinas Kehutanan Provinsi Lampung. 41 p.

SNI (Standard for Clean Water Requirements) 2002. Establishing Balance of Natural Resource: Part 1, Spatial of Water Resource [Penyusunan Neraca Sumberdaya: Bagian 1 Sumberdaya Air Spasial]. Jakarta, BSNI. 1 p. (in Indonesian). https://www.scribd.com/document/399443744/Standar-SNI-Kebutuhan-Air-Bersih

The World Bank 2019. Indonesia: Expanding Access to Clean Water for the Rural Poor. https://www.worldbank.org/en/results/2019/07/29/indonesia-expanding-access-to-clean-water-for-the-rural-poor

UNDP (United Nations Development Programme) 2015. United Nations. Department of Economic and Social Affairs. Sustainable Development. https://sdgs.un.org/goals

Webliana K.B., Ummiyati I.R., Akbar K., Faizin R., Supriyansyah, Ambiya W. 2023. Identification of Potential and Utilization of Water Environmental Services in Sanenrejo Village, Sanenrejo Resort, Meru Betiri National Park [Identifikasi Potensi Dan Pemanfaatan Jasa Lingkungan Air Di Desa Sanenrejo Resort Sanenrejotaman Nasional Meru Betiri]. Community Development Journal 4(2): 3535–3541 (in Indonesian). https://doi.org/10.31004/cdj.v4i2.15069

Wooldridge J.M. 2013. Introductory Econometrics: A Modern Approach. 5th edition. Mason, Ohio, USA, Cengage Learning. 836 p.

FORESTRY IDEAS, 2024, vol. 30, No 1 (67): 50–65

Chlorophyll fluorescence characteristics in *Robinia pseudoacacia* L. under conditions of urban forest ecosystems in Dnipro city

Svitlana A. Sytnyk[1], Viktoriia M. Lovynska[1], Kyrylo K. Holoborodko[2*], Natalia K. Vasylieva[1], Yurii I. Gritsan[1], Iryna M. Loza[2], Oleksandr Ye. Pakhomov[2], Liudmila P. Golodok[2], and Hynek Roubik[3]

[1]Dnipro State Agrarian and Economic University, 25 Sergey Efremov Str., 49600 Dnipro, Ukraine. E-mails: glub@ukr.net, sytnyk.s.a@dsau.dp.ua, gritsan@ua.fm
[2]Oles Honchar Dnipro National University, 72 Gagarin Av., 49010 Dnipro, Ukraine. E-mails: holoborodko.kk@gmail.com*, irinaloza23@gmail.com, a.pakhomov@i.ua, milagolodok@gmail.com
[3]Czech University of Life Sciences Prague, Kamycka 129, 16500, Praha-Suchdol, Czech Republic. E-mail: roubik@ftz.czu.cz

Received: 17 September 2023 / Accepted: 21 February 2024 / Available online: 01 March 2024

Open Access: This article is licensed under a Creative Commons Attribution 4.0 International License.

Abstract

The rapid technique for measuring of chlorophyll fluorescence photoinduction is one of modern informative methods for assessing the impact of abiotic factors (temperature, humidity, and environmental light intensity) on physiological traits of photosynthesis responsible for productivity. We explored alterations in activity of different types of chlorophyll fluorescence influenced by above mentioned basic abiotic factors which have been undergoing essential changes in Ukrainian Steppe zone in recent decades. The research object was the black locust, introduced tree species spread widely in the examined region as forest anti-erosion plantings and in the landscaping of industrial towns. To reveal background, stationary, maximum and variable chlorophyll fluorescence, we used a fluorimeter to measure spectrum of light absorption and reflection by leaves. The output was presented as Kautsky curve that depicted the fluorescence response changes over time. We clarified that the background concentration was minimal at low air temperature. With increasing temperature, there was an upward trend in the background fluorescence intensification. The increase in the air humidity caused the opposite effect. With raising temperature, the intensity of maximum fluorescence had the reverse trend compared to the background fluorescence. It decreased when the temperature got higher. Alike the background fluorescence, the stationary fluorescence was minimal at low air temperature, but its rise resulted in the decline in the stationary fluorescence intensity. The research outcomes are methods and mathematical models developed and offered for calculations of different fluorescence types. Statistically significant relationship between the fluorescence, temperature and light intensity was established. The obtained results allow defining the introduction of *Robinia pseudoacacia* L. as successful while its resistance to the impact of abiotic environmental factors can be identified as high. It allowed us to specify black locust as the up-to-date species when forming plantings, unless suitable care, management, and control have been fulfilled.

Key words: adaptation of introduced tree species, climatic factors, Kautsky curve, photosynthetic apparatus in trees, resistance of urban dendroflora, Steppe zone of Ukraine.

Introduction

Research on chlorophyll fluorescence intensity is a modern informative method applicable to ecological monitoring (Banks 2018, Holoborodko et al. 2022). The rapid technique of chlorophyll fluorescence photoinduction is one of the most effective methods intended to identify the impact of abiotic environmental factors on physiological conditions of introduced plant species. Timely diagnostics of plant physiological conditions through chlorophyll fluorescence allow obtaining key data on plant photosynthesis (Guidi et al. 2019, Lin et al. 2022).

The maintenance of active photosynthesis under physiological stress is usually associated with developing plant resilience to unfavourable environmental factors. Recently, the main scientific attention has been focused on exploring the plant response to different stressors. Namely, drought, high temperature (Farooq et al. 2009, Blum 2017, Urban et al. 2017, Zandalinas et al. 2018), and shading (Wan et al. 2020) were identified as the most extensive abiotic factors which cause alterations in plant physiological and biochemical reactions (Johnstone et al. 2014, Martínez-Ferri et al. 2016, Alonso et al. 2017, Baghbani et al. 2019, Lin et al. 2019, Berner et al. 2021, Shupranova et al. 2022).

Belgio et al. (2015) showed that with diminishing illumination of the plant habitat, the relative fluorescence quenching also decreases. It almost disappears when the light intensity varied within 20–30 lux or below. This may indicate a gradual decrease in photosynthetic activity in terms of chlorophyll the plants being shaded. As a result of subsequent structural rearrangements in the photosynthetic apparatus, a channel for a heat dissipation of the excitation energy of chlorophyll molecules opens, and the fluorescence decreases. This mechanism is assumed to play a protective role, defencing the photosynthetic apparatus against the damage caused by strong light and ensuring the optimal rate of electron transport between photosystems (Carvalho et al. 2015). An increase in temperature with a simultaneous increase in excitation light is explained by the protective effect of light against leaf damaging by high temperatures (Krüger et al. 2014).

For the last decades, climatic change has been developing on the local and global scale. The perception of photosynthesis that determines the primary productivity in response to fluctuations in air temperature, humidity, and environmental light intensity, belongs to topical scientific tasks (Kosova et al. 2018). It can be explained by the fact that autotrophic ecosystem component establishes the heterotroph functioning, being a driving environmental factor. Therefore, the analysis of photosynthesis activity in leaves exposed to stressful conditions has been a main focus of the major studies. The invention of next-generation fluorimeters that are easy to use and provide high resolution allowed quick kinetics of chlorophyll induction or fluorescence to be measured (Cheng et al. 2019). Parameters obtained by these means are widely utilised to examine responses of photosystem II to stress factors (Farquhar et al. 2001, Bürling et al. 2013, Chen et al. 2019).

Black locust (*Robinia pseudoacacia* L.) is a deciduous fast-growing woody species with wide range of environmental adaptations and native to North America. It has one of the widest distributions in Europe of any introduced plants (Martin 2019). The future climate is conducive to the northward expansion of black locust with a speed of 21 km per decade (Li et al.

2021). It is one of species most commonly introduced within artificial forests and urban plantations in Steppe zone of Ukraine. The functional categories of the analysed species are as follows: (i) plantations intended for environmental protection, scientific, historical and cultural purposes – 1831.1 ha; (ii) recreational-therapeutic plantations – 7173.5 ha; (iii) anti-erosion protection plantations – 8679.1 ha (Lovynska and Sytnyk 2016).

This work hypothesises that, being introduced in the Steppe zone of Ukraine, the black locust assimilation apparatus responded differently to abiotic factors of the environment in different ranges of their values. Therefore, the purpose of the work was to determine the changes in the chlorophyll fluorescence parameters at different values of air temperature, humidity, and light intensity, as well as to identify the abiotic factors that most significantly affect the chlorophyll fluorescence.

Materials and Methods

This study was carried out in black locust plantations in Steppe zone of Ukraine (Fig. 1).

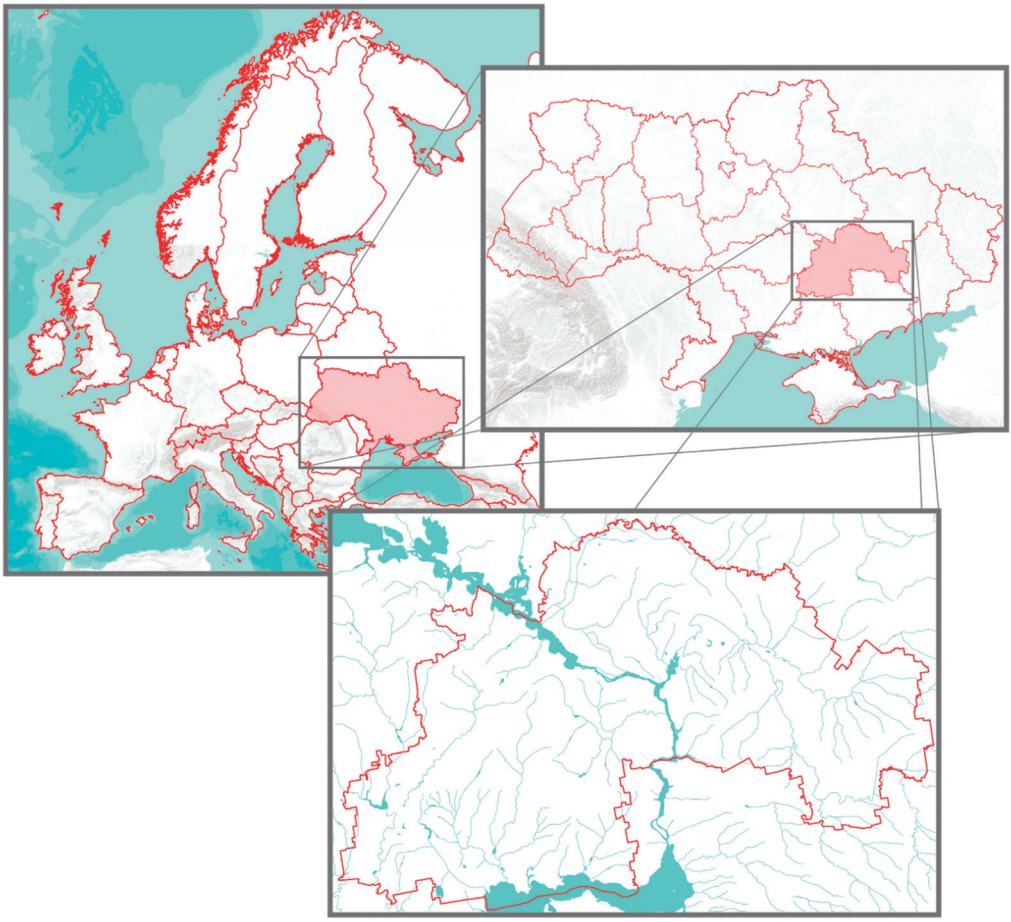


Fig. 1. The study region – Dnipro city, Ukraine.

Geographical parameters are the key regulators of the cultivation of introduced plant species. Their growth and development depend on numerous abiotic factors, but the climatic factors have the greatest limiting effect. Their consistency with ecological demands of the tree species ensures successful development and maintains further functions of tree plantations cultivated in novel geographical areas, essentially different from the relevant native areal.

The abiotic factors of air temperature, humidity, and environmental light intensity have significant effects on the progress of photosynthesis. To detect influence of the abiotic climatic factors, we analysed changes in air temperature and hydrothermic coefficient (HTC) as a ratio of a precipitation quantity (in mm) at a temperature above 10°C to the sum of temperatures for the same time period divided by 10. The considered climatic data were obtained from the Meteorological Site in Dnipro city (synoptic index 34504, altitude: 143 m, geographical coordinates: latitude 48°60´ N, longitude 34°97´ E) for 45 years from 1974 to 2018 (Weather and Climate 2004–2023).

The long-term averaged temperature in the coldest month of January was –3.6 °C, while in the hottest month of July it reached +22.1°C. However, in some years, the air temperature significantly deviated from a typical isotherm. The absolute minimum of –30.0 °C was recorded on January 11, 1950, while the absolute maximum of +40.9 °C was registered on August 8, 2010. Absolute minimum values of air temperature in winter were negative, whereas the corresponding maximum values were positive and equalled 13.6°C in December; 12.6°C in January; 17.5°C in February. The latter were recorded for the previous decade. The frost-free period usually lasts 160 to 220 days. In 1843, the average annual air temperature in Dnipro city was 9°C. It ranged from 6.3°C in 1987 to 10.8 °C in 2007. An annual amplitude between the average temperature in the warmest and coldest months was 25.7°C (Fig. 2).

A hydrothermal coefficient in Dnipro city had a wide range of values between 0.51 and 2.00 (Fig. 3). It meant that

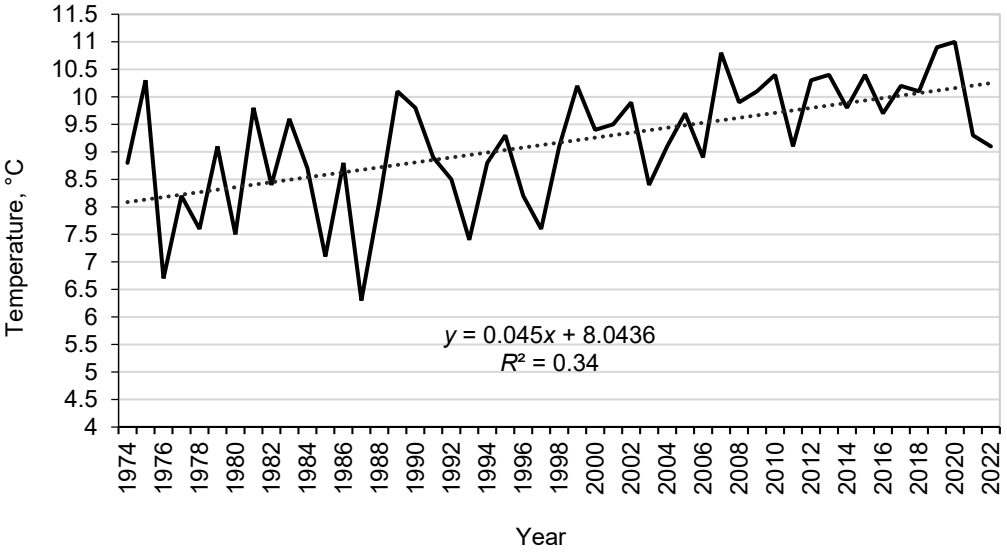


Fig. 2. Trend in average air temperature in Dnipro city.

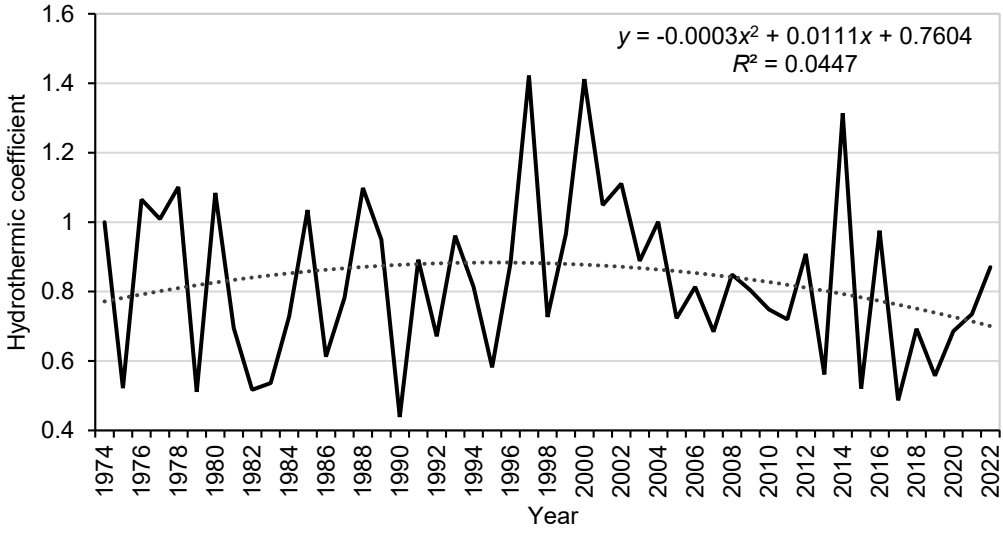


Fig. 3. Hydrothermic coefficient dynamics in Dnipro city.

there were alternating periods of severe droughts (when HTC ≤ 0.5) and excessive precipitations (HTC ≥ 1.5).

The climate of the Dnipropetrovsk region is moderately continental. The most common soil in the Dnipropetrovsk region is ordinary chernozem (or Mollisols in the US soil taxonomy) developed on loess and loess-like sediments. It is a dark-coloured soil containing a high percentage of humic, phosphorus and ammonia compounds. Chernozem is loose and can absorbs and holds water well, and at the same time is easily ventilated. All this creates favourable conditions for plant nutrition and growth. Subsoil water occurs, as a rule, at the depth of more than 5 m and does not influence the soil formation. The thickness of the humus layer varies from 40 to 80 cm. The humus content in the upper horizon of low-humus variety is 3.5–5.5 %, and in the medium-humus, 5.5–6.5 %. The reaction of the soil solution is subacid or near to neutral. The moisture content is subject to considerable seasonal and annual fluctuations (Kunakh et al. 2022).

In the place of the city areas, fine-textured low-humic ordinary chernozem, differently eroded had previously been naturally formed. In a megacity, anthropogenic activity in natural chernozems is often occurs with the formation of transformed soils. In Ukraine, the classification scheme of transformed soils includes the class 'Anthropogenic soils', group of types 'Technological soils' (technozems and lithozems). Soils of urbanized areas have specific differences from natural soils, such as formation of poured mixed upper horison with the presence of various construction and household wastes, shift of acid-alkaline balance towards its alkalization; contamination by heavy metals, oil products, emission components of industrial enterprises; change in physical-mechanical properties (lowered moisture capacity, increased density, rockiness ets.), decreasing buffering capacity (Khokhryakova 2020).

The plant photosystem conditions were explored using the induction in method of chlorophyll fluorescence ob-

served in the plant leaves. For such a reason, the spectra of light reflection and absorption were measured. The output was presented as Kautsky curve, which depicted the time dependence of chlorophyll fluorescence intensity. To study the alterations in native chlorophyll fluorescence of fresh (living) leaves, a portable fluorimeter 'Floratest' (Ukraine) was used (Romanov et al. 2013). Its remote optoelectronic sensor includes a LED that has a maximum radiation intensity at λ (470 + 20 nm). Irradiation indicators in the sensor were: radiation wavelength 470 + 15 nm; irradiated spot size not less than 15 mm^2; luminous intensity within the spot at least 2.4 $W \cdot m^{-2}$. Indicators for signal detection in optoelectronic sensor were: the spectral range of fluorescence intensity measurement 670–800 nm; receiving window size 9 mm^2; photodetector sensitivity at λ = 650 nm was 0.45 $A \cdot W^{-1}$. We carried out this research during the active vegetation season of *R. pseudoacacia* in May–September 2021. The critical parameters of Kautsky curve were measured monthly, namely on 23.05.2021, 20.06.2021, 21.07.2021, 23.08.2021, 20.09.2021 at 12:00 at the height of the sun activity.

Our study was performed in green areas in Dnipro city, and included 7 trees with similar morpho-taxational features. The critical parameters of Kautsky curve were measured on average leaves including 7 pieces of each tree. on the brightly lit side, as well as 7 pieces on the shaded side. The leaves were sampled in dry and sunny weather from the annual vegetative growth in a lower third of a tree crown in different compass points. The leaves were labelled for further comparison.

To clarify the impact of natural factors on fluorescence, we used a number of indicators (Holoborodko et al. 2021):

F_0 – baseline (background) fluorescence;

F_m – maximum fluorescence;

F_{st} – stationary fluorescence;

F_v/F_m – the index of internal or maximum quantum yield of photosystem II (PSII) calculated with the formula (1):

$$\frac{F_v}{F_m} = \frac{F_m - F_0}{F_m}. \quad (1)$$

To address the research goals, we applied mathematical analysis of variance, ANOVA. Like cluster and statistical methods, this approach is an efficient technique utilised to carry out research in miscellaneous fields of natural sciences, e.g. in forestry and agriculture (Vasylieva et al. 2015, 2021). In general, ANOVA allows clarifying the dynamics of parameters and identifying pivot points of significant changes that impact dependent variables in an essential way. In our study, ANOVA enables us to compare the averages of the fluorescence indicators between the groups of observations according to the specific ranges of the factors considered, such as air temperature, humidity, and environmental light intensity.

It involved checking null and alternative hypotheses, such as:

H_0: There is no significant difference between the averages of the compared groups;

H_a: There is significant difference between the averages of the compared groups.

If the impact was found to be insignificant, then the alternative hypothesis was rejected. In contrast, if the revealed influence was significant, then the null hypothesis should be rejected. ANOVA method is based on checking of Fisher criterion to evaluate the ratio of so-called between-group variability to within-group variability.

In more detail, let the entire data be

distributed into M groups consisting of N_m observations X_{mn}, $n = 1…N_m$, $m = 1…M$. Then the total number of observations is calculated by the formula (2):

$$N = \sum_{m=1...M} N_m \quad (2)$$

and, the total mean amounts were calculated by the formula (3):

$$\overline{X} = \frac{\sum_{m=1...M} \sum_{n=1...N} X_{nm}}{N}. \quad (3)$$

Similarly, the mean within the group m is determined by the formula (4):

$$\overline{X}_m = \frac{\sum_{n=1...N_m} X_{mn}}{N_m}, m = 1...M. \quad (4)$$

Fisher ratio is presented by the formula (5):

$$F_{calculated} = \frac{f_2 \sum_{m=1...M} N_m \left(\overline{X}_m - \overline{X}\right)^2}{f_1 \sum_{m=1...M} \sum_{n=1...N_m} \left(X_{mn} - \overline{X}_m\right)^2}, \quad (5)$$

where: $f_1 = M - 1$ is a degree of freedom of the variable between groups explained by an impact of the factor analysed, $f_2 = N - M$ is a degree of freedom of the variable within groups unexplained by the factor considered.

The critical value $F_{critical}$ of Fisher criterion depends on the chosen α level of significance. as well as degrees of freedom f_1 and f_2. Then the inequality $F_{calculated} \leq F_{critical}$ results in rejecting the alternative hypothesis H_α, in other words the changes in the considered factor have no effect on the relevant indicator with the probability of $(1-\alpha)$.

On the contrary, the inequality $F_{calculated} > F_{critical}$ disproves the null hypothesis H_0 and states that the relevant indicator depends on the changes in the factor considered factor with the probability of $(1-\alpha)$.

The calculations carried out covered up to $N = 199$ observations and the significance level of $\alpha = 0.05$.

Results

Several measured indicators of chlorophyll fluorescence intensity, as well as calculated parameters of the variance analysis performed are presented in tables 1, 2, and 3. The sample data size accounted for 60 observations for each of four indicators of fluorescence and each of three environmental parameters. Thus, the total number of the analysed values amounted to 720. For the sake of uniformity every data set was divided into 6 groups or clusters, each of which included 10 observations introducing 6 ranges of factor changes to analyze and compare. In tables 1–3, every cluster by each factor was described by the corresponding group average (AV) and coefficient of variance (CV) equal to ratio of the standard deviation to the group average.

The calculations were performed by means of free software Google Sheets. They are numbered in tables 1–3 and included only clusters relevant to the particular calculation. The clusters excluded from some calculations were marked with dashes (-).

To detect an impact of the abiotic factor conditioned by air temperature, chlorophyll fluorescence was examined within the temperature range of 16 °C to 41 °C. The absolute values of the background fluorescence varied within 304 to 560 relative fluorescence units. The minimum intensity of the background fluorescence was recorded at an air temperature from 18 °C to 19.9 °C. Its maximum was observed at the air temperature in the range of 29–30.9 °C. The applied ANOVA technique allowed the conclusion that temperature has a statistically significant effect on the target indicator. Data presented in Table 1 revealed that the indicator F_0 was essentially different within

Table 1. Chlorophyll fluorescence in *R. pseudoacacia* leaves depending on air temperature.

No	Fluorescence indicators		Range of temperature, °C						$F_{calculated}$	P	$F_{critical}$
			16.0–17.9	18.0–19.9	20.0–26.9	27.0–28.9	29.0–30.9	31.0–41.0			
1	F_0	AV	372.8	310.4	411.8	407.2	449.6	409.6	13.07	0.000	2.39
		CV	0.05	0.04	0.14	0.07	0.16	0.05			
2		AV	-	-	411.8	407.2	449.6	409.6	1.64	0.197	2.87
		CV	-	-	0.14	0.07	0.16	0.05			
3	F_m	AV	1542.4	1534.8	1347.6	1259.6	1361.6	1507.2	2.05	0.086	2.39
		CV	0.23	0.09	0.28	0.18	0.19	0.02			
4	F_{st}	AV	1473.6	1379.2	992.2	918.8	1014.4	1099.2	10.84	0.000	2.39
		CV	0.25	0.09	0.30	0.16	0.16	0.04			
5		AV	1473.6	1379.2	-	-	-	-	0.62	0.442	4.41
		CV	0.25	0.09	-	-	-	-			
6		AV	-	-	992.2	918.8	1014.4	1099.2	1.58	0.211	2.87
		CV	-	-	0.30	0.16	0.16	0.04			
7	F_v/F_m	AV	0.77	0.78	0.74	0.67	0.66	0.65	13.42	0.000	2.39
		CV	0.09	0.04	0.10	0.05	0.06	0.03			
8		AV	0.77	0.78	0.74	-	-	-	1.03	0.369	3.35
		CV	0.09	0.04	0.10	-	-	-			
9		AV	-	-	-	0.67	0.66	0.65	1.18	0.323	3.35
		CV	-	-	-	0.05	0.06	0.03			

the whole temperature range of 16 °C to 41 °C (Table 1, calculation 1). This was true because the calculated Fisher criterion was larger than the corresponding critical coefficient. However, fluctuations in the intensity of the background fluorescence turned out to be non-essential at an air temperature of 20 °C to 41 °C (Table 1, calculation 2).

The intensity of the maximal chlorophyll fluorescence developed a reverse trend compared to the background one. It decreases when the air temperature increases. The minimal average level of this physiological indicator of fluorescence was recorded within a temperature range of 27 °C to 28.9 °C. At the same time, this study detected no any significant impact of air temperature on maximal fluorescence F_m (Table 1, calculation 3). The stationary fluorescence showed a maximum intensity at low air temperature of 16°C to 17.9°C. Its growth resulted in a decrease in the stationary fluorescence values. Such tendency was confirmed by the calculated Fisher criterion. At the same time, indicator F_{st} was statistically uniform within temperature range of 16 °C to 19.9 °C, as well as 20 °C to 41 °C (Table 1, calculations 5 and 6). The index of the maximum quantum yield of PSII (F_v/F_m) varied from 0.59 to 0.86. According to the calculated Fisher criterion, this coefficient showed a clear downward trend triggered by an increase in air temperature. The significant decrease in the discussed index occurred

at the temperature of around 27 °C. Namely, indicator F_v/F_m was relatively stable within the temperature range of 16 °C to 26.9°C, as well as 27°C to 41 °C (Table 1, calculations 8 and 9).

Background, maximum and stationary chlorophyll fluorescence intensity were measured under the condition of relative air humidity from 31 % to 50 %. The background fluorescence associated with an ecological factor of relative air humidity reached its maximum, when the latter showed low values 31 % to 33.9 %. A further increase in humidity caused a reduction in the background fluorescence intensity. According to data accumulated in Table 2, the background fluorescence F_0 was relatively uniform within the range of humidity between 34.0 % and 43.9 % (Table 2, calculation 2).

The highest values of the maximum chlorophyll fluorescence in *R. pseudoacacia* leaves were observed at the air humidity of 31 % to 33.9 %, as well as of 44 % to 50 %. Meanwhile, stationary fluorescence reached its maximum when air humidity ranged from 39 % to 41.9 %. Its intensity dropped with the boundary values of air humidity. The research conducted conclude no essential reliable changes in maximum F_m or stationary F_{st} fluorescence associated with an increase in relative air humidity (Table 2, calculations 3 and 4). The average minimal index (0.62) of the maximum quantum yield of PSII was far from optimal at the air humidity of 31 % to 33.9 % (Table 2, calculation 5). With increasing environmental humidity, the active centres of PSII ensured stable functioning that resulted in growing of the ratio F_v/F_m. However, it was statistically stable within the rest of observed air humidity range (Table 2, calculation 6).

The study analysed the impact of the environment factors on *R. pseudoacacia* growth in phytocoenoses of Dnipro city with respect to different types of chlorophyll fluorescence. The research findings clarified that the maximum background fluorescence occurred under the condition when the light intensity was within the ranges of 150 to 299 lx and 700 to 999 lx.

Table 2. Chlorophyll fluorescence in *R. pseudoacacia* leaves depending on air humidity.

No	Fluorescence indicators		Range of air humidity, %						$F_{calculated}$	P	$F_{critical}$
			31.0–33.9	34.0–36.9	37.0–38.9	39.0–41.9	42.0–43.9	44.0–50.0			
1	F_0	AV	598.4	386.8	360.0	370.4	363.2	527.8	24.17	0.000	2.39
		CV	0.06	0.02	0.16	0.05	0.10	0.27			
2		AV	-	386.8	360.0	370.4	363.2	-	1.093	0.365	2.87
		CV	-	0.02	0.16	0.05	0.10	-			
3	F_m	AV	1532.8	1489.6	1369.6	1469.2	1412.8	1533.2	0.93	0.467	2.39
		CV	0.06	0.04	0.21	0.11	0.19	0.19			
4	F_{st}	AV	1080.0	1126.2	1131.2	1225.6	1084.8	1081.4	0.75	0.588	2.39
		CV	0.10	0.03	0.22	0.15	0.31	0.17			
5	F_v/F_m	AV	0.62	0.72	0.71	0.71	0.71	0.66	4.00	0.004	2.39
		CV	0.04	0.03	0.14	0.08	0.09	0.07			
6		AV	-	0.72	0.71	0.71	0.71	0.66	1.21	0.320	2.58
		CV	-	0.03	0.14	0.08	0.09	0.07			

Meanwhile, the corresponding minimum value associated with the environmental light intensity was 300 to 499 lx. The calculated Fisher criterion obtained using ANOVA technique was less than the critical one. It enabled us to reject the hypothesis that there is a significant relationship between the background fluorescence intensity F_0 and environmental light intensity (Table 3, calculation 1).

Both the maximum and stationary chlorophyll fluorescence depended on light intensity. In particular, the maximal fluorescence reached its peak when an environmental light intensity was within 300–499 lx, and dropped down when the light intensity was within 700–999 lx. Indicator F_m was statistically uniform when the light intensity varied between 150 and 699 lx, as well as from 1000 to 7450 lx (Table 3, calculations 3 and 4). The average values of the stationary chlorophyll fluorescence F_{st} were constant when the light intensity varied between 150 and 699 lx, as well as between 700 and 7450 lx (Table 3, calculations 6 and 7).

The coefficient of maximum quantum yield of PSII had a near-optimal value, except when light intensity was within 700–999 lx. However, the indicator F_v/F_m was

Table 3. Chlorophyll fluorescence in leaves of *R. pseudoacacia* depending on light intensity.

No	Fluorescence indicators		Range of light intensity, lx						$F_{calculated}$	P	$F_{critical}$
			150–299	300–499	500–699	700–999	1000–1699	1700–7450			
1	F_0	AV	454.4	363.2	369.2	441.0	364.8	367.6	9.29	0.000	2.39
		CV	0.06	0.04	0.05	0.17	0.18	0.06			
2		AV	1614.4	1636.8	1557.4	1110.4	1448.0	1435.8	6.39	0.000	2.39
		CV	0.04	0.03	0.06	0.17	0.31	0.22			
3	F_m	AV	1614.4	1636.8	1557.4	-	-	-	3.20	0.057	3.35
		CV	0.04	0.03	0.06	-	-	-			
4		AV	-	-	-	-	1448.0	1435.8	0.005	0.945	4.41
		CV	-	-	-	-	0.31	0.22			
5		AV	1190.4	1209.6	1141.6	895.6	1038.4	1105.4	4.21	0.003	2.39
		CV	0.03	0.03	0.15	0.13	0.25	0.25			
6	F_{st}	AV	1190.4	1209.6	1141.6	-	-	-	1.22	0.310	3.35
		CV	0.03	0.03	0.15	-	-	-			
7		AV	-	-	-	895.6	1038.4	1105.4	2.13	0.139	3.35
		CV	-	-	-	0.13	0.25	0.25			
8		AV	0.70	0.71	0.70	0.50	0.72	0.74	22.01	0.000	2.39
		CV	0.02	0.05	0.07	0.17	0.13	0.06			
9	F_v/F_m	AV	0.70	0.71	0.70	-	-	-	0.13	0.878	3.35
		CV	0.02	0.05	0.07	-	-	-			
10		AV	-	-	-	-	0.72	0.74	0.72	0.407	4.41
		CV	-	-	-	-	0.13	0.06			

relatively stable in the light intensity range of 150–699 lx, as well as 1000–7450 lx, showing a strong dependence on the light intensity of the environment (Table 3, calculations 9 and 10).

The next stage of the fulfilled research suggested establishing a mathematical relationship between different kinds of fluorescence and the analysed environmental factors by means of econometric non-linear regressions.

According to the data given, some of the modelled equations have statistically insignificant coefficients of determination. The one-factor models linked F_0 and F_{st} to temperature and also F_m and F_{st} to light intensity, had statistically reliable coefficients of their regressions. The two-factor models created linking F_{st} to temperature, and light intensity had statistically reliable coefficients (*a*, *b, c*) of their regressions. Statistically significant coefficients *a* and c were identified for F_m, while statistically significant coefficients *a* and *b* were detected for F_0. The most reliable three-factor regression (as a mathematical relationship based on temperature, humidity, and light intensity) was calculated for F_{st}. Overall, due to statistical analysis with regard to the mathematical models considered, this research revealed a fairly strong dependence of the fluorescence on the temperature and light intensity, but a similar relationship between the fluorescence and the humidity was not confirmed.

Discussion

PSII is considered to be the most sensitive to overheating. The thermal exposure was shown to cause disintegration of the components within PSII complex and a significant decrease in the efficiency of excitation energy transfer from light-harvesting pigments to PSII reaction centres. The background fluorescence F_0 (under normal conditions it corresponds to Chl_a when PSII reaction centres are fully open) was proposed to use as a test for the thermal stability of F_0 (Kalaji et al. 2012, 2016). Several authors (Crafts-Brandner and Salvucci 2002) found a significant increase in the F_0 level after heating of chrysanthemum leaves at temperatures above 38 °C for 30–120 min. At the same time, the researchers registered a sharp decrease in the F_v/F_m ratio, which characterizes the photochemical activity of PSII.

The value of background fluorescence (F_0) depends on the excitation energy lost during its transfer across a pigment matrix and also on the quantity of chlorophyll molecules without functional links to reaction centres (Sayed 2003, Zhang et al. 2020). This fact can be attributable to structural changes in a pigment complex caused by a combined impact of air temperature, humidity, and environmental light intensity. A decrease in the quantity of antenna chlorophylls reduces the initial level of fluorescence, and *vice versa* (Demmig-Adams et al. 2012). The non-photochemical decrease in the fluorescence intensity of PSII-associated chlorophyll is explained by the establishment of the proton gradient on the thylakoid membrane and redistributing the excitation energy in favour of PSI. The formation of ΔpH on the thylakoid membrane leads to the protonation of a special PsbS protein and the conversion of the carotenoid pigment violaxanthin into zeaxanthin. The mechanism for optimising the joint action of two photosystems includes reversible phosphorylation of a special light-harvesting chlorophyll-protein complex and its relocation between membrane areas with different content of PSI and PSII complexes (Mathur et al. 2011).

The parameter F_{st} describes the highest level of fluorescence; in other words, it is the maximum value on the induction curve. It tends to be the most variable due to its high adaptability (Zhao et al. 2018). The minimal indicators of F_{st} in the structure of a plant pigment complex were revealed in *R. pseudoacacia* trees to be affected by three factors: air temperature, humidity, and environmental light intensity. This combination is also responsible for a decrease in both light harvesting and antenna chlorophylls. The value of the stationary fluorescence F_{st} decreased coincidently with a downward trend for air temperature, humidity, and environmental light intensity (Sepúlveda and Johnstone 2019, Shupranova et al. 2019) This parameter featured a dynamic balance between processes that explain rising and decreasing (Ruban 2016).

The ratio F_v/F_m has been largely used as a sensitive indicator of plant photosynthetic performance (Guidi et al. 2019). Some scientists suggest that the decrease in this index indicates reducing PSII efficiency, namely photoinhibition. Being sensitive to inhibition of a light-dependent stage of photosynthesis, the parameter F_v/F_m provides an effective means to monitor the stressful effects on plants (Sonti et al. 2020**)**. This parameter is informative with regard to basic processes which boost changes in photosynthetic performance, in particular non-photochemical quenching (Uhrin and Supuka 2016, Uhrin et al. 2018). The values of F_v/F_m identify the maximum quantum yield of the potential PSII and are utilised as a sensitive productivity indicator of the plant photosystem. Its optimal value is close to 0.83 in major plants (Suchocka et al. 2021).

A sharp decrease in the ratio F_v/F_m, which characterises the maximum photochemical activity of PSII, also revealed the suppression of the functional activity in the photosynthetic apparatus after heating a leaf to over 38 °C. As for the background fluorescence level F_0 when PSII reaction centres open, it remains practically unchanged up to temperatures of 42 °C, which could indicate no significant disturbances in the aggregation of the light harvesting antenna and reaction centres (Janka et al. 2013). Perhaps, F_v/F_m is the parameter most frequently used for measuring of chlorophyll fluorescence and assessing plant responses to some stresses. However, some scientists concluded that F_v/F_m represents the plant resistance to moderate drought (Tezara et al. 1999, Oukarroum et al. 2007, Wan et al. 2020).

Our study disclosed that the discussed index varies between 0.65 and 0.66 regardless of the abiotic environmental factors considered. This means that its impact on plants growing in urban technogenic areas resulted in photoinhibition in all three cases associated with light intensity, temperature, and humidity. In this regard, a significant decrease in F_v/F_m can be interpreted as a factor of photo-damage, while an insignificant decline might be explained by photoprotection (Golan et al. 2015). In turn, some researchers associated a relatively moderate decrease in F_v/F_m with a reduced risk of photooxidative stress or so-called positive photoinhibition caused by activity of PSII-associated proteins (Giardi et al. 1996).

Conclusion

The absolute values of the background fluorescence fluctuated between 304 and 560 relative units. The minimum intensity of the background fluorescence was found at an air temperature of 18 °C to 19.9 °C.

The stationary fluorescence amounted to maximum when the air temperature dropped to 16–17.9 °C. The maximum level of background fluorescence was associated with low air humidity of 31 % to 34 %. The subsequent increase in humidity resulted in a decrease in background fluorescence intensity. The highest values of the maximum chlorophyll fluorescence produced by *R. pseudoacacia* were detected at humidity values of 31 % to 33.9 % and 44 % to 50 %. Stationary fluorescence amounted to its maximum intensity at an air humidity of 39 % to 41.9 %. Background fluorescence was the most active at a light intensity within 700–999 lx. The stationary fluorescence reached its maximum at a light intensity of 300–499 lx, but it was minimal when the light intensity increased to 700–999 lx. The coefficient of the maximum quantum yield of PSII was stable and relatively close to its optimum except for an environmental light intensity of 700–999 lx.

Our research resulted in confirming the hypothesis about different levels of influence of the studied abiotic factors on the photosynthetic processes observed in *R. pseudoacacia* under conditions of its introduction. Chlorophyll fluorescence appeared to be most sensitive to changes in light intensity levels. The marginal values of all types of fluorescence were determined for a wide range of values of the studied abiotic factors. According to data analysis, the values of chlorophyll fluorescence intensity varied significantly depending on abiotic factors. The research findings identified the values an air temperature, air humidity and light intensity at which background, maximum and stationary fluorescence reach their minimums and maximums.

References

Alonso L., Van Wittenberghe S., Amorós-López J., Vila-Francés J., Gómez-Chova L., Moreno J. 2017. Diurnal cycle relationships between passive fluorescence, PRI and NPQ of vegetation in a controlled stress experiment. Remote Sensing 9(8), 770. 16 p. https://doi.org/10.3390/rs9080770

Baghbani F., Lotfi R., Moharramnejad S., Bandehagh A., Roostaei M., Rastogi A., Kalaji M.H. 2019. Impact of *Fusarium verticillioides* on chlorophyll fluorescence parameters of two maize lines. European Journal of Plant Pathology 154(2): 1–10. https://doi.org/10.1007/s10658-018-01659-x

Banks J.M. 2018. Chlorophyll Fluorescence as a Tool to Identify Drought Stress in *Acer* genotypes. Environmental and Experimental Botany 155: 118–127. https://doi.org/10.1016/j.envexpbot.2018.06.022

Belgio E., Ungerer P., Ruban A.V. 2015. Light-harvesting superstructures of green plant chloroplasts lacking photosystems: Thylakoid grana without photosystems. Plant, Cell & Environment 38(10): 2035–2047. https://doi.org/10.1111/pce.12528

Berner J.M., Cloete H., Shuuya T. 2021. A baseline assessment of the photosynthetic potential of *Welwitschia mirabilis* using the JIP-test for monitoring and conservation purposes. Bothalia 51(1), a9. 7 p. http://dx.doi.org/10.38201/btha.abc.v51.i1.9

Blum A. 2017. Osmotic adjustment is a prime drought stress adaptive engine in support of plant production. Plant, Cell & Environment 40(1): 4–10. https://doi.org/10.1111/pce.12800

Bürling K., Cerovic Z.G., Cornic G., Ducruet J.M., Noga G., Hunsche M. 2013. Fluorescence-based sensing of drought-induced stress in the vegetative phase of four contrasting wheat genotypes. Environmental and Experimental Botany 89: 51–59. https://doi.org/10.1016/j.envex-

pbot.2013.01.003

Carvalho F.E., Ware M.A., Ruban A.V. 2015. Quantifying the dynamics of light tolerance in Arabidopsis plants during ontogenesis. Plant Cell & Environment 38(12): 2603–2617. https://doi.org/10.1111/pce.12574

Chen X., Mo X., Hu S., Liu S. 2019. Relationship between fluorescence yield and photochemical yield under water stress and intermediate light conditions. Journal of Experimental Botany 70(1): 301–313. https://doi.org/10.1093/jxb/ery341

Cheng D., Zhang Z., Zhou S., Peng Y., Zhang L. 2019. Relationships between leaf physiognomy and sensitivity of photosynthetic processes to freezing for subtropical evergreen woody plants. iForest 12(6): 551–557. https://doi.org/10.3832/ifor3196-012

Crafts-Brandner S.J., Salvucci M.E. 2002. Sensitivity of Photosynthesis in a C4 Plant, Maize, to Heat Stress. Plant Physiology 129(4): 1773–1780. https://doi.org/10.1104/pp.002170

Demmig-Adams B., Cohu C.M., Muller O., Adams W.W. 2012. Modulation of photosynthetic energy conversion efficiency in nature: from seconds to seasons. Photosynthesis Research. 113(1–3): 75–88. https://doi.org/10.1007/s11120-012-9761-6

Farooq M., Wahid A., Kobayashi N., Fujita D., Basra S. 2009. Plant drought stress: effects, mechanisms and management. Agronomy for Sustainable Development 29(1): 185–212. https://doi.org/10.1051/agro:2008021

Farquhar G.D., von Caemmerer S., Berry J.A. 2001. Models of photosynthesis. Plant Physiology 125(1): 42–45. https://doi.org/10.1104/pp.125.1.42

Giardi M., Cona A., Geiken B., Kuçera T., Masojidek J., Mattoo A. 1996. Long-term drought stress induces structural and functional reorganization of photosystem II. Planta 199: 118–125. https://doi.org/10.1007/BF00196888

Golan K., Rubinowska K., Kmieć K., Kot I., Górska-Drabik E., Łagowska B., Michałek W. 2015. Impact of scale insect infestation on the content of photosynthetic pigments and chlorophyll fluorescence in two host plant species. Arthropod Plant Interactions 9: 55–65. https://doi.org/10.1007/s11829-014-9339-7

Guidi L., Lo Piccolo E., Landi M. 2019. Chlorophyll Fluorescence, Photoinhibition and Abiotic Stress: Does it Make Any Difference the Fact to Be a C3 or C4 Species? Frontiers in Plant Science 10, 174. 11 p. https://doi.org/10.3389/fpls.2019.00174

Holoborodko K.K., Seliutina O.V., Ivanko I.A., Alexeyeva A.A., Shulman M.V., Pakhomov O.Y. 2021. Effect of *Cameraria ohridella* feeding on *Aesculus hippocastanum* photosynthesis. Regulatory Mechanisms in Biosystems 12(2): 346–352. https://doi.org/10.15421/022147

Holoborodko K.K., Sytnyk S.A., Lovynska V.M., Ivanko I.A., Loza I.M., Brygadyrenko V.V. 2022. Impact of invasive species *Parectopa robiniella* (Gracillariidae) on fluorescence parameters of *Robinia pseudoacacia* in the conditions of the steppe zone of Ukraine. Regulatory Mechanisms in Biosystems 13(3): 324–330. https://doi.org/10.15421/022242

Janka E., Körner O., Rosenqvist E., Ottosen C.O. 2013. High temperature stress monitoring and detection using chlorophyll a fluorescence and infrared thermography in chrysanthemum (*Dendranthema grandiflora*). Plant Physiology and Biochemistry 67: 87–94. https://doi.org/10.1016/j.plaphy.2013.02.025

Johnstone D., Tausz M., Moore G., Nicolas M. 2014. Bark and leaf chlorophyll fluorescence are linked to wood structural changes in *Eucalyptus saligna*. AoB Plants 6, plt057. 10 p. https://doi.org/10.1093/aobpla/plt057

Kalaji M.H., Carpentier R., Allakhverdiev S.I., Bosa K. 2012. Fluorescence parameters as early indicators of light stress in barley. Journal of Photochemistry and Photobiology B: Biology 112: 1–6. https://doi.org/10.1016/j.jphotobiol.2012.03.009

Kalaji M.H., Jajoo A., Oukarroum A., Brestic M., Zivcak M., Samborska I.A., Cetner M.D., Łukasik I., Goltsev V., Ladle R.J. 2016. Chlorophyll a fluorescence as

a tool to monitor physiological status of plants under abiotic stress conditions. Acta Physiologiae Plantarum 38, 102. 11 p. https://doi.org/10.1007/s11738-016-2113-y

Khokhryakova A. 2020. Classification and characteristic of soils in urban areas (on the example of Odessa city). EUREKA: Life Sciences 5: 3–15. https://doi.org/10.21303/2504-5695.2020.001404

Kosova K., Vitamvas P., Urban M.O., Prasil I.T., Renaut J. 2018. Plant abiotic stress proteomics: the major factors determining alterations in cellular proteome. Frontiers in Plant Science 9, 122. 22 p. https://doi.org/10.3389/fpls.2018.00122

Krüger T.P., Ilioaia C., Johnson M.P., Ruban A.V., van Grondelle R. 2014. Disentangling the low-energy states of the major light-harvesting complex of plants and their role in photoprotection. Biochimica et Biophysica Acta (BBA) – Bioenergetics 1837(7): 1027–1038. https://doi.org/10.1016/j.bbabio.2014.02.014

Kunakh O.M., Ivanko I.A., Holoborodko K.K., Lisovets O.I., Volkova A.M., Nikolaieva V.V., Zhukov O.V. 2022. Modeling the spatial variation of urban park ecological properties using remote sensing data. Biosystems Diversity 30(3): 213–225. doi: 10.15421/012223

Li G., Rogers P., Huang J. 2021. Black locust (*Robinia pseudoacacia* L.) range shifts in China: Application of a global model in climate change futures. Climate Change Ecology 2, 100036. https://doi.org/10.1016/j.ecochg.2021.100036.

Lin K.H., Wu C.W., Chang Y.S. 2019. Applying Dickson quality index, chlorophyll fluorescence, and leaf area index for assessing plant quality of *Pentas lanceolata*. Notulae Botanicea Horti Agrobotanici Cluj-Napoca 47(1): 169–176. https://doi.org/10.15835/nbha47111312

Lin X.Y., Wang X.X., Zeng Q.Y. 2022. Leaf structure and photosynthesis in *Populus alba* under naturally fluctuating environments. International Journal for Photosynthesis Research 60(2): 240–250. doi: 10.322615/ps2022.012

Lovynska V., Sytnyk S. 2016. The structure of Scots pine and Black locust forests in the Northern Steppe of Ukraine. Journal of Forest Science 62(7): 329–336. doi: 10.17221/120/2015-JFS

Martin G.D. 2019. Addressing geographical bias: A review of *Robinia pseudoacacia* (black locust) in the Southern Hemisphere. South African Journal of Botany 125: 481−492. https://doi.org/10.1016/j.sajb.2019.08.014

Martínez-Ferri E., Zumaquero A., Ariza M.T., Barceló A., Pliego C. 2016. Non-destructive detection of white root rot disease in avocado rootstocks by leaf chlorophyll fluorescence. Plant Disease 100(1): 49–58. https://doi.org/10.1094/PDIS-01-15-0062-RE

Mathur S., Allakhverdiev S.I., Jajoo A. 2011. Analysis of high temperature stress on the dynamics of antenna size and reducing side heterogeneity of Photosystem II in wheat leaves (*Triticum aestivum*). Biochimica et Biophysica Acta (BBA) – Bioenergetics 1807(1): 22–29. https://doi.org/10.1016/j.bbabio.2010.09.001

Oukarroum A., Madidi S.O.E., Schansker G., Strasser R.J. 2007. Probing the responses of barley cultivars (*Hordeum vulgare* L.) by chlorophyll a fluorescence under drought stress and re-watering. Environmental and Experimental Botany 60(3): 438–446. https://doi.org/10.1016/j.envexpbot.2007.01.002

Romanov V.O., Braiko Y.O., Imamutdinova R.G., Fedak V.S. Sarakhan E.V. (Eds) 2013. Portable fluorometer 'Floratest'. Operating instructions. Kyiv: Glushkov V.M. Institute of Cybernetics of the NAS of Ukraine. 24 p. (in Ukrainian).

Tezara W., Mitchell V., Driscoll S., Lawlor D. 1999. Water stress inhibits plant photosynthesis bydecreasing coupling factor and ATP. Nature 401: 914–917. https://doi.org/10.1038/44842

Ruban A.V. 2016. Nonphotochemical chlorophyll fluorescence quenching: mechanism and effectiveness in protecting plants from photodamage. Plant Physiology 170(4): 1903–1916. https://doi.org/10.1104/pp.15.01935

Sayed O.H. 2003. Chlorophyll fluorescence as a tool in cereal crop research. Photosynthetica 41(3): 321–330. doi: 10.1023/B:PHOT.0000015454.36367.e2

Sepúlveda P., Johnstone D. 2019. Novel way of assessing plant vitality in urban trees. Forests 10(1), 2. 18 p. https://doi.org/10.3390/f10010002

Shupranova L., Holoborodko K., Seliutina O., Pakhomov O. 2019. The influence of *Cameraria ohridella* (Lepidoptera, Gracillariidae) on the activity of the enzymatic antioxidant systemof protection of the assimilating organs of *Aesculus hippocastanum* in an urbogenic environment. Biosystem Diversity 27(3): 238–243. https://doi.org/10.15421/011933

Shupranova L., Holoborodko K., Loza I., Zhukov O., Pakhomov O. 2022. Assessment of *Parectopa robiniella* Clemens (Lepidoptera: Gracillariidae) effect on biochemical parameters of *Robinia pseudoacacia* under conditions of an industrial city in Steppe Ukraine. Ekológia (Bratislava) 41(4): 340–350. https://doi.org/10.2478/eko-2022-0035

Sonti N.F., Hallett R.A., Griffin K.L., Trammell T.L.E., Sullivan J.H. 2020. Chlorophyll fluorescence parameters, leaf traits and foliar chemistry of white oak and red maple trees in urban forest patches. Tree Physiology 41(2): 269–279. https://doi.org/10.1093/treephys/tpaa121

Suchocka M., Swoczyna T., Kosno-Jończy J., Kalaji H. 2021. Impact of heavy pruning on development and photosynthesis of *Tilia cordata* Mill. trees. PLoS One 16(8), e0256465. 22 p. https://doi.org/10.1371/journal.pone.0256465

Uhrin P., Supuka J. 2016. Quality assessment of urban trees using growth visual and chlorophyll fluorescence indicators. Ekológia (Bratislava) 35(2): 160–172. https://doi.org/10.1515/eko-2016-0013

Uhrin P., Supuka J., Billiková M. 2018. Growth adaptability of Norway maple (*Acer platanoides* L.) to urban environment. Folia Oecologia 45(1): 33–45. https://doi.org/10.2478/foecol-2018-0004

Urban L., Aarrouf J., Bidel L. 2017. Assessing the effects of water deficit on photosynthesis using parameters derived from measurements of leaf gas exchange and of chlorophyll *a* fluorescence. Frontiers in Plant Science 8, 2068. 18 p. https://doi.org/10.3389/fpls.2017.02068

Vasylieva N. 2021. Food security in times of Covid-19: price aspects in Ukraine and neighboring EU countries. Montenegrin Journal of Economics 17(3): 21–30. https://doi.org/10.14254/1800-5845/2021.17-3.2

Vasylieva N., Vinichenko I., Katan L. 2015. Economic and mathematical evaluation of Ukrainian agrarian market by branches. Economic Annals-XXI 154(9–10): 41–44. http://ea21journal.world/index.php/ea-v154-09/

Wan Y., Zhang Y., Zhang M., Hong A., Yang H., Liu Y. 2020. Shade effects on growth, photosynthesis and chlorophyll fluorescence parameters of three *Paeonia* species. PeerJournal 8, e9316. 19 p. https://doi.org/10.7717/peerj.9316

Weather and Climate 2004–2023. Reference and information portal 'Weather and Climate'. http://www.pogodaiklimat.ru/climate/34504.htm

Zandalinas S., Mittler R., Balfagon D., Arbona V., Gomez-Cadenas A. 2018. Plant adaptations to the combination of drought and high temperatures. Physiologia plantarum 162(1): 2–12. doi: 10.1111/ppl.12540

Zhang P., Zhang Z., Li B., Zhang H., Hu J., Zhao J. 2020. Photosynthetic rate prediction model ofnewborn leaves verified by core fluorescence parameters. Scientific Reports 10, 3013. 11 p. https://doi.org/10.1038/s41598-020-59741-6

Zhao F., Zhang W., Liu Y., Wang L. 2018. Responses of growth and photosynthetic fluorescent characteristics in *Ottelia acuminata* to a water-depth gradient. Journal of Freshwater Ecology 33(1): 285–297. https://doi.org/10.1080/02705060.2018.1443841

FORESTRY IDEAS, 2024, vol. 30, No 1 (67): 66–78

Light acclimation of European beech (*Fagus sylvatica* L.) saplings after canopy destruction

Svetoslav Anev*

Department of Dendrology, Faculty of Forestry, University of Forestry, 10 Kliment Ohridski Blvd., 1797 Sofia, Bulgaria. *E-mail: svetoslav.anev@ltu.bg

Received: 13 February 2024 / Accepted: 05 March 2024 / Available online: 08 March 2024

Open Access: This article is licensed under a Creative Commons Attribution 4.0 International License.

Abstract

Gas exchange response of European beech (*Fagus sylvatica* L.) saplings to canopy opening was studied in the 'Petrohan' training and experimental forest range in Western Stara Planina Mt. Experimental plots were set on various altitudes (700–1450 m a.s.l.) and were chosen by their different sylvicultural or disturbances histories. The results of this study point out that European beech saplings show significant acclimation potential to changed post-cutting or windthrow environmental conditions. The light response curves at saplings from the open and the closed sites were typical for the sun and the shade ecotype of European beech leaves. The maximal photosynthesis was higher in more illuminated saplings but, as with light-use efficiency, did not vary significantly with cutting type, disturbance, altitude and air temperature. These physiological indicators rather express the biological characteristics of the European beech more strongly than a common response to environmental changes. In contrast, respiration, transpiration, water-use efficiency and light-compensation points were highly correlated with altitude and temperature. Especially the respiration and the transpiration varied much less with cutting type and natural disturbance. The light-compensation point was the most sensitive to both the type of stand opening and illumination, which can indicate the acclimation response of European beech saplings to stand disturbances of different sizes and causes.

Key words: light-compensation point, light-use efficiency, photosynthesis, transpiration, water-use efficiency.

Introduction

European beech (*Fagus sylvatica* L.), a widely distributed European forest tree species, is at its south-eastern limit of distribution in the Bulgarian mountains between 600 and 1800 m elevation. Several factors, such as shade tolerance, manage species' position in forest succession. Pioneer species are generally shade intolerant and rapidly grow in open ground. Late succession species survive under shading are somewhat intolerant to high light and grow slower (Leuschner and Ellenberg 2017).

Forest cuttings or disturbances can significantly alter the light environment experienced by forest saplings (Kozlowski

2002, Dietze and Clark 2008). The extent and nature of these changes depend on factors, such as the type and intensity of cuttings or disturbances, spatial distribution of canopy opening, as well as the surrounding forest structure. The type and distribution of forest cuttings can lead to spatial heterogeneity in light availability. Forest cuttings create edges between the cut area and the surrounding forest. The resulting edge effects can include increase in light penetration into the adjacent forest, creating transitional zones with higher light levels than the forest interior (Matlack and Litvaitis 1999, Zheng and Chen 2000).

The impact of forest cuttings on light availability may vary over time. Initially, there may be a period of intense light exposure following a cutting event, which gradually decreases as vegetation regrows and canopy closure occurs. Over time, the light environment may stabilize, but the composition and structure of the forest may still be altered compared to pre-cut conditions (Kermavnar et al. 2019). In selective logging or partial cutting scenarios, residual vegetation may remain in the stand, providing shade and modifying the light environment for saplings. Residual trees or shrubs can create a dappled light environment with varying shade and sun flecks, influencing sapling growth and regeneration (Wagner et al. 2011).

On the other hand, significant canopy destructions create a highly altered environment that can be critically stressful for saplings (Oliver 1980), especially late successional species, such as European beech. Large canopy openings and disturbances may expose beech saplings to increased environmental stresses, such as higher temperatures and more significant fluctuations in soil moisture. However, Dountchev and Zhelev (2015) found high survivability after windthrow on the north-eastern slopes of Vitosha Mt., Bulgaria. They point out that beech and some pioneer species have a potential to restore windthrow areas effectively. In the large gaps, European beech is more adaptive, especially compared to high-sensitive to intense direct light species, e.g. silver fir. However, it does not realize such an advantage compared to spruce (Čater et al. 2014, Čater and Diaci 2017). Čater (2021) point out that the generally better adaptability of European beech after disturbances might be closely related to their annual foliage development, compared to conifers and the longevity of fir and spruce needles.

European beech retains its position after the windthrow due to the ample advance regeneration released by the disturbance (Szwagrzyk et al. 2018). European beech saplings can acclimate to canopy openings through physiological, morphological and growth-related responses (Lichtenthaler et al. 1981, 2007). These responses allow them to adjust to the changes in light availability, competition and other environmental factors associated with canopy openings (Thornley 2002). One of the most vital acclimation traits of the European beech to illumination change is its ability to develop leaves with different morphological characteristics – sun and shade ecotype leaves, which can enhance light capture and maximise photosynthetic rates in high-light environments (Wagner et al. 2010). Eschrich et al. (1989) point out that sun- and shade-leaf determination in European beech is triggered towards the end of July. When applied before July, changes in light conditions influence the structure of the next season's leaves. After the middle of August, an increase in irradiation has little or no influence on the structure of primordia

of the next season's leaves.

Sun and shade leaves grow in different light environments within a forest canopy (Niinemets 2010). These leaves exhibit several differences in photosynthetic characteristics to adapt to the varying light conditions. Sun leaves in beech typically have smaller surface areas but are thicker and with more packed chloroplasts than shade leaves (Closa et al. 2010). This acclimation allows sun leaves to maximise light absorption and photosynthetic efficiency in high-light environments. Shade leaves may have higher chlorophyll concentrations to optimise light capture and utilisation in low-light conditions (Closa et al. 2010, Anev et al. 2015).

Additionally, shade leaves may contain different ratios of chlorophyll a to chlorophyll b compared to sun leaves (Lichtenthaler et al. 2007). Sun leaves of European beech typically exhibit higher photosynthetic rates and maximal photosynthesis than shade leaves. This acclimation allows to capture and utilise the abundant light in high-light environments efficiently and maximise carbon assimilation. Shade leaves of European beech generally have lower photosynthetic rates and maximal photosynthesis due to the limited light availability in shaded environments (Lichtenthaler et al. 2013). However, shade leaves have a higher light-use efficiency in low-light conditions, in compare to sun leaves, due to their specialised morphology and light-harvesting capabilities (Lichtenthaler et al. 1981). European beech saplings successfully change their photosynthetic apparatuses to adapt to changes in light availability. This may include adjustments in chlorophyll content, chloroplast structure (Lichtenthaler et al. 1981, 2007), in the activity of photosynthetic enzymes (Kubiske and Pregitzer 1997) to optimize photosynthetic rates under different light conditions.

According to Kaiser et al. (2015), studying the light response curve is essential to understand various factors that influence the photosynthetic efficiency of plants and how they respond to changes in their environment. The light response curve of photosynthesis represents the relationship between the photosynthesis rate and light intensity. According to Thornley (2002), at low light intensities, the rate of photosynthesis increases rapidly as light intensity increases. This phase occurs because the available light energy is insufficient to saturate the plant's photosynthetic apparatus and for this reason the rate of photosynthesis increases close to linearly with increasing light intensity. The second phase occurs when light intensity is at a level that saturates the photosynthetic capacity of the plant but does not cause damage to the photosynthetic apparatus. Beyond a certain light intensity, the rate of photosynthesis reaches a maximum level and plateaus. This occurs because the plant's photosynthetic apparatus becomes saturated with light energy, and the further increases in light intensity do not lead to a rise in the rate of photosynthesis and can even lead to photoinhibition (Wimalasekera 2019), although Wyka et al. (2007) did not establish a relationship between photoinhibition and shade tolerance in European beech. The shape of the light response curve may vary depending on factors, such as plant species, environmental conditions and the availability of other resources, such as carbon dioxide and water (Čater and Diaci 2017).

This study aimed to evaluate the potential of European beech saplings to acclimate the main physiological processes to changes in light regime and other microclimatic factors after different types of forest cutting and a large windthrow.

Materials and Methods

Experimental sites and plots

European beech (*Fagus sylvatica* L.) saplings' physiological responses to canopy opening were studied in the 'Petrohan' training and experimental forest range in Western Stara Planina Mt. The climate is mountainous with a moderate continental influence. The mean annual temperature at 1450 m is 4.8 °C, and the mean annual precipitation is about 1080 mm, with higher values in spring (Koleva and Peneva 1990, Kutchukova 1983). The soil is brown acid (district eutric cambisol) developed on granite, with a mean depth exceeding 80 cm (Malinova and Petrova 2019). Experimental sites were set on various altitudes (700–1450 m a.s.l.) in mono-dominated by European beech stands and were chosen according to their different silvicultural or disturbances histories. Each site includes two plots – stands with destructed and thus open (O) and closed (C) canopy stands for control (Table 1).

In 2011, the canopy of the ES1-O plot was opened by cutting off all mature trees (120 years) in a gap with sizes 25 × 40 m (0.1 ha), which was not subsequently expanded further. In 2013, the canopy (120-year-old) of the ES2-O plot opened a circle gap with a diameter of 50 m, which was expanded to 80 m (~0.5 ha) in 2018. In the winter of 2013/2014, the 80-year-old stand (ES3-O) was disturbed by a windthrow of a total area of ~2.5 ha. The canopy of ES4-O was opened by cutting off eight mature trees (160 years), evenly distributed on a total area of 0.1 ha. The control C-plots were placed near the O-plots in the stands, which have not been subject to logging or natural disturbance in at least the last twenty years.

The temperatures measured during the physiological measurements indicated that the areas with the canopy destruction were warmer. The differences vary from 0.39 °C on EP1 to 2.25 °C on EP3. Unlike the air temperature, the differences in relative humidity between the O and C plots were not unambiguous. The air was

Table 1. Characteristic of the open (O) and closed (C) canopy plots in experimental sites.

Experimental plot	Latitude, ° ′ ″	Longitude, ° ′ ″	Elevation, m	T_{AIR}, °C	*HD*, %	PPFD, μmol(γ)·m^{-2}·s^{-1}	*n*	*N*	N_L, mg·g$_{dw}^{-1}$
ES1-C	43°7′32″	23°7′25″	1439	20.68 ±0.07	56.6 ±0.5	47.7 ±5.8	22	176	17.3 ±0.3
ES1-O	43°7′30″	23°7′23″	1450	21.07 ±0.05	46.8 ±0.2	912.7 ±197.3	25	200	18.3 ±0.4
ES2-C	43°8′22″	23°8′33″	970	22.72 ±0.03	55.8 ±0.2	39.0 ±12.2	22	176	16.3 ±0.2
ES2-O	43°8′23″	23°8′37″	1015	23.56 ±0.10	56.5 ±0.4	773.2 ±244.2	25	200	17.0 ±0.4
ES3-C	43°11′15″	23°7′32″	870	24.25 ±0.11	59.2 ±0.5	163.1 ±95.2	20	160	17.2 ±0.3
ES3-O	43°11′18″	23°7′33″	862	26.45 ±0.14	46.3 ±0.5	1125.5 ±186.5	23	184	19.2 ±0.7
ES4-C	43°9′29″	23°9′00″	713	25.11 ±0.07	57.6 ±0.3	171.5 ±10.7	25	200	15.8 ±0.2
ES4-O	43°9′27″	23°8′59″	718	26.22 ±0.06	58.6 ±0.4	385.2 ±42.2	25	200	17.1 ±0.3

Note: Average values ± standard error of air temperature (*T*, °C), relative air humidity (*HD*, %), and photosynthetic photon flux density (PPFD, μmol(γ)·m^{-2}·s^{-1}) during the physiological measurements are presented. The number of light-response curves (*n*) and total number of measurements ($N = 8 \cdot n$) of each plot after data filtering are presented in the last two columns. N_L is the leaf nitrogen content ±SE.

drier in plots with a large disturbed canopy compared to the control plots – on ES1 with 9.8 % and ES3 with 12.9 %. However, the differences were insignificant at the ES with smaller canopy openings.

Total nitrogen concentration by Kjeldahl (Jones 1991) was determined on 100 leaves per plot in mixed sample from each O and C plot with three replications in 2019. The leaves of the lighted saplings tended to accumulate more nitrogen than those under the canopy, which was most pronounced in ES3 (windthrow).

Gas-exchange measurements

Gas exchange measurements were carried out in five consecutive growing seasons during the period 2018–2022 on typical, cloudless July days on five randomly chosen saplings with a similar height of around 1.5 m at each O and C plot. Net-photosynthetic rate (A_N) and transpiration rate (E) were measured on a third leaf of branches in the upper part of sapling's crown with a portable photosynthesis system Li-6400 (LiCor Instruments, Lincoln, NE, USA), equipped with shielded thermocouples, a red light-emitting diode light source (6400-02) and a quantum PAR sensor (LI-190) in the chamber. Before measurements, the instrument was calibrated according to standard procedures (LiCor 2012). Simultaneously with the physiological indicators, the air temperature (T_{AIR}), relative air humidity (*HD*) and photosynthetic photon flux density (*PPFD*) were recorded in the field measurements with the sensors built into the Li-6400. The summarized levels of these indicators are presented in Table 1.

Following the protocol of Evans and Santiago (2014), light-response curves for each leaf were recorded between 09:00–12:00 at ambient levels of environmental factors: CO_2-concentration at about 400 μmol(CO_2)·mol^{-1}, leaf temperature 20–26 °C, 45–60 % relative humidity. Leaves were given at least 3 min. to acclimate to chamber conditions under a saturating irradiance of 1000 μmol(γ)·m^{-2}·s^{-1} until TotalCV decreased below 0.5 %. Subsequently, the *PPFD* was changed in incremental steps, using eight levels of illumination (2000, 1000, 500, 250, 100, 50, 25 and 0 μmol(γ)·m^{-2}·s^{-1}) changed by the auto program 'Light_curve', in which we set the following criteria: minimum acclimation time of the leaf when the *PPFD* in the camera changes 60 s; maximum time before values are recorded 120 s; 'match mode' before each measurement; and TotalCV < 0.5 % (Broadbent 2012).

Photosynthetic light responses were individually analysed for each leaf with the non-rectangular hyperbolic model (Leverenz and Jarvis 1979, Marshall and Biscoe 1980, Prioul and Chartier 1977, Norman et al. 1992). Light-use efficiency (*LUE*, μmol(CO_2)·μmol(γ)$^{-1}$), the maximal photosynthesis (A_{MAX}, μmol(CO_2)·m^{-2}·s^{-1}), the dark respiration rate (R_D, μmol(CO_2)·m^{-2}·s^{-1}) and the convexity (θ) of the light response curve were calculated for each sample. All regression lines were fitted to the data by applying the least-squares approach of the Microsoft Excel Solver routine using the Newton algorithm (Office 2019, Microsoft, Redmond, WA, USA). The light-compensation point (*LCP*, μmol(γ)·m^{-2}·s^{-1}) was calculated by the regression equations as the *PPFD*, at which photosynthesis and respiration equalise (A_N = 0). Transpiration rates E, mmol(H_2O)·m^{-2}·s^{-1} of each leaf were calculated as the average value of transpiration, recorded at eight levels of *PPFD* during the measurements for light curves. Water-use efficiency of each leaf was calculated as $WUE = A_N/E$,

$\mu mol(CO_2)\cdot mmol(H_2O)^{-1}$.

Data were filtered before statistical processing according to the following criteria: $A_{MAX} > 0 > R_D$; $LCP > 0$; $0.125 > LUE > 0$; $E > 0$. One-way ANOVA tests and Tukey post hoc analysis were performed to determine the difference between the average values of A_{MAX}, R_D, *LCP*, *LUE*, *E* and *WUE* of saplings in O and C plots of experimental sites. All statistical procedures were performed with MS Excel and user-defined functions in Visual Basic for Applications (MS VBA 7.1, Microsoft, Redmond, WA, USA). Only statistically significant results (as defined by a *P*-value < 0.05) were discussed.

Results

Light-response curves

At all experimental sites, light curves of photosynthesis in the O-plots were typical for sun leaves and in C-plots they were typical for shade leaves (Fig. 1).

Photosynthesis saturates with light, reaches 90 % of its maximum at *PPFD* between 250 and 500 $\mu mol(\gamma)\cdot m^{-2}\cdot s^{-1}$ for the shade leaves (C-plots). At the same time, the sun leaves (O-plots) need significantly more intense light and their photosynthesis saturates above 1000 $\mu mol(\gamma)\cdot m^{-2}\cdot s^{-1}$. The difference between the curves of the O and C plots is most significant at the highest altitude, while the curves converge at decreasing altitudes. Light curves of O and C plots in ES1 are crossed (A_N of O and C plots become equal) at 42 $\mu mol(\gamma)\cdot m^{-2}\cdot s^{-1}$, in ES2 and ES4 – at 84 $\mu mol(\gamma)\cdot m^{-2}\cdot s^{-1}$, and in ES3 – at 90 $\mu mol(\gamma)\cdot m^{-2}\cdot s^{-1}$. Only in few saplings from the C-plots we found lower photosynthesis at 2000 than at 1000 $\mu mol(\gamma)\cdot m^{-2}\cdot s^{-1}$, which corresponds to the findings of Wyka et al. (2007). Lichtenthaler et al. (1981) point out that the acclimation of saplings to high quanta fluence rates is correlated with a higher photosynthetic capacity and especially with a higher light saturation of CO_2-fixation. Čater and Diaci (2017) show that in beech, the acclimatization to light climate develops relatively faster than some evergreen species, which might be closely related to their annual foliage development compared to conifers and the longevity of fir and spruce needles (Čater 2021).

The maximal photosynthesis (A_{MAX}) is significantly higher in O-plots, than in C-plots, except for ES3, where the difference is minimal as there is measured the minimum Amax at illuminated saplings and the maximum A_{MAX} at shaded saplings among all sites (Fig. 2).

The A_{MAX} of illuminated saplings in ES1-O was 1.99 times higher than in ES1-C on a background of more than 19 times higher *PPFD* in the gap. In ES2-O, *PPFD* was 18.8 times higher than such in ES2-C, and yet the difference between A_{MAX} was 2.05 times in favour of the illuminated saplings. Differences in A_{MAX} between sun and shade leaves were similar to those previously described for European beech (Lichtenthaler et al. 1981, 2007). In the windthrow site (ES3-O), despite the highest average *PPFD*, compared to the other sites, it was only 6.9 times higher than the ES3-C and probably for this reason, an insignificant difference of A_{MAX} between ES3-O and ES3-C was observed. That may be due to the edge effects, which can increase light penetration into the nearby forest stands (Matlack and Litvaitis 1999, Zheng and Chen 2000). Čater (2021) establishes similar levels of A_{MAX} in European beech saplings in the second year after exposure to the rapid increase of light due to sleet damages to the mature canopy. He points out that the suc-

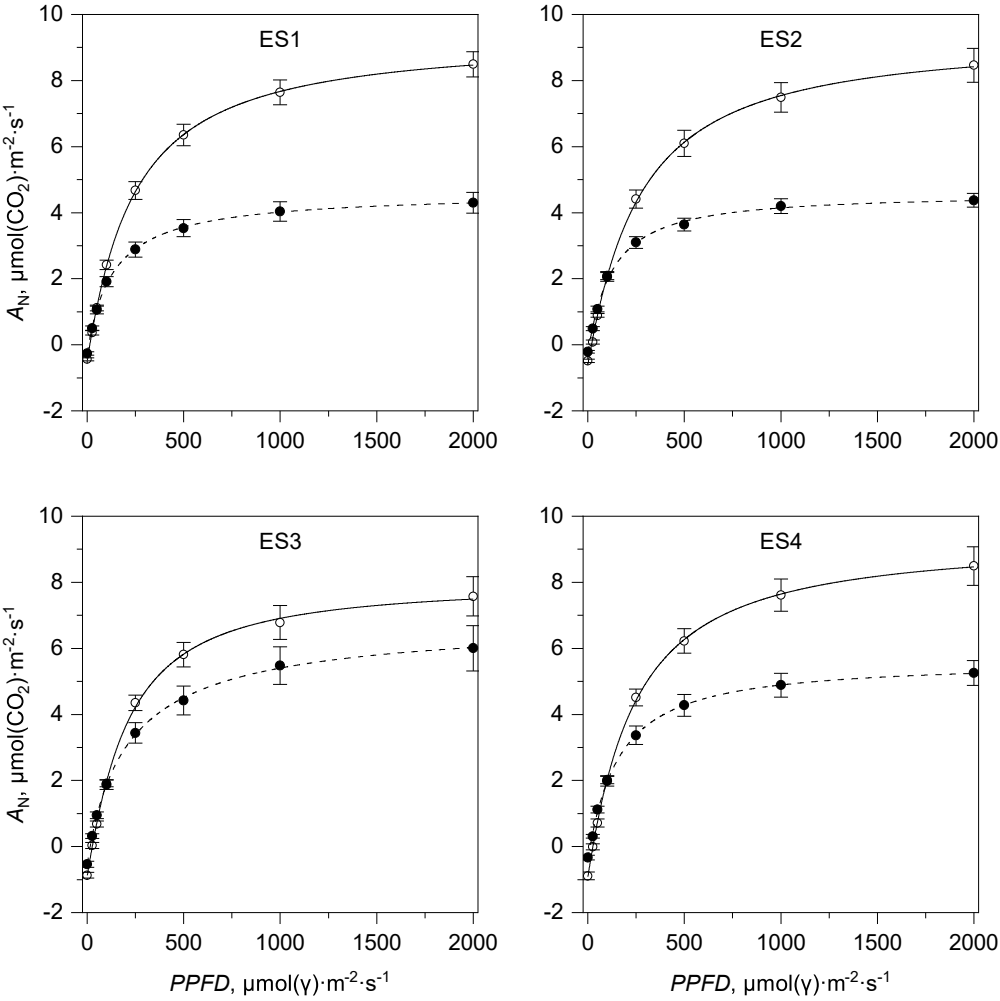


Fig. 1. Light-response curves of European beech saplings in the O-plots (—○—) and in the C-plots (- - ● - -) of experimental sites (ES1, ES2, ES3, and ES4).

Note: The mean values of net-photosynthetic rate (A_N) at various photosynthetic photon flux density (*PPFD*) are presented with circles. The standard errors of means are presented with whiskers. The lines presented regressions.

cessful acclimation of trees with advanced regeneration is mainly related to their ability to produce sun foliage. Reynolds and Frochot (2003) reported lag-missing in photosynthetic acclimation only four months after windthrow. This observation is similar to findings by Tognetti et al. (1994) for well-watered, shade-acclimated beech seedlings, in which an increase in photosynthetic rates began even by the end of the first week after transfer to high illumination and was nearly complete after only one month.

Despite the higher *PPFD* in the areas

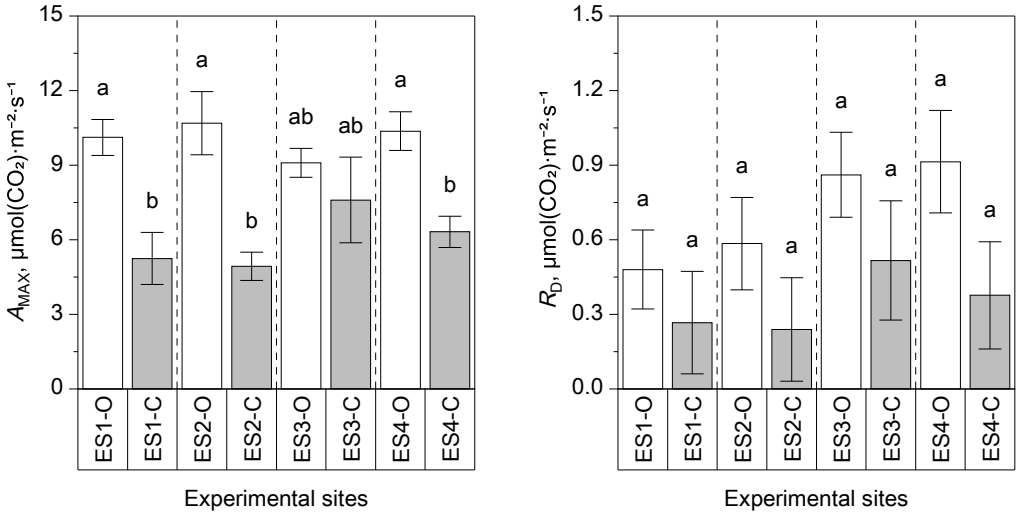


Fig. 2. Maximal photosynthesis (A_{MAX}) – left, and dark respiration rate (R_D) – right, of European beech saplings within saplings in the O-plots (□) and in the C-plots (■) of experimental sites (ES1, ES2, ES3, and ES4).

Note: The regression values (eq. 1) are presented with columns, and their standard errors are presented with whiskers. One-way ANOVA (Tukey) statistical test was applied to estimate the difference among all the variants. Different letters denote statistically significant differences.

with an open canopy, the air temperature was not appreciably affected (Table 1). This could explain the lack of significant differences between the R_D levels of the saplings in the open plots and under the assembly of the control areas. However, there was a strong negative correlation (Pearson correlation coefficient) between altitude and respiration rate (R = -0.47, P-value < 0.001) and a positive correlation between air temperature and respiration rate (R = 0.48. P-value < 0.001) of saplings in open canopy plots, already established by other authors (Hikosaka et al. 1999, Tjoelker et al. 2001, Smith and Dukes 2013).

The values of all the *LCP* of sun-acclimate saplings in O-plots were also significantly higher than the *LCP* of shade saplings in C-plots – 2.2 times on ES1, 2.43 times on ES2, 2.51 times on ES4 and only 1.71 times on windthrow (ES3) (Fig. 3). As Lichtenthaler et al. (1981, 2007) and Kolev and Anev (2022) point out, lower chlorophyll concentration and more intense respiration in sun leaves result in a higher *PPFD* to equalization photosynthesis and respiration. Like R_D, *LCP* in O-plots has a strong negative correlation (-0.340, P-value < 0.001) with altitude and a strong positive correlation (0.345, P-value < 0.001) with air temperature.

According to Čater (2021), quantum yield (or light-use efficiency) reflects the overall adaptation of the entire tree, especially in the upper third of the crown. He established that the *LUE* in European beech saplings increased in the years following the ice storm and windstorm. However, its studies have been carried out since the year after the destruction of the canopy, unlike ours, which occurs 5–7 years after cuttings or natural disturbance. In our experiment, *LUE* was not variate

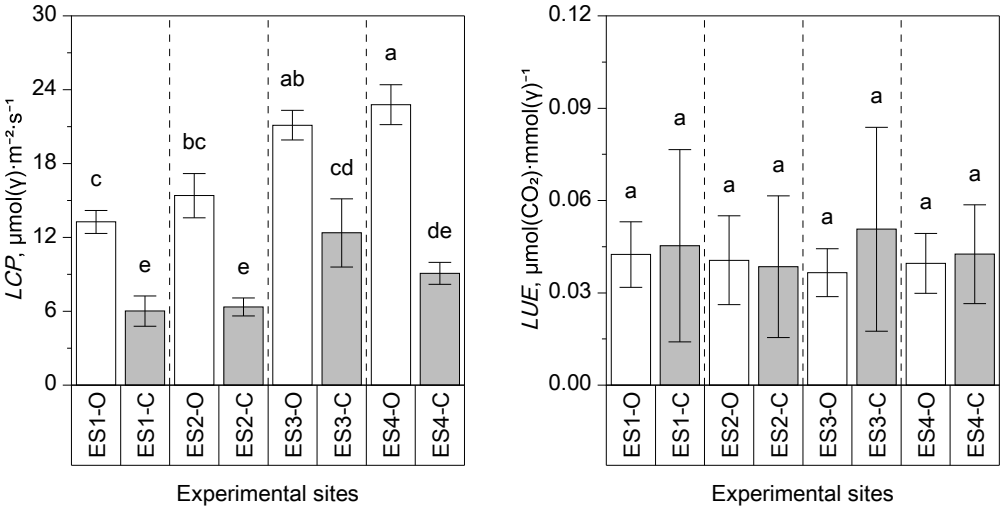


Fig. 3. Light-compensation point (*LCP*) – left, and light-use efficiency (*LUE*) – right, of European beech saplings in the O-plots (□) and in the C-plots (■) of experimental sites (ES1, ES2, ES3, and ES4).

Note: The regression values (eq. 1 and eq. 2) are presented with columns. The standard errors of regression values are presented with whiskers. One-way ANOVA (Tukey) statistical test was applied to estimate the difference among all the variants. Different letters denote statistically significant differences.

significant not only between the O-plots and the C-plots but also along the entire vertical profile of the experimental sites. This can be explained by, on one hand, the more minor scales of canopy destruction and, on the other hand, the more extended acclimatization period compared to similar experiments, e.g. Čater (2021).

The water regime of European beech saplings was much less affected than carbon assimilation. Both transpiration rates and *WUE* were not significantly different for saplings in O-plots and C-plots in all experimental sites (Fig. 4).

The results confirm our previous study (Anev and Marinova 2021), in which we hypothesized that the protective role of pioneer grass species allows European beech saplings to inhabit an environment with more humid air and maintain moderate levels of transpiration and *WUE*, even after canopy disturbance. Reynolds and Frochot (2003) confirm that functional (physiological) changes in response to the new environment occurred sooner than structural (morphological) changes. However, as with respiration and *LCP*, transpiration, although less pronounced, had a significant negative correlation (R = -0.29, P-value < 0.001) with altitude and a significant positive correlation (R = 0.30, P-value < 0.001) with air temperature.

Conclusions

The results of this study indicate that European beech saplings show significant assimilation acclimation potential to change post-cutting or windthrow environmental conditions. The light curves are

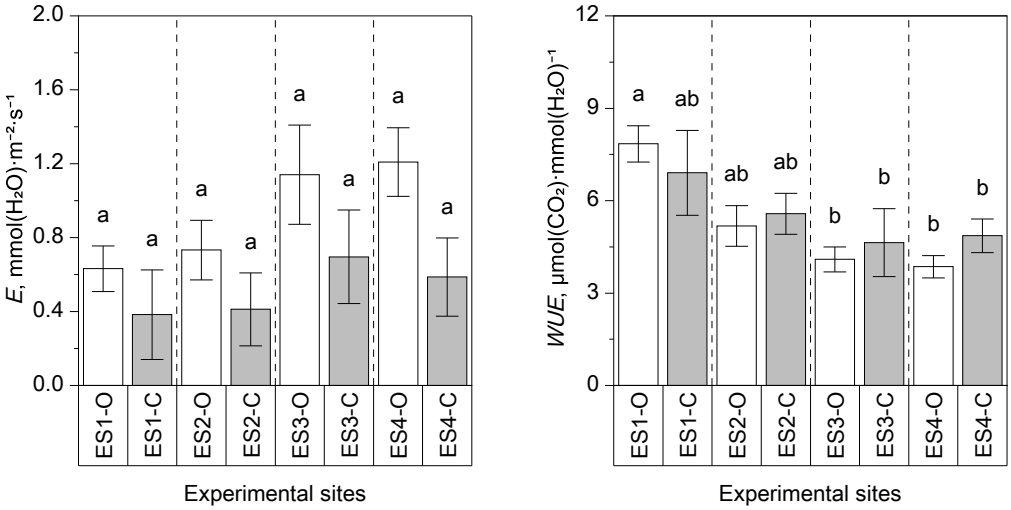


Fig. 4. Transpiration rate (*E*) – left, and water-use efficiency (*WUE*) – right, of European beech saplings in the O-plots (□) and in the C-plots (■) of experimental sites (ES1, ES2, ES3, and ES4).

Note: The mean values (eq. 3 and eq. 4) are presented with columns. The standard errors of mean values are presented with whiskers. One-way ANOVA (Tukey) statistical test was applied to estimate the difference among all the variants. Different letters denote statistically significant differences.

similar in all sites and visualize the typical change of photosynthesis with the change of illumination in the sun and in the shade ecotype of leaves. Maximal photosynthesis and light compensation points were higher in more illuminated plots. Dark respiration, light-use efficiency, transpiration rates and water-use efficiency did not vary significantly by cutting type or disturbance. We can conclude that these indicators reflect more strongly biological characteristics of the European beech typical sun and shade leaves than a response to environmental changes. Dark respiration, transpiration rate and light-compensation points were highly correlated with altitude and temperature. The light compensation point was the most sensitive to both the cause of stand opening and illumination, which can indicate the acclimation response of European beech saplings to stand disturbances of different sizes and causes.

Acknowledgements

The results of this study are product of several consecutive projects over time: Physiological aspects of natural regeneration in beech forests (NIS-159/2017); Adaptive changes in forests of European beech (*Fagus sylvatica* L.) after cutting or natural disturbance (NIS-B-1010); Physiological assessment of regeneration in European beech (*Fagus sylvatica* L.) forests using remote sensing methods (NIS-B-1144) and Assessment of the damage and recovery rate of the ice-breaking forests in the 'Petrohan' training and experimental forest range using remote sensing methods (NIS-B-1292). The author thanks the

teams of the above-mentioned projects for their assistance in the field measurements.

References

Anev S., Damyanova S., Tonchev T., Tzvetkova N. 2015. Transmittance coefficient of leaves from different crown parts of young beech (*Fagus sylvatica* L.) trees. Silva Balcanica 16(2): 53–59.

Anev S., Marinova A. 2021. Physiological adaptation of European beech (*Fagus sylvatica* L.) and wild cherry (*Prunus avium* L.) saplings after windthrow. Foresry Ideas 27(2): 436–445.

Broadbent E.N. 2012. Forest dynamics across temporal and spatial scales. PhD-thesis (Publication Number hs625bt1189). Stanford University. 287 p. http://purl.stanford.edu/hs625bt1189

Čater M. 2021. Response and mortality of beech, fir, spruce and sycamore to rapid light exposure after large-scale disturbance. Forest Ecology and Management 498: 119554. 8 p. https://doi.org/10.1016/j.foreco.2021.119554

Čater M., Diaci J. 2017. Divergent response of European beech, silver fir and Norway spruce advance regeneration to increased light levels following natural disturbance. Forest Ecology and Management 399: 206–212. https://doi.org/10.1016/j.foreco.2017.05.042

Čater M., Diaci J., Roženbergar D. 2014. Gap size and position influence variable response of *Fagus sylvatica* L. and *Abies alba* Mill. Forest Ecology and Management 325: 128–135. https://doi.org/10.1016/j.foreco.2014.04.001

Closa I., Irigoyen J.J., Goicoechea N. 2010. Microclimatic conditions determined by stem density influence leaf anatomy and leaf physiology of beech (*Fagus sylvatica* L.) growing within stands that naturally regenerate from clear-cutting. Trees 24(6): 1029–1043. https://doi.org/10.1007/s00468-010-0472-3

Dietze M.C., Clark J.S. 2008. Changing the gap dynamics paradigm: vegetative regeneration control on forest response to disturbance. Ecological Monographs 78(3): 331–347. https://doi.org/10.1890/07-0271.1

Dountchev A., Zhelev P. 2015. Natural and artificial regeneration of montane *Picea abies* forests in a cleared windthrow area in Vitosha nature park. Foresry Ideas 21(2): 293–305.

Eschrich W., Burchardt R., Essiamah S. 1989. The induction of sun and shade leaves of the European beech (Fagus sylvatica L.): anatomical studies. Trees 3(1): 1–10. https://doi.org/10.1007/BF00202394

Evans J.R., Santiago L.S. 2014. PrometheusWiki Gold Leaf Protocol: gas exchange using LI-COR 6400. Functional Plant Biology 41(3): 223–226. https://doi.org/10.1071/fp10900

Hikosaka K., Murakami A., Hirose T. 1999. Balancing carboxylation and regeneration of ribulose-1,5-bisphosphate in leaf photosynthesis: temperature acclimation of an evergreen tree, *Quercus myrsinaefolia*. Plant, Cell & Environment 22(7): 841–849. https://doi.org/10.1046/j.1365-3040.1999.00442.x

Jones J.B. (Jr.) 1991. Kjeldahl method for nitrogen determination. Micro-Macro Publishing, Athens. 79 p.

Kaiser E., Morales A., Harbinson J., Kromdijk J., Heuvelink E., Marcelis L.F.M. 2015. Dynamic photosynthesis in different environmental conditions. Journal of Experimental Botany 66(9): 2415–2426. https://doi.org/10.1093/jxb/eru406

Kermavnar J., Marinšek A., Eler K., Kutnar L. 2019. Evaluating Short-Term Impacts of Forest Management and Microsite Conditions on Understory Vegetation in Temperate Fir-Beech Forests: Floristic, Ecological, and Trait-Based Perspective. Forests, 10(10), 909. 22 p. https://doi.org/10.3390/f10100909

Kolev K., Anev S. 2022. Physiological aspects of natural regeneration in coppiced forest dominated by Quercus *frainetto* Ten. and Quercus *cerris* L. Foresry Ideas 28(2): 446–454.

Koleva E., Peneva R. 1990. Precipitation in Bulgaria. Climatic handbook. Bulgarian academy of science. 169 p. (in Bulgarian).

Kozlowski T.T. 2002. Physiological ecology of natural regeneration of harvested and disturbed forest stands: implications for forest management. Forest Ecology and Management 158(1–3): 195–221. https://doi.org/10.1016/S0378-1127(00)00712-X

Kubiske M., Pregitzer K.S. 1997. Ecophysiological responses to simulated canopy gaps of two tree species of contrasting shade tolerance in elevated CO_2. Functional Ecology 11(1): 24–32. https://doi.org/10.1046/j.1365-2435.1997.00050.x

Kutchukova M. 1983. Temperatures of air and soil. Climatic handbook. Bulgarian academy of science. 440 p. (in Bulgarian).

Leuschner C., Ellenberg H. 2017. Ecology of Central European Forests: Vegetation Ecology of Central Europe (Vol. I). Springer. 972 p. https://doi.org/10.1007/978-3-319-43042-3

Leverenz J.W., Jarvis P.G. 1979. Photosynthesis in Sitka Spruce. VIII. The effects of light flux density and direction on the rate of net photosynthesis and the stomatal conductance of needles. Journal of Applied Ecology 16(3): 919–932. https://doi.org/10.2307/2402865

Lichtenthaler H., Buschmann C., Döll M., Fietz H.-J., Bach T., Kozel U., Meier D., Rahmsdorf U. 1981. Photosynthetic activity, chloroplast ultrastructure, and leaf characteristics of high-light and low-light plants and of sun and shade leaves. Photosynthesis Research 2(2): 115–141. https://doi.org/10.1007/BF00028752

Lichtenthaler H.K., Ač A., Marek M.V., Kalina J., Urban O. 2007. Differences in pigment composition, photosynthetic rates and chlorophyll fluorescence images of sun and shade leaves of four tree species. Plant Physiology and Biochemistry 45(8): 577–588. https://doi.org/10.1016/j.plaphy.2007.04.006

Lichtenthaler H.K., Babani F., Navrátil M., Buschmann C. 2013. Chlorophyll fluorescence kinetics, photosynthetic activity, and pigment composition of blue-shade and half-shade leaves as compared to sun and shade leaves of different trees. Photosynthesis Research 117(1): 355–366. https://doi.org/10.1007/s11120-013-9834-1

LiCor 2012. Using the LI-6400 / LI-6400XT portable photosynthesis system. LI-COR Biosciences. 1324 p.

Malinova L., Petrova K. 2019. Petrohan training and experimental forest range cambisols classification. Forestry Ideas 25(1): 147–160.

Marshall B., Biscoe P.V. 1980. A model for C3 leaves describing the dependence of net photosynthesis on irradiance. Journal of Experimental Botany 31(1): 29–39. https://doi.org/10.1093/jxb/31.1.29

Matlack G.R., Litvaitis J.A. 1999. Forest edges. In: Hunter M. (Ed.), Maintaining biodiversity in forest ecosystems. Cambrige University Press: 210–233. https://doi.org/10.1017/CBO9780511613029.008

Niinemets Ü. 2010. A review of light interception in plant stands from leaf to canopy in different plant functional types and in species with varying shade tolerance. Ecological Research 25(4): 693–714. https://doi.org/10.1007/s11284-010-0712-4

Norman J.M., Welles J.M., McDermitt D.K. 1992. Estimating canopy light-use and transpiration efficiencies from leaf measurements. Application Note #105. Li-Cor Biosciense. 19 p.

Oliver C.D. 1980. Forest development in North America following major disturbances. Forest Ecology and Management 3: 153–168. https://doi.org/10.1016/0378-1127(80)90013-4

Prioul J.L., Chartier P. 1977. Partitioning of Transfer and Carboxylation Components of Intracellular Resistance to Photosynthetic CO_2 Fixation: A Critical Analysis of the Methods Used. Annals of Botany 41(4): 789–800. https://doi.org/10.1093/oxfordjournals.aob.a085354

Reynolds P., Frochot H. 2003. Photosynthetic acclimation of beech seedlings to full sunlight following a major windstorm event in France. Annals of Forest Science 60(7): 701–709. https://doi.org/10.1051/forest:2003064

Smith N.G., Dukes J.S. 2013. Plant respiration and photosynthesis in global-scale models: incorporating acclimation to temperature and CO_2. Global Change Biology 19(1): 45–63. https://doi.org/10.1111/j.1365-2486.2012.02797.x

Szwagrzyk J., Maciejewski Z., Maciejewska E., Tomski A., Gazda A. 2018. Forest recovery in set-aside windthrow is facilitated by fast growth of advance regeneration. Annals of Forest Science 75(3), 80. 12 p. https://doi.org/10.1007/s13595-018-0765-z

Thornley J.H.M. 2002. Instantaneous canopy photosynthesis: analytical expressions for sun and shade leaves based on exponential light decay down the canopy and an acclimated non-rectangular hyperbola for leaf photosynthesis. Annals of Botany 89(4): 451–458. https://doi.org/10.1093/aob/mcf071

Tjoelker M.G., Oleksyn J., Reich P.B. 2001. Modelling respiration of vegetation: evidence for a general temperature-dependent Q10. Global Change Biology 7(2): 223–230. https://doi.org/10.1046/j.1365-2486.2001.00397.x

Tognetti R., Michelozzi M., Borghetti M. 1994. Response to light of shade-grown beech seedlings subjected to different watering regimes. Tree Physiology 14(7–8–9): 751–758. https://doi.org/10.1093/treephys/14.7-8-9.751

Wagner S., Collet C., Madsen P., Nakashizuka T., Nyland R.D., Sagheb-Talebi K. 2010. Beech regeneration research: From ecological to silvicultural aspects. Forest Ecology and Management 259(11): 2172–2182. https://doi.org/10.1016/j.foreco.2010.02.029

Wagner S., Fischer H., Huth F. 2011. Canopy effects on vegetation caused by harvesting and regeneration treatments. European Journal of Forest Research 130(1): 17–40. https://doi.org/10.1007/s10342-010-0378-z

Wyka T., Robakowski P., Zytkowiak R. 2007. Acclimation of leaves to contrasting irradiance in juvenile trees differing in shade tolerance. Tree Physiology 27(9): 1293–1306. https://doi.org/10.1093/treephys/27.9.1293

Wimalasekera R. 2019. Effect of Light Intensity on Photosynthesis. In: Ahmad P. et al. (Eds), Photosynthesis, Productivity and Environmental Stress. Chapter 4: 65–73. https://doi.org/10.1002/9781119501800.ch4

Zheng D., Chen J. 2000. Edge effects in fragmented landscapes: a generic model for delineating area of edge influences (D-AEI). Ecological Modelling 132(3): 175–190. https://doi.org/10.1016/S0304-3800(00)00254-4

FORESTRY IDEAS, 2024, vol. 30, No 1 (67): 79–92

Kraft pulping of 3-year-old *Acacia* hybrid (*A. mangium* × *A. auriculiformis*) clonal wood

Salwaa Ainayya[1], Awanda Sifa Maharani[1], Sri Sunarti[2], Arif Nirsatmanto[2], and Ganis Lukmandaru[1*]

[1]Department of Forest Products Technology, Faculty of Forestry, Gadjah Mada University, Yogyakarta 55281, Indonesia. *E-mail: glukmandaru@ugm.ac.id
[2]National Research and Innovation Agency, West Java 16912, Indonesia.

Received: 15 February 2024 / Accepted: 03 April 2024 / Available online: 19 April 2024

Open Access: This article is licensed under a Creative Commons Attribution 4.0 International License.

Abstract

Clonal propagation is a silvicultural method that is often employed due to its advantages in terms of speed and flexibility. This method is typically combined with a reduction in rotation age to enhance the quality of pulp derived from *Acacia* wood. Therefore, this study aims to determine the basic wood properties, pulp and paper characteristics of a 3-year-old clonal *Acacia* hybrid (Aha and Ah044 clones) using the kraft process. Obtained samples were cooked using different cooking times, active alkali levels and sulfidity concentrations to obtain the optimum conditions (screened yield > 50 %). Pulp and paper properties were tested at different beating degrees. The result showed that at the optimum conditions of 120 min cooking time, 15 % active alkali and 20 % sulfidity, screened yield and kappa number ranged from 55–59 % and 33–34, respectively. The optimum levels of beating degree were 255–285 mL CSF, which produced handsheets with an average burst index, tear index, tensile index, brightness and opacity of 3.11 $kPa \cdot m^2 \cdot g^{-1}$, 4.56 $mN \cdot m^2 \cdot g^{-1}$, 39.26 $Nm \cdot g^{-1}$, 23.42 % and 93.66 %, respectively. At the same conditions, the Ah044 clone gave a higher screened yield but lower reject and kappa number values compared to the Aha clone. Although screened yield of clones was higher compared to samples from older trees in previous studies, the paper strength properties were generally poorer, indicating the high proportion of juvenile wood and high kappa number.

Key words: active alkali, beating degree, cooking time, physical properties, pulp wood, sulfidity.

Introduction

The significance of *Acacia mangium* Willd as a fundamental raw material is widely acknowledged due to its extensive industrial applications within the pulp and paper industries in Indonesia. The natural cross-breeding of *A. mangium* and *A. auriculiformis* A.Cunn.ex Benth often lead to the production of *Acacia* hybrid with a combination of the superior characteristics of both parents. These characteristics include fast growth, cylindrical and straight stems, enhanced wood quality, adaptability to marginal terrains and increased resistance to pest/disease attacks (Sunarti

et al. 2014). Therefore, the introduction of this hybrid serves as a strategic measure to rectify the prevailing imbalance between the supply and demand of raw materials for pulp and paper products.

Over the years, only few studies have been carried out on the pulp and paper characteristics of *Acacia* hybrid. A previous related study was conducted by Yamada et al. (1992), using a 9-year-old tree in Malaysia. The results of this study revealed that the screened yield and the physical properties of the paper exhibited higher levels compared to the two-parent species, namely *A. mangium* and *A. auriculiformis*. Similar trend was also observed by Haque et al. (2019), who studied *Acacia* hybrid wood aged 8 years from Bangladesh. However, the tensile and burst indices values were lower compared to those obtained by Yamada et al. (1992).

Government of Indonesia, through the Centre for Forestry Instruments Standard Assessment under the Ministry of Environment and Forestry, has developed intensive silviculture methods for *Acacia* species. These methods involve the maximization of production through appropriate genetic improvement and the use of growth enhancement measures, followed by shortening of rotation age (Miranda and Perreira 2002). To achieve improved plants from the breeding program to the plantation, clonal propagation techniques have been extensively explored due to their advantages in terms of speed and flexibility. The breeding process for fibre materials and the evaluation of superior clones are directly related to the yield, quality and economic benefits. Several studies have identified that the adoption of a shorter rotation can increase the probability of higher juvenile wood content in the harvested materials (Myers et al. 1996), but there are limited insights concerning their wood properties and pulp viability.

In previous reports, paper made from juvenile wood chemical pulp showed lower yield and strength properties compared to mature samples (Kirk et al. 1972, Zobel and van Buijtenen 1989, Severo et al. 2013). Juvenile pulps also tended to exhibit lower tear strength and opacity but higher burst and folding strength compared to matured variants (Shmulsky and Jones 2011). However, an exception to this trend was observed in the case of loblolly pine juvenile wood, where the paper showed superior strength and optical properties compared to mature samples when subjected to thermomechanical pulping (Myers 2002). These studies are expected to provide the needed information to aid in clonal and product developments. Therefore, this study aims to determine kraft pulp yields and physical paper properties of trees cultivated with clonal propagation (Aha and Ah044 clones) and harvested at 3 years based on optimum conditions of cooking with less concentration of chemicals and beating.

Material and Methods

Sample preparation

Wood material used in this study was obtained from 3-year-old *Acacia* hybrid (*A. mangium* × *A. auriculiformis*) trees with clone number Ah044 (dbh = 17.9 cm, tree height = 15.5 m, heartwood proportion = 30.4 %) and Aha (dbh = 9.6 cm, tree height = 10 m, heartwood proportion = 18.0 %). Furthermore, clones showed good growth properties and were from the multiplication of superior *Acacia* hybrid tissue culture developed by the Centre for Forestry Instruments Standard Assessment, Ministry of Environment and For-

estry, Jogjakarta. After felling, logs were debarked and manually made into wood chips (approximate dimensions of 12 × 12 × 5 mm). To provide a single composite chip, samples from various heights were combined. Sampled chips were then converted into wood meal (40–60 mesh size), which was used for chemical analysis.

Physical and chemical properties

Chemical values were obtained using the following test procedures: 1) ethanol-toluene extractive – ASTM D1107-96 (ASTM 2007), 2) hot-water soluble extractive – ASTM D1110-84, (ASTM 1984), 3) lignin content – ASTM D1106-84 (ASTM 1984), 4) holocellulose content (Wise method, Browning 1967), 5) alpha-cellulose content – Rowell et al. 2005), 6) solubility in 1% NaOH – ASTM D1109-84 (ASTM 1984) and 7) ash content – ASTM D1102-1984 (ASTM 1984).

Basic wood density was measured using the water displacement method. For fibre dimension and derived value measurements, match-stick size was cut from sampled chips. Sticks were then macerated in hot hydrogen peroxide and glacial acetic acid (20:1, v/v). Furthermore, fibres were stained with safranin, dehydrated in alcohol and mounted on Canadian balsam on glass slides. From each sample, microscopic images of the cross sections were collected using an Olympus digital microscope connected to a personal computer and stored in a digital format for image analysis (Image Pro Plus). The fibre length (L), diameter (D), lumen diameter (d) and cell wall thickness (W) were measured. Derived values were also determined for Runkel ratio ($2W/d$), slenderness ratio (L/D), flexibility ratio [$d/(D \cdot 100)$] and coefficient of rigidity (W/D) to evaluate the fibre quality for paper production (Yanez-Espinosa et al. 2004, Ohshima et al. 2005).

Kraft pulping process

Kraft (sulphate) pulps were prepared in an electrically heated rotary digester (KRK, laboratory scale). Chips (150 g) were cooked under different conditions, such as cooking for 60 to 150 min at maximum temperature. Active alkali level was also adjusted within the range of 15 to 21 % (as Na_2O) along with sulphidity from 15 to 30 %. Furthermore, the parameters used for the procedures included 170 °C maximum temperature, 45 min cooking time, 4:1 liquor to wood ratio (liters:kg) and 5-liter batch digester volumetric capacity. To obtain commercial level, the target screened yield was > 50 %. Digested chips were washed with water and then passed through a laboratory flat stationary screen, consisting of 200 mesh wire bottoms for the removal of residual cooking chemicals and pulp washing. Pulp was hand-squeezed and sampled for moisture content, and determination of the yield was carried out. TAPPI standard T2 14m-50 with slight modification was used to measure the kappa number of samples, and duplicate kraft cooks were made on each pulping condition.

Pulp beating process

The pulp used for beating process was selected based on the experimental results at optimum cooking conditions. The process was carried out using different beating times, including 0 (control), 10, 20 and 30 min. Samples were withdrawn from the Niagara beater after beating intervals of 0, 10, 20 and 30 min for Canadian Standard Freeness (CSF) testing (TAPPI standard T227, TAPPI 1992) and handsheet forma-

tion (TAPPI standard T205, TAPPI 1992). The beaten pulp was then moulded and tested to determine the value of the physical and optical properties of produced paper.

Handsheet testing

Physical properties of paper consisted of brightness, opacity, as well as burst, tear and tensile indices. Testing was carried out based on the TAPPI procedures (TAPPI 1992), where the burst, tear and tensile indices were evaluated using TAPPI T403, TAPPI T414 and TAPPI T494, respectively. Brightness and printing opacity were measured with a whiteness meter WSB-3 apparatus based on TAPPI Test Method T525.

Data analysis

Mean values of wood chemical and physical properties, as well as pulp properties, were compared by independent sample Student's t-test and a significance level of 0.05. Simple linear regression was used to relate measured handsheet strength values to pulp freeness. For comparison, strength values at 250 ml CSF levels were estimated for different beating times. Statistical analyses were done using SPSS ver. 16.

Results and Discussion

Basic properties

To assess its suitability for pulp and papermaking, the proximate chemical analysis of *Acacia* hybrid is presented in Table 1. Furthermore, the carbohydrate composition of *A.* hybrid could affect its pulp yield and the development of physical properties. The α-cellulose content of raw materials had a strong correlation with the yield (Al-Maruf and Jahan 2015). It was found that only the property of lignin content was significantly different according to t-test results at $p < 0.05$ significance level. Ah044 clone significantly had more lignin content than Aha clone. Apart from lignin content, both clones examined in this study showed only a slight difference in other parameters.

Table 1. Chemical properties of 3-year-old *Acacia* hybrid clonal wood and *Acacia* hybrid from previous researches.

Chemical properties	*Acacia* hybrid				
	Clone Ah044	Clone Aha	7 years[1]	9 years[2]	7 years[3]
Ethanol-toluene solubility, %	3.9	3.6	2.90	3.8	4.7
Hot water solubility, %	3.2	3.2	-	2.5	6.5
NaOH 1% solubility, %	19.6	19.6	-	13.9	15.4
Holocellulose, %	80.4	81.5	82.88	79.3	67.9
α-cellulose, %	47.4	47.8	45.45	47.3	45.5
Hemicellulose, %	33.0	33.6	37.43	32.0	22.4
Lignin, %*	26.3	23.6	30.91	26.6	29.0
Ash, %	0.44	0.53	-	0.59	1.6

Source: [1]Yahya et al. (2010) grown in Indonesia; [2]Yamada et al. (1992) grown in Malaysia; [3]Haque et al. (2019) grown in Bangladesh. * – values between the clones were significantly different at the 0.05 level by t-test.

The results revealed that clones had lower ash and lignin contents, as well as higher 1% NaOH solubilities compared to older trees obtained by seed propagation from previous studies. Clones also had lower lignin content and higher α-cellulose compared to *Acacia mangium* (Yahya et al. 2010) and *Acacia crassicarpa* (Martins et al. 2020) woods grown in Indonesia. Lignin was commonly known as an unfavourable wood component for pulp uses (Shmulsky and Jones 2011). This indicated that a reduction in its content through breeding could lead to production of raw materials with more desirable properties for pulping. According to previous studies, lower ash content could reduce the consumption of chemicals during cooking, pulp washing and beating (Biermann 1996). However, pulp yield was negatively correlated with the extractive content (ethanol-benzene, 1% NaOH, and water solubles), indicating that a higher value in 1% NaOH solubilities of samples often led to a reduction in yield.

Based on previous studies, wood density affected the fibre properties and pulp yield of samples (Downes et al. 2006). Among the clones, Ah044 showed slightly higher values in basic density, fibre length, lumen diameter, slenderness ratio and flexibility ratio compared to Aha (Table 2). However, t-test results introduced that there is no significant effect of clone differences on density, fibre dimension and derived values samples.

Density levels of clonal wood were lower compared to the 7-year-old samples from Indonesia (Yahya et al. 2010). In terms of fibre dimension, these clone samples had slightly lower values in length, cell wall thickness, lumen diameter and slender ratio but had higher diameter and flexibility ratio. Furthermore, long fibres increased the paper strength, particularly bursting strength and folding endurance (Tamolang and Wangaard 1961, Ona et al. 2001). Lower levels of density and fibre length in this experiment were possibly due to the high proportion of juvenile wood.

Table 2. Density, fibre dimension, and derived values of 3-year-old *Acacia* hybrid clonal wood.

Characteristics	*Acacia* hybrid		
	Ah044 Clone	Aha Clone	7 years[1]
Density, g·cm^{-3}	0.44	0.42	0.49
Fibre length, mm	0.91	0.87	1.08
Fibre diameter, μm	16.66	17.50	13.74
Fibre wall thickness, μm	1.74	2.26	2.51
Lumen diameter, μm	13.18	12.99	13.74
Runkel ratio	0.27	0.37	0.37
Slenderness ratio	55.52	51.10	57.4
Flexibility ratio	0.79	0.74	0.73
Coefficient of rigidity	0.11	0.13	0.13

Source: [1]Yahya et al. (2010) grown in Indonesia.

The derived values of *A.* hybrid fibres for both clones were comparable to the sample used by Yahya et al. (2010). The fibres of both clones had a good Runkel ratio and high flexibility coefficient. A previous study stated that low Runkel ratios were expected to increase fibre-to-fibre bonding and pulp yield (Ona et al. 2001, Oshima et al. 2005). The high levels of flexibility coefficient (> 0.7) were predicted to produce paper with high tensile and bursting strength values (Bektas et al. 1999). The low values of coefficient rigidity (< 0.5) were desirable in paper manufacturing, as they had a great influence on the quality of the product (Tamolang and Wangaard 1961). However, the ratio of length to width of both clones also referred to as slenderness ratios was lower compared to the conventional variants.

The slenderness ratio had a positive effect on the paper tear index (Ona et al. 2001), indicating that the clones could be predicted to produce paper with weaker tear strength.

Effects of cooking condition on pulp properties

Table 3 shows the pulping process, which was carried out at four different cooking times at 15 % active alkali and 25 % sulphidity. According to the results of t-tests applied to pulp properties, screened yield, reject and kappa number values have significant differences in term of cooking time (60 and 120 min), whereas the effect of clone is found to be insignificant on total yield. The values of Aha clone found for screened yield were determined to be higher, whereas reject and kappa number levels to be lower to those of Ah044 clone. The combination gave the highest screened and total yield at cooking time of 120 min for both clones. Results also revealed that the lowest level of reject was found at 150 min and the levels of kappa number were still high (26–33) > 60 min. This indicated that at 150 min of cooking, the residual lignin contents decreased sharply, while the degradation of carbohydrate fractions also increased, leading to reduced pulp yield. Therefore, based on experimental data at this stage, a maximum cooking time of 120 min could be considered as an optimum cooking condition for kraft pulping of *A.* hybrid.

Table 3. Yield and kappa number of kraft pulping with different cooking times of 3-year-old *Acacia* hybrid clonal wood.

Pulp properties	Cooking time, min	Clone	
		Ah044	Aha
Screened yield, %	60*	43.68	51.51
	90	52.47	52.90
	120*	55.54	58.81
	150	51.54	52.83
Reject, %	60*	15.94	7.34
	90	7.08	6.43
	120*	5.29	1.97
	150*	4.28	1.12
Total yield, %	60	59.61	58.85
	90	59.55	59.33
	120	60.83	60.78
	150	55.82	53.95
Kappa number	60*	50.19	37.94
	90	34.13	35.52
	120	33.93	33.21
	150*	31.34	26.12

Note: cooking condition: active alkali of 15 %, sulphidity of 25 %. * – values between the clones were significantly different at the 0.05 level by t-test.

Table 4 revealed that pulp yield, rejects, and kappa number decreased with increasing active alkali from 15 to 19 % (as Na_2O) at 120 min and sulphidity of 25 %. This indicated that the excessive active alkali charge could cause a decrease in lignin and polysaccharide contents. The results of the t-test, which were applied to reveal effect of clone, showed differences on screened yield and reject (active alkali of 15%), as well as kappa number (active alkali of 17%). At those concentrations, Aha clone showed significantly higher values in screened yield and kappa number than those Ah044 clone. The highest screened yield was observed in the Aha clone at an active alkali of 15 % (58.81 %). Although the amount of reject decreased with increasing active alkali, screened and total yields did not show an increase. Preliminary cooks were made at 13 % concentration, leading to low yield and high reject values (data not shown). The high kappa number at a low level of 15 %, which was considered the optimum cooking dose, indicated the high con-

sumption of cooking chemicals for *A*. hybrid to achieve lower kappa number.

Table 4. Yield and kappa number of kraft pulping with different active alkali charge of 3-year-old *Acacia* hybrid clonal wood.

Pulp properties	Active alkali, %	Clone	
		Ah044	Aha
Screened yield, %	15*	55.54	58.81
	17	51.71	52.32
	19	47.91	47.51
	21	48.27	49.70
Reject, %	15*	5.29	1.97
	17	2.00	2.49
	19	1.76	1.84
	21	1.12	1.13
Total yield, %	15	60.83	60.78
	17	53.71	54.30
	19	49.39	52.13
	21	48.91	49.41
Kappa number	15	33.93	33.21
	17*	22.56	26.04
	19	22.02	24.12
	21	18.27	18.27

Note: cooking condition: 120-minute cooking, 25 % sulphidity. * – values between the clones were significantly different at the 0.05 level by t-test.

Table 5 shows the effect of sulphidity on pulp yield, kappa number at distinct cooking time (120 min) and active alkali (15 %). The amounts of rejects and kappa number decreased with increasing sulphidity. The screened and total yield slightly decreased when the pulps were studied at 25 % sulphifidity. At the same cooking conditions, the Ah044 clone gave a higher screened yield but lower reject and kappa number values compared to the Aha clone. The Student´s t-test showed that the recorded screened yield, reject and kappa number differences between the clones were all statistically significant at sulphidity of 20 and 25 %. Aha clone significantly had lower reject and kappa number levels and also higher screened yield compared to those of Ah044. Based on the results, the magnitude of reduction in all parameters among sulphidity levels was slightly pronounced compared to those in active alkali, as shown in Table 4. This study showed that there were only slight variations between sulphidity of 20 and 25 % on pulp properties. Therefore, 20 % suphfidity could be considered an optimum dose, as there was practically no gain during the use of higher concentrations.

Table 5. Yield and kappa number of kraft pulping with different sulphidity charge of 3-year-old *Acacia* hybrid clonal wood.

Pulp properties	Sulphidity, %	Clone	
		Ah044	Aha
Screened yield, %	15	52.61	54.04
	20*	**55.94**	**59.06**
	25*	55.54	58.81
	30	53.25	56.07
Reject, %	15	5.64	3.65
	20*	**5.45**	**2.00**
	25*	5.29	1.97
	30*	3.36	1.95
Total yield, %	15	58.25	57.69
	20	**61.39**	**61.05**
	25	60.83	60.78
	30	56.61	58.02
Kappa number	15	35.06	34.73
	20*	**34.46**	**32.85**
	25*	33.93	31.21
	30	29.14	26.34

Note: cooking condition: 120-minute cooking, 15 % active alkali; bold numbers indicate pulps to be further processed into papers. * – values between the clones were significantly different at the 0.05 level by t-test.

Yamada et al. (1992) reported screened pulp yields of 55.9 % and a kappa number of 16.2 for a 7-year-old *A.* hybrid from Malaysia digested at a 13 % active alkali range. Meanwhile, Haque et

al. (2019) obtained screened pulp yields of 46.8 % and a kappa number of 28.7 for a 9-year-old sample from Bangladesh digested at 16 % active alkali. In this study, the results were higher in screened yield, particularly for the Aha clone (59.06 %) with a kappa number of 32.85. The lowest kappa number (18.27) was achieved at a 21 % active alkali with a lower screened yield (49.70 %). The comparatively low content of lignin (23.6 %) for the Aha clone than Ah044 clone (Table 1) explained the cause of the low kappa number. According to a previous study, mature wood showed greater yields compared to juvenile variants in other species (Hatton 1997, Severo et al. 2013). This indicated that tree age and geographical condition were some of the factors affecting kraft pulp yields.

Beating properties

Beating or refining was a mechanical process carried out in an aqueous environment, leading to important chemical and physical alterations in the fibre structure (Sparnochia and Castro 2019). This process had also been shown to improve fibre quality, enhance fibre-fibre adhesion, increase flexibility and reduce pulp sheet porosity. In this study, pulp freeness was measured as CSF. The freeness, which was mainly influenced by fibre fibrillation and the number of fine elements, showed values 645 mL CSF (Aha clone) and 675 mL CSF (Ah044) for the unbeaten pulps from optimum cooking conditions (120 min cooking time, 15 % active alkali and 20 % sulphidity). Beating process produced several tiny fibres and smaller pieces in the pulp that worsened pulp filtering, leading to a decrease in beating degree. As shown in Figure 1, time increased along with degree, thereby presenting a trend of linear growth. Based on the results, there were no large differences in beating response observed between the clone pulps evaluated. Furthermore,

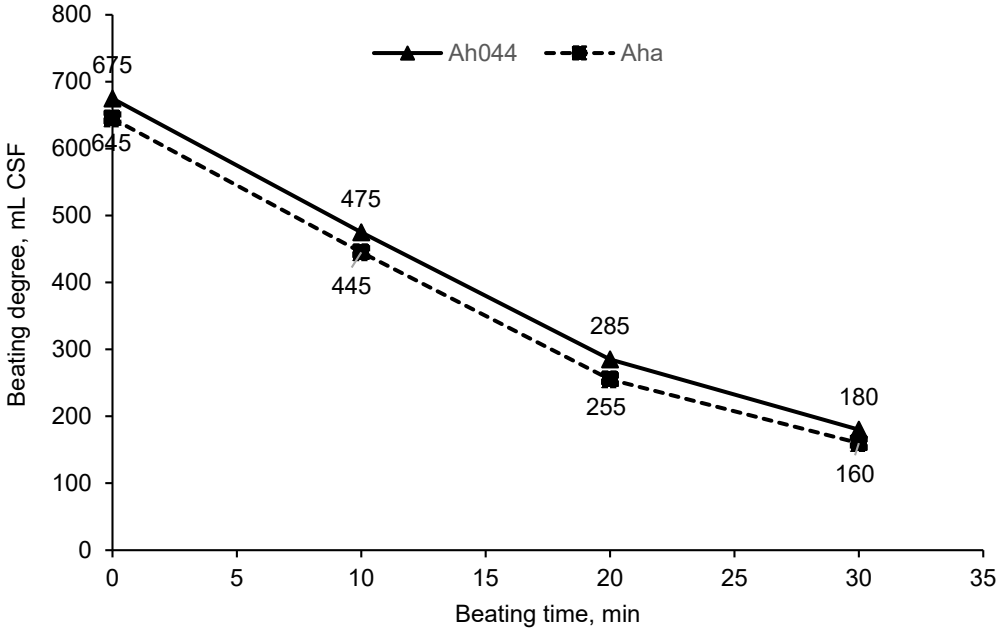


Fig. 1. The effect of beating time on beating degrees.

lesser time was required to reach a given freeness for pulps obtained from the Aha clone. The relative amounts of lignin components in the pulp fibres shown by the kappa number could account for differences in beatability (Rosli et al. 2011), with the Aha clone showing a slightly lower kappa number (Table 5).

Effects of beating on physical properties of handsheets

Pulps must be subjected to beating process to render them useful in making paper with acceptable properties. The two clones showed similar patterns in mechanical properties, as shown in Figure 2. However, slight difference was observed in the burst index, with Aha clone having higher values compared to the Ah044 clone. The burst index increased along with increasing beating time or decreasing degree. The results revealed that tear and tensile indices increased with decreasing beating degree and reached a maximum value at 20 min corresponding to beating level of 255 mL CSF (Aha clone) and 285 mL CSF (Ah044) as an optimum degree.

As beating time gradually increased due to cutting action, external and internal fibrillation and brushing action, tear strength experienced a decrease. Meanwhile, all other properties, which depend on hydrogen bonding except tear strength, improved with pulp beating (Dutt et al. 2009). Previous results on *A.* hybrid (Yamada et al. 1990) showed that the maximum value for burst and tensile indices was achieved at 263 mL CSF, while the maximum tear index was obtained at 509 mL CSF (unbeaten pulp). When the average fibre length decreased at 30 min (160–180 mL CSF), it became the main factor affecting tear and tensile indices, causing their reduction. Fibre cutting or reduction in the length could reduce the paper strength values, such as tensile index and tearing resistance (Brännvall 2009, Rosli et al. 2011).

The measured optical properties in this study, namely brightness and opacity, were important printability characteristics of paper. Brightness levels were found to decrease along with beating degree, while opacity increased, as shown in Figure 3. It was assumed that beating decreased the scattering coefficient of the paper and then reduced its brightness degree. The process caused more even distribution of residual lignin containing highly coloured chromophoric groups on fibre surfaces, which reduced this optical parameter (Serkov and Alen 2004). Pulps from the Aha clone showed higher brightness values compared to the Ah044 clone. This trend was also slightly observed for the opacity values, particularly at a low-level beating degree. The brighter pulps indicated fewer amounts of coloured substances and a reduction of the light scattering coefficient (Brännvall 2009). The lower kappa number of Aha clone pulps (Table 5) caused a higher level of brightness.

Opacity was defined as the ability of the paper sheet to conceal the printing on its backside (Brännvall 2009). This parameter increased along with the level of light scattering. An increase in the opacity level was related to the light scattering coefficient of the pulps, which increased with the intensity of beating (Gomide et al. 2005).

For comparison, values of handsheet mechanical properties of samples were obtained from a regression analysis set to beating degree of 250 mL CSF. The *A.* hybrid clones showed inferior strength properties compared to older trees from previous results (Table 6). The clones

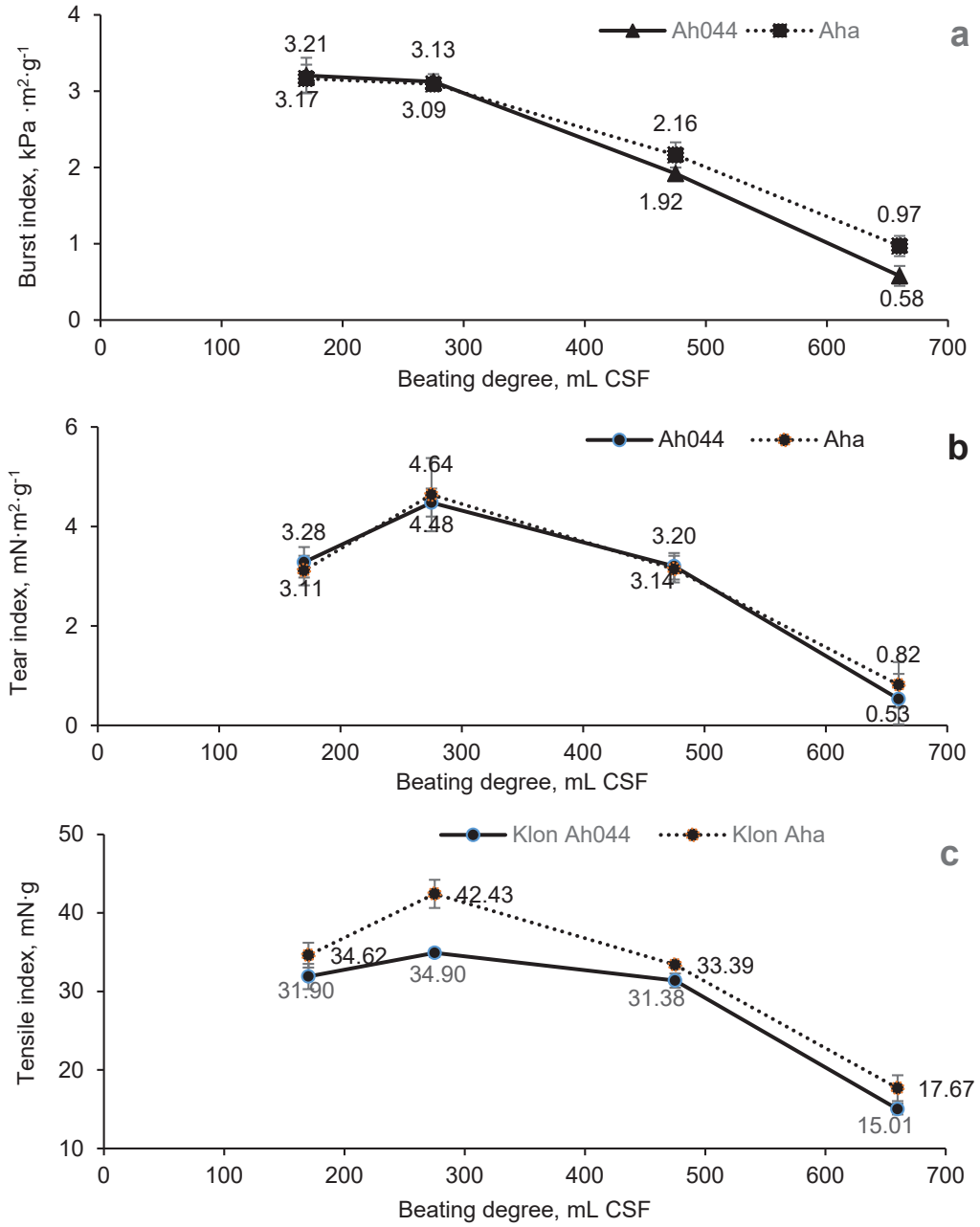


Fig. 2. The effect of the beating degree on the mechanical properties of the handsheets: (a) burst index, (b) tear index, (c) tensile index.

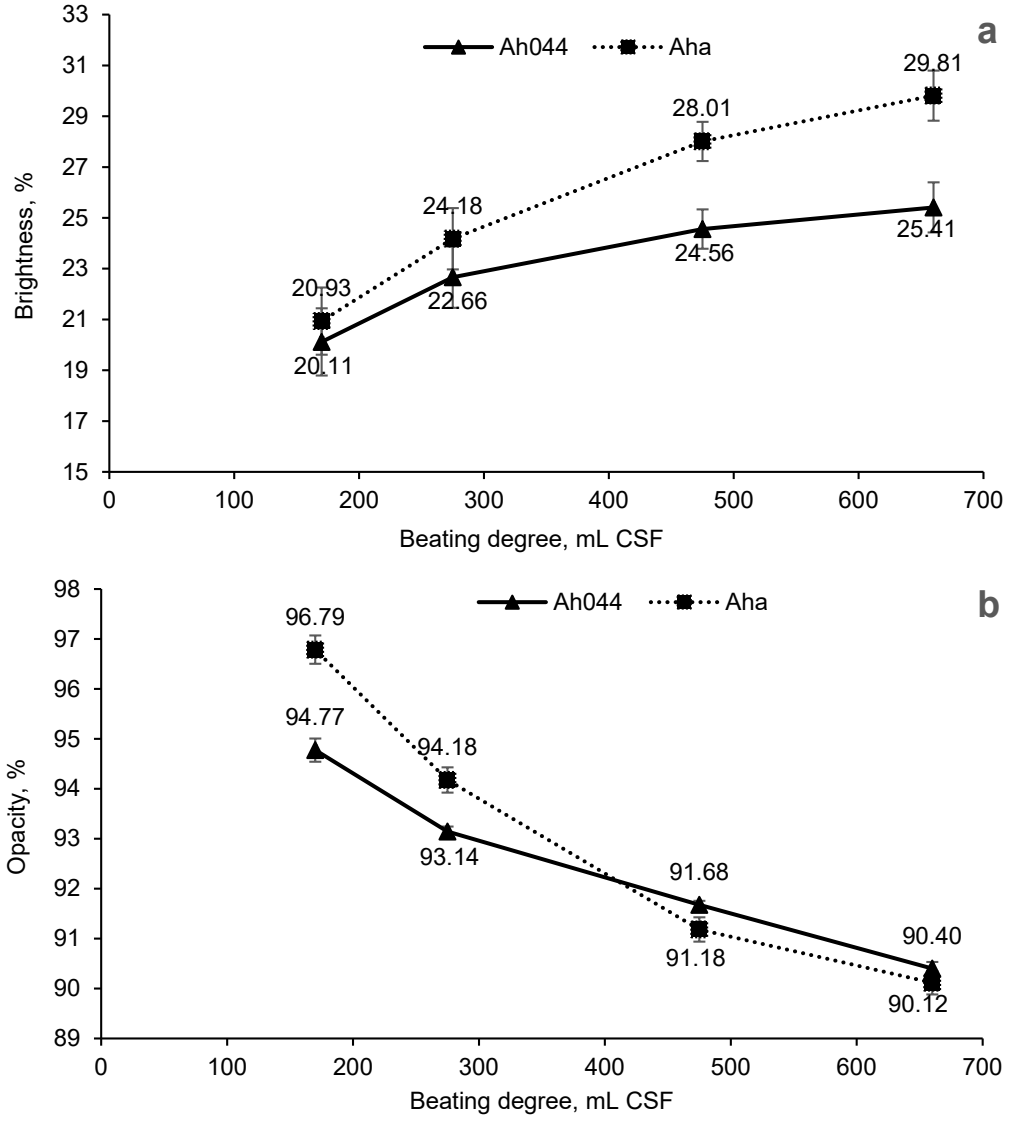


Fig. 3. The effect of the beating degree on the brightness and printing opacity of the handsheets: (a) brightness, (b) opacity.

handsheets also exhibited lower strength properties than those of *Acacia nilotica* (Lukmandaru et al. 2019) and *Acacia mangium* (Kardiansyah and Sugesty 2020) handsheets. This was possibly caused by the shorter fibre length and lower slenderness ratio levels. Furthermore, lower basic densities could contribute to the inferior strength of clone samples. This pattern had also been previously observed in other species (Myers et al. 1996, Santos and Sansigolo 2007). Another explanation could be that milder cooking kraft conditions in this exper-

Table 6. Mechanical properties of the handsheets of *Acacia* hybrid wood.

Sample	Burst index, $kPa \cdot m^2 \cdot g^{-1}$	Tear index, $mN. m^2 \cdot g^{-1}$	Tensile index, $Nm \cdot g^{-1}$
Ah044 Clone	3.06	5.04	38.80
Aha Clone	2.94	4.82	43.79
Acacia hybrid[1]	8.2	9.9	106
Acacia hybrid[2]	5.5	10	85.1

Note: Set to beating degree of 250 ml CSF. Source: [1]Yamada et al. (1992) 9 years, grown in Malaysia; [2]Haque et al. (2019) 8 years, grown in Bangladesh.

iment caused ineffective delignification, as indicated by the comparatively high kappa number (values: 32–34) obtained. Technically, lignin reduction increases the hydrogen bonding capacity of the fibres and consequently the strength of the fibre network. Furthermore, the kappa number within acceptable range for bleaching are from 18 to 20 for alkaline pulpings. The results showed that more intense cooking conditions were required to achieve satisfactory delignification levels, such as at a high 21 % active alkali (Table 4).

Examined wood properties were measured at an early age of clonal experiment and reported results could only apply to samples with juvenile characteristics. The information was expected to be helpful, as the amount of juvenile wood dominated the final merchantable volume under short-rotation forestry (Zobel and van Buijtenen 1989). Furthermore, these properties were expected to increase even further with 3 or 4 years of additional growth, leading to a significant increase in average fibre length.

Conclusions

In conclusion, according to the obtained results, clone Ah044 showed significantly higher lignin content compared to Aha clone. The optimum kraft cooking condition was 15 % active alkali charge and 20 % sulphidity with 120 min of cooking. At the same cooking conditions, Ah044 had a higher screened yield but lower reject and kappa number values compared to Aha. Furthermore, in terms of handsheet mechanical strength, Ah044 had lower values in the burst index compared to Aha. The clones in this study produced higher pulp yield but had higher kapa number, as well as lower handsheet strength, compared to samples produced from older trees with seed propagation in previous reports. Wood from clonal propagation was an interesting material, which was expected to possess the required properties for pulp and paper production over time.

Acknowledgements

This study was funded by Thesis Recognition Grant (Rekognisi Tugas Akhir/RTA) 2023 Gadjah Mada University.

References

Al-Maruf A., Jahan M.S. 2015. Pulping and papermaking potential of six mangrove species in Bangladesh. Journal Indian Academy of Wood Science 12(2): 116–121. https://doi.org/10.1007/s13196-015-0153-3

ASTM 1984. Annual book of ASTM standards. American Scociety for Testing and Material. Race St., Philadelphia.

ASTM 2007. Annual book of ASTM standards. Section Four Construction Volume 04.10 Wood. Baltimore.

Biermann C.J. 1996. Handbook of pulping and papermaking. Second Edition. Aca-

demic Press, California. 776 p.

Bränvall E. 2009. Pulp characterisation. In: Ek M., Gellerstedt G., Henrikkson G. (Eds), Pulp and paper chemistry and technology. Volume 2, Pulping Chemistry and Technology, Berlin, New York: De Gruyter. https://doi.org/10.1515/9783110213423

Browning B.L. 1967. Methods of wood chemistry. Volume 2. New York, Interscience Publisher, A Division of John Wiley and Sons, Inc. 498 p.

Downes G., Worledge D, Schimleck L., Harwood C., French J., Beadle C. 2006. The effect of growth rate and irrigation on the basic density and kraft pulp yield of *Eucalyptus globulus* and *E. nitens*. New Zealand Journal of Forest Science 51(3): 13–22. https://api.semanticscholar.org/CorpusID:138500341

Dutt D., Upadhyay J.S., Singh B., Tyagi C.H. 2009. Studies on *Hibiscus cannabinus* and *Hibiscus sabdariffa* as an alternative pulp blend for softwood: An optimization of kraft delignification process. Industrial Crops and Products 29(1): 16–26. https://doi.org/10.1016/j.indcrop.2008.03.005

Gomide J.L., Colodette J.L., Oliveira R.C., Silva C.M. 2005. Caracterização tecnológica, para produção de celulose, da nova geração de clones de eucalipto do Brasil. *Árvore* 29(1): 129–137. https://doi.org/10.1590/S0100-67622005000100014

Hatton J.V. 1997. Pulping and papermaking properties of managed second-growth softwoods. TAPPI Journal 80(1): 178–184.

Haque M.M., Aziz M.I., Hossain M.S., Quaiyyum M.A., Alam M.Z., Jahan M.S. 2019. Pulping of hybrid *acacia* planted in a social forestry program in Bangladesh. Cellulose Chemistry and Technology 53(7–8): 739–745. https://doi.org/10.35812/CelluloseChemTechnol.2019.53.72

Kardiansyah T., Sugesty S. 2020. Effect of active alkali on characteristic of *Acacia mangium* and *Eucalyptus pellita* bleached kraft pulp. Jurnal Selulosa 10(1): 9–20 (in Indonesian). http://dx.doi.org/10.25269/jsel.v10i01.291

Kirk D.G., Breeman L.G., Zobel B.J. 1972. A pulping evaluation of juvenile loblolly pine. TAPPI Journal 55(11): 1600–1604.

Lukmandaru G., Setiaji F., Siagian R.M. 2019. Effects of mixing ratio of heavily beaten *Pinus merkusii* pulp on physical properties of kraft *Acacia nilotica* pulp sheets. Wood Research Journal 10(2): 53–60. doi: 10.51850/wrj.2019.10.2.53-60

Martins G.S., Yuliarto M., Antes R., Sabki, Prasetyo A., Unda F., Mansfield S.D., Hodge G.R., Acosta J.J. 2020. Wood and pulping properties variation of *Acacia crassicarpa* Cunn. ex Benth. and sampling strategies for accurate phenotyping. Forests 11(10): 1–20. https://doi.org/10.3390/f11101043

Miranda I., Pereira H. 2002. The variation of chemical composition and pulping yield with age and growth factors in young *Eucalyptus globulus*. Wood and Fiber Science 34(1): 140–145.

Myers G.C. 2002. Thermomechanical pulping of loblolly pine juvenile wood. Wood and Fiber Science 34(1): 108–115.

Myers G.C., Arola R.A., Horn R. A., Wegner T.H. 1996. Chemical and mechanical pulping of aspen chunkwood, mature wood, and juvenile wood. TAPPI Journal 79(12): 161–168. https://api.semanticscholar.org/CorpusID:32402085

Ona T., Sonoda T., Ito K., Shibata M., Tamai Y., Kojima Y., Ohshima J., Yokota S., Yoshizawa N. 2001. Investigation of relationships between cell and pulp properties in Eucalyptus by examination of within-tree variations. Wood Science and Technology 35(3): 229–243. https://doi.org/10.1007/s002260100090

Oshima J., Yokota S., Yoshizawa N., Ona T. 2005. Examination of within-tree variations and the heights representing whole-tree values of derived wood properties for quasi-non-destructive breeding of *Eucalyptus camaldulensis* and *Eucalyptus globulus* as quality pulpwood. Journal of Wood Science 51(2): 102–111. https://doi.org/10.1007/s10086-004-0625-3

Rosli W.D.W., Mazlan I., Law K.N. 2011. Effect of lignin on *Acacia mangium* kraft pulp refining behaviour. Cellulose Chemistry and Technology 45(9–10): 643–648. https://api.

semanticscholar.org/CorpusID:136046784

Rowell R., Petersen R., Han J.S., Rowell J.S., Tshabalala M.A. 2005. Cell wall chemistry. In: Rowell R. (Eds), Handbook of wood chemistry and wood composites, CRC Press, Boca Raton, London, New York, Washington, D.C.: 63–64.

Santos S.R., Sansígolo C.A. 2007. Influência da densidade básica da madeira de clones de *Eucalyptus grandis* × *urophylla* na qualidade da polpa branqueada. *Ciencia Florestal* 17(1): 53–63. https://doi.org/10.5902/198050981935

Serkov A.A., Alen R. 2004. Beating-induced yellowing of TCF- and ECF-bleached pulps. TAPPI Journal 3(1): 3−6.

Severo E.T.D., Sansigolo C.A., Calonego F.W., Barrieros R.M. 2013. Kraft pulp from juvenile and mature woods of *Corymbia citriodora*. BioResources 8(2): 1657–1664. doi: 10.15376/biores.8.2.1657-1664

Shmulsky R., Jones P.D. 2011. Forest products and wood science: An introduction, 7th Edition. Oxford, Wiley-Blackwell. 504 p.

Sparnochia L., Castro M.A. 2019. Cell wall changes caused by refining in fibre of *Eucalyptus grandis* W. Hill ex Maiden bleached kraft pulp: a ultra- and nano-structural approach. Wood Science and Technology 53: 911–925. https://doi.org/10.1007/s00226-019-01103-1

Sunarti S., Nirsatmanto A., Setyaji T. 2014. Hybrid acacia (*A. mangium* × *A. auriculiformis*): New variety for raw materials of pulp and paper [Akasia hibrida (*A. mangium* x *A. auriuliformis*): varietas baru untuk bahan baku industri pulp dan kertas]. Jakarta, IPB Press. 6 p. (in Indonesian).

Tamolang F.N., Wangaard F.F. 1961. Relationship between hardwood fiber characteristics and pulp sheet properties. TAPPI Journal 44(3): 200–216.

TAPPI 1992. TAPPI test methods 1992–1993. Atlanta, Georgia. TAPPI Press. 800 p

Yahya R., Sugiyama J., Silsia D., Grill J. 2010. Some anatomical features of an *Acacia hybrid*, *A. mangium* and *A. auriculiformis* grown in Indonesia with regard to pulp yield and paper strength. Journal of Tropical Forest Science 22(3): 343–351. http://www.jstor.org/stable/23616663

Yanez-Espinosa L., Terrazas T., Lopez-Mata L., Valdez-Hernandez J.I. 2004. Wood variation in *Laguncularia racemosa* and its effect on fibre quality. Wood Science and Technology 38: 217–226. https://doi.org/10.1007/s00226-004-0228-6

Yamada N., Khoo K.C., Yusoff N.M. 1992. Sulphate pulping characteristics of *Acacia* hybrid, *Acacia mangium* and *Acacia auriculiformis* from Sabah. Journal of Tropical Forest Science 4(3): 206–214. http://www.jstor.org/stable/43594803

Zobel B.J., van Buijtenen J.P. 1989. Wood variation: Its causes and control. New York, Springer-Verlag. 363 p.

FORESTRY IDEAS, 2024, vol. 30, No 1 (67): 93-106

Grafting of *Syringa vulgaris* L. cultivars

Teodora Lyubomirova[1], Nasko Iliev[2*], and Ivan Iliev[1]

[1]Department of Landscape architecture, University of Forestry, 10 St. K. Ohridski Blvd., 1797 Sofia, Bulgaria. E-mails: tlyubomirova@gmail.com (TL), ivilievltu@yahoo.com (II)
[2]Department of Forestry, University of Forestry, 10 St. K. Ohridski Blvd., 1797 Sofia, Bulgaria.
[*]E-mail: ilievnasko@abv.bg

Received: 26 February 2024 / Accepted: 19 April 2024 / Available online: 26 April 2024

Open Access: This article is licensed under a Creative Commons Attribution 4.0 International License.

Abstract

Spring and autumn grafting of *Syringa vulgaris* L. and its cultivars Charles Joly and Mme Florent Stepman have been researched using chip budding, top wedge graft and splice graft methods. Two-year-old vegetative saplings of *Ligustrum ovalifolium* Hassk. were used as rootstocks. Chip budding showed the worst results in both spring and summer. Successful bud adhesion reached 56.7 % ('Charles Joly') and 70.0 % ('Mme Florent Stepman'), respectively. It has been established that propagation can be successfully achieved through grafting in both seasons. The graft adhesion reached 76.7 % in spring and 85 % in summer grafting by spice graft. Better growth indicators of the scions were observed during summer grafting. This outlines the recommendation to use summer splice grafting.

Key words: chip budding, top wedge, splice graft.

Introduction

Common lilac (*Syringa vulgaris* L.) is famous for its great diversity of ornamental cultivars and hybrids (Krüssmann 1986, Dirr and Heuser 1987, Dirr 1998, Fiala 2008, Rudolf 2008). However, their cloning in a generative way is impossible because of the heterozygosity of this species (Fiala 2008). *Syringa vulgaris* cuttings are generally considered difficult-to-root (Patience and Alderson 1984, Waldenmaier and Bünemann 1991, Howard and Ridout 1992, Howard 1993, Marks and Simpson 2000, Ford et al. 2002, Tyatyushkina 2007) and vary between the cultivars (Schmidt 1978, Bassuk et al. 1984, Tyatyushkina 2007), their age (Waldenmaier and Bünemann 1991), period of cuttings collection (Schmidt 1978) and different part of the shoots (Bojarczuk and Jankiewicz 1975, Schmidt 1978).

The *in vitro* multiplication depends on the cultivar (Pinker et al. 1993, Tomsone et al. 2007), the rooting of shoots in some cultivars is low (Hildebrandt and Harney 1983, Refouvelet et al. (1998) and depends on their rejuvenation (Nesterowicz et al. 2006) by continuous subculturing (Pierik et al. 1993, Lyubomirova and Il-

iev 2013) and auxin pulse treatment (Lyubomirova and Iliev 2013). Also, the acclimatisation could be problem and *in vitro* is expensive method of propagation (Refouvelet et al. 1998).

The grafting is used to overcome these limits when valuable cultivars cannot be propagated through rooting of cuttings and *in vitro* propagation (Coggeshall 1977, Wedge 1977, Hand 1978, Mezzit 1978, Hartmann and Kester 1983, Einset and Alexander III 1984, Waldenmaier and Bünemann 1991, Hartmann et al. 2002, Cameron et al. 2003). It is performed onto rootstocks produced by seed (Krüssmann 1964, Waldenmaier and Bünemann 1991, Cameron et al. 2003) or onto plants, propagated by rooted cuttings (Hartmann et al. 2002). According to Hartmann et al. (2002), factors influencing the success of grafting include: 1) compatibility between the rootstock and scion, 2) suitable physiological condition of the rootstock and scion, 3) direct contact between the conducting tissues of the components, 4) grafting method, and 5) environmental conditions during and after grafting and care for the grafted plants.

The rootstock influences the morphological characteristics of the grafted plant. Krüssmann (1964), Waldenmaier and Bünemann (1991), and Mac Cartaigh and Spethmann (2000) recommend using seedlings stocks of the species for propagating cultivars of *Syringa vulgaris*. A major drawback of these rootstocks is the formation of root shoots, which if not removed, can overgrow and suppress the scion (Krüssmann 1964, Dirr and Heuser 1987, Waldenmaier and Bünemann 1991). According to Krüssmann (1964), the use of other closely related species that do not form sprouts is a possible alternative, but *S. japonica* (Maxim.) Decne, *S. josikaea* J.Jacq. ex Rchb., *S. villosa* Vahl, *S. reticulata* (Blume) H.Hara and *S. tomentella* Bureau & Franch. are unsuitable due to poor shoot growth. Other species suitable for grafting common lilac cultivars include *Ligustrum ovalifolium* Hassk. (Krüssmann 1964, Mac Cartaigh and Spethmann 2000), *Fraxinus pensilvanica* Marshall (Krüssmann 1964, Dirr and Heuser 1987), and *Fraxinus ornus* L. (Krüssmann 1964). The same author reported that using *Fr. ornus* rootstocks resulted in later development of seedlings but with rapid growth. The use of vegetative propagated rootstocks allowed avoidance of genetic variation and cloning of disease-resistant genotypes (Krüssmann 1964, Hartmann et al. 2002). Krüssmann (1964) recommended one-year-old rooted mature cuttings of *Ligustrum* as rootstocks. On them, the scion grows vigorously for several years (eg one-year-old grafted plants reach 30–90 cm depending on the cultivar), but then the leaves become sparse, suffer from chlorosis, and growth slows down. Standard practice in the USA is to deeply plant the grafted plant the following year so that the scion can form its own roots. This typically takes around 3 years. Shoots can later be detached from the resulting own-rooted plants (Krüssmann 1964, Mac Cartaigh and Spethmann 2000, Fiala 2008). This practice also allows rejuvenation of the obtained shrubs after a certain age by cutting the stem to the ground, allowing the shrub to regenerate from its root shoots (Fiala 2008).

According to some studies, timing is the most significant factor affecting the success of grafting (Iliev and Petrakieva 2007). Suitable physiological condition for the scion means that the buds are dormant, while the tissues are capable of forming the callus necessary for adhesion. The rootstock may be dormant or

actively growing depending on the grafting time (Hartmann et al. 2002). An important indicator for the appropriate period is the ease of separating the bark from the wood and the presence of active cambium (Kolev 1977, Hartmann et al. 2002, Dancheva 2012). Optimal grafting periods are: 1) late winter and early spring (Krüssmann 1964, Mac Cartaigh and Spethmann 2000, Schmid 2002, Alexandrov 2007, Iliev and Petrakieva 2007) and 2) summer (July-September), after the height growth and the development of summer wood are over (Bodjakov et al. 1962, Dirr and Heuser 1987, Waldenmaier and Bünemann 1991, Mac Cartaigh and Spethmann 2000, Schmid 2002, Iliev and Petrakieva 2007, Dancheva 2012). Summer grafting is preferred for outdoor application in nurseries, as higher temperatures at that time facilitate secure union, and there is no need to store the scions (Dirr and Heuser 1987, Waldenmaier and Bünemann 1991, Hartmann et al. 2002, Dancheva 2012). However, according to some authors, later grafting is undesirable due to the risk of graft damage in winter (Bodjakov et al. 1962, Krüssmann 1964, Dirr and Heuser 1987, Alexandrov 2007, Iliev and Petrakieva 2007, Dancheva 2012). When grafting is done in winter or early spring, scions are obtained from branches developed in the previous growing season. They are stored at low humidity and temperature to prevent bud development. For storage lasting 2–3 weeks, a temperature of about 5 °C is recommended, and for periods of 1 to 3 months, about 0 °C. For summer grafting, scions are obtained from one-year-old branches of the current season's growth. The lower parts of the shoots are preferred, as the upper ones may not have hardened enough (Hartmann et al. 2002).

The choice of an appropriate method is a significant factor for the success of grafting (Iliev and Petrakieva 2007). Different methods are recommended for cultivars of *S. vulgaris* depending on the site of grafting and the diameter of the components – splice grafting (Dirr and Heuser 1987, Mac Cartaigh and Spethmann 2000), whip and tongue grafting (Krüssmann 1964), cleft grafting (Krüssmann 1964, Mac Cartaigh and Spethmann 2000), and T-budding (Waldenmaier and Bünemann 1991). According to Krüssmann (1964), Pierik et al. (1988), and Waldenmaier and Bünemann (1991), the most widely used method for grafting common lilac cultivars is budding. The advantages of this method include good tissue union, reduced risk of wind damage, and effective use of scions. This is especially useful when obtaining scions is limited to a cultivar specimen (Bodjakov et al. 1962, Hartmann et al. 2002, Alexandrov 2007).

In the grafting, it is necessary to ensure a direct contact between the rootstock conductive tissues and the scion (Hartmann et al. 2002). In order for the tissues of both components to fuse successfully, a new vascular cambium should be formed (Yeoman and Brown 1976). The cambium layers of the rootstock and scion should be close enough for the newly formed parenchyma cells to fuse (Hartmann et al. 2002). It is recommended the graft wounds to be the same in size to complete matching of both components' tissues (Alexandrov 2007). Cut surfaces should be tightly fixed to each other and protected from drying out by an elastic bandage, wax or parafilm (Hartmann et al. 2002). Temperature during and after grafting is important for callus formation. At temperatures below 0 °C callus is not formed, above 32 °C callus formation slows down and cell damage occurs, and above 40 °C they die (Hartmann et al.

2002). The same author indicated optimal temperatures between 20 and 28 °C, low air humidity can also suppress callus formation.

The aim of the present study was to investigate the effect of grafting method, working period and stock plant genotype on the successful grafting of *Syringa vulgaris* and its ornamental cultivars Charles Joly and Mme Florent Stepman onto *Ligustrum ovalifolium* rootstocks.

Material and Methods

As rootstocks for grafting, 2-year-old individuals of *L. ovalifolium*, propagated by rooting of cuttings and grown in pots with a volume of 2 L and containing peat were used. The peat (sphagnum) was with the following parameters: structure 0.5 mm; 20 $kg \cdot m^{-3}$ bulk density; pH = 5.5–6.5 in water; electrical conductivity 35–45 $mS \cdot m^{-1}$ ±25 %; enriched with NPK (nitrogen 14 : phosphorus 10 : potassium 18) 1.5 $kg \cdot m^{-2}$.

Scions were obtained from *S. vulgaris* and its ornamental cultivars Charles Joly and Mme Florent Stepman. To assess the physiological condition of the rootstock and scion, spring (March 4th–7th) and summer (August 28th – September 9th) grafting were performed. The following grafting methods were researched during the specified periods: chip budding, top wedge graft and splice grafting. Each of the studied factors (genotype, physiological condition of the rootstock and scion, and grafting method) was replicated 3 times, with each replication containing 20 grafts. Scions were collected immediately before grafting from one-year-old shoots of mature individuals. For spring grafting, scions and dormant buds from cuttings obtained before vegetation beginning were used and stored in a refrigerator under 4 ℃ for 2 weeks. For summer grafting, scions were collected immediately before grafting, and their leaves were removed, leaving 0.5–1.0 cm of the leaf stalk. The grafting site was tied with an elastic band. Grafted plants were grown in greenhouse conditions with care provided permanent removal of shoots from the rootstock. Spring grafting was performed in the greenhouse of the University of Forestry (Fig. 1) at a temperature of 20–24 °C and 70 % air humidity provided by an automatic misting system. Summer grafting was performed outdoors in ‘Sequoia’ nursery (Fig. 2). The grafts were irrigated once during the night with duration of 40 min.



Fig. 1. Spring greenhouse grafting.



Fig. 2. Summer outdoors grafting.

Results and Discussion

Spring grafting

Regarding the dynamics of fusing and development of the grafts, the results indicated that on the 14th day after grafting, swelling of the buds was observed, and development of some of the grafts began. The grafts by the wedge grafting method develop the fastest, with the percentage of developed grafts reaching 58.3 ±10.1 % and 51.7 ±6.7 % respectively for *S. vulgaris* and 'Charles Joly' on the 28th day after grafting. This process progressed more slowly for 'Mme Florent Stepman', with only 24.4 ±8.0 % of developed grafts on the 28th day (Table 1).

Budded scions grafted by budding method develop the slowest. On the 42nd day after grafting, the percentage of developed grafts reached 36.7 ±13.3 %, 23.3 ±4.4 %, and 31.1 ±9.7 % respectively for *S. vulgaris*, 'Charles Joly', and 'Mme Florent Stepman' (Table 1). Comparative analysis of the results showed that after 180 days, at the end of the experiment, the highest percentage of successful graft adhesion from spring grafting was obtained with 'Charles Joly' using the splice grafting method (76.7 ±12 %). The results for *S. vulgaris* and 'Mme Florent Stepman' (73.3 ±10.1 % and 71.1 ±5.9 % respectively) did not statistically differ from it. The obtained results for successfully fused grafts by wedge graft method were very

Table 1. Percentage of developed and successfully grafted scions grafted onto *L. ovalifolium* rootstocks for (1) *S. vulgaris*, (2) 'Charles Joly', and (3) 'Mme Florent Stepman'.

Period	Cultivar	Method	14th day	28th day	42nd day	180th day
Spring	1	1	0.0 ±0.0 a A	3.3 ±3.3 ab A	36.7 ±13.3 d-g B	51.7 ±10.9 abc B
		2	6.7 ±1.7 c A	58.3 ±10.1 e B	61.7 ±3.3 hi B	73.3 ±10.1 cde B
		3	3.3 ±1.7 abc A	33.3 ±4.4 d B	53.3 ±1.7 gh B	73.3 ±10.1 cde C
	2	1	0.0 ±0.0 a A	6.7 ±1.7 ab A	23.3 ±4.4 cde B	56.7 ±7.3 a-d C
		2	1.7 ±1.7 ab A	51.7 ±6.7 e B	71.7 ±4.4 I BC	73.3 ±3.3 cde C
		3	0.0 ±0.0 a A	26.7 ±12.0 cd B	40.0 ±12.6 efg B	76.7 ±12.0 e C
	3	1	0.0 ±0.0 a A	19.9 ±7.6 bcd AB	31.1 ±9.7 def B	40.0 ±7.7 ab B
		2	2.2 ±2.2 ab A	24.4 ±8.0 cd AB	42.2 ±2.2 fg B	71.1 ±2.2 cde C
		3	4.4 ±2.2 bc A	26.7 ±7.7 cd B	53.3 ±10.2 gh B	71.1 ±5.9 cde C
Summer	1	1	0.0 ±0.0 a A	0.0 ±0.0 a A	0.0 ±0.0 a A	38.3 ±7.3 ab B
		2	0.0 ±0.0 a A	0.0 ±0.0 a A	0.0 ±0.0 a A	76.7 ±4.4 de B
		3	0.0 ±0.0 a A	15.0 ±2.9 abc B	23.3 ±4.4 cde B	55.0 ±5.0 a-d C
	2	1	0.0 ±0.0 a A	0.0 ±0.0 a A	0.0 ±0.0 a A	28.3 ±6.0 a B
		2	0.0 ±0.0 a A	0.0 ±0.0 a A	3.3 ±1.7 ab A	85.0 ±0.0 e B
		3	0.0 ±0.0 a A	0.0 ±0.0 a A	10.0 ±5.0 abc A	63.3 ±8.3 b-e B
	3	1	0.0 ±0.0 a A	0.0 ±0.0 a A	0.0 ±0.0 a A	70.0 ±0.0 cde B
		2	0.0 ±0.0 a A	0.0 ±0.0 a A	1.7 ±1.7 a A	66.7 ±8.3 cde B
		3	5.0 ±2.9 bc A	6.7 ±4.4 ab A	21.7 ±6.0 bcd B	80.0 ±5.8 e C

Note: The means ± standard error within a column followed by the same small letter and within a row followed by the same capital letter were not significantly different, estimated by One-Way ANOVA followed by a *post hoc* LSD test at $p \leq 0.05$. Method: 1 – chip budding, 2 – wedge grafting, 3 – splice grafting.

close, and no statistical difference was found between them (Fig. 3).
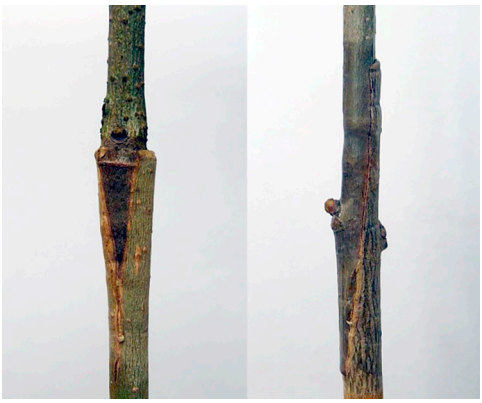


Fig. 3. Successfully fused components in wedge grafting (left) and splice grafting (right).

At the end of the experiment, budding showed the least successful graft adhesions (40.0 ±7.7 % to 56.7 ±7.3 %) compared to the other two grafting methods. Only for *S. vulgaris*, there was no statistical difference between the results obtained with the three methods applied (Table 1).

Summer grafting

During summer grafting, the scions did not develop during the current growing season. An exception was observed with the splice grafting method, where development of some buds on the scion began immediately after grafting, and the developed grafts reached 10.0 ±5.0 % to 23.3 ±4.4 % for the cultivars (Table 1). The obtained shoots successfully lignify outdoors and form new growth in the following growing season. With the wedge grafting method, there was observed bud breakage in a small number of buds in September, but there was no subsequent growth of shoots. There was no swelling or growth observed in the grafted buds. Their development only began in the following spring and was relatively delayed compared to the other two methods. The highest percentage of successful graft adhesion was achieved with autumn splice grafting of 'Mme Florent Stepman' (80.0 ±5.8 %). Comparative analysis of the results after 180 days, at the end of the experiment, shows that splice and wedge grafting methods were equally effective for all three cultivars, ensuring successful graft adhesion. Budding ranked third, with an exception noted for 'Mme Florent Stepman', where a graft fusion of 70.0 ±0.0 % was recorded. Results for this method with *S. vulgaris* and 'Charles Joly' were significantly lower (28.3 ±6.0 % and 38.3 ±7.3 % respectively) (Table 1).

The statistical analysis of the obtained results showed that among the factors studied, the duration of the grafting period had the greatest influence on the grafting success (Table 2, $F = 429.716$, $p = 0.000$). In second place was the timing (Table 2, $F = 176.612$, $p = 0.000$), and in third was the grafting method (Table 2, $F = 56.906$, $p = 0.000$). However, the genotype of the studied cultivars did not affect the success of grafting (Table 2, $F = 0.701$, $p = 0.498$). These results support the conclusion made by some authors that both spring (February-March) and summer (August-September) grafting are successful for cultivars of *S. vulgaris* (Mac Cartaigh and Spethmann 2000), and splice graft is an effective method for their grafting, ensuring successful adhesion between scion and stock (Krüssmann 1964, Dirr and Heuser 1987, Mac Cartaigh and Spethmann 2000). Although, to the best of our knowledge, there is no published data regarding its usage with common lilac cultivars, the wedge graft method proves to be equally successful in terms of percentage

Table 2. Significance of factors and their interaction on the mean percentage of grafted scions estimated by a *post hoc* LSD test.

Factors	Mean difference (*F*)	Level of significance (*p*)
CV	0.701	0.498
M	56.906	0.000
DR	429.716	0.000
SR	176.612	0.000
CV × M	6.090	0.000
CV × DR	1.187	0.317
CV × SR	5.346	0.006
M × DR	6.604	0.000
M × SR	10.853	0.000
DR × SR	50.325	0.000
CV × M × DR	1.330	0.208
CV × M × SR	0.196	0.940
CV × DR × SR	1.263	0.278
M × DR × SR	6.013	0.000
CV × M × DR × SR	3.593	0.000

Note: Significant effect at $p \leq 0.05$, F – Fisher's criterion. R-squared = 0.931 (Adjusted R-squared = 0.897), $p < 0.05$. Legend: CV = cultivar, M = grafting method, DR = graft union duration, SR = grafting season.

of successfully grafted scions. A disadvantage of using the California Privet may be the formation of a large number of water sprouts from the stock, which need to be regularly removed.

When using the budding method, only one shoot developed from the grafted bud, which did not branch during the current growing season. With the splice grafting and wedge graft methods, one or more shoots developed from the grafted scion (Table 3). Priority was given to the shoots at the top of the scion compared to those at the bottom. However, some lateral shoots also developed on some grafts. During spring grafting, shoot development statistically increased until the 28th day. Although the mean values at the end of the experiment were higher than those at day 28th and 42nd, a statistical difference between the results was only observed with the wedge grafting for *S. vulgaris* (Table 3). During summer grafting, as shoots started their development in the following growing season, the highest average value was recorded at the end of the experiment for all variants. Using the wedge graft method, the highest values were obtained during autumn grafting for 'Charles Joly' and 'Mme Florent Stepman' – 1.7 ±0.1. This result does not statistically differ from the result for *S. vulgaris* (1.6 ±0.1), but it differs from all results of spring grafting by this method - respectively 1.5 ±0.1, 1.3 ±0.1, and 1.4 ±0.1 developed buds on the scion for *S. vulgaris*, 'Charles Joly', and 'Mme Florent Stepman'. No statistically significant difference was found between the wedge graft and splice graft methods regarding the average number of developed buds on the scion. An exception to this trend was autumn grafting for *S. vulgaris*, which yielded 1.6 ±0.1 and 1.4 ±0.1 developed

Table 3. Mean number of developed buds on a scion during grafting of (1) *S. vulgaris*, (2) 'Charles Joly', and (3) 'Mme Florent Stepman' onto *L. ovalifolium* rootstocks.

Period	Cultivar	Method	14th day	28th day	42nd day	180th day
Spring	1	1	0.0 ±0.0 a A	1.0 ±0.0 b B	1.0 ±0.0 b B	1.0 ±0.0 a B
		2	1.0 ±0.0 b A	1.1 ±0.1 b A	1.2 ±0.1 d A	1.5 ±0.1 bc B
		3	1.5 ±0.5 c AB	1.1 ±0.1 b A	1.2 ±0.1 cd AB	1.3 ±0.2 b B
	2	1	0.0 ±0.0 a A	1.0 ±0.0 b B	1.0 ±0.0 bc B	1.0 ±0.0 a B
		2	1.0 *	1.2 ±0.1 de A	1.2 ±0.1 bcd A	1.3 ±0.1 b A
		3	0.0 ±0.0 a A	1.3 ±0.1 e B	1.3 ±0.2 def B	1.4 ±0.1 b B
	3	1	0.0 ±0.0 a A	1.0 ±0.0 b B	1.0 ±0.0 bc B	1.0 ±0.0 a B
		2	1.0 ±0.0 b A	1.2 ±0.1 d AB	1.4 ±0.1 ef B	1.4 ±0.1 bc B
		3	1.0 ±0.0 b A	1.1 ±0.1 bc A	1.2 ±0.1 bcd AB	1.4 ±0.1 b B
Summer	1	1	0.0 ±0.0 a A	0.0 ±0.0 a A	0.0 ±0.0 a A	1.0 ±0.0 a B
		2	0.0 ±0.0 a A	0.0 ±0.0 a A	0.0 ±0.0 a A	1.6 ±0.1 cd B
		3	0.0 ±0.0 a A	1.1 ±0.1 cd B	1.2 ±0.1 cde B	1.4 ±0.1 b C
	2	1	0.0 ±0.0 a A	0.0 ±0.0 a A	0.0 ±0.0 a A	1.0 ±0.0 a B
		2	0.0 ±0.0 a A	0.0 ±0.0 a A	1.0 ±0.0 bcd B	1.7 ±0.1 d C
		3	0.0 ±0.0 a A	0.0 ±0.0 a A	1.0 ±0.0 bcd B	1.6 ±0.1 cd C
	3	1	0.0 ±0.0 a A	0.0 ±0.0 a A	0.0 ±0.0 a A	1.0 ±0.0 a B
		2	0.0 ±0.0 a A	0.0 ±0.0 a A	1.0 *	1.7 ±0.1 d B
		3	1.0 ±0.0 b A	1.0 ±0.0 b A	1.5 ±0.1 f B	1.8 ±0.1 d C

Note: The means ± standard error within a column followed by the same small letter and within a row followed by the same capital letter were not significantly different, estimated by One-Way ANOVA followed by a *post hoc* LSD test at $p \leq 0.05$. Method: 1 – chip budding, 2 – wedge grafting, 3 – splice grafting. Results marked with * are not included in the statistical comparison, as there is only one value for the respective variant.

buds for both methods. During the spring term of splice grafting, no statistical differences were found between the results for the three cultivars (1.3 ±0.2, 1.4 ±0.1, and 1.4 ±0.1 developed buds). The highest value (1.8 ±0.1) during the autumn term was recorded for 'Mme Florent Stepman' when grafted using the splice grafting. All studied factors and their combinations influenced the number of developed buds on the scion (Table 4). The duration of the graft adhesion period had the greatest influence (Table 4, $F = 401.622$, $p = 0.000$), followed by the grafting method used (Table 4, $F = 140.075$, $p = 0.000$).

The length of the obtained shoots increased naturally with the progression of the vegetative period for both grafting periods (Table 5). During spring grafting, the developed shoots on the 14th day after grafting had an average length ranging between 2.8 ±0.3 and 3.2 ±0.2 cm, reaching 6.2 ±0.6 cm on the 28th day, and 9.0 ±1.3 cm on the 42nd day. Until the 42nd day, no statistically significant differences in shoot length were observed for the respective cultivar. At the end of the experiment, the shoots obtained on grafts made by the budding method stand out with the greatest length. An exception to this trend was observed during spring grafting of 'Mme Florent Stepman' and autumn grafting of *S. vulgaris*, where the results for the splice grafting (10.7 ±1.4 cm and 40.3

Table 4. Significance of factors and their interaction on the mean number of proliferated shoots estimated by a *post hoc* LSD test.

Factors	Mean difference (*F*)	Level of significance (*p*)
CV	23.418	0.000
M	140.075	0.000
DR	401.622	0.000
SR	73.051	0.000
CV × M	21.959	0.000
CV × DR	8.192	0.000
CV × SR	4.010	0.018
M × DR	25.599	0.000
M × SR	8.298	0.000
DR × SR	128.200	0.000
CV × M × DR	8.795	0.000
CV × M × SR	2.912	0.020
CV × DR × SR	15.097	0.000
M × DR × SR	33.881	0.000
CV × M × DR × SR	2.577	0.002

Note: Significant influence demonstrated at $p \leq 0.05$, *F* – Fisher's criterion. *R*-squared = 0.412 (Adjusted *R*-squared = 0.402), $p < 0.05$. Legend: CV – cultivar, M – grafting method, DR – duration of graft union, SR – season of grafting.

±3.4 cm, respectively) exceed the value obtained for budding (10.1 ±1.6 cm and 35.1 ±2.5 cm). However, no statistically significant differences were found between the results of both methods for the respective cultivar. On the 180th day, the longest shoots were observed on *S. vulgaris* grafted by chip budding, reaching a length of 67.5 ±4.5 cm (Fig. 4). This result differed statistically from the other grafting methods of *S. vulgaris* (48.3 ±3.8 cm for the wedge grafting and 37.2 ±5.1 cm for the splice grafting) and for both ornamental cultivars.

The developed shoots of 'Charles Joly' and 'Mme Florent Stepman' were notably shorter compared to *S. vulgaris*. For 'Charles Joly', the highest result obtained from spring grafting is by the chip budding method, 14.1 ±3.8 cm, which statistically differed from the results of the other two methods – 9.4 ±2.5 cm for wedge grafting and 8.3 ±1.8 cm for splice grafting. For 'Mme Florent Stepman', the length of the shoots varied between 9.1 ±2.1 cm and 10.7 ±1.4 cm, but no statistical difference was found between these values. A similar trend was observed for autumn grafting. The shortest shoots were observed in 'Charles Joly' – 7.3 ±0.8 cm for splice grafting and 7.8 ±0.7 cm for wedge grafting. 'Mme Florent Stepman' also exhibited a minimal increase, with shoots measuring 8.6 ±0.5 cm and 8.2 ±0.8 cm for both methods. Budding produced longer shoots – 14.8 ±1.1 cm for 'Mme Florent Stepman' and 21.8 ±2.5 cm for 'Charles Joly'. The greatest height increased in shoots with various budding methods was also reported by Iliev and Petrakieva (2007) in wild cherry grafting (*Prunus avium* L.). While budding from a bud resulted in growth of only one shoot, grafting from a scion lead to the growth of several shoots, resulting in a shorter terminal shoot length (Iliev and Petrakieva 2007).

Table 5. Mean length (cm) of the shoots after grafting of (1) *S. vulgaris*, (2) 'Charles Joly' и (3) 'Mme Florent Stepman' on rootstocks of *L. ovalifolium*.

Period	Cultivar	Method	14th day	28th day	42nd day	180th day
Spring	1	1	0.0 ±0.0 a A	2.8 ±0.3 bc AB	6.1 ±0.7 de B	67.5 ±4.5 g C
		2	2.8 ±0.1 b A	3.9 ±0.2 c A	5.5 ±0.3 cd A	48.3 ±3.8 f B
		3	2.8 ±0.3 b A	3.7 ±0.2 c A	4.6 ±0.3 bc A	37.2 ±5.1 f B
	2	1	0.0 ±0.0 a A	2.0 ±0.5 b A	5.1 ±1.2 bcd A	14.1 ±3.8 bcd B
		2	2.5 *	3.0 ±0.3 bc A	3.5 ±0.2 b A	9.4 ±2.5 abc B
		3	0.0 ±0.0 a A	4.0 ±1.5 cde AB	4.9 ±0.9 bcd AB	8.3 ±1.8 ab B
	3	1	0.0 ±0.0 a A	4.3 ±0.6 cd AB	8.2 ±1.2 f B	10.1 ±1.6 abc B
		2	3.0 ±0.2 c A	6.2 ±0.6 f A	9.0 ±1.3 f A	9.1 ±2.1 abc A
		3	3.2 ±0.2 d A	5.6 ±0.5 ef AB	7.4 ±0.9 ef AB	10.7 ±1.4 abc B
Summer	1	1	0.0 ±0.0 a A	0.0 ±0.0 a A	0.0 ±0.0 a A	35.1 ±2.5 f B
		2	0.0 ±0.0 a A	0.0 ±0.0 a A	0.0 ±0.0 a A	33.4 ±27.1 ef B
		3	0.0 ±0.0 a A	4.8 ±0.8 de B	6.3 ±1.0 de B	40.3 ±3.4 f C
	2	1	0.0 ±0.0 a A	0.0 ±0.0 a A	0.0 ±0.0 a A	21.8 ±2.5 de B
		2	0.0 ±0.0 a A	0.0 ±0.0 a A	3.0 ±0.5 a-d AB	7.8 ±0.7 a B
		3	0.0 ±0.0 a A	0.0 ±0.0 a A	2.7 ±0.1 b A	7.3 ±0.8 ab B
	3	1	0.0 ±0.0 a A	0.0 ±0.0 a A	0.0 ±0.0 a A	14.8 ±1.1 cd B
		2	0.0 ±0.0 a A	0.0 ±0.0 a A	2.5 *	8.2 ±0.8 ab B
		3	2.8 ±0.2 b A	3.1 ±0.2 bc A	3.0 ±0.2 b A	8.6 ±0.5 ab B

Note: The means ± standard error within a column followed by the same small letter and within a row followed by the same capital letter were not significantly different, estimated by One-Way ANOVA followed by a *post hoc* LSD test at $p \leq 0.05$. Method: 1 – chip budding, 2 – wedge Grafting, 3 – splice Grafting. Results marked with * are not included in the statistical comparison, as there is only one value for the respective variant.



Fig. 4. Intensive shoot growth after budding.

This may explain the obtained results, as for *S. vulgaris*, 'Charles Joly', and 'Mme Florent Stepman', a greater number of developed shoots through splice grafting and wedge grafting methods has been statistically proven (Table 3). According to Iliev and Petrakieva (2007), another possible explanation for the more intense height growth could be the better contact between the cambium of the stock and the shield during budding. The length of obtained shoots during grafting was significantly influenced by growth duration (Table 6, $F = 392.959$, $p = 0.000$), followed by the genotype of respective cultivar (Table 6, $F = 85.365$, $p = 0.000$), and the grafting period (Table 6, $F = 26.069$,

Table 6. Significance of factors and their interaction on the mean length of proliferated shoots estimated by a *post hoc* LSD test.

Factor	Average difference (*F*)	Level of significance (*p*)
CV	85.365	0.000
M	1.718	0.180
DR	392.959	0.000
SR	26.069	0.000
CV × M	1.194	0.311
CV × DR	115.873	0.000
CV × SR	4.112	0.016
M × DR	14.380	0.000
M × SR	2.932	0.053
DR × SR	1.204	0.307
CV × M × DR	1.360	0.178
CV × M × SR	4.641	0.001
CV × DR × SR	7.459	0.000
M × DR × SR	1.262	0.272
CV × M × DR × SR	6.275	0.000

Note: Significant influence proved at $p \leq 0.05$, *F* – Fisher's criterion. *R*-squared = 0.707 (Adjusted *R*-squared = 0.699), $p < 0.05$. Legend: CV – cultivar, M – grafting method, DR – duration of graft union, SR – grafting season.

$p = 0.000$). The grafting method (Table 6, $F = 1.718$, $p = 0.180$), as well as the combinations CV × M (Table 6, $F = 1.194$, $p = 0.311$), M × SR (Table 6, $F = 2.932$, $p = 0.053$), DR × SR (Table 6, $F = 1.204$, $p = 0.307$), CV × M × DR (Table 6, $F = 1.360$, $p = 0.178$), and M × DR × SR (Table 6, $F = 1.262$, $p = 0.272$) did not influence the obtained results.

Grafting is a widely practiced and preferred method for propagating species and cultivars where there are numerous limiting factors for their vegetative propagation (Coggeshall 1962, Krüssmann 1964, Einset and Alexander III 1984, Waldenmaier and Bünemann 1991, Hartmann et al. 2002, Cameron et al. 2003). It has been established that the rooting of cuttings of *S. vulgaris* and its ornamental cultivars has variable success rates (0–100 %) and is highly dependent on genotype, exogenous auxin treatment, and the phenological state of stock plants, being possible only during a limited period during full bloom (Bojarczuk 1975, 1978, 1979; Bojarczuk and Jankiewicz 1975; Schmidt 1978; Dirr and Heuser 1987; Dirr 1998; Ford et al. 2002; Hartmann et al. 2002; Cameron et al. 2003; Tyatyushkina 2007). Studies have shown that grafting, unlike rooting, can eliminate the influence of genotype on the success (%) of cloning (Table 2) and extend the period during which it is possible. For instance, with 'Mme Florent Stepman', where the percentage of cutting rooting barely reaches 33.3 ±13.6 % (Table 2), an 80.0 ±5.8 % success rate was achieved by grafting using the splice grafting (Table 1). It has been found that the graft adhesion success of both scion and rootstock depends on the physiological condition of the components (Hartmann et al. 2002, Iliev and Petrakieva 2007, Dancheva 2012). Various time frames and methods are recommended for the successful grafting of

common lilac in the literature. It is suggested to be done early in the spring, in February-March, while the rootstock and scions are dormant (Krüssmann 1964, Mac Cartaigh and Spethmann 2000, Schmid 2002, Alexandrov 2007). Other authors indicated August or the first half of September as the optimal period (Bodjakov et al. 1962, Dirr and Heuser 1987, Waldenmaier and Bünemann 1991, Mac Cartaigh and Spethmann 2000, Schmid 2002, Iliev and Petrakieva 2007, Dancheva 2012) because the bark of both rootstocks and scions easily separates during this time, and buds on mature scions are well-developed (Schmid 2002, Iliev and Petrakieva 2007). Studies showed that the two grafting seasons – spring (February-March) and summer (August-September) – provide statistically equal graft success rates (Table 1), allowing for their use with equal success in grafting common lilac cultivars, thus extending the propagation period from 3 weeks to 3 months per year. The grafting method is cited as one of the main factors influencing grafting success (Hartmann et al. 2002, Iliev and Petrakieva 2007, Dancheva 2012). Although according to Krüssmann (1964), Pierik et al. (1988), and Waldenmaier and Bünemann (1991), the most widely applied method for grafting lilac cultivars is bud grafting, there is no data on the success of different methods when using different rootstocks. The obtained results show that the wedge grafting and splice grafting have an advantage. While during spring grafting, the results from budding did not statistically differ from those of the wedge grafting and splice grafting, in the case of autumn grafting, this method was significantly less effective (Table 1). According to Mac Cartaigh and Spethmann (2000), successful budding should be performed in mid-July, which may explain the lower results obtained when grafting at later times (late August – early September). It is pointed out that compatibility between the scion and rootstock was crucial for the success of grafting and that the rootstock may influence the growth and development of the grafted plant (Hartmann et al. 2002, Iliev and Petrakieva 2007). Common Privet (*L. ovalifolium*) is recommended for grafting 112 cultivars of common lilac (Krüssmann 1964, Waldenmaier and Bünemann 1991, Mac Cartaigh and Spethmann 2000) due to its easy vegetative propagation and absence of root sprouts. It provides good graft adhesion with scion tissues and a relatively high success rate (71.1 ±5.9 % – 85.0 ±0.0 %) for the best methods and seasons (Table 1). However, it was reported that after grafting, plants suffer from chlorosis on the leaves, and after 3–5 years, their growth is significantly delayed (Chester 1931, Krüssmann 1964). In spring grafting experiments, where plants were grown in greenhouses, chlorosis of the leaves was observed after mid-July. A similar trend was not observed in plants grown outdoors. Therefore, subsequent deep planting of the grafted plants for their rooting above the graft site is considered advisable, a practice adopted in the USA (Mac Cartaigh and Spethmann 2000, Fiala 2008).

Conclusion

To avoid the occurrence of root shoots as rootstocks for grafting, individuals of *Ligustrum ovalifolium* can be used. Chip budding showed poorer results of adhesion in comparison of grafting in both seasons of operation.

Grafting should be performed in spring or summer using the splice grafting or wedge grafting. The graft adhesion

reached 76.7 % in spring and 85 % in summer grafting by spice graft.

Better growth indicators of the scions were observed during summer grafting. This outlines the recommendation to use summer splice grafting.

References

Alexandrov P. 2007. Nurseries for ornamental plants. Dionis. 151 p. (in Bulgarian).

Bassuk N., Miske D., Maynard B. 1984. Stock plant etiolation for improved rooting of cuttings. Combined Proceedings, International Plant Propagators' Society 34: 543–550.

Bodjakov P., Prokopiev E., Ganchev A., Popov J. 1962. Production of ornamental tree and shrub species. Zemizdat. 368 p. (in Bulgarian).

Bojarczuk K. 1975. Effect of auxin cofactors on rooting and effect of gibberellic acid on shoot growth of lilac softwood cuttings. Proceedings of the International Plant Propagators' Society 25: 485–491.

Bojarczuk K. 1978. Propagation of green cuttings of lilac (*Syringa vulgaris* L.) cultivars using various substances stimulating rooting. Arboretum Kornickie 23: 53–100.

Bojarczuk K. 1979. Studies on rooting cofactors in lilac (*Syringa vulgaris* L.) cuttings. Acta Horticulturae 91: 501–506.

Bojarczuk K., Jankiewicz L.S. 1975. Rooting of *Syringa vulgaris* soft wood cuttings using auxin, vitamins, phenolic substances, indole SADH and abscisic acid. Acta Agrobotanica 28(2): 229–239. https://doi.org/10.5586/aa.1975.016

Cameron R., Harrison-Murray R., Fordham M., Judd H., Ford Y., Marks T., Edmondson R. 2003. Rooting cuttings of *Syringa vulgaris* cv. Charles Joly and *Corylus avellana* cv. Aurea: the influence of stock plant pruning and shoot growth. Trees 17(5): 451–462. https://doi.org/10.1007/s00468-003-0255-1

Chester K.S. 1931. Graft-blight: a disease of lilac related to the employment of certain understocks in propagation. Journal of the Arnold Arboretum 12(2): 79–146. http://www.jstor.org/stable/43780585

Coggeshall R.G. 1962. Hybrid lilacs from softwood cuttings. American Nurseryman 115(12): 7–8.

Coggeshall R.G. 1977. Propagating French hybrid lilacs by softwood cuttings. Combined Proceedings of the International Plant Propagators' Society 27: 442–444.

Dancheva D. 2012. Cloning possibilities of Mountain ash (*Fraxinus excelsior* L.). PhD thesis. Sofia, UF, 133 p. (in Bulgarian).

Dirr M.A. 1998. Manual of woody landscape plants: their identification, ornamental characteristics, culture, propagation and uses. Fifth Edition. Stipes publishing L. L. C. Champaign. Illinois. 1187 p.

Dirr M.A., Heuser C.W. 1987. The reference manual of woody plant propagation: from seed to tissue culture. Varsity Press, Inc. Athens, Georgia: 203–205.

Einset J.W., Alexander J.H. III 1984. Multiplication of *Syringa* species and cultivars in tissue culture. Proceedings of the International Plant Propagators' Society 34: 628–636.

Fiala J.L. 2008. Lilacs: a gardener's encyclopedia. 2nd. ed. Timber Press, Inc. Portland, Oregon. 416 p.

Ford Y.-Y., Bonham E.C., Cameron R.W.F., Blake P.S., Judd H.L., Harrison-Murray R.S. 2002. Adventitious rooting: examining the role of auxin in an easy- and a difficult-to-root plant. Plant Growth Regulation 36(2): 149–159. https://doi.org/10.1023/A:1015013025513

Hand N.P. 1978. Propagation of lilacs. Proceedings of the International Plant Propagators' Society 28: 348–350.

Hartmann H.T., Kester D.E. 1983. Plant Propagation: Principles and Practices. 4th Ed. Prentice-Hall, Inc., Englewood Cliffs, New Jersey. 726 p.

Hartmann H.T., Kester D.E., Davies F.T., Geneve R.L. 2002. Hartmann and Kester's plant propagation. Principles and practices. Seventh edition. Prentice Hall. Upper Saddle River, New Jersey. 880 p.

Hildebrandt V., Harney P.M. 1983. *In vitro* propagation of *Syringa vulgaris* 'Ves-

per'. HortScience 18(4): 432–434. doi: 10.21273/HORTSCI.18.4.432

Howard B. 1993. Understanding vegetative propagation. Combined Proceedings, International Plant Propagators' Society 43: 157–162.

Howard B.H., Ridout M. 1992. A mechanism to explain increased rooting in leafy cuttings of *Syringa vulgaris* 'Madame Lemoine' following dark-treatment of the stock plant. Journal of Horticultural Science 67: 103–114.

Iliev N., Petrakieva A. 2007. Propagation of wild cherry by grafting (*Prunus avium* L.). Forest Science (Nauka za gorata) 4: 3–15 (in Bulgarian).

Kolev N. 1977. Grafting of forest trees. Zemizdat. 155 p. (in Bulgarian).

Krüssmann G. 1964. Die Baumschule, Paul Parley, Berlin und Hamburg. 391 p.

Krüssmann G. 1986. Manual of cultivated broad-leave trees & shrubs. Timber press. Portland, Oregon, vol. III. 448 p.

Mac Cartaigh D., Spethmann W. 2000. Krüssmanns Gehölzvermehrung. Blackwell Wissenschafts-Verlag, Berlin. 453 p.

Marks T.R., Simpson S.E. 2000. Interaction of explant type indole-3-butyric acid during rooting *in vitro* in a range of difficult and easy-to-root woody plants. Plant Cell, Tissue and Organ Culture 62: 65–74. https://doi.org/10.1023/A:1006443124007

Mezzit E.V. 1978. Propagation by cuttings of lilacs and other hard-to-root species by the sub-irrigation method. Proceedings of the International Plant Propagators' Society 28: 494–496.

Nesterowicz S., Kulpa D., Moder K., Kurek J. 2006. Micropropagation of an old specimen of common lilac (*Syringa vulgaris* L.) from the dendrological garden at Przelewice. Acta Scientiarum Polonorum Hortorum Cultus 5(1): 27–35.

Patience P.A., Alderson P.G. 1984. Improving the rooting of *Syringa vulgaris* cuttings by etiolation. Combined Proceedings, International Plant Propagators' Society 34: 316–327.

Pierik R.L.M., Steegmans H.H.M., Elias A.A., Stiekema O.T.J., van der Velde A.J. 1988. Vegetative propagation of *Syringa vulgaris* L. *in vitro.* Acta Horticulturae 226: 195–204. https://doi.org/10.17660/ActaHortic.1988.226.22

Refouvelet E., Le Nours S., Tallon C., Daguin F. 1998. A new method for in vitro propagation of lilac (*Syringa vulgaris* L.): regrowth and storage conditions for axillary buds encapsulated in alginate beads, development of a pre-acclimatisation stage. Scientia Horticulturae 74(3): 233–241. https://doi.org/10.1016/S0304-4238(98)00088-0

Rudolf P.O., Slabaugh P.E., Shaw N.L. 2008. *Syringa* L.: (lilac). In: Bonner F.T.; Karrfalt R.P. (Eds), The Woody Plant Seed Manual. Agric. Handbook No. 727. Washington, DC. U.S. Department of Agriculture, Forest Service: 1083–1086.

Schmidt G. 1978. Studies on some factors concerning the rooting of green cuttings of common lilac (*Syringa vulgaris*). Acta Horticulturae 79: 79–88.

Schmid H. 2002. Grafting of fruit trees and shrubs. Dionis. 223 p. (in Bulgarian).

Tomsone S., Galeniece A., Akere A., Priede G., Zīra L. 2007. *In vitro* propagation of *Syringa vulgaris* L. cultivars. Biologija 53(2): 28–31.

Tyatyushkina T.A. 2007. Evaluation of rhizogenic activity of stem cuttings of promising common lilac varieties. Russian Agricultural Sciences 33(2): 92–93. https://doi.org/10.3103/S1068367407020073

Waldenmaier S., Bünemann G. 1991. *Ex vitro* effects in micropropagation of *Syringa* L. Acta Horticulturae 300: 201–209. https://doi.org/10.17660/ActaHortic.1992.300.29

Wedge D. 1977. Propagation of hybrid lilacs. Proceedings of the International Plant Propagators' Society 27: 432–436.

Yeoman M.M., Brown R. 1976. Implications of the formation of the graft union for organization of the intact plant. Annals of Botany 40(6): 1265–1276. https://doi.org/10.1093/oxfordjournals.aob.a085247

FORESTRY IDEAS, 2024, vol. 30, No 1 (67): 107–119

Financial analysis of cat's eye resin business in West Coast Regency, Lampung province, Indonesia

Muhammad Irfan Affandi[1*], Alifia Hasyimi[2], and Fembriarti Erry Prasmatiwi[3]

[1]Agribusiness Department, Faculty of Agriculture, University of Lampung, Jl. Prof. Dr. Sumantri Brojonegoro No. 1, Bandar Lampung 35145, Indonesia. *E-mail: irfan.affandi@fp.unila.ac.id
[2]Master of Urban and Regional Planning, Postgraduate University of Lampung, Indonesia.
[3]Agribusiness Department, Faculty of Agriculture, University of Lampung, Indonesia.

Received: 04 January 2024 / Accepted: 19 April 2024 / Available online: 07 May 2024

Open Access: This article is licensed under a Creative Commons Attribution 4.0 International License.

Abstract

This study aimed to analyse the financial feasibility business of cat's eye resin in West Coast Regency. The method used in this research was the survey method. Primary and secondary data were collected in this study. Sampling used census sampling. The number of respondents consisted of 60 farmers. The data collection was carried out in June 2023. All financial feasibility criteria, such as *NPV*, Gross B/C, Net B/C ratio, IRR and Payback Period of cat's eye resin business in West Coast Regency, are feasible. The results showed that the business is feasible to run based on an analysis of the financial feasibility.

Key words: business analysis, financial feasibility, non-producing plant, revenue.

Introduction

West Coast Regency is the only underdeveloped region in Lampung Province that has been determined in Presidential Regulation Number 63 of 2020 of the Republic of Indonesia, concerning the determination of underdeveloped regions for 2020–2024. Based on Law No. 22/2012, this regency began to separate itself from West Lampung Regency. The regional development missions are to achieve the vision of 'Realizing a Civilized, Independent and Prosperous West Coast Community'. Overcoming the development of underdeveloped regions includes the development of economic, social, cultural and security aspects (Cabinet Secretariat of the Republic of Indonesia 2024). West Coast Regency has several economic sectors that can be relied upon and has geographical advantages and potential resources, if it can be managed properly, it will improve the economy and welfare of the community and has a very large forest area of more than sixty percent of the area, so the forestry sector also has a significant contribution to the economy

(Regional Development Planning Agency of West Coast Regency 2015).

Resin is the leading commodity in Lampung Province, only found in the West Coast Regency. Resin is one of Indonesia's native timber plants that is spread across Sumatra, Kalimantan, Sulawesi, Maluku and Papua. Resin is usually utilized for its wood because it has a fairly high selling value, especially used for carpentry trees of the meranti-Iranian Dipterocarpaceae tribe, grows predominantly in the lowland forests of Southeast Asia, therefore resin is commonly known in Western Indonesia (Michon et al. 1996).

West Coast Regency produces resin with the number one quality known as 'Mata Kucing' resin. According to Michon et al. (1996), resin has been cultivated by the people of the West Coast since the Dutch era until now. Mastic is one part of the local community's farming system, as is the cultivation of other crops (Makmur et al. 2018).

Cat's eye resin (extracted from the plant *Shorea javanica* Koord. & Valet.) is a superior commodity from Lampung Province, especially in West Coast Regency. This commodity has been famous since the 19th century and has been cultivated by the community in Pesisir Barat Regency in agroforests (cultivation of forestry plants together with agricultural crops) for generations. The cat's eye resin (sap) is used as raw material for paint, ink, cosmetics and food additives industry and can be used as termite repellent and anti-fungal, as well. The sap produced from repong resin from Pesisir Barat is of high quality, highly demanded by importers so its existence and sustainability are very important in the cat's eye resin trade chain in Indonesia. Cat's eye resin in Pesisir Barat has the potential to be developed. Mastic cultivation has two benefits at once: forest conservation and economy (Appanah and Trunbull 1998).

Resin, a non-timber forest product, is extensively cultivated and employed by the indigenous communities residing for generations along the periphery of the rainforest in South Sumatra, specifically in West Coast, Lampung Province (Mary and Michon 1986, Anasis and Ratna Sari 2015, Gilbert 2016). The forest management techniques originated and refined by indigenous communities have demonstrated their effectiveness in meeting essential household requirements and providing the sustainable utilization of natural resources for over a century (Murniati et al. 2001, Kusters et al. 2008). From the perspective of conserving forest resources, the agroforest system sustains a rich biodiversity and preserves the ecological functions of the forests (Michon et al. 1986). The configuration of the agroforest system provides long-term productivity sustainability by preserving soil water quality, along with offering additional environmental advantages, like carbon sequestration. It also plays role in safeguarding the diversity of forest plants, as well as invertebrate and vertebrate animals (Nyhus and Tilson 2004, Mutuo et al. 2005). When applied within buffer zones, the agroforestry system is anticipated to contribute to the safeguarding of the remaining natural forests (Nyhus and Tilson 2004). Economically, the agroforestry system offers diverse income opportunities for both rural and urban households, as well as the participants involved in the dammar gum trading chain (Bouamrane 1996).

Cat's eye resin is an important part of people's lives in West Coast Regency, both for farmers who own resin businesses, people involved in resin tapping (tapping laborers, sorting laborers, resin

porters, renting transportation for transporting resin), and the buying and selling process (large traders, collectors). There is a dependence on the income from the resin sold in determining the level of welfare of farmers and their next generation. The importance of this research can be seen from several aspects: 1) local economic growth, 2) environmental conservation, 3) local community empowerment. Through previous research by Maryati (2020), it was explained that cat's eye resin is the main livelihood for most of the people of Pahmungan village, West Coast Regency. Therefore, authors want to examine whether the cat's eye resin business is feasible or not to be cultivated. Based on the existing problems and information, the primary objective of this research is to thoroughly examine the financial feasibility of the cat's eye resin business in West Coast Regency.

Object and Methods

The research location is in the West Coast Regency area, Lampung Province. It was chosen purposively with the consideration that West Coast Regency is the only regency in Lampung Province that is included in the status of underdeveloped regencies based on the Presidential Regulation Number 63 of 2020 of the Republic of Indonesia, concerning the determination of underdeveloped regions for 2020–2024, while this district area has abundant natural resources and has great potential to be developed.

Respondents of business actors in this study are farmers who do business based on superior commodities of West Coast, which is done by saturated sampling also called census technique. There were 60 farmers representing the respondents in this study who came from 3 sub-districts with the highest cat's eye resin land area in West Coast Regency, namely Way Krui Sub-district, Karya Penggawa Sub-district and Pesisir Selatan Sub-district (Fig. 1).

The research method used is the survey method, using questionnaires as a research tool conducted on large and small populations, but the data studied is from samples taken from these populations, so that relative incidence, distribution and relationships between variables, sociological and psychological are found (Sugiyono 2013). Primary and secondary data were collected in this study. Primary data in this research was obtained by conducting interviews with 60 cat's eye resin farmers, while secondary data used in this research was data from the Regional Spatial Plan of West Coast Regency 2017–3017.

The production of cat's eye resin is the result obtained by farmers during the implementation of the business, from the beginning of the business, cultivation, to the end of the economic life of the plant. The production of the plant used in this study is the result of direct interviews with 60 farmers regarding the production of cat's eye resin sap for the last five years, where each farmer has a different starting year.

The cost of the cat's eye resin business is incurred from the beginning of the resin business until the end, which is calculated per one hectare of land. The costs of the resin business include costs incurred during the non-producing plant and costs incurred during the producing plant. Expenditures include the purchase of seeds, fertilizers family labour, business equipment and taxes.

The data has been compiled and processed in tabulated form with a financial aspect approach with the assumption that:

- all input and output prices used in this analysis are based on prices prevailing

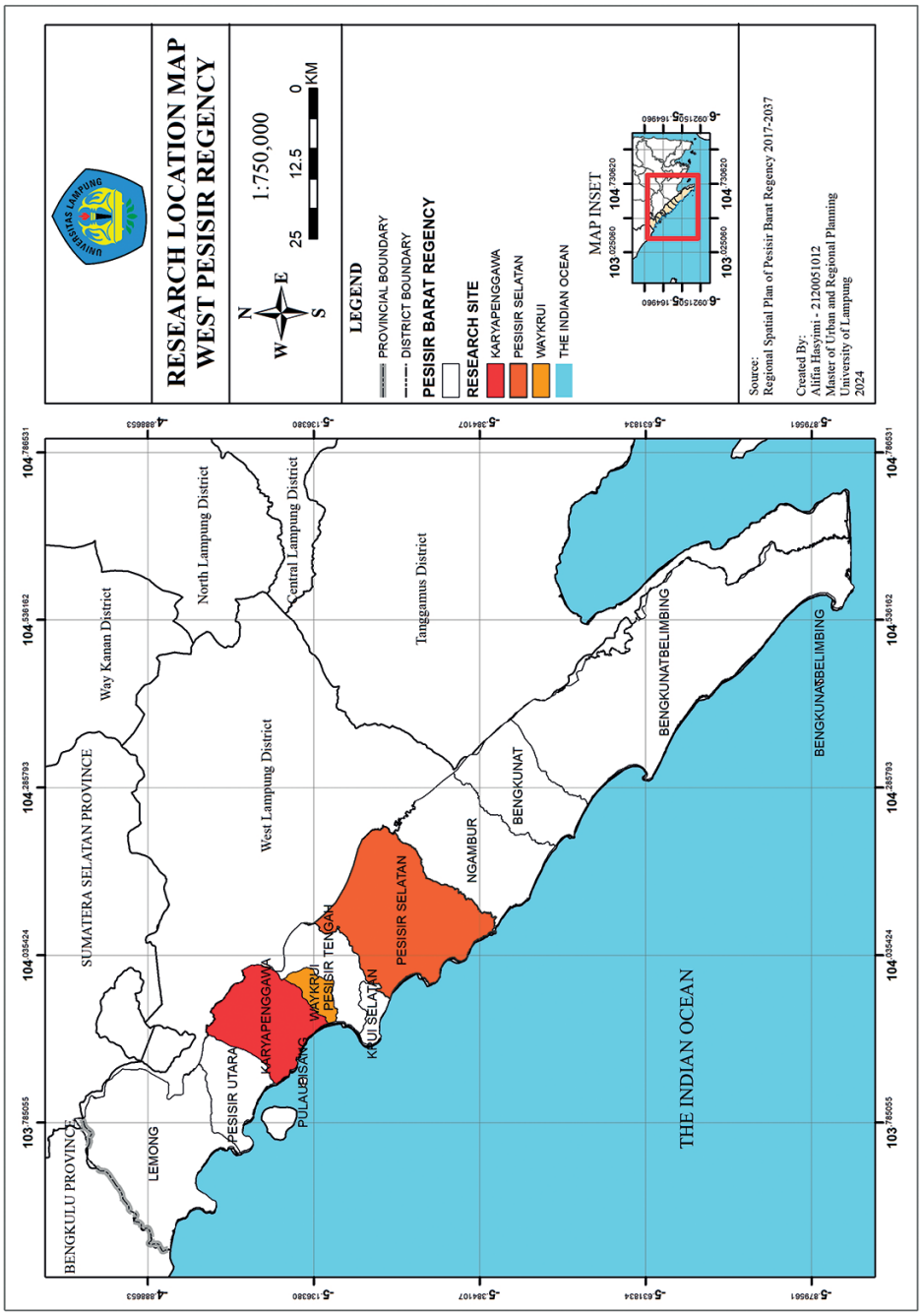


Fig. 1. Map of research location, Way Krui Sub-district, Karya Penggawa Sub-district, and Pesisir Selatan Sub-district.
Source: Regional Spatial Plan of West Coast Regency 2017–2037.

during the research year at the research location;

- using an interest rate of 6%;
- the state of the country's economy is stable during the study period;
- the unit used is Rupiah per year per ha;
- working day is valued at the prevailing wage in the location;
- income starts to be calculated when the land that has been planted is producing;
- repong resin income is calculated when the age of the resin > 20 years;
- non-gum income is calculated according to fruiting periodization.

Cat's eye resin plants are assumed to have an economic life or productive life of 50 years.

The calculation of business profit is calculated using an average for each year from 21 years to 50 years. The calculation results obtained are then valued using compound factors and discount factors to determine the value of benefits provided in the past and future.

Net present value (*NPV*) was a method that calculated the difference between benefits/receipts and costs/expenses with formula (1) (Rustiadi et al. 2011).

$$NPV = \sum_{t=0}^{n} \frac{Bt - Ct}{(1+t)^t}, \quad (1)$$

where: *Bt* is benefits of the business; *Ct* is cost of the business; *i* is interest rate 6%; *t* is number of *t*-time periods, years.

The three investment criteria are:

- if *NPV* > 0, the business is profitable and can be implemented;
- if *NPV* < 0, then the business is loss-making and not feasible to implement;
- if *NPV* = 0, then the business is neither profitable nor loss-making (break event point).

Net B/C ratio is the comparison between net benefits that have been discounted by positive factors and net benefits that have been discounted negatively. To determine B/C we used formula (2) (Novianti 2021).

$$Net\frac{B}{C} = \frac{\sum_{t=1}^{n} \frac{Bt - Ct}{(1+t)^t}}{\sum_{t=1}^{n} \frac{Bt - Ct}{(1+t)^t}}, \quad \begin{matrix} \text{for } Bt - Ct > 0 \\ \text{for } Bt - Ct < 0 \end{matrix} \quad (2)$$

where: *Bt* is benefit in a year *t*; *Ct* is cost in year *t*, IDR; *i* is interest rate 6%; *t* is number of *t*-time periods, years.

Feasibility criteria:

- if net B/C > 1, then the business is feasible;
- if net B/C < 1, then the business is not feasible to implement;
- if net B/C = 1, then the business is in a state of break event point.

To calculate the Gross benefit cost ratio (gross B/C) value, we used formula (3) (Novianti 2021).

$$\text{Gross B/C} = \frac{\sum_{t=1}^{n} \frac{Bt}{(1+t)^t}}{\sum_{t=1}^{n} \frac{Ct}{(1+t)^t}}, \quad (3)$$

where: *Bt* is benefit in year *t*, IDR; *Ct* is cost in year *t*, IDR; *i* is interest rate 6%; *t* is number of *t*-time periods, years.

Indicators of investment assessment based on gross B/C are:

- if the gross B/C value > 1, then the business is worth continuing;
- if gross B/C < 1, then the business is not worth continuing;
- if gross B/C = 1, then then the business is in a state of break event point.

Internal rate of return (*IRR*) is an interest rate that shows *NPV* is equal to the sum of all project investments or in other words the interest rate that results in *NPV* = 0. To determine *IRR,* we used formula (4) (Tarigan 2004).

$$IRR = i_1 + \frac{NPV_1}{NPV_1 + NPV_2} \cdot (i_2 - i_1), \quad (4)$$

where: NPV_1 is positive present value; NPV_2 is negative present value; i_1 is discount factor, if $NPV > 0$; i_2 is discount factor, if $NPV < 0$.

The resulting *IRR* value must be greater than the prevailing interest rate, which is 6% to assume that the cat's eye resin business is able to pay when making credit loans. *IRR* is calculated in an indirect way, namely by calculating the *NPV* of two discounts whose value is close to zero and whose value is negative (Grey et al. 2002).

Investment criteria:

- if the *IRR* value > the interest rate, then the business is feasible;
- if the *IRR* value < the interest rate, then the business is not feasible;
- if the *IRR* value = the interest rate, then the business breaks event point.

Payback period is an investment appraisal of a project based on the repayment of investment costs based on the net benefits of a business.

Criteria for feasibility:

- if the payback period is shorter than the economic life of business, the project is viable;
- if the payback period is longer than the economic life of the business, the project is not viable.

Result and Discussion

Cost of non-producing plant

Farmers buy cat's eye resin seedlings for IDR 3000 per stem. One hectare of planting land requires 277 seeds with spacing 6×6 m, so the cost of seeds that must be incurred by farmers is IDR 831,000 (the exchange rate of Indonesian Rupiah is 1 IDR = $59 \cdot 10^{-6}$ €).

However, not all cat's eye resin farmers spend money on seeds, because the majority of farmers have plantations from the inheritance of parents or from generation to generation.

Business equipment is used to support and facilitate farmer activities. The types of equipment used in the cat's eye resin sap business include axes for hollowing out, axes for harvesting sap, machetes, bebalang or baskets, ambons, sacks and buckets. The use of cat's eye resin business equipment in West Coast Regency amounted IDR 464,006.11.

Non-producing plant fertilizer costs are calculated based on the use of 1 fertilizer per year. The types of fertilizers used during the non-producing plant period of the cat's eye resin business are NPK fertilizer and manure. Fertilization is done once a year. The use of fertilizer during non-producing plant period of the cat's eye resin business amounted to IDR 547,400.

In addition to requiring agricultural inputs, such as fertilizers, cat's eye resin business also requires labour to carry out its business activities. The labour used can come from within the family, namely domestic family labour, or from outside the family, namely outside family labour. In this business, the labour used is entirely from within the family. The breakdown of labour costs based on the cat's eye resin business activity amounted to IDR 3,257,250.

Tax is something that must be paid by the people of Indonesia. Taxes are paid as mandatory community contribution to support the development of the Indonesian state. Planting land that is owned by farmers is subject to annual tax fees. Tax costs incurred by the farmers depend on the size of the land, type of land and location. The tax cost incurred by cat's eye resin farmers is IDR 515,483 per ha per year.

All costs incurred during the non-pro-

ducing plant period of the business were calculated as non-producing plant costs. The length of time to return non-producing plant costs that had been incurred was calculated using the payback period calculation, indicating how long it took for the business to recover the costs incurred before the plant produced. This entire cost includes the cost of intercropping crops.

Cost of producing plants

Producing plant costs were costs that had to be incurred in the business and were used up in one use during the period of the plant production. Producing plant costs were incurred annually until the productive age of the resin plant was exhausted and had to be incurred in the form of labor costs and taxes.

The labour used is from in-family labour, which also includes the use of labour for intercropping crops. There are differences in the use of labour during the non-producing plant and producing plant periods. This difference is caused by different business activities during the non-producing plant and producing plant periods. The amount of male and female labour during the producing plant period is IDR 75,000 per person per day and IDR 50,000 per person per day. Based on the research results, the average cost of labour use during the producing plant period in West Coast Regency was IDR 2,030,208.

Taxes incurred by farmers during the period are assumed to be the same as those incurred during the non-producing plant period. Tax costs incurred by the farmers amounted to IDR 515,483 per year.

The business costs incurred in the cat's eye resin also include the cost of intercropping. The business costs incurred by the farmers are assumed to be the same amount during this period until the end of the productive life of the plant. This is because, based on the results of the study, there were no significant differences in the costs incurred by farmers each year. The overall costs incurred by cat's eye resin farmers from year 1 to year 50 are detailed in Table 1.

Production and revenue of cat's eye resin sap business

Cat's eye resin plants in years 1 to 20 have not yet produced production. The plants produce sap from year 21 to year 50. The results showed that the production of cat's eye resin fluctuated from year to year. The results of the plant production from year 21 to year 50 can be seen in Figure 2.

The selling price of cat's eye resin in West Coast Regency fluctuates every year. In this study, the selling price of resin used is the selling price of dirty resin (unclassified resin), the average selling price of cat's eye resin in West Coast Regency for the last 5 years is IDR 16,800 per kg. Based on the results of the research, the selling price of cat's eye resin in West Coast Regency received by cat's eye resin farmers is IDR 13,000 per kg, the price is the selling price from 2022 to 2023.

Acceptance of cat's eye resin production is calculated by multiplying the amount of the production by the prevailing resin selling price. Acceptance of this business is obtained from the acceptance of the resin production and intercropping plants. In addition, the costs incurred have also included the cost of intercropping.

From year 10 to year 20, cat's eye resin farmers get revenue from the production of intercropping crops. Jensen (2007) states that increased profits for farmers may cause them to change the scale of

Table 1. Total revenue and total cost of cat's eye resin business per hectare per year in West Coast Regency.

Age of resin, years	Cat's eye resin		Age of resin, years	Cat's eye resin	
	Revenue, IDR	Cost, IDR		Revenue, IDR	Cost, IDR
1	0	2,302,729	26	63,864,244	3,847,859
2	0	69,225	27	64,756,020	3,745,608
3	0	69,225	28	64,962,050	3,734,358
4	0	69,225	29	66,358,121	3,859,108
5	0	69,225	30	66,639,913	3,734,358
6	0	900,475	31	68,651,636	3,790,184
7	0	900,475	32	68,269,364	3,892,434
8	0	900,475	33	70,903,750	3,790,184
9	0	900,475	34	69,287,895	3,778,934
10	0	900,475	35	63,497,516	3,903,684
11	15,450,741	1,415,958	36	67,795,222	3,778,934
12	15,450,741	1,388,614	37	67,545,267	3,790,184
13	15,450,741	1,388,614	38	57,987,292	3,892,434
14	15,450,741	1,388,614	39	71,899,714	3,790,184
15	15,450,741	1,388,614	40	68,670,000	3,778,934
16	15,450,741	1,381,583	41	62,333,333	3,804,158
17	15,450,741	1,381,583	42	72,308,333	3,679,408
18	15,450,741	1,381,583	43	60,742,333	3,690,658
19	15,450,741	1,381,583	44	63,522,500	3,792,908
20	15,450,741	1,778,278	45	58,213,500	3,690,658
21	61,150,667	4,012,012	46	51,377,000	3,558,158
22	71,326,000	4,000,684	47	64,859,000	3,682,908
23	68,076,000	4,125,434	48	56,509,000	3,558,158
24	66,588,667	4,000,684	49	63,570,000	3,569,408
25	66,501,455	4,011,934	50	55,357,338	3,671,658

production and marketing decisions; they may farm more intensively, sell in larger quantities, adopt new technologies and move land from non-agricultural uses.

From year 21 to year 50 farmers earn revenue from the total receipts of the production and intercropping. The intercrops include jengkol (*Archidendron pauciflorum* (Benth.) I.C.Nielsen), durian (*Durio zibethinus* L.), petai (*Parkia speciose* Hassk.), cempedak (*Artocarpus integer* Merr.) and duku (*Lansium parasiticum* (Osbeck) Sahni & Bennet). Based on the data in Table 1, it is known that the difference between the total cost and total revenue of the business shows that the cat's eye resin business provides profit.

Financial feasibility analysis

The financial feasibility analysis in this study was used to determine the financial viability of cat's eye resin business. Financial analysis is very important because farmers will be willing to do the business if it provides a profit. The profit of the farmers calculated in this analysis comes from the overall profit obtained by farmers during

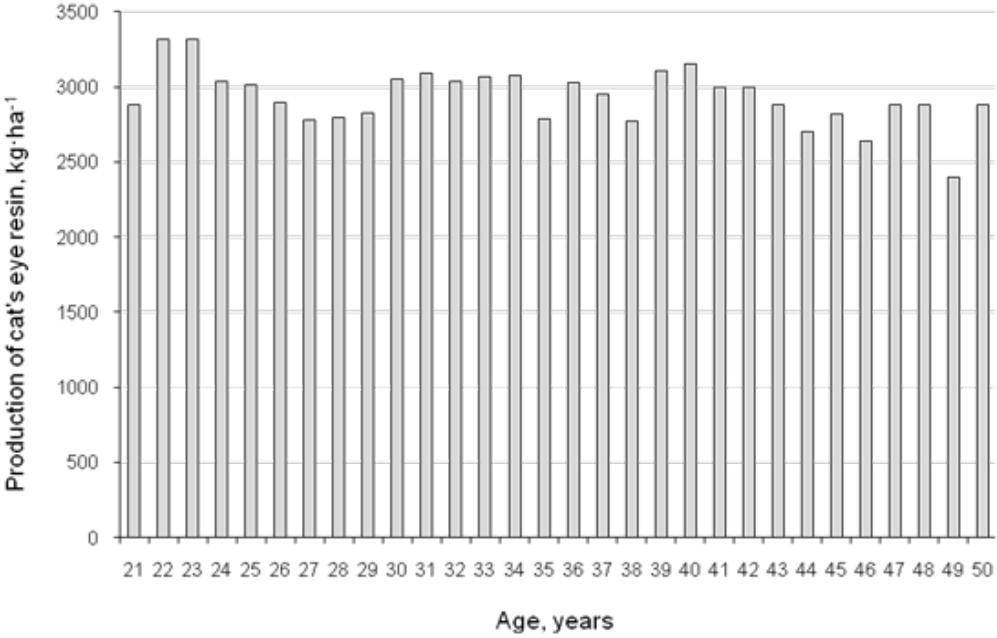


Fig. 2. Production of cat's eye resin in West Coast Regency from year 21 to year 50.

the economic life of the business. Cat's eye resin plants are assumed to have an economic life or productive life of 50 years.

The calculation of business profit is done using an average for each year from 21 years to 50 years of cat's eye resin. Obtained results are then valued using compound factors and discount factors to determine the value of benefits provided in the past and future. This research uses an interest rate of 6% based on the Bank Rakyat Indonesia People's Business Credit interest rate. This interest rate has the same value as the interest rate in 2022. This relatively low-interest rate is expected to support small and medium enterprises, especially businesses in the agricultural sector. The calculation and results of the financial feasibility of the cat's eye resin business per hectare can be seen in Table 2 and Table 3.

The data in Table 3 shows that the business produced a net present value of IDR 4,491,493,713. The business is feasible to implement because the resulting net present value is greater than zero (*NPV* > 0). So, it is concluded that the business is profitable to cultivate. The results of this study are in line with the research of Koeswindarti et al. (2021), the results of net present value financial analysis of rubber plants in the area of PT Inhutani III Tanah Laut Regency were obtained at IDR 11,384,378,028, where the net present value > 0 and categorized as feasible. Gross B/C of 12.71, this value is greater than one (gross B/C>1) indicating that the business is feasible. Payback period value of the business is 21.60, meaning that the payback period is 21 years and 6 months. The payback period of non-producing plant costs in this business is faster than the productive life of the business (50 years), so the business

Table 2. Financial feasibility analysis of cat's eye resin business per hectare at 6% interest rate in West Coast Regency.

Year	Investment cost, IDR	Operational cost, IDR	Total cost (CT), IDR	Benefit (*Bt*), IDR	Net (*Bt-Ct*), IDR	Interest rate (6%)	CT*6%, IDR	BT*6%, IDR	*NPV*, IDR
	1	2	3 = 1 + 2	4	5 = 4 – 3	6	7 = 3 * 6	8 = 4 * 6	9 = 5 * 6
1	2,302,729	0	2,302,729	0	-2,302,729	12.99	29,902,052	0	-29,902,052
2	69,225	0	69,225	0	-69,225	12.25	848,038	0	-848,038
3	69,225	0	69,225	0	-69,225	11.56	800,036	0	-800,036
4	69,225	0	69,225	0	-69,225	10.90	754,751	0	-754,751
5	69,225	0	69,225	0	-69,225	10.29	712,029	0	-712,029
6	900,475	0	900,475	0	-900,475	9.70	8,737,766	0	-8,737,766
7	900,475	0	900,475	0	-900,475	9.15	8,243,175	0	-8,243,175
8	900,475	0	900,475	0	-900,475	8.64	7,776,581	0	-7,776,581
9	900,475	0	900,475	0	-900,475	8.15	7,336,397	0	-7,336,397
10	900,475	515,483	1,415,958	15,450,741	14,034,783	7.69	10,883,176	118,755,736	107,872,560
11	873,131	515,483	1,388,614	15,450,741	14,062,127	7.25	10,068,877	112,033,714	101,964,836
12	873,131	515,483	1,388,614	15,450,741	14,062,127	6.84	9,498,941	105,692,183	96,193,242
13	873,131	515,483	1,388,614	15,450,741	14,062,127	6.45	8,961,265	99,709,606	90,748,341
14	873,131	515,483	1,388,614	15,450,741	14,062,127	6.09	8,454,023	94,065,666	85,611,643
15	873,131	515,483	1,388,614	15,450,741	14,062,127	5.74	7,975,494	88,741,195	80,765,701
16	866,100	515,483	1,381,583	15,450,741	14,069,158	5.42	7,485,953	83,718,108	76,232,155
17	866,100	515,483	1,381,583	15,450,741	14,069,158	5.11	7,062,219	78,979,347	71,917,128
18	866,100	515,483	1,381,583	15,450,741	14,069,158	4.82	6,662,471	74,508,818	67,846,347
19	866,100	515,483	1,381,583	15,450,741	14,069,158	4.55	6,285,350	70,291,338	64,005,988
20	1,237,258	515,483	1,752,741	15,450,741	13,698,000	4.29	7,522,539	66,312,583	58,790,044
21	1,237,258	2,774,754	4,012,012	61,150,667	57,138,655	4.05	16,244,375	247,595,053	231,350,678
22	1,226,008	2,774,676	4,000,684	71,326,000	67,325,316	3.82	15,281,613	272,447,464	257,165,852
23	1,350,758	2,774,676	4,125,434	68,076,000	63,950,566	3.60	14,866,157	245,314,413	230,448,256
24	1,226,008	2,774,676	4,000,684	66,588,667	62,587,982	3.40	13,600,581	226,372,407	212,771,827

25	1,237,258	2,774,676	4,011,934	66,501,455	62,489,520	3.21	12,866,817	213,279,174	200,412,357
26	1,339,508	2,508,350	3,847,859	63,864,244	60,016,386	3.03	11,642,079	193,227,626	181,585,547
27	1,237,258	2,508,350	3,745,608	64,756,020	61,010,411	2.85	10,691,237	184,835,642	174,144,406
28	1,226,008	2,508,350	3,734,358	64,962,050	61,227,692	2.69	10,055,778	174,928,040	164,872,262
29	1,350,758	2,508,350	3,859,108	66,358,121	62,499,013	2.54	9,803,492	168,572,965	158,769,473
30	1,226,008	2,508,350	3,734,358	66,639,913	62,905,555	2.40	8,949,607	159,706,430	150,756,823
31	1,237,258	2,552,926	3,790,184	68,651,636	64,861,452	2.26	8,569,242	155,214,756	146,645,514
32	1,339,508	2,552,926	3,892,434	68,269,364	64,376,929	2.13	8,302,283	145,613,655	137,311,372
33	1,237,258	2,552,926	3,790,184	70,903,750	67,113,566	2.01	7,626,596	142,672,276	135,045,680
34	1,226,008	2,552,926	3,778,934	69,287,895	65,508,960	1.90	7,173,546	131,529,111	124,355,565
35	1,350,758	2,552,926	3,903,684	63,497,516	59,593,832	1.79	6,990,904	113,714,381	106,723,477
36	1,226,008	2,552,926	3,778,934	67,795,222	64,016,288	1.69	6,384,430	114,538,601	108,154,172
37	1,237,258	2,552,926	3,790,184	67,545,267	63,755,082	1.59	6,040,978	107,656,893	101,615,915
38	1,339,508	2,552,926	3,892,434	57,987,292	54,094,857	1.50	5,852,782	87,191,446	81,338,664
39	1,237,258	2,552,926	3,790,184	71,899,714	68,109,530	1.42	5,376,449	101,991,119	96,614,670
40	1,226,008	2,552,926	3,778,934	68,670,000	64,891,066	1.34	5,057,067	91,895,950	86,838,884
41	1,323,675	2,480,483	3,804,158	62,333,333	58,529,175	1.26	4,802,662	78,694,397	73,891,735
42	1,198,925	2,480,483	3,679,408	72,308,333	68,628,925	1.19	4,382,234	86,120,382	81,738,148
43	1,210,175	2,480,483	3,690,658	60,742,333	57,051,675	1.12	4,146,823	68,250,086	64,103,262
44	1,312,425	2,480,483	3,792,908	63,522,500	59,729,592	1.06	4,020,482	67,333,850	63,313,368
45	1,210,175	2,480,483	3,690,658	58,213,500	54,522,842	1.00	3,690,658	58,213,500	54,522,842
46	1,198,925	2,359,233	3,558,158	51,377,000	47,818,842	0.94	3,356,753	48,468,868	45,112,115
47	1,323,675	2,359,233	3,682,908	64,859,000	61,176,092	0.89	3,277,775	57,724,279	54,446,504
48	1,198,925	2,359,233	3,558,158	56,509,000	52,950,842	0.84	2,987,498	47,446,046	44,458,548
49	1,210,175	2,359,233	3,569,408	63,570,000	60,000,592	0.79	2,827,305	50,353,394	47,526,089
50	1,312,425	2,359,233	3,671,658	55,357,338	51,685,680	0.75	2,743,676	41,366,223	38,622,547
Total	53,962,486	81,813,360	135,775,846	2,113,481,281	1,977,705,435	216.96	383,583,010	4,875,076,722	4,491,493,713

Table 3. Result of financial feasibility analysis of cat's eye resin business per hectare at 6% interest rate in West Coast Regency.

Criteria		Cat's eye resin	
		Value	Result
Net present value, IDR	> 0	4,491,493,713	Feasible
Net B/C ratio	> 1	69.98	Feasible
Gross B/C ratio	> 1	12.71	Feasible
Payback period, year	< 25	21.60	Eligible
Internal rate of return, %	> 6	38.73	Eligible

is feasible to cultivate. Internal rate of return value is 38.73 %. This shows that the business is feasible to cultivate because the resulting internal rate of return value is greater than 6 %. These results are in line with Azizah et al. (2016) research, the results of the internal rate of return financial feasibility analysis of the rubber industry in Musi Rawas Regency, South Sumatra amounted to 18.6 % and fell into the feasible category.

The results of the calculation of this financial feasibility analysis can be used as a consideration for farmers to decide which business to pursue. These results can help farmers in making decisions to switch to doing cat's eye resin business because this business is feasible and profitable to run.

Conclusion

Based on these results, all criteria for the financial feasibility of the cat's eye resin business in West Coast Regency were found to fall into the feasible category. Therefore, the study concluded that the cat's eye resin business in West Coast Regency, Lampung province, provides benefits and is feasible to run, offering diverse income opportunities for both rural and urban households and contributing to the welfare of the community.

References

Anasis A.M., Ratna Sari M.Y.A. 2015. Geographical indication protection of cat's eye Damar (*Shorea javanica*) as a forest conservation effort (Study in Pesisir Barat Regency, Lampung Province) [Perlindungan Indikasi Geografis terhadap Damar Mata Kucing (*Shorea javanica*) sebagai Upaya Pelestarian Hutan (Studi di Kabupaten Pesisir Barat Propinsi Lampung)]. Jurnal Hukum IUS QUIA IUSTUM. 22(4): 566–593 (in Indonesian). https://doi.org/10.20885/iustum.vol22.iss4.art3

Appanah S., Turnbull J.M. (Eds) 1998. A Review of Dipterocarps: Taxonomy, Ecology, and Silviculture. CIFOR. Bogor. 220 p. https://www.cifor.org/knowledge/publication/463/

Azizah F.A., Wijana A., Effendi M. 2016. Technical and financial feasibility analysis of the small scale industrial rubber processing in Musi Rawas Regency of South Sumatera [Analisis Kelayakan Teknis and Finansial pada Industri Pengolahan Karet Skala Kecil di Kabupaten Musi Rawas Sumtera Selatan]. Jurnal Industria 4(1): 53–65 (in Indonesian).

Bouamrane M. 1996. A season of gold-putting a value on harvest from Indonesian agroforests. Agroforestry Today 8(1): 8–10.

Cabinet Secretariat of the Republic of Indonesia 2024. Presidential Regulation no. 63 of 2020 concerning Determination of Disadvantaged Areas for 2020–2024. https://setkab.go.id/en

Gilbert M. 2016. Brydson's Plastics Materi-

als. Eight ed. Elsevier, Oxford. 892 p.

Grey C., Simanjuntak P., Sahur L.K., Masyaitella P.F.I., Yarley R.C.G. 2002. Introduction to Project Evaluation [Pengantar Evaluasi Proyek]. PT Gramedia Pustaka Utama. Jakarta. 178 p. (in Indonesian).

Jensen R. 2007. The Digital Provides: Information (Technology), Market Performance, and Welfare in the South Indian Fisheries Sector. The Quarterly Journal of Economics 122(3): 879–924. https://www.jstor.org/stable/25098864

Koeswindarti E., Rezekiah A.A., Helmi M. 2021. Financial Analysis of Rubber Plants (*Hevea brasilliens*) Area of PT. Inhutani III Joint Operation (KSO) with PT. Citra Putra Kebun Asri Tanah Laut Regency [Analisis Finansial Tanaman Karet (*Hevea brasiliensis*) Areal PT. Inhutani III Kerjasama Operasi (KSO) dengan PT. Citra Putra Kebun Asri Kabupaten Tanah Laut]. Jurnal Sylva Scienteae 4(2): 264–273 (in Indonesian).

Kusters K., Perez M.R., de Foresta H., Dietz T., Rostonen M., Belcher B., Wollenberg E. 2008. Will agroforestry vanish? The case of Damar agroforests in Indonesia. Human Ecology 36(3): 357–370. https://doi.org/10.1007/s10745-008-9168-3

Makmur E., Imron A., Maskun M. 2018. Repong Damar for coastal communities in Karya Penggawa District, Pesisir Barat Regency [Repong Damar bagi masyarakat pesisir di Kecamatan Karya Penggawa Kabupaten Pesisir Barat]. FKIP Universitas Lampung. Bandar Lampung. Journal of Pesagy 3(1). 13 p. (in Indonesian).

Maryati R. 2020. Analysis of the Role and Contribution of Repong Damar to Community Household Income in an Islamic Economic Perspective [Analisis Peran dan Kontribusi Repong Damar terhadap Pendapatan Rumah Tangga Masyarakat dalam Perspektif Ekonomi Islam]. Skripsi. Raden Intan Lampung State Islamic University. Bandar Lampung. 79 p. (in Indonesian).

Michon G., Mary F., Bompard J. 1986. Multistoried Agroforestry Garden System in West Sumatra, Indonesia. Agroforestry Systems 4: 315–338. https://doi.org/10.1007/BF00048106

Michon G., de Foresta H., Aliadi A. 1996. Damar Resins from Extraction to Cultivation: an 'Agroforestry Strategy' for Resource Appropiation. In: Proceedings of the IVth International Congress of Ethnobiology, Lucknow, India, November 1996: 454–459.

Murniati, Garrity D.P., Gintings A.N. 2001. The contribution of agroforestry systems to reducing farmers' dependence on the resources of adjacent national parks: a case study from Sumatra, Indonesia. Agroforestry Systems 52(3): 171–184. https://doi.org/10.1023/A:1012047602192

Mutuo P.K., Cadisch G., Albrecht A., Palm C.A., Verchot L. 2005. Potential agroforestry for carbon sequestration and mitigation of greenhouse gas emissions from soils in the tropics. Nutrient cycling in Agroecosystems 71(1): 43–54. https://doi.org/10.1007/s10705-004-5285-6

Novianti T. 2021. Project Evaluation [Evaluasi Poyek]. Universitas Terbuka, Tangerang Selatan. 227 p. (in Indonesian).

Nyhus P.J., Tilson R. 2004. Agroforestry, elephants, and tigers: Balancing conservation theory and practice in human-dominated landscapes of Southeast Asia. Agriculture, Ecosystems and Environment 104(1): 87–97. https://doi.org/10.1016/j.agee.2004.01.009

Regional Development Planning Agency of West Coast Regency 2015. Cluster-Based Invesment Profile of West Coast Regency in 2015. Krui. 53 p.

Rustiadi D., Saefulhakim S., Panuju D.R. 2011. Regional Planning and Development [Perencanaan dan Pengembangan Wilayah]. Second edition. Indonesian Obor Library Foundation, Jakarta. 514 p.

Sugiyono 2013. Quantitative, Qualitative and R&D Research Methodologies [Metodologi Penelitian Kuantitatif, Kualitatif dan R&D]. ALFABETA. Bandung. 334 p. (in Indonesian).

FORESTRY IDEAS, 2024, vol. 30, No 1 (67): 120–138

Preservation and optimisation of ‘Dubynka’ historical planting of National dendrological park ‘Sofiyivka’

Yuriy O. Rumiankov[1], Olga Porokhniava[1], Volodymyr Hrabovyi[1], Hryhoriy I. Muzyka[1], Tetyana Kopylova[1], Volodymyr Vitenko[2*], Iryna Pushka[2], and Vasyl Zayachuk[3]

[1]Department of Dendrology and Park Construction, National Dendrological Park ‘Sofiyivka’ of the National Academy of Sciences of Ukraine, 12a Kyivska Str., Uman, Ukraine.
[2]Department of Forestry, Faculty of Forestry and Landscape Gardening, Uman, National University of Horticulture, 1 Institutska Str., Uman, Ukraine. *E-mail: uman.vitenko@ukr.net
[3]Ukrainian National Forestry University, 103 General Chuprinka Str., Lviv, Ukraine.

Received: 28 December 2023 / Accepted: 18 April 2024 / Available online: 07 May 2024

Open Access: This article is licensed under a Creative Commons Attribution 4.0 International License.

Abstract

In the course of coenosis development, changes in the quantitative and species structure took place in certain areas of ‘Dubynka’ historical planting. The aim of the study is to find out possible ways to optimise and propose measures to restore the quantitative structure of *Quercus robur* in it. The research was carried out by field (continuous inventory), analytical and mathematical, and statistical methods. Throughout the historical development of the coenosis, *Carpinus betulus* has been the dominant species in the tree stand. The low number of *Acer platanoides* and *Fraxinus excelsior* in certain age groups indicates an unbalanced removal of trees during felling. It was proved that the beginning of the decay of the primary planting of *Q. robur* began 100–118 years after its establishment. A stable tendency to reduce its quantitative indicators in the structure due to the death of trees and weak natural recovery during the last 109–127 years was revealed. The loss of the ability to natural recovery of *Q. robur* during the last 54–72 years was also revealed. The impracticality of using artificial measures to reduce the mass fraction of dominant species at the planting in favour of self-regeneration of *Q. robur* has been proven. It was found that under the conditions of this coenosis *Ulmus laevis* is unpromising. The care strategy for the area of the historical planting, which takes into account the coenotic features of development, has been determined. Recommendations are made for restoring the proportion of *Q. robur* to return the historic planting to its appropriate status.

Key words: age groups, artificial origin, dominant species, natural recovery, park coenosis, species composition.

Introduction

Park coenoses, which at the time were artificially formed from native plants, are currently the basis of the National dendrological park ‘Sofiyivka’ of the National Academy of Sciences of Ukraine. Historically, the planting ‘Dubynka’ was created in 1796–98 by seedlings of native species. In scientific works, it was indicated that from the very beginning of the construction of the park, this entire territory was

planted mainly with oaks, with addition of such species as hornbeam, ash, maple, linden (Lypa 1948, Kosarevsky 1951, Kosenko et al. 1996). Unfortunately, mass share of each species in the structure of planting was not reported. Monitoring of plantations and detection of undesirable changes made it possible to adjust the structure of the coenosis in time to restore the historical composition of plantations.

As a result of a regular inspection of the plantations, in 2019 we noted a sharp deterioration in the phytosanitary condition of pedunculate oak (*Quercus robur* L.) plantations on the plateau, which led to accelerated tree mortality. At the same time, on the slope of the valley, no such trend of its accelerated die-off and massive appearance of recently deceased oak trees was detected (Rumiankov 2019).

Over the past hundred years, in Europe, *Q. robur* has been characterised by a weakened resistance to diseases and pests, and is not competitive in forest communities, so as a result of these trends, it is subject to accelerated extinction (Gensiruk 2002, Doležal et al. 2016).

The last decline in the number of *Q. robur* was observed in Europe in 2011–2020. A study conducted over several decades has shown that the number of living oaks has been declining since 1935. It was also found that the death of plantations along with the disruption of natural regeneration can threaten not only the oak population, but also species dependent on it (Larsson 2021). Since 2013, the death of *Q. robur* has been observed in the Ardennes region of Belgium. Given the direct and delayed effects of the extreme drought of 1976 and the subsequent disruption of the water balance due to winter frosts and moderate spring droughts, the condition of the scrub oak is of concern in the context of climate change (Losseau et al. 2020). The projected increase in temperature and extreme summer droughts, which negatively affect the growth of *Q. robur*, contribute to the decline of its local population in the warm southeastern part of the Czech Republic. In addition, such oaks are often infested with mistletoe (*Loranthus europaeus* Jacq.) and suffer from competition from neighbouring trees (Zlatanov 2006, Doležal et al. 2016). In the temperate forests of Europe, the die-off of *Q. robur* and reduced growth were caused by extreme climatic events, such as dry and cold periods, the negative impact of which was intensified by the general climate warming (Bose et al. 2021, Camarero et al. 2021, Vospernik et al. 2023). It has been found that in Europe, after a series of seasonal droughts without any obvious consequences, already weakened *Q. robur* trees can die as a result of another minor drought. The cumulative effect of the negative impact of droughts is associated with the low ability of oak trees to reduce the impact of the initial drought, which causes the risk of high tree loss in the context of global climate warming (DeSoto et al. 2020, Harvey et al. 2020). According to many experts, the reason for the massive drying out of oak forests may be the influence of a complex of factors: global climate change; long-term, selective felling of the best oak trees for economic needs; and the growing anthropogenic load (Kelly et al. 1989, Lutsyshyn and Lavnyy 2012).

The first observations of the accelerated dying off of gully forests in Ukraine were recorded in the 1940s (Borodaevsky 1909). In studies conducted in three typical ravine forests of the southern part of the Ukrainian Steppe in Zaporizhzhya, recreational impacts revealed a slight decrease in regeneration potential and an increase in the proportion of generative and

post-generative individuals in the coenopopulations of Generalka and Khortytska beams. However, in Shyroka Gully, due to the reduction of anthropogenic impact, all coenopopulations of *Q. robur* are young and have significant adaptive potential (Yakovlieva-Nosar and Bessonova 2021).

In a study on the vital status of the dendroflora of Nemyrivskyi Park in Vinnytsia region, was found that the age-old park plantations of *Q. robur* were in good condition, the trees had normal shoot growth without signs of weakening, but the leaf blade had a slight fungal infection, and they bear fruit (Vitenko et al. 2022).

The experience of forestry specialists showed that oak regeneration in the Ukrainian Steppe is hopeless. In the specific climatic and anthropogenic conditions of the southeast of Ukraine, the viability of woody plants was significantly reduced, and their durability was shortened (Levon 2008, Matusyak 2016, Kopiy et al. 2017).

Under unfavourable conditions, the course of ontogeny changes, the periodisation of which may proceed according to a shortened program (Rabotnov 1950, Sklyar 2013).

The age structure of woody plantations determines the dynamics of structural diversity, the ability to self-renewal and the degree of resistance to the impact of natural and anthropogenic factors. Monitoring the age spectrum of park plantations is the basis for a substantive assessment and forecast of the feasibility of developing and implementing certain optimization measures (Fizyk et al. 2016, Zvarych et al. 2016).

Natural regeneration process in plantations is largely determined by natural and climatic factors, and specific conditions of coenosis (Ostapchuk 2013, Ischuk 2017).

Therefore, the study of the species and age structure of the artificial planting of the same climatic zone, but under individual coenotic conditions in different parts of the massif is relevant.

In the process of development of the artificial coenosis of the historical planting, there were changes in its species structure, the scale and trends of which differed depending on the forest and vegetation conditions of individual areas of the planting and the degree of anthropogenic impact (Rumiankov et al. 2021). Currently, our task is to determine the species and age structure of the stand and its undergrowth on the slope of the valley, which is characterised by a better hydrological regime and minimal impact of anthropogenic factors on the development of coenosis, and to identify the reasons for the lack of natural oak regeneration in sufficiently optimal conditions for many species in this area. Therefore, the aim of our study is to provide practical recommendations for plantation care, and propose measures to restore share of oak. The scientific novelty of the work is to determine the characteristic features of the development of the coenotic structure of a separate section on the slope of the valley, which will allow us to propose a specific direction of the plantation care strategy to restore share of oak.

Object and Methods

The object of our research was historical planting ‘Dubynka’ of the National dendrological park ‘Sofiyivka’. Its geographic coordinates are 48°45‘36″ N, 30°13‘59″ E (Fig. 1).

The subject of our research was the species and age structure on the slope of the valley. In June 2023, a study of the species and age structure of the plantations was carried out using the continuous inventory method. The named method

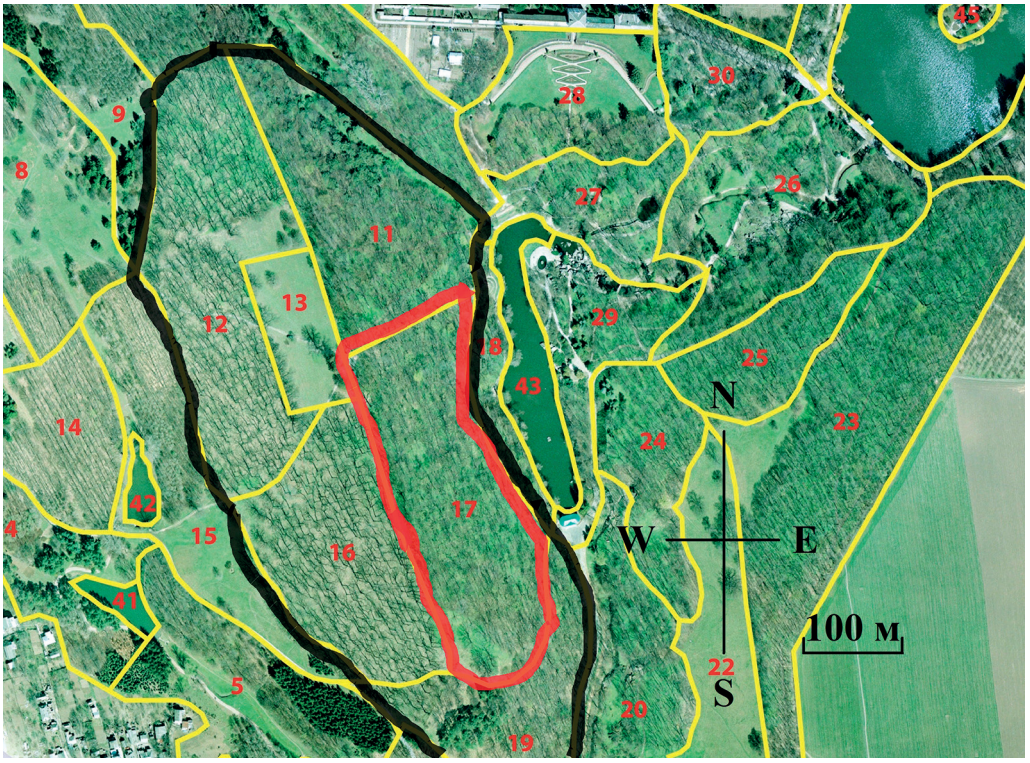


Fig. 1. Planting 'Dubynka' of quarter No 17 of the National dendrological park 'Sofiyivka' of NAS of Ukraine.

Note: black line – the entire plantation, the red line – the valley part of the plantation (object of our research).

involves the individual enumeration of all trees, bushes and self-seeding plants of each species in a continuous manner on an area of 4.1 ha, which was highlighted on the map with a red line. To achieve this goal, we used methodical instructions for conducting field work on the inventory of forests of the Polissky region of Ukraine (Storozhuk 2006), methodical recommendations for inventorying, taxation and monitoring of perennial plantings in historical parks of Ukraine (Kosenko et al. 2014). We analysed the species and age structure of the plantations using the scientific works of: Lypa (1948), Kosarevsky (1951), and Kosenko et al. (1996). We determined the approximate age of oak trees by counting annual cambial layers of the trunk of cut dry trees. When analysing the age structure, we determined the age of the tree indirectly through the trunk diameter, since its thickness depends on the tree's life expectancy. The trees were conventionally divided into age groups, where each subsequent group contains trees 10 cm larger than the trunk diameter of the previous one. Self-seeding of trees was divided into three age groups by plant height. The first age group includes plants which height is from 0.1 to 1 m, the second – from 1 to 5 m, and the third – from 5 to 10 m.

The climate is characterised as moderately continental, with an average annual

air temperature of 7.3–9.4 °C. The coldest month is January with an average temperature of -5.6 to 6.1 °C, and the warmest is July with an average temperature of 19.2–20.8 °C. The absolute minimum air temperature is -34 to -38 °C. The absolute maximum temperature of 36–39 °C is observed in July–August. The transition of the average daily temperature through 0 °C occurs on March 15–16 and November 22–24. There are 242–255 days in a year with an air temperature above 0 °C. The average annual rainfall is 570–630 mm, of which only 300–310 mm falls during the period with a temperature of more than 10°C. During the year, precipitation is unevenly distributed, the most falls in June–July (90–100 mm), and the least in January–February (Shkvaruk and Zapatiy 1960, Lipinsky et al. 2003).

The soil cover of the park is dominated by regraded chernozems and dark gray forest podsol. The acidity varies between pH 4.8–7.3, but the majority of soils have a neutral reaction. Most of dark gray forest soils are heavy loamy by mechanical composition. The content of humus in a 30-centimeter layer of soil is 2.7–3.8 %; nitrogen content – 8.9 mg per 100 g; of mobile compounds of phosphorus and potassium, respectively, 10.8–12.5 and 14.3–16.4 mg per 100 g. Groundwater lies at a depth of 1.7 to 22.0 m. In general, the soils are highly fertile (Shkvaruk and Delemenchuk 1969, Shlapak 2021).

Results and Discussion

As a result of stand species structure analysis, based on the size of the quantitative share, species were conditionally divided into two categories. The first category includes species which share from 5 to 36 %. The second category includes species with a share of only 0.8 % of the total number of trees (Fig. 2).

The first category includes *C. betulus*,

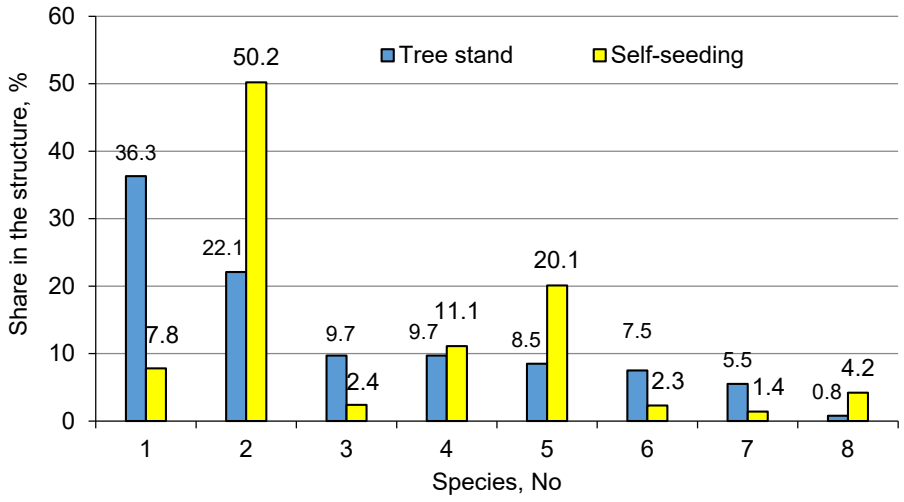


Fig. 2. The species structure of the tree stand and self-seeding.

Note: 1. *Carpinus betulus* L., 2. *Acer platanoides* L., 3. *Quercus robur* L., 4. *Acer campestre* L., 5. *Fraxinus excelsior* L., 6. *Ulmus laevis* Pall., 7. *Tilia cordata* Mill., 8. species that are found in single specimens.

A. platanoides, *Q. robur*, *A. campestre*, *F. excelsior*, *U. laevis*, *T. cordata*.

The second category includes single specimens of: *Prunus padus* L., *Quercus rubra* L., *Prunus avium* L., *Picea abies* L., *Celtis occidentalis* L., *Crataegus oxyacanta* L., *Prunus cerasifera* Ehrh., *Sorbus torminalis* L., *Acer pseudoplatanus* L., *Morus alba* L., *Styphnolobium japonicum* (L.) Schott, *Juglans cinerea* L.

Currently, species of the second category, have a minimal impact on this park coenosis, but their presence determines a certain reserve in case of loss of perspective of any species from the first category as a result of climate changes. In addition to the reserve function, species of the second category in the plantation can also perform the role of decorative elements. For example, *M. alba*, which adaptive potential in studies was assessed as high (Vitenko et al. 2023), acquires a higher decorative effect with the use of grafted forms. The method of grafting mulberry trees directly in the stand itself allows to avoid such an operation as transplantation, thereby maintaining the growth rate of the rootstock, and also lengthen the life of the grafted tree. *M. alba* trees of the forms ‘Pendula’, ‘Globosa’, ‘Pyramidalis’, ‘Contorta’, ‘Macrophylla’ were grafted by the method of improved copulation according to the conclusions of Vitenko et al. (2019) quickly fuse, and the grafting sites are completely covered with protective tissue. The use of single *M. alba* trees of various grafted forms on the edges of forests will help to enrich the park’s dendrostructure and, bringing local colour, will increase the decorative effect of the planting.

C. betulus and *A. platanoides* occupy the largest mass share in the plantation (36.3 and 22.1 %, respectively). The smallest share in the first category is occupied by *T. cordata* — 5.5 %. *Q. robur, A. campestre, F. excelsior* and *U. laevis* have the average mass fraction (9.7, 9.7, 8.5 and 7.5 % respectively).

The identified main species composition of the plantation generally coincides with the structure formed at the beginning of the park construction (1796), except for *U. laevis*, which was not mentioned in historical sources. Taking into account the existing quantitative composition, the investigated plantation only partially corresponds to the original composition, since instead of *Q. robur*, which is mentioned in historical sources, the structure of the tree stand is dominated by *A. platanoides* and *C. betulus*. Describing the tree stand in 1948, Lypa (1948) wrote that ‘hornbeam dominates here, forming almost everywhere a single tree massif. Only very rarely and in small quantities, other species occur: ash, oak, maple, pear, linden and others‘ so now we have every reason to confirm the relevance of the dominance of *C. betulus* in this coenosis. In addition, given the dominant position of hornbeam described by Lypa in 1948 and the fact that we have found its dominant position in the tree stand over the past 90–110 years, we consider the trend of *C. betulus* dominance in the park’s coenosis to be historical. It is also interesting to note that as of 1948, oak, ash and maple occupied an insignificant part in the structure of the tree stand, which at that time also did not allow this plantation to be called a oak tree stand, and therefore did not correspond to its historical name.

Among the species composition of the self-seeding, *A. platanoides* and *F. excelsior* have the largest mass fraction (50.2 and 20.1 %, respectively) (Fig. 2). *Q. robur, U. laevis* and *T. cordata* have the smallest share in self-seeding (2.4, 2.3 and 1.4 %, respectively). *A. campestre*

and *C. betulus* (11.1 and 7.8 %, respectively) have average values of the mass share of self-seeding in the plantation.

The largest amount of self-seeding in all three age groups was found in *A. platanoides* (Table 1).

Table 1. Quantitative characteristics of age groups of self-seeding.

Species	Number by plant height			Total number of self-seeding
	I / 0.1–1 m	**II / 1.1–5** m	**III / 5–10** m	
Acer platanoides L.	2656	732	408	3796
Fraxinus excelsior L.	1361	142	16	1519
Acer campestre L.	489	313	35	837
Carpinus betulus L.	442	112	33	587
Quercus robur L.	181	0	0	181
Ulmus laevis Pall.	113	90	11	214
Tilia cordata Mill.	43	27	33	103

In age group I, the quantitative index of maple self-seeding (2656 pcs.) is twice as large as that of such a strong edificator as ash (1361 pcs.).

The biggest difference between the quantitative indicators was determined in age group III, where the maple is 25 times more than the ash. The highest number of self-seeding in all three age groups of *A. platanoides* convincingly demonstrates the significant natural potential of the species, which leads to a high ability to self-renewal, competitiveness in the park coenosis and provides the possibility of a corresponding dominant position in the stand.

F. excelsior also has a large amount of viable self-seeding (1519 pieces) (Table 1). However, there were no ash trees in age groups I and II (trunk diameter from 10 to 30 cm), and only 2 trees in age group III.

The introduction of measures to regulate the proportion of *A. platanoides* and *F. excelsior* in the past was not unreasonable, given that such a strong unifier as *Q. robur* in this forest community has reduced its influence due to natural causes. For example, in the presence of 181 oak self-seeding plants (Table 1), no *Q. robur* trees were found in age groups I and III, and only a tree in age group II (Fig. 3).

The absence of a sufficient number of *Q. robur* trees in age groups I–III in a row indicates a decrease in competitiveness and leads to the loss of the edificator function in the coenosis.

At first glance, the presence of 181 pcs. self-seeding of oak should guarantee its presence, as in the case of linden, when even the smallest number of self-seeding ensures a full-fledged age structure (Table 1). However, the type of placement of self-seeding plants of these species on the plantation territory is somewhat different. Linden self-seeding, as in most species, is distributed fairly evenly over the entire area, while in oak it is only on one side of the plantation. It was found that the oak seeds germinated on the border of the forest edge-park alley on the northern side, where direct sunlight only gets in the morning and evening, but there is enough diffused light during the day. Of course, such a place will be more humid, because it is close to the park alley. The alley is lined with bricks, under which moisture easily gets and stays. According to our observations, outside the stand tent, in conditions of partial shade and moderate soil

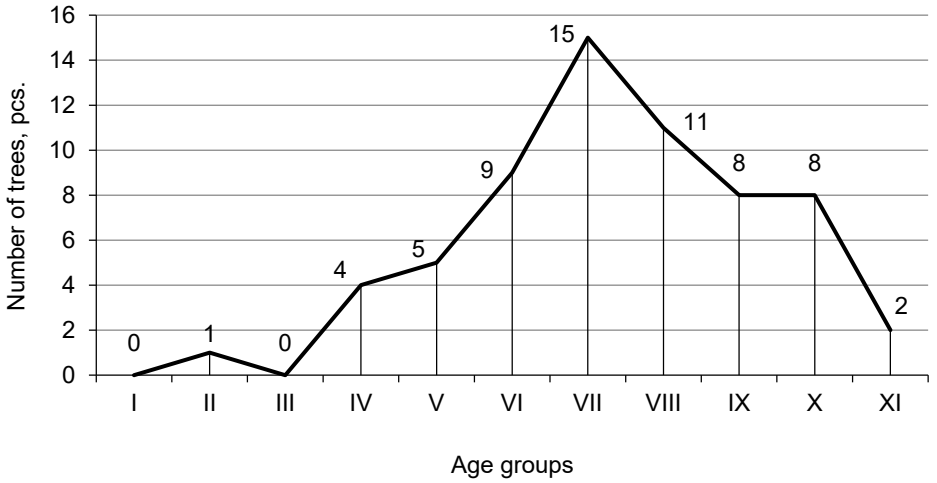


Fig. 3. Quantitative characteristics of *Q. robur* trees by the age structure.

moisture, *Q. robur* seeds can germinate, but young plants are not able to survive.

Studying the regularities of the reforestation process under the canopy of oak-hornbeam plantations in fresh oak forests of the Korsun-Shevchenkivskyi forestry, Ishchuk (2017) determined that low illumination under the canopy of high-completeness oak-hornbeam forests reaches 0.5–3.0 % of total illumination and leads to the gradual death of self-seeding and oak undergrowth in the second or third year of life. Taking into account the author's conclusions, the conditions of natural oak-hornbeam groups do not contribute to the success of oak restoration due to insufficient lighting under the dense canopy of hornbeam. Therefore, if we take into account the dominant impact of hornbeam found in our research – 36.3 % in the species structure (Fig. 2), it should be stated that the dense canopy of hornbeam becomes an obstacle to the successful restoration of oak. It is certain that such a statement should be put in the form of a question.

A similar situation was described in studies on the regeneration of *Q. robur* in deciduous and mixed forests, where the level of photosynthetically active radiation under the tent rarely reaches 15 %, which is insufficient for the successful growth and development of oak self-seeding (von Lüpke 1998). Comparing the findings of Ishchuk (2017), who believed that 0.5–3.0 % of total illumination leads to the gradual death of self-seeding and undergrowth of oak, with the findings (von Lüpke 1998) that the level of photosynthetically active radiation in natural forests 15 % (this is 5 times more than the previous value) was still insufficient for the development of oak, we can note that the limiting factor for the restoration of oak is most likely not the amount of light. For example, in our research, even in completely open areas under the crowns of oak plantations, self-seeding of oak was not detected at all. In other words, how, with all components being equal, did the oak still continue to regenerate in natural forests when it was so critically lacking in light?

Studies of reforestation processes in 110–165-year-old oak forests of 'Roztochia' Nature Reserve have shown that

the undergrowth of common oak, compared to other species, is more sensitive to insufficient light and other factors of the under-tent environment (Zvarych et al. 2016). The authors established that on most of the area, almost all oak self-seeding was very weakened and unsustainable, therefore, no plants taller than 25 cm and older than 2–3 years were found on the territory of the reserve. It should be noted the similarity of the results obtained in our study, when analysing the age structure of oak self-seeding in the stand, it was established that it was absent in age groups II and III (Table 1). The presence of self-sowing oak of only the age group I indicates that one of the limiting factors of the viability of oak growth is insufficient lighting under the tree canopy. In order to discuss this question from the other side, the following seemingly similar situation should be considered.

Accordingly, with a decrease in the efficiency of photosynthesis in leaves, which are often affected by the fungus *Phytophthora* de Bary, according to Bobiec et al. (2018), young oaks could lose their former ability to survive and grow in forest conditions, but at the same time, they remained strong competitors in well-lit non-forest areas. In our research, sufficiently well-lit areas (clearings, gaps, glades) were also found on the territory of the forest stand, in addition, the sunny edges of the plantation perimeter were examined, but no self-seeding oak plants were found. Therefore, well-lit areas do not guarantee young oak plants the opportunity to show their competitiveness.

Taking into account the formation of the stand mainly from common oak, in the future, even in the absence or minimised influence of competing tree species, according to observations by a number of authors, oaks are not able to regenerate themselves directly under their own canopy (Palmer et al. 2004, Strandberg et al. 2005, Perrin et al. 2006), which was also proved by previous research (Rumiankov 2019), that established the absence of natural regeneration in artificially created oak plantations, where the undergrowth of other species was regularly removed. For now, it should be noted regarding our debatable question about the importance of lighting conditions, from the point of view of the degree of illumination of this area, we can confidently state that in relation to this factor, the possibility of oak restoration was not limited.

At the same time, research in the artificial plantations of the Sinytsky Forestry of the 'Uman Forestry' State Enterprise showed their high productivity in the composition of 48 % of common oak, 19 % of common ash, 19 % of European beech, 9 % of sharp-leaved maple, and less than 5 % of such as elm, aspen, hornbeam and linden (Koval et al. 2022). In plantations dominated by *Q. robur* under the conditions of its simultaneous planting and a uniform placement scheme, oak trees received the first class of quality assessment. Comparing the specified structure of the plantation with the structure in our plantation, it should be noted that the species structure of our object of research corresponds to a greater extent to the structure of natural oak-hornbeam communities (Fig. 2), which should contribute to the restoration of oak, but as it turned out, the plantation formed as a natural oak-hornbeam coenosis does not yet ensure the success of oak restoration.

The only continuous tree canopy which conditions could allow oaks to regenerate is a translucent crown architecture that can leave young oak plants with enough photosynthetically active radiation to grow and develop. This semi-permeable prop-

erty of the canopy is possessed by pine stands, which are widely cultivated by forestry in most European biogeographic regions, often in an ecological niche for deciduous forests (Kuiters and Slim 2003, Onaindia et al. 2013). Taking into account the openwork of the crown of pine plantations, we consider it expedient to introduce *Pinus sylvestris* L. into the planting as an alternative for enriching the dendrostructure, which could realise the natural potential of oak regeneration. Therefore, we recommend the establishment of scots pine plantations in certain areas stand, which will open up new prospects for research, observing in the future how this measure will remain justified in the individual conditions of the existing coenosis for both oak and pine.

Studying the reproduction of oak stands naturally in forestry in Ukraine, it was found that in forest areas with clearfelling, where the stand was cut after the acorn fell in a harvest year, the lowest decline of self-seeding oak (19.3–28.5 %) is typical (Kopiy et al. 2017). Analysing the areas of clear-cutting of oak forest stands in Podillia, Matusyak (2016) shows that under optimal conditions it is possible to ensure the natural regeneration of common oak at the level of 3000–5000 pcs. per ha in the next 1–2 years after clear-cutting. These studies have shown that oak self-seeding in areas of the forest with clearfelling was characterised by much faster growth. In our opinion, this indicates that in the presence of fresh fallen oak seeds under favourable lighting conditions, there is a real opportunity to obtain self-seeding of oak, which can quantitatively ensure the full reproduction of oak plantations. Taking into account the fact that there is an opportunity to obtain viable oak plants in the open area and the proven fact of the failure of natural regeneration in our case, leads us to use an artificial means of restoring the species structure of *Q. robur* by planting young trees.

It should be noted, that in temperate climates, there are forest habitats where oaks retain their dominant position due to their stress resistance over other species that cannot withstand boreal and arid conditions. Harsh natural biotic factors specific to acidophilous oak forests on silicate rocks, xerophilous oak forests on limestone, Euro-Siberian steppe forests, Pannonian-Balkan oak forests, and old-growth oak forests of the British Isles (habitats 9190, 91I0, 91M0, 91A0 – European Commission 2013) reduce interspecific competition and prevent the development of dense shade-tolerant stands, and therefore promote the regeneration of *Q. robur.* In our opinion, the existence of the listed habitats shows that the oak feels more comfortable even in harsh conditions of high soil acidity or on limestone outcrops, without a sufficient amount of water and without the structure of officially recognised associations, which were obliged to perform the functions of preserving species diversity. In difficult conditions for most species, the oak is able to form a coenosis with a full-fledged age structure, which indicates regular natural regeneration. If we mention the presence of the habitat of the old-growth oak forests of the British Isles, then this fact indicates that even in such conditions *Q. robur* is able to maximally show its potential as a long-lasting species. In addition to the above, we can note that similar conclusions were also reached by other researchers, for example Johnson et al. (2009), who gave oak culture a special ecological niche, as the formation of similar habitats with the natural regeneration of oak without the influence of exogenous factors they called by a separate term

such as 'intrinsic oak accumulator'.

Analysing the discussion of the views of the presented researchers regarding the possibility of oak restoration in the conditions of tree groups, we can conclude that the oak plantation should not be perceived as a self-regenerating formation, but only as an initiating forest grouping, in which the oak in the process of historical development of the coenosis no longer finds an ecological niche for its development. Taking into account the contradictions of the data presented by a number of scientists and forestry specialists regarding the determination of the conditions for the natural restoration of oak, it should be recognised that it forms a special category of plantations with artificial support for the conditions of its cultivation and reproduction function. Therefore, taking into account the special status of oak given by individual scientists, it becomes clear why, according to researchers (Bobiec et al. 2018), the problem of successful restoration and replenishment of oak habitats is solved by creating modern oak formations, represented mainly by non-forest natural or artificial habitats.

Currently, on the territory of the planting, we can only state a complete loss of the ability of *Q. robur* to regenerate naturally, as evidenced by the absence of oak trees for three consecutive age groups, except for a single specimen in age group II (Fig. 3). However, the fact that there is an ecological niche that still allows the formation of single specimens of *Q. robur* gives us reason to recommend the use of existing glades in the stand for artificial planting of young oak trees. The event involves the use of not only existing glades, but also other open spaces that do not contain full-fledged trees with the obligatory clearing from self-seeding, shrubs and grass vegetation to ensure proper light conditions young oak plants. Given that only one out of 181 oak self-seeding plants survives (often none) (Table 1) and the reduced moisture supply of open areas, we recommend that in addition to clearing, which should be done during the growing season, regular watering should be provided. The proposed possibility of restoring the quantitative structure of *Q. robur* is quite relevant for returning the appropriate status to the historical planting.

As a result of age structure analysis, the two oldest trees of *Q. robur* in age group XI were found (Fig. 3). We found that the growth of oak in the trunk diameter in this area is on average 5.5 mm per year. The trunk diameter of these trees is 115 and 117 cm, which is about 209- and 212-year-old, respectively. Given that from the very beginning of the park's construction, this entire area was planted mainly with oaks (Lypa 1948, Kosarevsky 1951, Kosenko et al. 1996), only two of these trees remain in the planting. We can conditionally consider these two trees to be contemporaries of the construction of the park, which is now 227-years-old. It is planned to install commemorative plaques on granting the status of historic trees to two long-lived specimens of *Q. robur.*

The highest number of common oak trees was recorded at the age of 127–145 years – 15 trees (age group VII) (Fig. 3). Probably 127–145 years ago, oak was still the dominant species in the community. That is, for 80–98 years from the establishment, the oak still held a quantitative advantage. A 40 % decrease in the number of oak trees 109–127 years ago (age group VI) indicates significant losses in the structure of the stand and determines the beginning of the decay plantation of oak in the structure of the coenosis.

It is important to note that the decline in the quantitative characteristics of oak in

relation to other dominant species began in an overripe state, which it reached in the 100–118th year of the planting existence. After that, there was a steady downward trend in the quantitative structure due to the death of old trees and weak natural regeneration. This makes it possible to state that at the initial stage of the park coenosis development, the dominance of *Q. robur* was based only on a quantitative advantage during the establishment of planting.

The next reduction in the quantitative composition occurred 90–109 years ago (age group V) by 44 %, which confirms the tendency of a decrease in quantitative indicators 116–135 years after the establishment plantation of *Q. robur* (Fig. 3).

The presence of oak trees (4 pcs.) aged 72–90 (age group IV) in the stand certainly indicates some natural regeneration (Fig. 3), but its intensity and viability were already declining and could not ensure the proper quantitative share of *Q. robur* as the dominant species. Over the past 54–72 years (age group I–III), only one oak tree has grown, which indicates a critically low capacity for natural regeneration of *Q. robur* trees.

Analysing the age structure of self-seeding, we can note the presence of its full-fledged structure in the form of three age groups for all the listed species, but this pattern does not apply to *Q. robur*. In the age structure of *Q. robur* self-seeding, there are no plants of age groups II and III, while there are 181 plants in age group I (Table 1).

The detected self-seeding of oak only in age group I indicates a sufficient intensity of fruiting trees and the quality of acorns that formed this self-seeding, and at the same time insufficient stability of self-seeding of age groups II and III (Table 1). If we take into account the inability of the oak tree to self-regenerate on the territory of the planting in our time and the revealed steady tendency to reduce its quantitative structure throughout the entire development of the coenosis, then hypothetically, there is every reason to think that self-seeding *Q. robur* was not competitive enough from the establishment.

The quantitative advantage of the maple over the ash in the age groups is preserved only in the I one (Fig. 4). If we analyse their age structure from age groups II to IX, *F. excelsior* takes quantitative priority. In addition, its maximum one-time quantitative indicator in age group V (19 pcs.) testifies its high potential viability in the park coenosis in the absence of control by anthropogenic factors over the quantitative structure of species with a high reproduction rate. Therefore, given the significant potential for self-seeding of maple and ash, low quantitative indicators in age groups II and III are not typical, which indicates active anthropogenic interference in the development coenosis.

We consider the decrease in the number of *A. platanoides* and *F. excelsior* in age groups II and III as the implementation of measures to artificially reduce their dominant potential in this coenosis.

Taking into account the loss of the status of *Q. robur* as an edificator in the past, measures to artificially reduce the mass fraction of *A. platanoides* and *F. excelsior* as potentially dominant species were carried out in order to improve the lighting regime and creation of a favourable microclimate for self-regeneration of *Q. robur*. However, at the moment we can observe the impracticality of using artificial measures to reduce the mass share of dominant species in the planting, which could contribute to the natural recovery of *Q. robur*. In connection with this, we are planning to implement measures to regularly

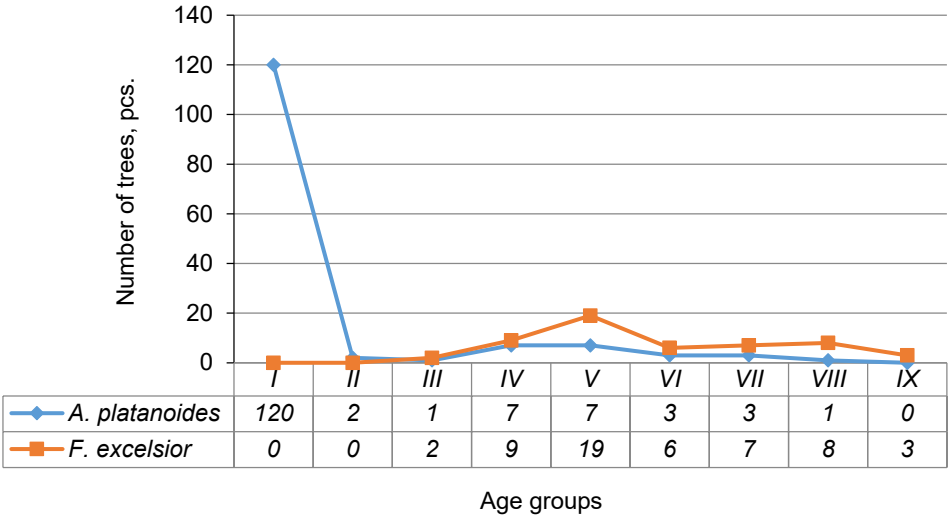


Fig. 4. Comparative characteristics of *A. platanoides* and *F. excelsior* number in the age structure.

control the quantitative indicators of competitive young trees *A. platanoides* and *F. excelsior* to maintain the mass share of dominant species in the park coenosis at the level of 20–25 %.

The quantitative composition in age group I of self-seeding *A. campestre* and *C. betulus* is almost the same: 489 and 442 pcs. respectively (Table 1). In age group III of self-seeding, the ratio of these species remained in the same balance, but quantitatively decreased by 14 times (35 and 33 pcs., respectively), showing the same degree of viability. However, if we analyse the quantitative characteristics of the age groups of *A. campestre*, it turns out that the field maple very quickly loses its quantitative share with each subsequent age group, and it was not detected already in age group IV (Fig. 5), which indicates the insufficient longevity of *A. campestre* in the conditions of this coenosis.

Compared to *A. campestre*, the quantitative characteristics of *C. betulus* age groups in the tree stand differ in a more gentle and uniform decline, keeping high indicators (from 89 to 26 pcs.). It should be noted that even in the last age group, the number of hornbeam trees remains quite high, whereas for all the studied species the presence of senescent trees in single specimens is more typical. Therefore, the absence of long-lived trees in *C. betulus* is determined by the massive death of a large number of old trees in the last age group.

U. laevis and *T. cordata* are characterised by the lowest quantitative self-seeding potential, with indicators in age group I of 113 and 43 pcs. respectively (Table 1). Compared to linden, elm loses its quantitative indicators much faster, because in self-seeding of age group III, 10 times fewer plants were found than at the beginning.

A similar trend of rapid loss of quantitative indicators of *U. laevis* is also observed in the tree stand, when already in age group III there are only two trees left (Fig. 6), which is 15 times less than in the first.

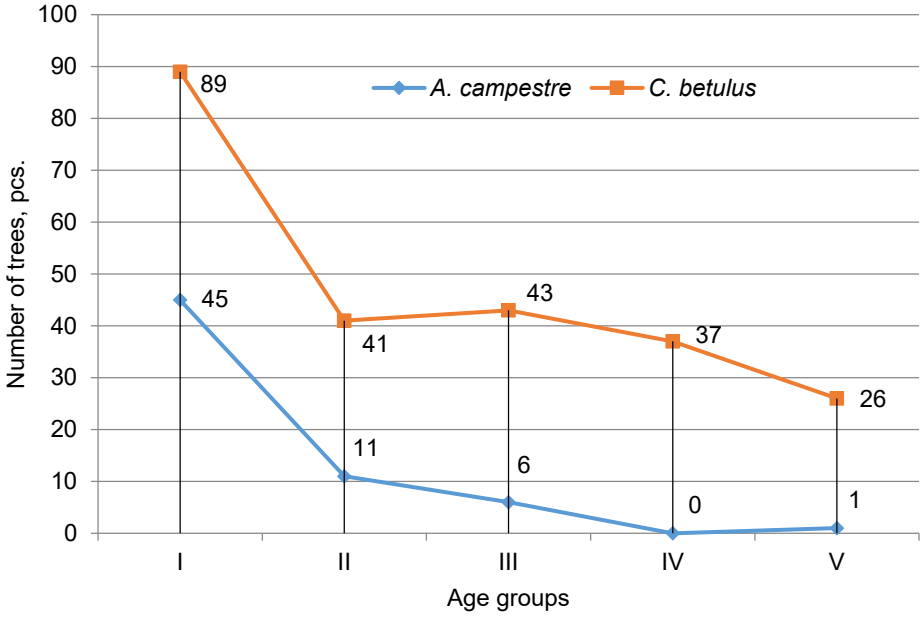
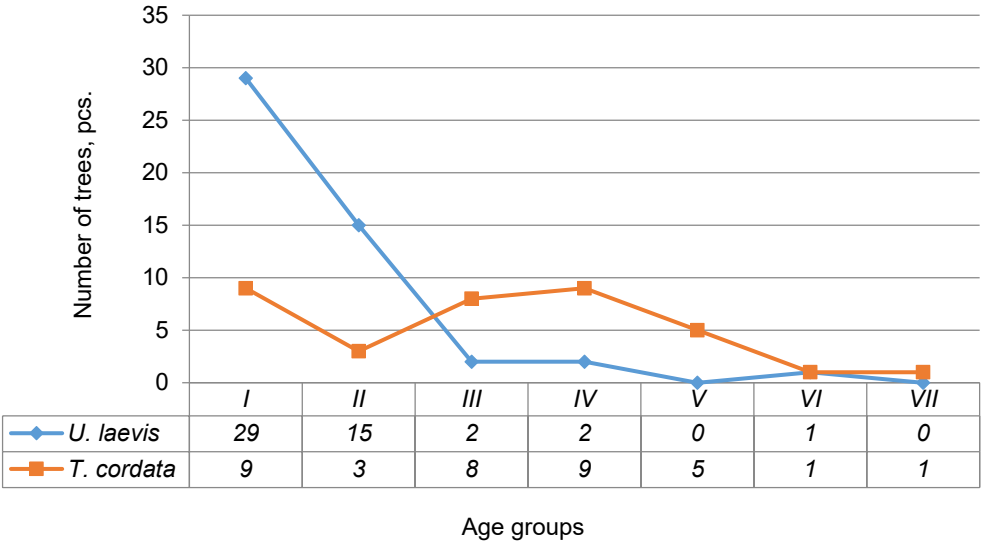


Fig. 5. Comparative characteristics of *A. campestre* and *C. betulus* number in the age structure.



	I	II	III	IV	V	VI	VII
U. laevis	29	15	2	2	0	1	0
T. cordata	9	3	8	9	5	1	1

Fig. 6. Comparative characteristics of *U. laevis* and *T. cordata* number in the age structure.

In the age structure 89.7 % of the quantitative potential of elm is concentrated only in the first two age groups out of the six identified, which indicates the short-

lived nature of *U. laevis* and, accordingly, its low prospects in this coenosis.

The initial self-seeding potential of *T. cordata* in age group I was the lowest among all species (43 pieces) (Table 1). In age group III, 1.3 times less self-seeding linden remained than in I (33 pcs.). This is the lowest rate of natural thinning of self-sowing among all studied species, which indicates the high viability of *T. cordata* in this coenosis (Table 1).

Compared to *U. laevis*, the quantitative indicators of *T. cordata* in age groups I–IV are distributed fairly evenly. However, it should be noted a sharp decrease in the number of linden trees in age group II – 3 pcs., which is 66 % less than in age group I (Fig. 6). In our opinion, the regulation of the quantitative composition of *T. cordata* by anthropogenic factors is unlikely, since is natural regeneration is the least intensive (Table 2). For this reason, a violation of the characteristic stability of quantitative indicators and a decrease in the viability of linden trees occurred due to natural factors.

Analysing the quantitative structure of age groups among the studied species, it was found that the most long-lived in this coenosis are *Q. robur* in the amount of 2 pcs. (Fig. 3) and *F. excelsior* – 3 pcs. (Fig. 4), which belong to age groups XI and IX, respectively. The rest of the studied species were placed in descending order of longevity as follows: *A. platanoides*, *T. cordata*, *U. laevis*, *C. betulus* and *A. campestre* – in the last place.

Conclusions

Currently, the plantation does not correspond to its original composition due to the lack of the quantity of *Q. robur* stipulated by the founders of the park. Throughout the historical development of the coenosis, *C. betulus* has been the dominant species in the tree stand. The absence of separate age groups of *A. platanoides* and *F. excelsior* was found, which indicates an unbalanced anthropogenic regulation of their number. Considering the high natural self-sowing potential of *F. excelsior* and *A. platanoides*, these two species are candidates for dominance. The high viability and prospects of *T. cordata* and the low prospects of *U. laevis* in the conditions of this park coenosis were revealed. Two long-lived trees of *Q. robur*, aged about 209 and 212 years, corresponding to the status of historical trees, were found on the territory of the plantation.

It was proved that the decay of the primary plantation of *Q. robur* began 100–118 years after its establishment. A steady downward trend in the quantitative structure due mortality and weak natural regeneration over the past 109–127 years was revealed. The loss of the ability to natural recovery of oak on the territory of the planting over the past 54–72 years has been proven. The reason for the lack of natural recovery is probably the non-competitiveness of oak seedlings in age group I.

The inexpediency of using artificial measures to reduce the mass fraction of potentially dominant species *A. platanoides* and *F. excelsior* in the plantations to promote self-regeneration of *Q. robur* was revealed. It was established that the basis of the dominance of *Q. robur* in the territory of the planting was only its quantitative advantage during the creation of the park.

Recommended:

- Regular monitoring of quantitative indicators of self-seeding of competitive species *A. platanoides* and *F. excelsior* to achieve optimal values of the mass frac-

tion of dominant species in the park coenosis up to 20–25 %.

- Restoration of the quantitative structure of *Q. robur* to restore the appropriate status to the historic planting by artificially planting young oak trees in open areas (clearings, gaps, glades). Ensure regular watering of young oak trees and clearing of overgrowth (self-seeding trees, bushes).

- Creation of plantations of *P. sylvestris* in certain areas of the stand as an element of the dendrostructure with a semi-permeable canopy that promotes the natural renewal of *Q. robur*.

- Reducing the mass fraction of *U. laevis* by removing its self-seeding in favour of other promising species such as *F. excelsior, A. platanoides* or *T. cordata.*

The provided recommendations for controlling the quantitative and restoration of species structure are the basis of the care strategy for the plantations, which takes into account the coenotic features of development.

References

Bobiec A., Reif A., Öllerer K. 2018. Seeing the oakscape beyond the forest: a landscape approach to the oak regeneration in Europe. Landscape Ecology 33: 513–528. https://doi.org/10.1007/s10980-018-0619-y

Borodaevsky L.S. 1909. Drying of the forest in the Mayatsky dacha of the Mayatsky forestry of the Kharkov province. Forest Journal 6: 688–711 (in Russian).

Bose A.K., Scherrer D., Camarero J.J., Ziche D., Babst F., Bigler C., Bolte A., Dorado-Liñán I., Etzold S., Fonti P., Forrester D.I., Gavinet J., Gazol A., González de Andrés E., Karger D.N., Lebourgeois F., Lévesque M., Martínez-Sancho E., Menzel A., Neuwirth B., Nicolas M., Sanders T.G.M., Scharnweber T., Schröder J., Zweifel R., Gessler A., Rigling A. 2021. Climate sensitivity and drought seasonality determine post-drought growth recovery of *Quercus petraea* and *Quercus robur* in Europe. Science of the Total Environment 784, 147222. 13 p. https://doi.org/10.1016/j.scitotenv.2021.147222

Camarero J.J., Colangelo M., Gazol A., Azorín-Molina C. 2021. Drought and cold spells trigger dieback of temperate oak and beech forests in northern Spain. Dendrochronologia 66, 125812. 13 p. https://doi.org/10.1016/j.dendro.2021.125812

DeSoto L., Cailleret M., Sterck F., Jansen S., Kramer K., Robert E.M.R., Aakala T., Amoroso M.M., Bigler C., Camarero J.J., Čufar K., Gea-Izquierdo G., Gillner S., Haavik L.J., Hereş A-M., Kane J.M., Kharuk V.I., Kitzberger T., Klein T., Levanič T., Linares J.C., Mäkinen H., Oberhuber W., Papadopoulos A., Martínez-Vilalta J. 2020. Low growth resilience to drought is related to future mortality risk in trees. Nature Communications 11, 545. 9 p. https://doi.org/10.1038/s41467-020-14300-5

Doležal J., Lehečková E., Sohar K., Altman J. 2016. Oak decline induced by mistletoe, competition and climate change: a case study from central Europe. Preslia 88(3): 323–346. https://www.preslia.cz/article/pdf?id=72

European Commission 2013. Interpretation manual of european union habitats. DG Environment, Brussels, Belgium. 144 p. https://www.miteco.gob.es/content/dam/miteco/es/biodiversidad/temas/espacios-protegidos/doc_manual_intp_habitat_ue_tcm30-207191.pdf

Fizyk I.V., Kopiy S.L., Ahiyy V.O., Kopiy O.I., Kaganiak Yu.Yo., Kopiy L.I. 2016. Influence of forest management on the structure hornbeam-oak stands under Transcarpathia. Scientific Bulletin of UNFU 26(4): 147–156 (in Ukrainian). https://doi.org/10.15421/40260423

Gensiruk S.A. 2002. Forests of Ukraine. 'NTSh' Publishing House. 352 p. (in Ukrainian).

Harvey J.E., Smiljanić M., Scharnweber

T., Buras A., Cedro A., Cruz-García R., Drobyshev I., Janecka K., Jansons Ā., Kaczka R., Klisz M., Lääänelaid A., Matisons R., Muffler L., Sohar K., Spyt B., Stolz J., van der Maaten E., van der Maaten-Theunissen M., Vitas A., Weigel R., Kreyling J., Wilmking M. 2020. Tree growth influenced by warming winter climate and summer moisture availability in northern temperate forests. Global Change Biology 26(4): 2505–2518. https://doi.org/10.1111/gcb.14966

Ischuk G. 2017. Natural Regeneration of Oak and Hornbeam under the Canopy and Log Cabins in the State Enterprise 'Korsun-Shevchenko Forestry'. Scientific Bulletin of UNFU 27(1): 15–18 (in Ukrainian). http://nv.nltu.edu.ua/index.php/journal/article/view/152

Johnson P.S., Shifley S.R., Rogers R. 2009. The ecology and silviculture of Oaks. 2nd edn. CABI Publishing, Oxon. 580 p.

Kelly P.M., Munro M.A.R., Hughes M.K., Goodness C.M. 1989. Climate and signature years in west European oaks. Nature 340: 57–60. https://doi.org/10.1038/340057a0

Kopiy L.I., Fizyk I.V., Baran S., Lavnyy V.V., Kopiy S.L., Presner R.B., Agij V.O. 2017. Natural seed reproduction of oak plantations as an element close to the nature of forestry. Scientific Bulletin of UNFU 27(9): 9–13 (in Ukrainian). https://doi.org/10.15421/40270901

Kosarevsky I.A. 1951. State reserve 'Sofiyivka'. Publishing house of the Academy of Architecture of the Ukrainian SSR. 120 p. (in Russian).

Kosenko I.S., Grabovyi V.M., Muzyka G.I. 2014. Methodical recommendations for inventory, taxation and monitoring of perennial plantations in historical parks of Ukraine. VPC 'Vizavi' (Publisher 'Sochinsky'). 64 p. (in Ukrainian).

Kosenko I.S., Khraban G.Y., Mitin V.V., Garbuz V.F. 1996. Dendrological Park 'Sofiyivka'. Scientific thought. 186 p. (in Ukrainian).

Koval S., Ostapchuk O, Shlapak V, Bayura O., Sovakov O., Vitenko V., Podzerei R., Lazariev O. 2022. Condition and productivity of marginal oak and beech plantations in the southern part of the Right Bank Forest Steppe of Ukraine. Forestry Ideas 29(1): 3–14.

Kuiters A.T., Slim P.A. 2003. Tree colonisation of abandoned arable land after 27 years of horse-grazing: the role of bramble as a facilitator of oak wood regeneration. Forest Ecology and Management 181(1–2): 239–251. https://doi.org/10.1016/S0378-1127(03)00136-1

Larsson J. 2021. Changes in the oak (*Quercus robur*) population in Dalby Söderskog national park 2011–2020: stem size distribution, spatial distributions, vitality and mortality. Second cycle, A2E. Alnarp: SLU, Southern Swedish Forest Research Centre. http://urn.kb.se/resolve?urn=urn:nbn:se:slu:epsilon-s-17153

Levon F.M. 2008. Green plantations in an anthropogenically transformed environment. Monograph. NNC IAE. 364 p. (in Ukrainian).

Lipinsky V.M., Dyachuka V.A., Babichenko V.M. (Eds) 2003. Climate of Ukraine. Raevsky Publishing House. 343 p. (in Ukrainian).

Losseau J., Jonard M., Vincle C. 2020. Pedunculate oak decline in southern Belgium: a long-term process highlighting the complex interplay among drought, winter frost, biotic attacks, and masting. Canadian Journal of Forest Research 50(4): 380–389. https://doi.org/10.1139/cjfr-2019-0341

Lutsyshyn V.Ye., Lavnyy V.V. 2012. Impact of recreational pressure on natural regeneration of trees in the recreational and health forests of Rostochia. Scientific Bulletin of UNFU 22(13): 87–92 (in Ukrainian). https://nv.nltu.edu.ua/Archive/2012/22_13/87_Luc.pdf

Lypa A.L. 1948. Sofiyivka Uman State Reserve (1796–1946). Publisher of the Academy of Sciences of the Ukrainian SSR. 110 p.

Matusyak M.V. 2016. The Assessment of the effectiveness of applying natural regeneration of pedunculate oak (*Quercus robur* L.) at reforestation in solid blockhouse in the conditions of fresh hornbeam oak forests in Podillya. Scientific Bulletin of UNFU

26(4): 110–116 (in Ukrainian). https://doi.org/10.15421/40260417

Onaindia M., Ametzaga-Arregi I., Sebastian M.S., Mitxelena A., Rodriguez-Loinaz G., Pena L., Alday J.G. 2013. Can understorey native woodland plant species regenerate under exotic pine plantations using natural succession? Forest Ecology and Management 308: 136–144. https://doi.org/10.1016/j.foreco.2013.07.046

Ostapchuk O.S. 2013. Formation of forest natural regeneration under oak forest canopy in southern part of Right-Bank Forest-Steppe of Ukraine. Scientific Bulletin of UNFU 23(6): 52–57 (in Ukrainian). https://nv.nltu.edu.ua/Archive/2013/23_6/11.pdf

Palmer S.C.F., Mitchell R.J., Truscott A.M., Welch D. 2004. Regeneration failure in Atlantic oakwoods: the roles of ungulate grazing and invertebrates. Forest Ecology and Management 192(2–3): 251–265. https://doi.org/10.1016/j.foreco.2004.01.038

Perrin P.M., Kelly D.L., Mitchell F.J. 2006. Long-term deer exclusion in yew-wood and oakwood habitats in southwest Ireland: natural regeneration and stand dynamics. Forest Ecology and Management 236(2): 356–637. https://doi.org/10.1016/j.foreco.2006.09.025

Rabotnov T.A. 1950. Life cycle of perennial herbaceous plants in meadow coenoses. Tr. BIN Academy of Sciences of the USSR. Geobotany. USSR Academy of Sciences 3: 7–204 (in Russian).

Rumiankov Yu.O. 2019. Accelerated dieback of pedunculate oak (*Quercus robur* L.) in the park phytocoenosis of the planting ‘Dubynka’ of the National Dendrological Park ‘Sofiivka’ of the NAS of Ukraine. Journal of Native and Alien Plant Studies 15: 125–132 (in Ukrainian). https://doi.org/10.37555/.15.2019.184913

Rumiankov Yu.O., Porokhniava O.L., Muzyka H.I., Hrabovyi V.M. 2021. *Quercus robur* L. in historical planting of the Sofiivka National Dendrological Park of the NAS of Ukraine in different phytocoenotic conditions. Scientific Bulletin of UNFU 31(3): 34–40 (in Ukrainian). https://doi.org/10.36930/40310305

Shkvaruk M.M., Delemenchuk M.I. 1969. Soil science. Harvest. 412 p. (in Russian).

Shkvaruk M.M., Zapatiy S.E. 1960. Natural conditions of the Uman district. Collection of Scientific Works of the Uman Agricultural Institute 12: 89–100 (in Russian).

Shlap2103ak V.P. 2021. The strength of the soil profile and the content of nutrients in the soils of the dendrological park ‘Sofiyivka’ of the National Academy of Sciences of Ukraine. Studies and materials. Czartoryski Gardens 10(16): 241–244.

Sklyar V.G. 2013. Peculiarities of the ontogenetic development of the sharp-leaved maple in the forests of the Novgorod-Siversky Polissia. Herald of Cherkasy University. Series: Biological Sciences 2: 115–120 (in Ukrainian). http://nbuv.gov.ua/UJRN/VchuB_2013_2_22

Storozhuk V.F. 2006. Methodical instructions for conducting field work on forest inventory of the Polissya region of Ukraine. Scientific and information center of forest management. 74 p. (in Ukrainian).

Strandberg B., Kristiansen S.M., Tybirk K. 2005. Dynamic oak-scrub to forest succession: effects of management on understorey vegetation, humus forms and soils. Forest Ecology and Management 211(3): 318–328. https://doi.org/10.1016/j.foreco.2005.02.051

Vitenko V.A., Goncharuk V.V., Podzerei R.V., Kulivnuk V.S., Koval S.A. 2022. Dendroflora of Nemyriv Park in the Vinnytsia Region. Scientific Bulletin of UNFU 32(6): 18–24 (in Ukrainian). https://doi.org/10.36930/40320603

Vitenko V.A., Manziy O.M., Koval S.A., Bayura O.M., Adamenko S.M. 2023. Adaptive potential of *Morus alba* L. in the conditions of the Sofiivka National Arboretum NAS of Ukrainian. Scientific Bulletin of UNFU 33(1): 14–20 (in Ukrainian). https://doi.org/10.36930/40330102

Vitenko V., Shlapak V., Kozachenko I., Kulbitskyi V., Maslovata S., Koval S., Lazariev O. 2019. Results of grafting of *Morus alba* L. ornamental forms. Forestry Ideas 25(2): 413–424.

von Lüpke B. 1998. Silvicultural methods of oak regeneration with special respect to shade tolerant mixed species. Forest Ecology and Management 106(1): 19–26. https://doi.org/10.1016/S0378-1127(97)00235-1

Vospernik S., Heym M., Pretzsch H., Pach M., Steckel M., Aldea J., Brazaitis G., Bravo-Oviedo A., Del Rio M., Lof M., Pardosi M., Bielak K., Bravo F., Coll L., Cerný J., Droessler L., Ehbrecht M., Jansons A., Korboulewsky N., Jourdan M., Nord-Larsen T., Nothdurft A., Ruiz-Peinado R., Ponette Q., Sitko R., Svoboda M., Wolff B. 2023. Tree species growth response to climate in mixtures of *Quercus robur/Quercus petraea* and *Pinus sylvestris* across Europe – a dynamic, sensitive equilibrium. Forest Ecology and Management 530, 120753. 15 p. https://doi.org/10.1016/j.foreco.2022.120753

Yakovlieva-Nosar S., Bessonova V. 2021. State of coenopopulations of *Quercus robur* L. growing in ravines located in the Dnieper river's rapids section (recreation zone of the city of Zaporizhzhya), Ukraine. Forestry Ideas 27(1): 256–270.

Zlatanov Ts. 2006. Successional trends in pedunculate oak (*Quercus robur* L.) dominated forests along the upper reaches of Tundzha river – Southern Bulgaria. Austrian Journal of Forest Science 123(4): 185–197.

Zvarych O.D., Zaika V.K., Stryamec G.V., Zvarych Yu.V., Parobiy S.B. 2016. The natural regeneration in old forest stands of the nature reserve 'Roztochya'. Scientific Bulletin of UNFU 26(7): 77–85 (in Ukrainian). https://doi.org/10.15421/40260711

FORESTRY IDEAS, 2024, vol. 30, No 1 (67): 139–159

Utilisation of multitemporal SAR data for mapping and statistical analysis of ice and snow breakage of mountainous mixed forest in Bulgaria with Sentinel-1

Zlatomir Dimitrov[1*], Radka Koleva[2], Toma Tonchev[2], and Hristo Nikolov[1]

[1]Space Research and Technology Institute, Bulgarian Academy of Sciences, Georgy Bonchev Blvd., Block 1, 1113 Sofia, Bulgaria. [*]E-mail: zlatomir.dimitrov@space.bas.bg
[2]University of Forestry, 10 Kliment Ohridski Blvd., 1797 Sofia, Bulgaria.

Received: 07 December 2023 / Accepted: 29 April 2024 / Available online: 14 May 2024

Open Access: This article is licensed under a Creative Commons Attribution 4.0 International License.

Abstract

This study represents analysis of abiotic forest disturbance in mountainous mixed forest, based on change detection and statistical analysis from C-band Synthetic Aperture Radar (SAR) multitemporal SAR data, provided from ESA's Sentinel-1 satellite mission. Statistical means from the backscatter coefficients in both polarisations were calculated, with the dual-pol Radar Vegetation Index (*dRVI*), applying change detection before and after the disaster event. Study period was the summer of 2020 and 2021. The proposed methodology was tested at the Training and Experimental Forest Range of 'Petrohan' hosted by University of Forestry – Sofia. Mean estimates from SAR descriptors with emphasis on *dRVI* sowed high sensitivity to the forest type. The calculated differential orbit-averaged SAR descriptors utilised in change detection analysis, exhibited correlation with the optical Enhanced Vegetation Index 2 (EVI2), with highest sensitivity being the cross-pol Gamma-Nought $(\Delta\overline{\gamma^0_{VH}})$. The conducted statistical analysis has demonstrated significant differences in backscatter mean values, with the highest sensitivity observed among the three differential SAR descriptors again being the $(\Delta\overline{\gamma^0_{VH}})$. However, clear identification of the disturbances via SAR descriptors was not possible, primarily due to the mechanism of the disaster event (stem breakage) that resulted in an increased dihedral scattering. Accuracy was also influenced by the geometric distortions due to mountainous relief, which biased the SAR measurements. In conclusion, statistical analysis of multitemporal SAR is well utilised in studying forest disturbances on mixed coniferous mountainous forest. Results suggest need for an *in situ* data and high-resolution quad-pol POL-SAR measurements in a stem breakage disturbed forest.

Key words: forest disturbances, dual-pol RVI, EDUSAR, EVI2, Synthetic Aperture Radar.

Introduction

Forest ecosystems are widely studied by satellite Synthetic Aperture Radar (SAR) based systems, giving vast of methodological approaches to derive forest biophysical parameters and forest status, in depend on the frequency (Cloude and Pa-

pathanassiou 1998, Fernandez-Ordonez et al. 2009, Le Toan et al. 2011, Caicoya et al. 2012, Kugler et al. 2014). Studying biophysical parameter's diversity via different SAR systems, such as C-band Radarsat-2 and L-band ALOS PALSAR-2 by SAR polarimetry is vital for forest management and deforestation monitoring (Englhart et al. 2011, Stelmaszczuk-Górska et al. 2018). A time series SAR approach by employing Sentinel-1 SAR GRD products were widely assessed for the biophysical parameters estimation, and variation over time (Nasirzadehdizaji et al. 2019).

Forest disturbance plays a key role in forest management, whilst abiotic disturbances[1] could cause a significant gap in the forest canopy (Anev and Marinova 2021). For 2019 the Forest State Agency (FSA) reported that most significant for the disturbances in Bulgarian forests are the biotic factors (e.g. bark beetle and fungal pathogens). Despite that FSA registered a significant increase of the abiotic disturbances for 2022 than 2021 (BNA 2022). The analysis of coniferous forest stands damaged by biotic and abiotic factors established that the abiotic ones are the largest for the stressors ice breakage, followed by snow breakage and the snow uproot (Tonchev et al. 2018). The summary of the databases created in different stages of the project CORINE Land Cover – Bulgaria ascertains that the forested areas in the forest territories of Bulgaria decreased by 67,103.9 ha for the period 1990–2018, which is exactly 2 % of the total forested area in 1990 (Koleva et al. 2019). The abiotic forest disturbances, such as snowthrow[2] and icethrow[3] are more often investigated by SAR based acquisitions in higher frequencies, such as C-band (Tomppo et al. 2019). That is because the snowthrow as an abiotic disturbance factor at those frequencies leads to significant lowering of the backscatter (Akbari and Solberg, 2022). Disturbances are mostly studied by means of time series approach, by freely available SAR acquisitions from ESA's satellite mission – Sentinel-1. Akbari and Solberg (2022) have found that most of the limitations that bias the results are encompassed in the environmental factors, such as wetness, rainfall, and topography. They recommend a combination of both SAR orbits – ascending and descending to be used to overcome the local incidence angle limitations. Ruiz-Ramos et al. (2020) utilise an approach based on a long time series from Sentinel-1 – Ground Range Detected (GRD) products, to identify clear cuts in Scotland, by reporting the importance of the dual polarization of the SAR data (Ruiz-Ramos et al. 2020). An approach by using change detection between averaged backscatter coefficients from RADARSAT-2 C-band SAR data, is implemented successfully to map selective logging in tropical forests (Antropov et al. 2021). Statistically mean values significantly improve the identification of disturbed forest, before and after the disaster event (Tomppo et al. 2019).

This paper introduces a SAR based method for mountainous disturbed forest

[1] Hereafter, we shall adopt the term 'Abiotic disturbances' to denote the mechanical damages, caused in our case by ice and snow breakage.

[2] Snowthrow, is braking of branches or even part of the stem caused by heavy wet snow during warm winter, with temperatures around zero. It is a synonym of snow breakage and causes abiotic disturbances.

[3] Icethrow – ice breakage in winter.

mapping in rugged terrain, which is implemented for first time by Bulgarian scientists to investigate abiotic forest disturbances. A change detection of approach based on multitemporal SAR data is utilised with statistical mean estimates. The method is based on the Sentinel-1 GRD data products, freely provided by ESA COPERNICUS SAR mission. A comparison between normalised radar cross-section in both polarisations, the dual-pol Radar vegetation index (*dRVI*) and optical (EVI2) is made, aiming values differences in disturbed forest stands, before and after the disaster event.

This study represents a pioneering endeavour for Bulgarian environmental sciences, whereas to the best of the authors' knowledge, no comparable investigation has been conducted on the Bulgarian disturbed temperate forests in mountainous regions solely by SAR methods.

The general objective of this investigation is to employ a classical remote sensing approach, exclusively relying on remotely sensed data, for the derivation of specific environmental parameters and status of forest ecosystem. The central hypothesis under scrutiny is the assessment of the suitability and efficacy of time-series analysis by means of Ground Range Detected (GRD) products from ESA's C-band SAR – Sentinel-1, for the mapping, characterisation, and possible identification of abiotic disturbances within mountainous forest.

In that case, the following aims were pursued:

- to implement multitemporal change detection SAR approach, for two reference periods in the summer, employing two acquisition orbits (descending and ascending);
- to calculate the dual-pol Radar Vegetation Index (*dRVI*);
- to calculate statistical mean values in order to eliminate stochastic factors;
- to map mixed forest by means of statistical mean SAR estimates;
- to test a method for identification of forest disturbances in mountainous mixed forest, by means of statistical mean SAR estimates;
- to estimate accuracy and consistency of the used methods.

Data and Methods

Study site

The proposed SAR based methods for forest mapping and disturbances identification was tested in mountainous mixed forest, located at the Training and Experimental Forest Range (TEFR) 'Petrohan', managed by University of Forestry – Sofia. The test site comprises the whole territory, with a total area of 7192 ha situated in the Western Balkan Mountain, north of the capital of Sofia. The forest areas are among the oldest, where its management took place for the first time in 1893 (University of Forestry 2023). The relief is steep mountainous with the lowest point being at 350 m a.s.l., and highest at 1900 m. Most of the territory is steep (about 48 %), where 13 % is very steep. Moderate continental climate is present at the test site. The studied forest is mainly deciduous, where the predominant species is European beech (*Fagus sylvatica* L.) that occupies 82 % of the territory, while the coniferous forest is represented mostly by Scots pine (*Pinus sylvestris* L.) – 5.8 %) and Norway spruce (*Picea abies* (L.) H. Karst.) – 4 %.

Forest disturbances registered in TEFR 'Petrohan'

In January 2021, as a result of microclimatic conditions – thick fog combined with precipitation and a temperature of around 0 °C, damage was caused to the forests. It mainly resulted in branches breakage and stems broken in the middle. The total volume of damaged forests, which are state property managed by University of Forestry, as reported was more than 115,000 m^3. The private property forests were not considered. The damaged forest areas are in the altitude range of 550–1000 m, with the largest share of deciduous stands being between 750–950 m. In the areas occupied by coniferous species, a relatively even distribution of the affected areas was observed, predominant areas are established in the range of 650–850 m. In the sake of unavailability of *in situ*, terrain, or aerial measurements it was not possible to assess the fraction of the damaged trees for the entire study area.

A large part (about 80 %) of the forest area, subject of the present study, is located on sloping and steep terrains (11–30 degrees), and this is valid for both coniferous and deciduous forests. Regarding the distribution of the studied area by exposure to the terrain, an approximately equal distribution of the affected coniferous plantations is observed, while areas of shady exposure prevail in the case of broad-leaved ones. Regarding the distribution by age classes, the most areas of plantations between 50 and 60 years were found for coniferous forests, while for broad-leaved forests the largest share of the area is those between 50 and 80, and the data show a relatively small area of forest stands in the range of 100–140 years. It is noteworthy that for the oldest beech stands (>140 years) the share of the damaged stock of state forests is over 15,000 m^3.

Methodology

The methodology is based on a change detection approach solely from C-band SAR, derived from Sentinel-1 SAR acquisitions, where to identify and quantify changes in the forest structure due to disturbances. Its emphasis is on statistical mean estimates of the Gamma-Nought backscatter coefficient before and after the disaster event. It employs the existing differences in backscatter at both cross-pol (VH) and co-pol (VV) polarisations, represented by the normalised radar cross-sections – 'Gamma-Nought' (γ^0_{VH}, γ^0_{VV}). Sentinel-1 dual-polarisation SAR has proven its successful implementation in land cover mapping of the natural scatterers (Abdikan et al. 2016). Polarisation difference is also exploited via the introduced *dRVI* (Trudel et al. 2012, Mandal et al. 2020). Despite utilisation of the different orbit direction, orbit averaged products are also examined ($\overline{\gamma^0_{VH}}$, $\overline{\gamma^0_{VV}}$, $\overline{dRVI}$). The spatial resolution used is 10 m for all SAR products. The considered disaster event is snowthrow that happened in January 2021. Two summer periods with time span from 30th June, till 31st August are considered, for statistical mean estimates – before the disaster event in 2020, and after the disaster event in 2021. SAR data processing was carried out both in ESA Sentinel Application Platform (SNAP), and QGIS.

In this study detailed *in situ* information was not used, because firstly it was unavailable due to lack of terrain measurements, neither any aerial nor visual observation. Thus, it was not reasonable to perform traditional thematic mapping of forest disturbances with concurrent accuracy assessment. Nonetheless, a kind of

such a mapping is performed in terms of testing.

Reference data

As a reference, the forest cadastre with disturbed forest stands is used, preliminary processed from the University of Forestry, Department of Forest Management. For October 2022, the activated stands for sanitary cuts are 132, while the upcoming ones are 69, with the total number of disturbed forests stands at TEFR 'Petrohan', are 201. Percentage ratio from total area is 12.99 %, or 855.9 ha (Fig. 1).

We have no information about any sanitary logging before the summer of 2021. Also, a forest cadastre from the Executive Forest Agency, at TEFR 'Petrohan' is downloaded and processed with software – LESOTEST-2©, in shapefile format, CRS: WGS84 UTM34N. Two classifications are elaborated from the output shapefile, to represent per forest stand the growing stock volume ($m^3 \cdot ha^{-1}$), and the mean stand height (or forest volume height – h_v, m). Optical imagery from Sentinel-2 is used as reference, before (acquisition, on 22.06.2020) and after (acquisition, on 27.06.2021) the disaster event, with 20 m spatial resolution. As reference calculated are EVI, and two spectral combinations – NIR-SWIR-Red (B08-B11-B04 on Fig. 2A), and RGB Natural Colours

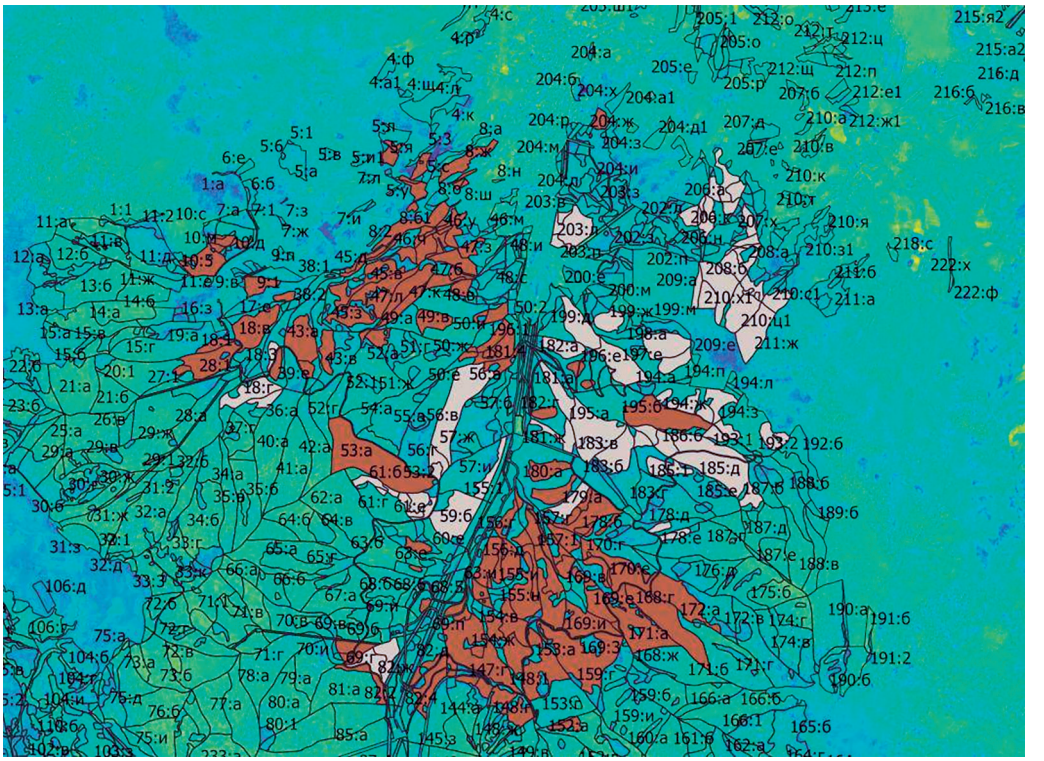


Fig. 1. Activated (brown) and pending (beige) forest stands for sanitary cuts, on disturbed forest cadastre at TEFR 'Petrohan', provided by University of Forestry.

Note: EVI2 index is used to visualise changes in forest structure, calculated from Sentinel-2 acquisition (2021-06-22), after the disaster event.

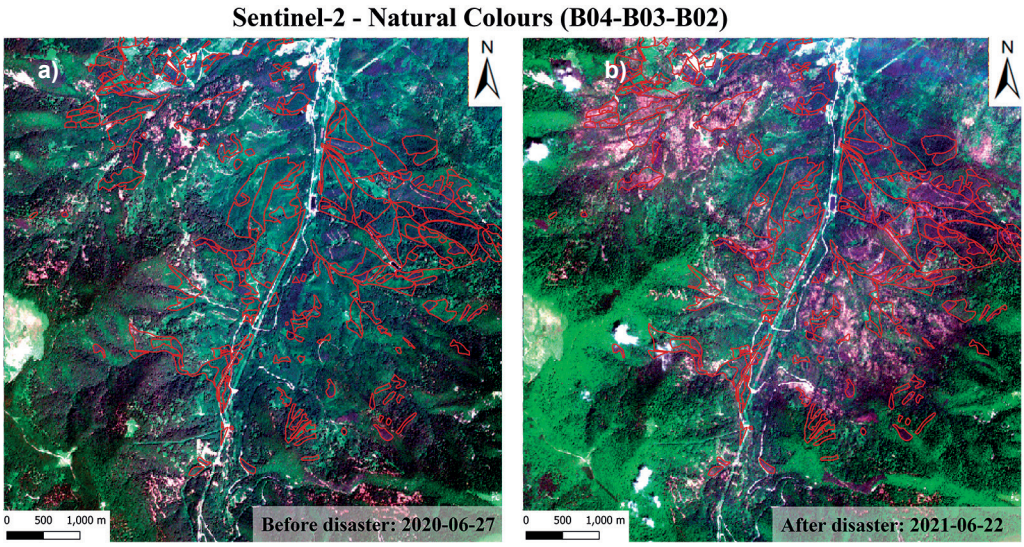


Fig. 2A. Sentinel-2 reference imagery in two band combinations (noted in title), where: a) before disaster – 2020-06-27, b) after disaster – 2020-06-27.

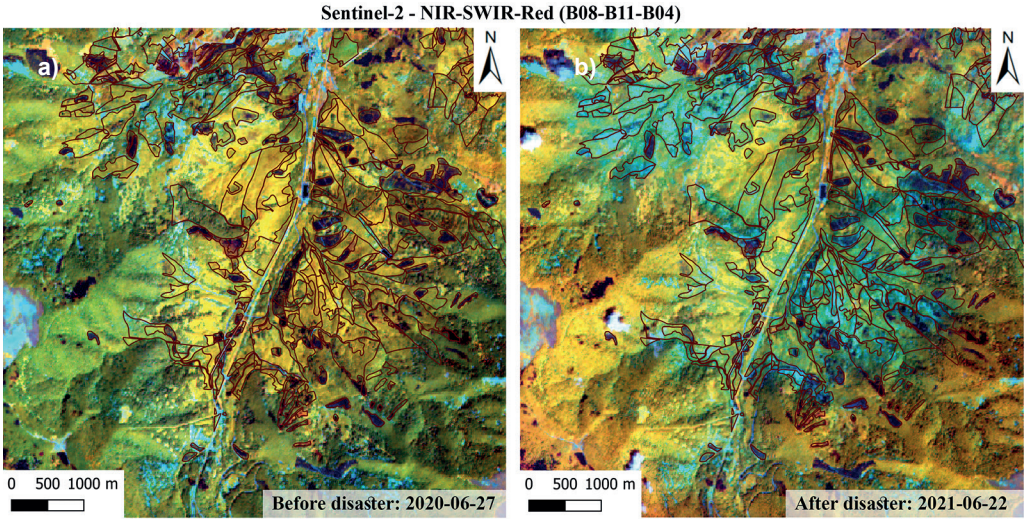


Fig. 2B. Sentinel-2 reference imagery in two band combinations (noted in title), where: a) before disaster – 2020-06-27, b) after the disaster event of snowthrow in the winter 2020/2021.

Note: disturbed forest stands from disturbed forest cadastre are also overlaid in dark red.

(B04-B03-B02, in Fig. 2B).

Copernicus Services HRL 2018 are also used – Dominant Leaf Forest (DLT-2018), and Tree Cover Density (TCD-2018). The bright colours recognized in Figure 2 are mostly due to reflection from the terrain, rather from the trees. The reason to appear bright in the spectral image

from S2 is that only the stem is left from the whole tree, with no reflection from the leaves. In general, S2 spectral composites are only used to represent changes in the forest before and after the disturbances. On the other hand, EVI2 also takes a major part in the comparison analysis with the SAR observables in the disturbed forest stands.

SAR data processing

Relative Orbit Numbers for GRD products are selected, according to the assumption of an equal incidence angle at the test site. This means that for Ascending this is N29, and for Descending is N80 (Fig. 3).

Twenty scenes were downloaded for summer periods of 2020 and 2021 obtained by both satellites – Sentinel-1A and Sentinel-1B. In addition, to study geometric properties during leaf off eight scenes were downloaded, single orbit only, by Sentinel-1A (refer to Table 1).

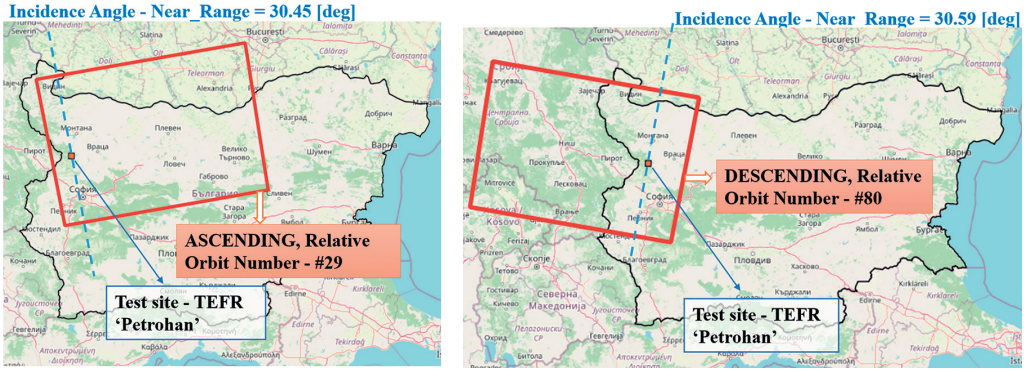


Fig. 3. Relative Orbit Number selection, according to the same incidence angle at the test site, which falls in the near range of both Sentinel-1 orbits (left: ascending, right: descending).

Table 1. Number of downloaded Sentinel-1 scenes, in ascending (A) and descending (D) orbits, for years 2020 and 2021.

	2020/Before												2021/After											
Month	I	II	III	IV	V	VI	VII	VIII	IX	X	XI	XII	I	II	III	IV	V	VI	VII	VIII	IX	X	XI	XII
S-1B							6	4			4	2	2	4					4	6				
S-1A							4	6			2	4	4	2					6	4				
Orbit							A+D	A+D			D	D	D	D					A+D	A+D				
Total							20				4		4						20					

Note: in title rows – greenish points to non-disturbed forest, orange points to disturbed forest after the disaster event; greenish background relates to summer time series, bluish – to winter ones.

The following processing steps are used to elaborate the SAR time series (ESA 2021): import GRD data in ESA SNAP; subset to Area of interest (AOI) of the test site; calibrate to γ^0_{VV}, γ^0_{VH}; Speckle filtering – R. Lee (with window size of 5×5 pixels); convert linear to Decibel (dB); Terrain flattening to remove topography (Small et al. 2010); Geocode by using Range-Doppler; Export to GeoTIFF. Automation is performed via Graph Builder in SNAP (Fig. 4).

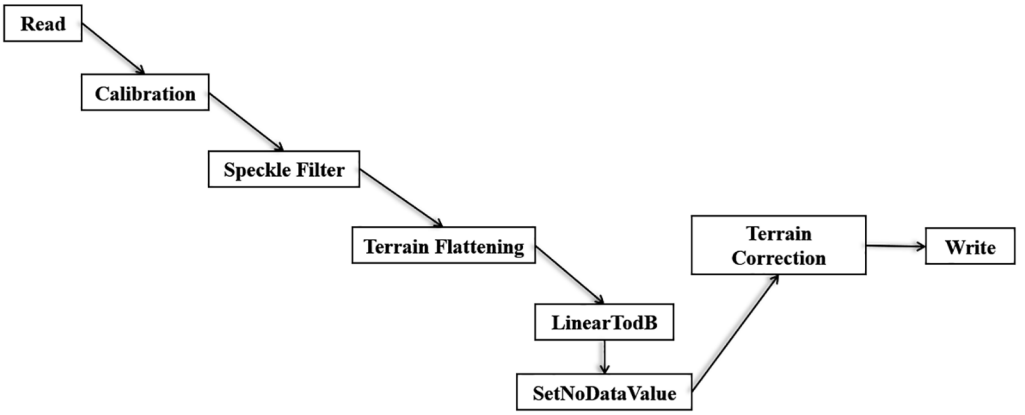


Fig. 4. Processing graph in SNAP.

The reason why Gamma Nought (γ^0) is preferred and used in the methodology instead of Sigma Nought (σ^0), is because γ^0 is a normalised version of σ^0 and therefore it is preferable to be utilised in mountainous rugged terrain. Sigma nought represents the raw radar backscatter coefficient, and its values are influenced by various factors, as variances of the incidence angle from the underlying topography, polarisation, and surface roughness (Abdikan et al. 2016).

During processing different averaging windows in Speckle filtering are tested – 5×5, 7×7, and 9×9 pixels. Also, two types of incoherent algorithms are tested – non-adaptive (Boxcar), and adaptive (R. Lee). To preserve the objects geometry – the adaptive one is implemented. As an output a geocoded and terrain flattened Gamma-Nought, for Ascending (ASC) and Descending (DESC) orbits, as well as for co-/cross-polarisations a GeoTIFF files are produced. The *dRVI* index is dimensionless, but in purpose of the physical interpretation a conversion of linear values in decibels (dB) is introduced.

Geometric distortions such as foreshortening, in general bias the interpretation of SAR observations. Foreshortening, predominantly occurring at low values of the local incidence angle, is a very common issue in rugged terrain. Consequently, it is imperative to exclude such areas from analysis due to the inherent unreliability of resultant findings.

Results and Discussion

Statistical estimates are calculated via Raster Calculator in QGIS. Also, the *dRVI* is calculated, per orbit direction, using the formula (Trudel et al. 2012):

$$dRVI = \frac{4\gamma_{VH}}{\gamma^0_{VV} + \gamma^0_{VH}}, \quad (1)$$

where: γ^0_{VH} – is cross-polarised Gamma-Nought, γ^0_{VV} – is co-polarised Gamma-Nought.

Coniferous *vs* broadleaf

A consistency of *dRVI* with the forest type (coniferous, deciduous) is observed in the descriptors with the DLT-2018. The reason for this is that the depolarisation of the signal in coniferous forest is much higher than in the deciduous one. This leads to higher response at γ^0_{VH}, rather than in γ^0_{VV}. The physics behind is that the coniferous leaves interact more with the polarisation vector of the signal in lower wavelengths, such as C-band (Fig. 5).

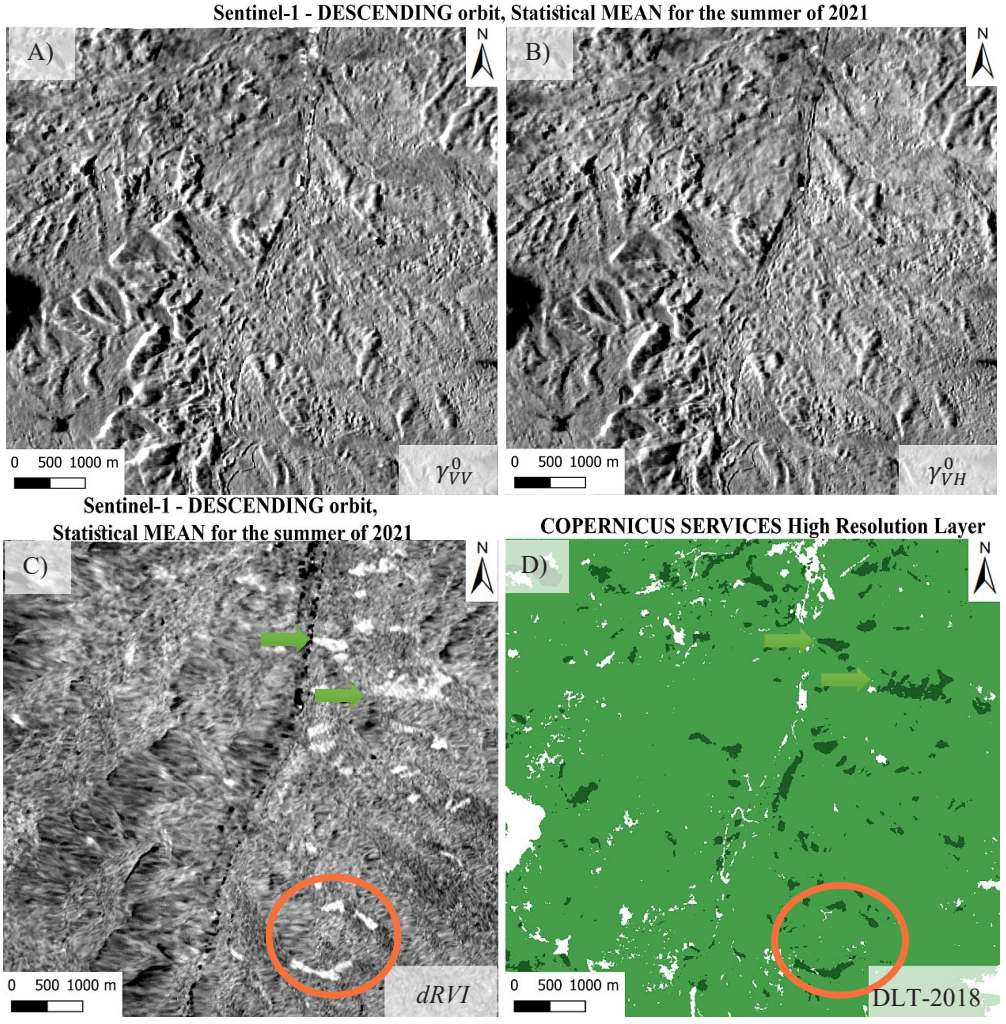


Fig. 5. Three SAR descriptors in DESC – orbit for the summer of 2021, where: A) γ^0_{VV}, B) γ^0_{VH}, C) *dRVI,* and D) Dominant Leaf Type for 2018 (DLT-2018).

Note: consistency of *dRVI* with the forest type is observed, where the white patches found on *dRVI,* match the coniferous forest patches (dark green) on DLT-2018.

This leads to a change of polarisation state and lowering the intensity of the signal. This fact is mostly observed on the polarimetric ratios, such as *dRVI*.

Differences in orbits

The resulting statistical means estimates of the polarimetric products – descriptors are studied for orbit differences. At the backscatter descriptors – γ^0_{VV} and γ^0_{VH} the geometric distortions caused by topography (effect of foreshortening) are well recognised but have different imprints and depend on the orbit direction (or the direction to Radar line of sight – RLOS) (Fig. 6).

As reported in other studies here the co-polarised descriptor (γ^0_{VV}) is much more influenced by geometric distortions rather than the cross-polarised (γ^0_{VH}) (Dimitrov 2022). The orbit difference is most obvious on the *dRVI* descriptor, where the coniferous forest (see the white patches on Fig. 6) is seen differently on both orbits – Ascending (ASC) and Descending (DESC). This is because of the different orientation of the target vector to the RLOS.

Seasonality differences

A comparison of the different seasonality involving the summer and winter descriptors shows that in winter it is not possible to discriminate coniferous forest from deciduous one, which is obvious on *dRVI* in both orbits (Fig. 7 – A and C: *dRVI* in summer; B and D: *dRVI* in winter).

From Figure 7, it could be concluded that the winter multitemporal does not entail sensitivity to the forest type regarding the summer one. Despite that could be stated that the ascending orbit multitemporal is less influenced by the geometric distortions (i.e. foreshortenings).

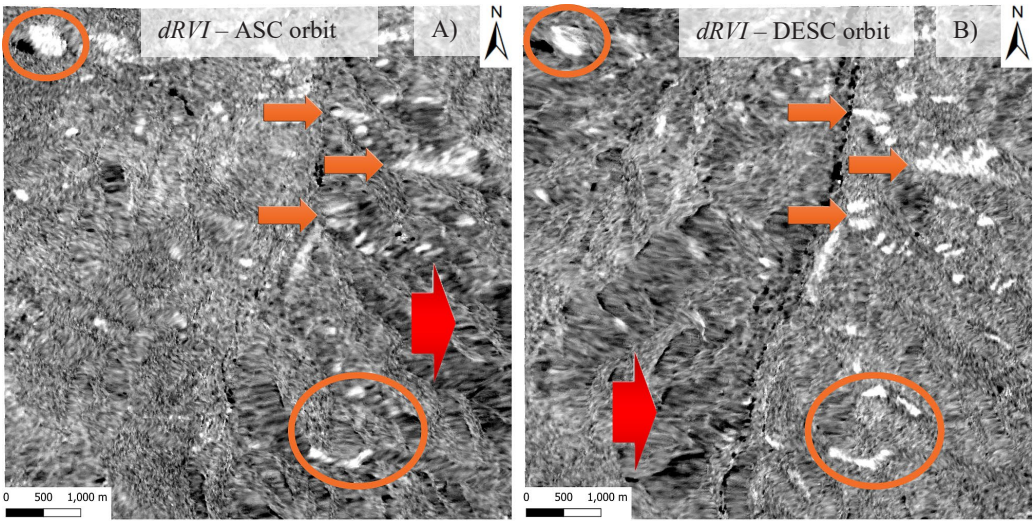


Fig. 6. Comparison of *dRVI* for the summer of 2021, in – A) DESC orbit, B) ASC orbit.
Note: certain differences are observed, due to different orbit direction, hence the incidence angle and position of the target vector to the RLOS.

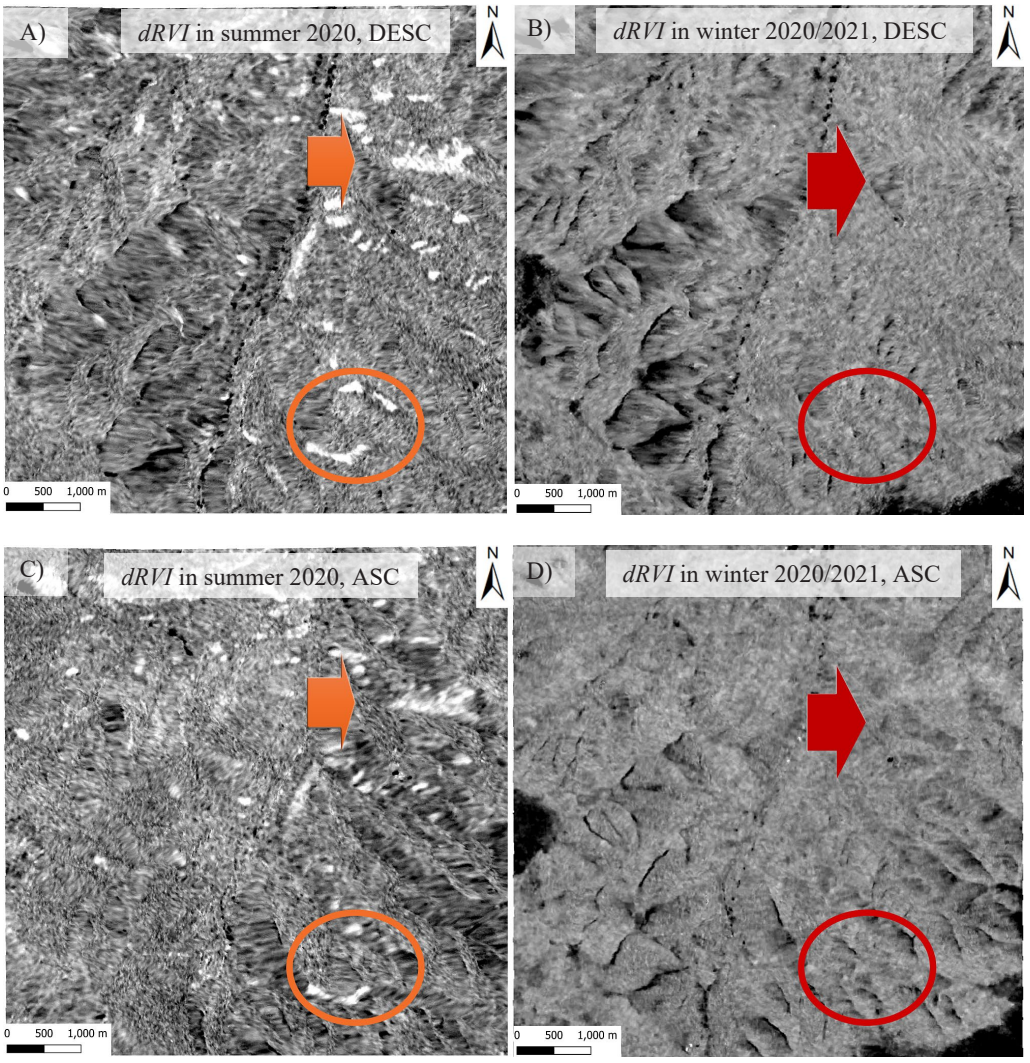


Fig. 7. Comparison of different seasonality, where: A) *dRVI* for the summer of 2020 in DESC orbit, and C) same for ASC orbit; B) *dRVI* for the winter of 2020/2021 in DESC orbit, and D) same for ASC orbit.

Note: Please, note that on the summer multitemporal mean (A and C), the forest type is indicated, where white spots represent the coniferous forest. Despite that the winter multitemporal mean (B and D) does NOT entail such a sensitivity. One of the reasons why the summer multitemporal is preferable.

Orbit averaging

Following the recommendation outlined in the study of Akbari and Solberg (2020) an orbit averaging is performed for the summer seasons only, by using the formulas (2, 3, and 4):

$$\overline{\gamma^0_{VH}} = \frac{\gamma^{0\ ASC}_{VH} + \gamma^{0\ DESC}_{VH}}{2}, \qquad (2)$$

$$\overline{\gamma^0_{VV}} = \frac{\gamma^{0\ ASC}_{VV} + \gamma^{0\ DESC}_{VV}}{2}, \quad (3)$$

$$\overline{dRVI} = \frac{dRVI^{ASC} + dRVI^{DESC}}{2}, \quad (4)$$

where: *ASC* – descriptors are in ascending orbit; *DESC* – descriptors are in descending orbit.

Therefore, the geometric distortions are slightly diminished with a smaller impact on the descriptors. Backscatter intensities are less biased from the speckle effect, which leads to a smooth improvement regarding the separate orbits.

Differential layers

To complete the analysis a computation of layer differencing (or, differenced descriptors), by math subtraction are calculated, aiming the orbit averaged ones for summer of 2020 (before), and for summer of 2021 (after). The produced four differenced descriptors – *ΔEVI2,* $\Delta\overline{\gamma^0_{VV}}$, $\Delta\overline{\gamma^0_{VH}}$, $\Delta\overline{dRVI}$ are examined in QGIS with disturbed forest cadastre overlaid. Negative values are considered, due to the assumption that the backscatter BEFORE is higher, than after the disaster event (Akbari and Solberg 2020, Antropov et al. 2021). This is especially true at the cross-polarised differenced descriptor, because of the diminished volume backscatter in the rest understory and low vegetation. In this regard, the backscatter at the disturbed forest stands is observed to be higher in the co-pol $\Delta\overline{\gamma^0_{VV}}$, rather than the cross-pol $\Delta\overline{\gamma^0_{VH}}$.

Forest disturbances analysis with SAR and optical data

In the analysis the disturbed forest cadastre is used, provided by the University of Forestry, Department of Forest Management. The disturbed forest cadastre was overlaid with the optical EVI2 layer differencing (differenced descriptor – ΔEVI2), from the summer of 2020 and 2021, but also the SAR differenced descriptors – $\Delta\overline{\gamma^0_{VV}}$, $\Delta\overline{\gamma^0_{VH}}$, $\Delta\overline{dRVI}$.

Therefore, the Δ*EVI2* negative values should be clearly related to the possible forest loss, due to lack of vegetation in the post-disaster period in the summer of 2021. Instead, dark values (negative pixels) are also found away from the disturbed forest stands, which is embarrassing. Reanalysis showed bias from environmental factors that considers opposite slopes with North aspect that leads to low irradiation fluxes from the Sun, and differences in woods growth altitude. This had led to specification of the wood's development in those areas and therefore lowered the values of EVI2 at the time of S2 acquisition in the summer of 2021.

This leads to the conclusion that Δ*EVI2*'s negative values could not be solely used for identification of the disturbed forest in our case (Fig. 8).

As observed from Figure 8 the negative values of SAR differenced layers (differenced descriptors) *ΔEVI2* and $\Delta\overline{\gamma^0_{VH}}$, does not fully identify as expected damaged woods, where negative values in bluish does not completely correlate with the disturbed forest stands boundaries in reddish. Must be stated that the Figure 8 has representative character about the layer differencing results only, therefore it does not represent identification results of actual snow and ice damages. The other two $\Delta\overline{\gamma^0_{VV}}$ and $\Delta\overline{dRVI}$ are less representative and does not visually represent changes. This is discussed in the statistical analysis later, aiming how much they correlate with *ΔEVI2.*

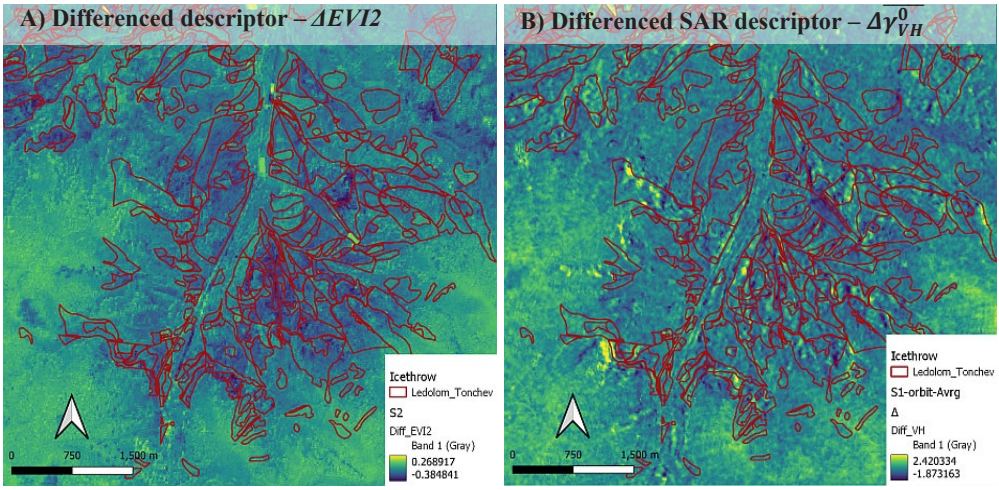


Fig. 8. Layer differencing results (or, differenced SAR descriptors), with overlaid disturbed forest cadastre (in dark reddish), where: A) *ΔEVI2*, B) $\Delta\overline{\gamma^0_{VH}}$.

Comparison of the differenced descriptors showed that SAR ones are less sensitive to the differences in forest changes, rather than *ΔEVI2*. This arise an important question why we observe such a result? One of the answers given is related with the specifics of the snow and ice breakage. On Figure 9 are represented the damaged woods, where stem breakage is present in general, but mixed with undamaged standing trees also! This leads into two things: 1) much lower index values in EVI2 after disturbances, which also lead to a higher negative value observed in *ΔEVI2,* because the lack of crowns with needles that hold the chlorophyll; 2) small differences in the SAR backscatter before and after the disaster event, where after the disaster higher dihedral with surface scattering almost replaces volume scattering before the disaster event. This is why in this snow/ice breakage, it could not be solely stated that SAR differenced descriptors are more sensitive to the forest change, in respect to the optical one (Fig. 9).

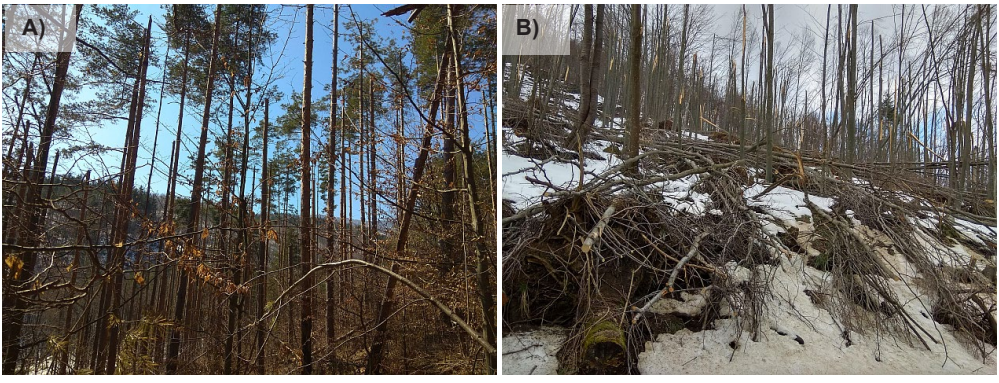


Fig. 9. Two disturbed forest stands, both having stem breakage that is mainly observed as a common breakage type at test area, where: A) young conifers, B) young beech.

That is clearly observed on the following Figure 10, where a zoomed in area into the damaged forest stands is represented, showing the two photos taken from the damaged woods and pinned as yellow points, including the Sentinel-2 post-disaster acquisitions in July 2021, together with the differenced optical and SAR descriptors of *ΔEVI2,* $\Delta\overline{\gamma^0_{VH}}$ and $\Delta\overline{dRVI}$ (Fig. 10).

Statistical analysis

Statistical analysis is performed on disturbed forest stands solely. Statistically it was found that the Δ*EVI2* change cor-

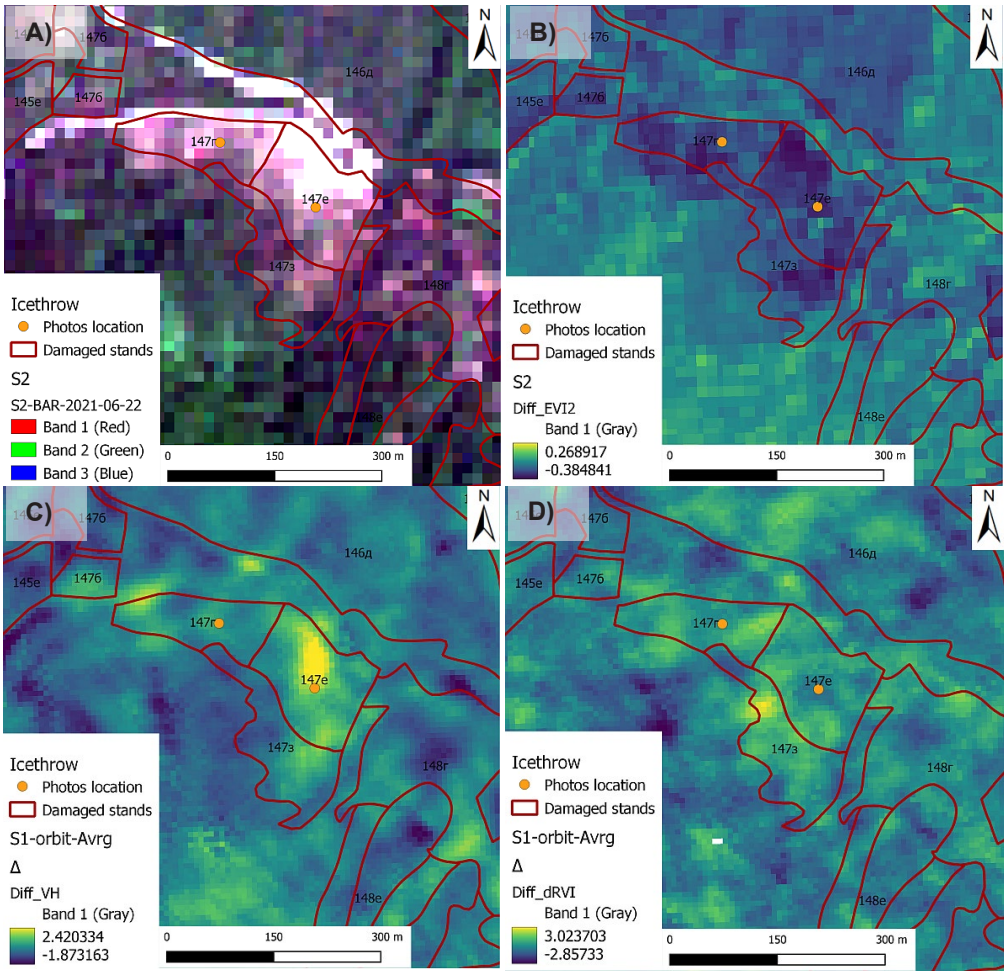


Fig. 10. A zoomed in disturbed forest cadastre with two photos taken from visited damaged forest in 2021, after the disaster of snow/icethrow happened (yellow points), where: A) the Sentinel-2 post-disaster acquisition from July 2021, showing lack of chlorophyll in damaged forest area; the differenced descriptors are: B) *ΔEVI2* with negative values in bluish that truly represents damaged woods; C) $\Delta\overline{\gamma^0_{VH}}$ **that exhibits non-consistent positive values; D)** $\Delta\overline{dRVI}$ **.**

relates, mostly with the cross-pol – $\Delta\overline{\gamma^0_{VH}}$ and least with the $\Delta\overline{dRVI}$ (Table 2). The last could be true, because the cross-pol channel (VH) is clearly more sensitive to the forest volume rather than the co-pol and *dRVI*.

Applying zonal statistics instruments via ArcGIS, represents the mean-value changes across disturbed and non-disturbed forest stands, by statistically averaged values. Except the $\Delta\overline{\gamma^0_{VV}}$ whole mean values at disturbed forest stands from the difference layers are negative, whilst at the non-disturbed forest stands those are positives. Regarding SAR data the highest change is observed at the $\Delta\gamma^0_{VH}$ (more than 0.2), while $\Delta\overline{dRVI}$ certainly changes its sign. Positive changes observed at non-disturbed forest stands should be correlated with the forest environmental factors changes. Forest regrowth for one year is too small to be a reason.

The ANOVA test, performed on the mean values of the six SAR data series – $\overline{\gamma^0_{VV}}$, $\overline{\gamma^0_{VH}}$, $\overline{dRVI}$ from both summer periods (i.e. 2020 and 2021), is applied to measure similarities in between. In addition, correlation and covariance are also calculated to those data series. The results showed that for both summer periods the $\overline{dRVI}$ differs more than the – $\overline{\gamma^0_{VH}}$ and $\overline{\gamma^0_{VV}}$. This is confirmed also on the covariance estimation of both series of $\overline{dRVI}$ (see Table 3). Correlations between series from both years show relatively low correlation in between, where differences should be due to environmental changes that influenced both summer periods, but also the forest disturbances.

Looking for a certain indication at the differenced SAR descriptors (i.e. *ΔEVI2,* $\Delta\overline{\gamma^0_{VV}}$, $\Delta\overline{\gamma^0_{VH}}$, $\Delta\overline{dRVI}$), separation of disturbed from non-disturbed forest stands is performed, by using the available forest cadastre layers. Implementing zonal statistical tools in ArcGIS©, average values (mean estimates) are calculated for the differenced SAR descriptors. This showed certain differences for disturbed and non-disturbed forest stands (Fig. 9). Looking at the disturbed forest, values of the differenced SAR descriptors are much lower, rather than those representing the healthy forest. Highest sensitivity to the disturbed forest is found in the changes of mean of the cross-pol difference SAR descriptor – $\text{Mean}_{\overline{\Delta\gamma^0_{VH}}}$. Observed change is with more than 0.23 dB in respect to the co-pol – $\text{Mean}_{\overline{\Delta\gamma^0_{VV}}}$, which also shows higher change. This leads to clear identification of forest disturbances, leading to physical changes of forest geometry (Fig. 11).

From both graphs on Figure 11 it could be concluded that a certain difference is observed between disturbed forest stands (on A) and non-disturbed (on B). This is a certain indication of the snow/ice breakage (resulted from the snowthrow and icethrow disaster events) of the forest causing abiotic stress. Besides, the SAR differenced descriptors are showing sensitivity to this change, where more sensible is the backscatter (i.e. $\Delta\overline{\gamma^0_{VV}}$ and $\Delta\overline{\gamma^0_{VH}}$), rather than the $\Delta\overline{dRVI}$. To point out the magnitude of those differences a subtraction is made of mean-estimates without forest disturbances (i.e. MEAN NonDisturbed) from the disturbed ones (i.e. MEAN Disturbed) (Table 4), from which it is seen that actually most sensitive SAR descriptor is namely $\Delta\overline{\gamma^0_{VH}}$.

Notably from Figure 11, only $\text{Mean}_{\Delta EVI2}$ shows negative value changes in the disturbed forest area in respect to the non-disturbed one, which is negative but very close to zero. To study these differences a division is performed on broadleaf

Table 2. Correlation results from differenced descriptors from Sentinel-1 and Sentinel-2.

Coefficient of determination	$\Delta EVI2 \sim \Delta\overline{\gamma^0_{VH}}$	$\Delta EVI2 \sim \Delta\overline{\gamma^0_{VV}}$	$\Delta EVI2 \sim \Delta\overline{dRVI}$
R	0.4547	0.3436	0.2167

Note: the backscatter in both polarisations only shows some degree of similarity with the – *ΔEVI2*.

Table 3. Statistical accuracy estimation – ANOVA, correlation, and covariance, on series for both summer periods that constitutes from mean orbit averaged SAR descriptors.

Applied test	$\overline{dRVI}$	$\overline{\gamma^0_{VH}}$	$\overline{\gamma^0_{VV}}$
ANOVA	77.963	50.927	54.050
Correlation	0.7706	0.7597	0.7275
Covariance	0.2092	0.1335	0.1377

Note: tests are applied over both series from summer of 2020 and summer of 2021.

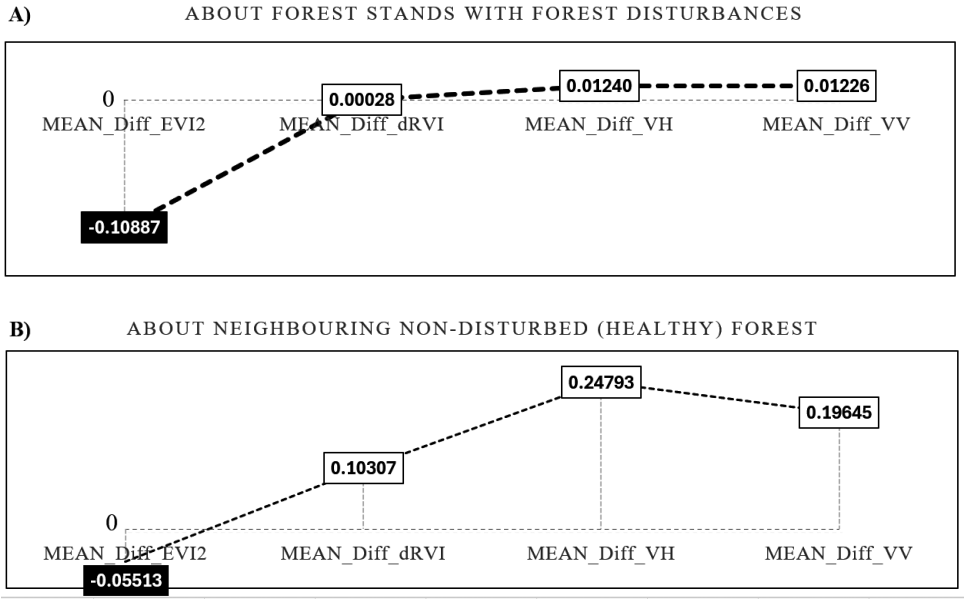


Fig. 11. Mean values of the differenced SAR descriptors and optical EVI2, statistically averaged over forest stands, where: A) Forest stands with disturbances caused from the icethrow disaster event; B) Non-disturbed (or healthy) forest stands nearby.

Note: Negative values are with black background. Differenced descriptors (*ΔEVI2*) and their mean values from zonal statistics are noted as: MEAN_Diff_EVI2, MEAN_Diff_VV, MEAN_Diff_VH, Mean_Diff_dRVI.

Table 4. Computed differences of the statistically averaged over forest stands mean values of the differenced descriptors, between those with forest disturbances from those without.

ΔMEAN	MEAN_Diff_EVI2	MEAN_Diff_dRVI	MEAN_Diff_VH	MEAN_Diff_VV
MEAN Disturbed – MEAN NonDisturbed	-0.05374	-0.10280	-0.23553	-0.18419

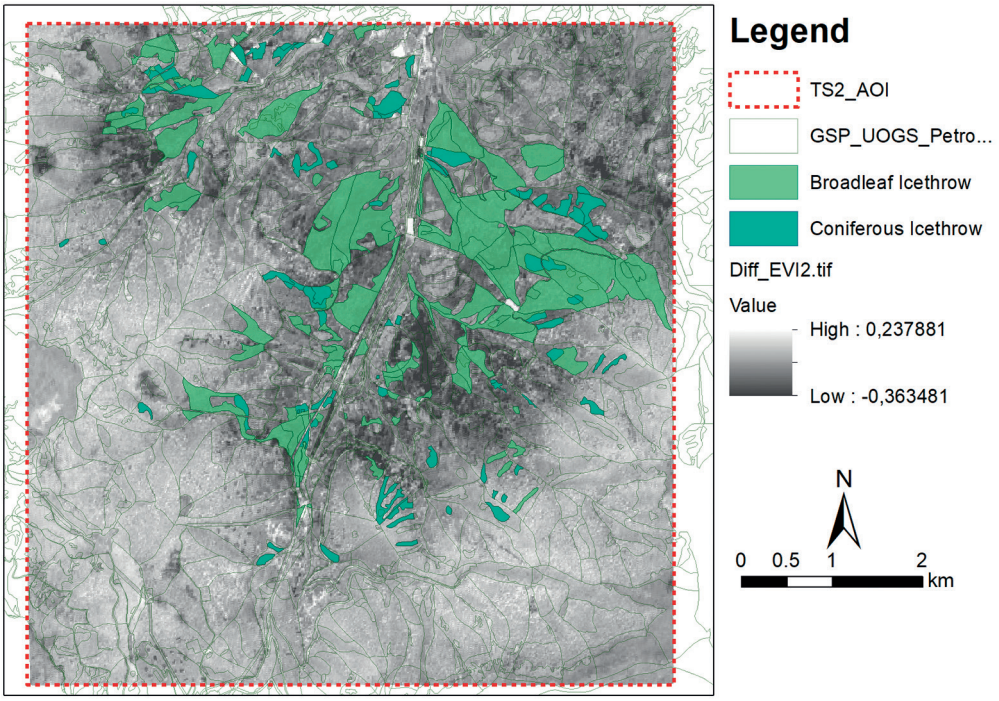


Fig. 12. Disturbed forest stands are divided by forest type in GIS.

versus coniferous forest stands (Fig. 12).

Thus, disturbed forest stands are divided by forest type in GIS, where 142 forest stands resulted as broadleaf, and 93 as coniferous ones (Fig.12). The next statistics utilises mean estimates per forest stand derived from zonal statistics in ArcGIS, from the orbit averaged SAR descriptors, or $\overline{dRVI}$, $\overline{\gamma^0_{VH}}$, $\overline{\gamma^0_{VV}}$, for both summer periods of 2020 and 2021. The overall statistical means are calculated, denoted again as – $\text{Mean}_{\overline{dRVI}}$, $\text{Mean}_{\overline{\gamma^0_{VH}}}$ and $\text{Mean}_{\overline{\gamma^0_{VH}}}$, for both forest types and summer periods (Table 5).

Highest differences are observed at $\text{Mean}_{\overline{dRVI}}$ showing lower depolarisation of the signal in post-disaster period, with notable positive values for coniferous forest at both periods. This is because coniferous forest exhibits higher depolarisation of the signal than the broadleaf one. It seems that differences between both periods for the backscatter are very low, with maximum difference of 0.054 for the $\text{Mean}_{\overline{\gamma^0_{VH}}}$ in coniferous forest. Influence from geometric distortions may influence those low differences in between. This leads to conclusion that $\overline{dRVI}$ show

Table 5. Statistics for both summer periods, of the three SAR descriptors, in respect to the forest type, from disturbed forest stands.

Mean estimates	Mean $_{\overline{dRVI}}$		Mean $_{\overline{\gamma^0_{VH}}}$		Mean $_{\overline{\gamma^0_{VH}}}$	
Summer periods	Broadleaf	Coniferous	Broadleaf	Coniferous	Broadleaf	Coniferous
Summer 2020	-0.7851	0.3840	-13.506	-13.235	-7.093	-7.406
Summer 2021	-0.6199	0.2275	-13.477	-13.262	-7.147	-7.355

better sensitivity to changes in the structure of the forest, with better delineation on forest type. Hereafter, the elaborated boxplots derived from the zonal statistics in ArcGIS in the above visually represent the statistical distributions and mean values change, before and after the disaster event (Fig. 13).

Due to the highest difference is for $\overline{dRVI}$ it is shown only in the figure. Statistics for $\overline{\gamma^0_{VH}}$ and $\overline{\gamma^0_{VV}}$ are overlapping for both periods and are not representative for the forest change. The boxplots are not so much representative for the forest change, despite that mean values differ. This is related with the already discussed fact that before and after the disaster event, the backscatter is high in the damaged forest stands. Nonetheless, changes are observed in between. Also, the geometric distortions also introduce higher backscatter and bias the interpretation.

As a final, the following statistics are calculated aiming to study dependencies in age of the forest species. Analysis is based on the disturbed forest cadastre and the estimated mean values of the differenced SAR descriptors (i.e. Mean $_{\Delta EVI2}$ and Mean $_{\overline{\Delta\gamma^0_{VH}}}$) (Fig. 14).

Results showed higher value diversity of Mean $_{\overline{\Delta\gamma^0_{VH}}}$, in respect to the forest age, having an outlier at the age of 120, where value is 0.584. The reason could be due to geometric distortions, which could strongly bias the values of the Mean $_{\overline{\Delta\gamma^0_{VH}}}$ in a mountainous region. Nonetheless, SAR

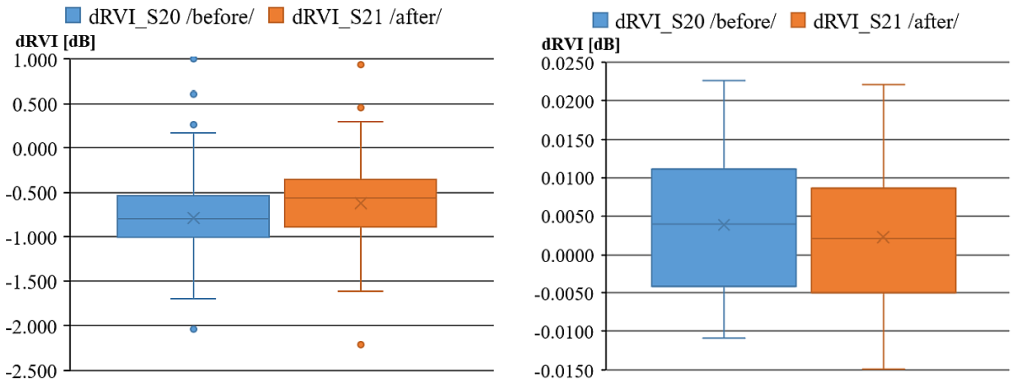


Fig. 13. Statistical analysis of time series data conducted for the summer periods of 2020 (pre-disaster) and 2021 (post-disaster) for $\overline{dRVI}$, with particular attention to variations across different forest types, such as coniferous (left) and broadleaf (right) forests.
Note: pre-disaster period is in bluish, posts-disaster period is in orange.

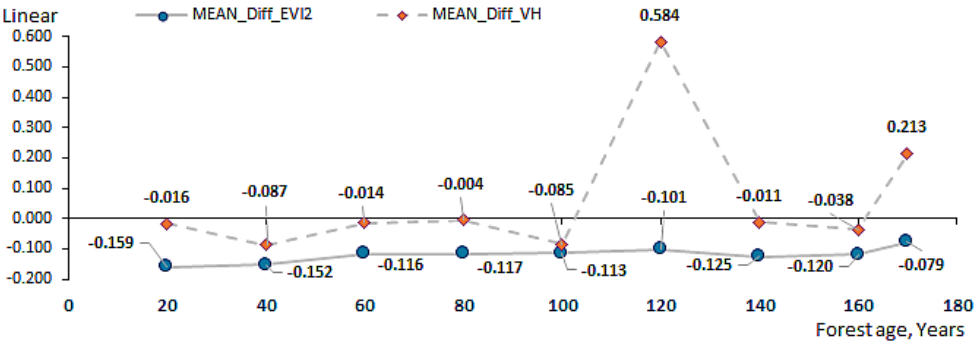


Fig. 14. Mean values change in respect to the forest age, for $\overline{\Delta\gamma^0_{VH}}$ (Mean_Diff_VH), and *ΔEVI2* (Mean_Diff_EVI2).

Note: for the purpose of comparability both $\overline{\Delta\gamma^0_{VH}}$ and ***ΔEVI2*** are represented in linear values.

is much more sensitive to the geometry of forest and therefore could be pointed out that Mean$_{\overline{\Delta\gamma^0_{VH}}}$ is more sensitive to the dependency of forest age, than Mean$_{\Delta EVI2}$.

Conclusions

In this study a large-scale forest mapping and statistical analysis, by employing a C-band Synthetic aperture radar (SAR) multitemporal approach was performed, proving that ESA's Sentinel-1 is fully capable to distinguish forest type and geometry changes of the forest canopy.

This sensitivity plays a key role in studying forest disturbances in temperate forest located in rugged terrain. Study is held in a complex forest structure, such as Bulgarian mountainous forest in TEFR 'Petrohan', of University of Forestry, by means of mean estimates from multitemporal SAR acquisitions (or, *SAR descriptors*) in both orbit directions – ascending and descending (i.e., $\overline{\gamma^0_{VH}}$, $\overline{\gamma^0_{VV}}$, $\overline{dRVI}$). A change detection approach is held, by referencing summer periods before the disaster in 2020 and after snow and ice breakage in the summer of 2021, showing high utilisation value of the mean estimates. In this manner the SAR descriptors represents highest possible centre of mass of the scattering centres, besides this approach fully determine the forest type, and almost fully correlates (i.e. $r^2 > 0.91$) with the reference layer from COPERNICUS HRL Dominant Leaf Type (DLT-2018).

Utilisation of the mean SAR descriptors is made by referring to the optical index (EVI2). The differenced SAR descriptors ($\Delta\overline{dRVI}$, $\Delta\overline{\gamma^0_{VH}}$, $\Delta\overline{\gamma^0_{VV}}$), and the differenced optical one (*ΔEVI2*), showed certain changes in forest structure within disturbed forest, apart from the non-disturbed one. Statistical analysis showed that highest change is observed at Mean$_{\overline{\Delta\gamma^0_{VH}}}$ and *ΔEVI2,* whereas most meaningful differenced layer is $\Delta\overline{dRVI}$. Changes in coniferous forest were most significant at the $\overline{dRVI}$ apart from the backscatter (i.e., $\overline{\gamma^0_{VH}}$ and $\overline{\gamma^0_{VV}}$). It could be concluded that in general $\overline{dRVI}$ shows better sensitivity to changes in the structure of the forest, with better delineation on forest type. It could be stated that to study complex temperate forests in mountainous regions by means of Sentinel-1

SAR data and methods, the methodology should rely on statistical mean estimations in dual polarimetry (VV and VH). This approach overcomes the stochastic factors, speckle, and geometrical distortions that accompany SAR measurements.

It must be noted that the GRD data products are slightly unreliable for the purpose of the study. Improvement should be made with the SLC data products that hold the original speckle pattern per each pixel, representing the original geometry of the backscatter process. Further research will include a dual-pol special case (i.e. HH+VV), or fully polarimetric data (i.e. HH+VV+HV), to fully represent the snow/ice breakage via POL-SAR data.

Acknowledgement

Authors wish to thank to ESA PECS. This study is part of project – 'EDUSAR', ESA Contract No. 4000134001/21/NL/CBi, held in SRTI-BAS, in partnership with the University of Forestry.

References

Abdikan S., Sanli F.B., Ustuner M., Calò F. 2016. Land cover mapping using sentinel-1 SAR data. The International Archives of the Photogrammetry, Remote Sensing and Spatial Information Sciences XLI-B7: 757–761. https://doi.org/10.5194/isprs-archives-XLI-B7-757-2016

Akbari V., Solberg S. 2022. Clear-cut Detection and Mapping Using Sentinel-1 Backscatter Coefficient and Short-term Interferometric Coherence Time Series. IEEE Geoscience and Remote Sensing Letters 19, 4006405. 5 p. https://doi.org/10.1109/lgrs.2020.3039875

Anev S., Marinova A. 2021. Physiological adaptation of European beech (*Fagus sylvatica* L.) and wild cherry (*Prunus avium* L.) saplings after windthrow. Forestry Ideas 27(2): 436–445.

Antropov O., Rauste Y., Praks J., Seifert F.M., Häme T. 2021. Mapping Forest Disturbance Due to Selective Logging in the Congo Basin with RADARSAT-2 Time Series. Remote Sensing 13(740), 740. 16 p. https://doi.org/10.3390/rs13040740

Caicoya A.T., Kugler F., Hajnsek I., Papathanassiou K. 2012. Boreal Forest Biomass Classification with TanDEM-X. In: International Geoscience and Remote Sensing Symposium (IGARSS). IEEE International Geoscience and Remote Sensing Symposium (IGARSS), 22–27.07.2012, Munich, Germany. 4 p. doi: 10.1109/IGARSS.2012.6350681

Cloude S.R., Papathanassiou K.P. 1998. Polarimetric SAR Interferometry. IEEE Transactions on Geoscience and Remote Sensing 36(5): 1551–1566.

Dimitrov Z. 2022. Application of mean statistics derived from Sentinel-1 time series on forest – examine forest type and correlation with biomass layers. 2nd National Workshop with Workshop with International Participation on EU Copernicus Programme 28 July 2020, 6 October 2020 Sofia, Bulgaria. Zenodo: 61–78. doi: 10.5281/zenodo.6497740

Englhart S., Keuck V., Siegert F. 2011. Aboveground biomass retrieval in tropical forests – The potential of combined X- and L-band SAR data use. Remote Sensing of Environment 115: 1260–1271. http://dx.doi.org/10.1016/j.rse.2011.01.008

ESA 2021. Time-series analysis with Sentinel-1. 31 p.

Fernandez-Ordonez Y., Soria-Ruiz J., Leblon B. 2009. Forest Inventory using Optical and Radar Remote Sensing. Advances in Geoscience and Remote Sensing. InTech: 539–555. http://dx.doi.org/10.5772/8330

Koleva R., Tepeliev Y., Dimitrov V. 2019. Changes in the afforested areas of the

forest territories of Bulgaria in the period 1990 – 2018, set out by the results of the Corine land cover project. XXVIII International Symposium Modern Technologies, Education and Professional Practice in Geodesy and Related Areas, 08–09 November, Sofia. Geodesy, cartography and land management 2019(1–2): 7–12 (in Bulgarian).

Kugler F., Schulze F.D., Hajnsek I., Pretzsch H., Papathanassiou K. 2014. TanDEM-X Pol-InSAR Performance for Forest Height Estimation. IEEE Transactions on Geoscience and Remote Sensing 52(10): 6404–6422. https://doi.org/10.1109/TGRS.2013.2296533

Le Toan T., Quegan S., Davidson M.W.J., Balzter H., Paillou P., Papathanassiou K., Plummer S., Rocca F., Saatchi S., Shugar H., Ulander L. 2011. The BIOMASS mission: Mapping global forest biomass to better understand the terrestrial carbon cycle. Remote Sensing of Environment 115(11): 2850–2860. https://doi.org/10.1016/j.rse.2011.03.020

Mandal D., Kumar V., Ratha D., Dey S., Bhattacharya A., Lopez-Sanchez J.M., McNairn H., Rao Y.S. 2020. Dual polarimetric radar vegetation index for crop growth monitoring using sentinel-1 SAR data. Remote Sensing of Environment 247, 111954. 17 p. https://doi.org/10.1016/j.rse.2020.111954

Nasirzadehdizaji R., Sanli F.B., Abdikan S., Cakir Z., Sekertekin A., Ustuner M. 2019. Sensitivity Analysis of Multi-Temporal Sentinel-1 SAR Parameters to Crop Height and Canopy Coverage. MDPI, Applied Sciences 9(4), 655. 18 p. https://doi.org/10.3390/app9040655

Ruiz-Ramos J., Marino A., Boardman C., Suarez J. 2020. Continuous Forest Monitoring Using Cumulative Sums of Sentinel-1 Timeseries. Remote Sensing 12(18), 3061. 23 p. https://doi.org/10.3390/rs12183061

Small D., Miranda N., Zuberbühler L., Schubert A., Meier E. 2010. Terrain-corrected Gamma: improved thematic land-cover retrieval for SAR with robust radiometric terrain correction. Proceedings of ESA Living Planet Symposium, held on 28 June – 2 July 2010 at Bergen in Norway. 8 p. https://doi.org/10.5167/uzh-41236

Stelmaszczuk-Górska M.A., Urbazaev M., Schmullius C., Thiel C. 2018. Estimation of Above-Ground Biomass over Boreal Forests in Siberia Using Updated In Situ, ALOS-2 PALSAR-2, and RADARSAT-2 Data. Remote Sensing 10(10), 1550. 20 p. https://doi.org/10.3390/rs10101550

Tomppo E., Antropov O., Praks J. 2019. Boreal Forest Snow Damage Mapping Using Multi-Temporal Sentinel-1 Data. Remote Sensing 11(4), 384. 20 p. https://doi.org/10.3390/rs11040384

Tonchev T., Koleva R., Tepeliev Y. 2018. Detection and mapping of coniferous forests in western Bulgaria damaged by biotic and abiotic factors in the frame of the 'CORINE land cover 2018' Project. Forestry ideas 24(2): 131–140.

Trudel M., Charbonneau F., Leconte R. 2012. Using RADARSAT-2 polarimetric and ENVISAT-ASAR dual-polarization data for estimating soil moisture over agricultural fields. Canadian Journal of Remote Sensing 38(4): 514–527. https://doi.org/10.5589/m12-043

University of Forestry 2023. Petrohan – Training and Experimental Forest Range (the village of Barziya). https://ltu.bg/en/university/training-and-sport-centres/training-centres/petrohan-training-and-experimental-forest-range-the-village-of-barziya

FORESTRY IDEAS, 2024, vol. 30, No 1 (67): 160–172

Comparative characteristics of the leaf surface ultrastructure of plants of genus *Populus* L.

Liubov Ishchuk[1*], Volodymyr Hrabovyj[1], Halyna Ishchuk[2], Inna Didenko[3], Tatiana Kovalchuk[3], and Svetlana Kurka[2]

[1]Sofiyivka National Dendrological Park of the National Academy of Sciences of Ukraine, 12A Kyivska Str., 20305 Uman, Ukraine, *E-mails: ishchuk29@gmail.com* (LI), konf_sofievka2011@ukr.net (VH)

[2]Department of Forestry, Uman National University of Horticulture, 1 Instytutska Str., 20305 Uman, Ukraine. E-mails: sobaka.kot2011@gmail.com (HI), Svetlana9075@ukr.net (SK)

[3]Department of Herbaceous Plants of the Sofiyivka National Dendrological Park of the National Academy of Sciences of Ukraine, 12A Kyivska Str., 20305 Uman, Ukraine, E-mails: fritillaria2007@gmail.com (ID), rhus2017@gmail.com (TK)

Received: 06 February 2024 / Accepted: 29 April 2024 / Available online: 14 May 2024

Open Access: This article is licensed under a Creative Commons Attribution 4.0 International License.

Abstract

The article analyses the ultrastructure and morphometric characters of cells and stomata on the adaxial and abaxial surfaces of leaves in *Populus deltoides* Bartr. ex Marsh., *Populus trichocarpa* Torr. & A. Grey, *Populus suaveolens* Fisch. and *Populus nigra* cv. Italica (Du Roi) Moench (Salicaceae). The aim is to identify species-specific and diagnostically significant features at different taxonomic levels under introduction conditions. For the ultrastructure investigation, the middle part of the leaf blade was fixed on brass stubs, coated with a thin layer of gold and examined using a scanning electron microscope. Most important features are shape, size, nature of the leaf surface and the presence of specific structures. The density of epidermal cells and the number of stomata on the adaxial and abaxial surface of the leaf were determined. The hypostomatous leaf type and collenchymatous ultrastructure type were identified in *P. trichocarpa* and *P. suaveolens*, while the amphistomatous leaf type and stomato-faveolus ultrastructure type are observed on both leaf surfaces of *P. deltoides* and on the adaxial leaf surface of *P. nigra* cv. Italica. Morphometric traits of the leaf surface indicate a higher density of adaxial epidermal cells in *P. nigra* cv. Italica, *P. suaveolens* and *P. trichocarpa* compared to the abaxial surface. Structural organization of the leaf in *P. deltoides*, *P. nigra* cv. Italica, *P. suaveolens* and *P. trichocarpa* allows to identify these taxa on the basis of micromorphological features and suggests their broad ecological plasticity.

Key words: abaxial surface, adaxial surface, cells, epidermis, morphometric features, stomata, stomatal index.

Introduction

The influence of the environment on plants is determined not only by the nature of the acting factors but also by the genetic specificity of the organism, characterized by its ecological nature. The most flexible organ of plants is the leaf, whose structure re-

flects not only the eco-climatic conditions, in which the species developed, but also the organism's response to the conditions of the external environment in which the plant is currently situated (Ishchuk 2016, Ishchuk and Ishchuk 2018). The study of the anatomical and morphological structure of leaves allows deeper ecological characterization of the plant organism and helps determine the degree of its adaptation to environmental conditions, especially during the process of introduction (Gorlacheva 2010, Brailko 2014). Due to the difficulties that arise in distinguishing species within critical genera of flowering plants based on a series of macro-morphological leaf characteristics, data from other studies are employed, particularly those related to the anatomical structure of leaves (Metcalfe and Chalk 1950, Juniper 1959, Aneli 1975, Carolin, 1980, Chakrabarty and Mukherjee 1986, Shetler and Morin 1986, Barthlott et al. 1998). Waxes are an essential structural element of the surface and of fundamental functional and ecological importance for the interaction between plants and their environment (Barthlott et al. 1998).

Such studies are particularly relevant for the identification of hybrids within genus *Populus*, whose leaves are morphologically very similar. Researchers have attributed crucial importance to the features of the ultrastructure of the leaf surface as diagnostic criteria for distinguishing taxa and understanding the ecological characteristics of species (Chen et al. 2008, Su et al. 2009). Characters, such as shape, size and density of stomatal complexes, were very useful in differentiating Salix species. Variation in features of stomatal apparatus in Salix is wider than previously known. Moreover, the type of stomatal complex proved to be very helpful in discriminating *Chosenia* Nakai as members of genus *Salix* (Ghahremaninejad et al. 2012). Leaf ultrastructure is also closely associated with drought resistance of species (Mytyna 2007, Ishchuk 2017, Ishchuk and Ishchuk 2019) and resistance to pollution by dust and heavy metals (Ishchuk et al. 2018, Ishchuk and Ishchuk 2020).

American scientists (Russin and Evert 1984) studied the vascular system and the spatial relationship of various orders of vascular bundles to the moesophyll of *P. deltoides* leaves in field conditions and in special growth chambers. They found that the adaxial and abaxial parenchyma of isolateral leaves grown in growth chambers had thinner lobes, a greater proportion of air space and greater interveinal spacing than in field-grown plants.

Chinese researchers, analysing the anatomical structure of leaves in polyploid hybrids of *P. ussuriensis* Kom., found that tetraploid hybrids were characterized by the thickest leaves, epidermis, columnar parenchyma tissues and the ratio of columnar to spongy parenchyma tissues compared to diploid hybrids of this species (Chuan 2010).

Therefore, the goal of our study was to establish the features of the ultrastructure of leaf epidermis in introduced species and hybrids of *Populus deltoides* Bartr. ex Marsh., *Populus trichocarpa* Torr. & A. Grey, *Populus suaveolens* Fisch. and *Populus nigra* cv. Italica (Du Roi) Moench., and to identify the species-specific and diagnostic significance of these characteristics at various taxonomic levels under introduction conditions.

Materials and Methods

The material for the study consisted of leaves from the middle part of the crown of young 8–10-year-old plants of *Popu-*

lus deltoides, *Populus nigra* cv. Italica, *Populus suaveolens* and *Populus trichocarpa* from the collection of the Botanical Garden of Bila Tserkva National Agrarian University. The studied species come from different regions of the globe. The natural range of *P. deltoides* occupies the eastern regions of North America, *P. trichocarpa* – the western part of North America, *P. suaveolens* – Eastern Siberia, Mongolia and Northern China, *P. nigra* cv. Italica is the territory of Central and Asia Minor (Ishchuk 2019). For the ultrastructure investigation, the middle part of the leaf blade was fixed on brass stubs and coated with a thin layer of gold. The surface ultrastructure was examined using a scanning electron microscope (SEM) JSM-6060 LA. Digital images were captured with an AxioCam MRc-5 camera and processed using the Axio Vision 4.8 software. The study was conducted with five replicates. The ultrastructure of the leaves was described using the commonly accepted methodology and terminology (Aneli 1975). Among the external characteristics, most important were shape, size, surface characteristics of the leaf and the presence of specific structures. According to Barthlott and Wollenweber (1981), primary and secondary structures of the leaf epidermis are distinguished.

The primary structure is determined by:

- General outlines of cells in the paradermal plane (isodiametric or elongated);
- Shape of the external periclinal wall (convex, concave, flat);
- Shape of anticlinal walls (straight, wavy, thickened, not thickened);
- Outlines of visible cell boundaries on the surface.

The secondary structure is primarily determined by the morphological features of the cuticle (Barthlott and Wollenweber 1981). Following the widely accepted botanical terminology (Stern and Morris 1992), in cells of elongated shape, the anticlinal walls farthest from the cell centre are referred to as distal, while those closer to the cell centre and perpendicular to the distal walls are termed proximal.

The quantity of cells per 1 mm^2 of the adaxial and abaxial epidermis of the leaf was determined. If the quantity of cells on the adaxial surface is less than 400 and on the abaxial surface is less than 600 per 1 mm^2, they are considered very large. If the quantity of cells on the adaxial surface of the epidermis is between 401–900, and on the abaxial surface is between 601–1350 per 1 mm^2, these cells are classified as large according to the author's classification. Cells of medium size on the adaxial surface may be present in quantities of 901–1600 per 1 mm^2 on the adaxial surface and 1351–2400 on the abaxial surface. Conversely, cells in quantities of 1601–2500 on the adaxial surface and 2401–3750 per 1 mm^2 are considered small, and if their quantity is even greater, the author considers them very small.

If the quantity of stomata per 1 mm^2 on the adaxial surface of the leaf is less than 10, they are classified as solitary; if they are between 11 and 100, it is considered small quantity; 101–150 is an average quantity; 151–250 is a large quantity, and above 251 is considered very large. For the abaxial surface, if the quantity of stomata is less than 100 per 1 mm^2, their sizes are classified as very small; 101–160 as small; 161–250 as medium; 251–360 as large; 361–490 as very large, and above 491 as extremely large stomatal quantity.

The quantity of stomata was determined in the microscope field by counting per 1 mm^2 of the epidermal surface. The stomatal index was expressed as the ratio

of the quantity of guard cells of stomata to the total quantity of epidermal cells, including both guard cells and other epidermal cells, on the same area, expressed as a percentage by formula (1)

$$I = \frac{100 \cdot 2n}{2n + m}, \quad (1)$$

where: I is stomatal index, %; n is quantity of guard cells of stomata per 1 mm^2; $m$is total quantity of epidermal cells per 1 mm^2 (including guard cells and other epidermal cells).

The statistical analysis of the obtained data was performed using the Microsoft Excel software application.

Results

Among the species of genus *Populus*, we investigated the ultrastructure of the leaf surfaces of four species: *P. deltoides*, *P. nigra* cv. Italica, *P. suaveolens* and *P. trichocarpa*, the descriptions are provided below.

The projections and outlines of epidermal cells vary: in the region of vascular bundles, cells with elongated projections and straight outlines are observed, while above the moesophyll, cells are angular (four- to five-sided) with straight, uniformly thickened anticlinal walls. The external periclinal walls are characterized by a granular texture. The surface relief is reticulate, and the subtype is reticulate-comminuted. The cuticle is well-developed, and the epicuticular wax is represented by flakes.

For *P. deltoides*, the leaf is characterized by an amphistomatous structure, with paracytic and anomocytic stomata evenly distributed on both surfaces of the leaf blade at the same level as the main epidermal cells. The adaxial surface of the leaf blade of this species is reticulate (Fig. 1).

In *P. deltoides*, the abaxial surface is structurally similar to the adaxial one (Fig. 2) but differs primarily in a more pronounced wrinkling of the cuticle compared to the adaxial surface.

For *P. nigra* cv. Italica, the leaf is characterized by an amphistomatous type, with anomocytic and paracytic stomata evenly distributed on both upper and lower epidermis of the leaf blade, at the same level as the main epidermal cells. The ad-

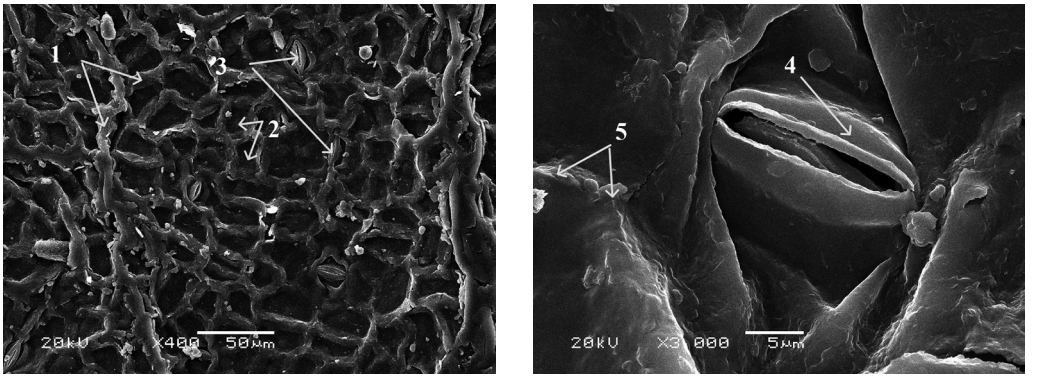


Fig. 1. Ultrastructure of the adaxial epidermis of the leaf blade of *P. deltoides*: 1 – anticlinal walls of epidermal cells, 2 – periclinal walls of epidermal cells, 3 – stomata, 4 – stoma, 5 – epicuticular wax.

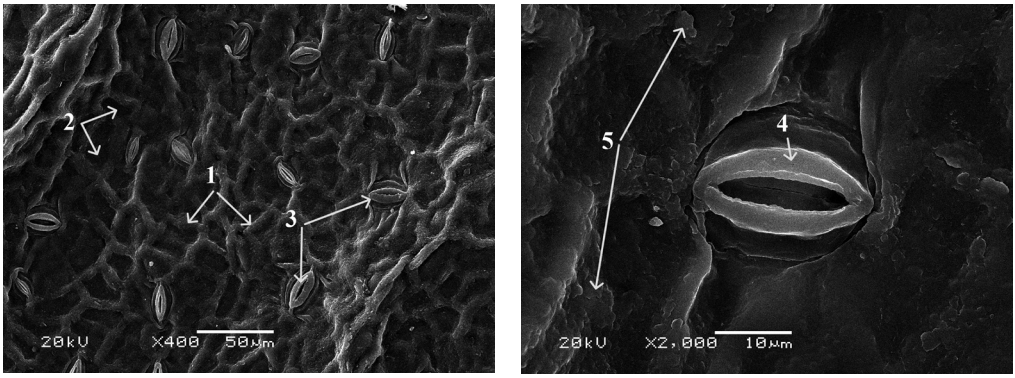


Fig. 2. Ultrastructure of the abaxial epidermis of the leaf blade of *P. deltoides*: 1 – anticlinal walls of epidermal cells, 2 – periclinal walls of epidermal cells, 3 – stomata, 4 – stoma, 5 – epicuticular wax.

axial epidermis of the investigated hybrid is characterized by a reticulate-comminuted subtype of relief with deeply concave periclinal walls of cells and a granular ultrasculpture (Fig. 3).

The cell boundaries are on the adaxial surface of *P. nigra* cv. Italica distinct. Projections and outlines of epidermal cells vary: in the area of vascular bundles, cells with elongated projections and straight outlines are observed, while above the mesophyll, cells are angular (triangular, quadrangular) with straight, thickened anticlinal walls. The cuticle is well-developed. Epicuticular wax is represented by wax flakes and wax plates.

In the studied hybrid *P. nigra* cv. Italica, the abaxial surface differs from the adaxial one. On the abaxial surface there are stomata of the paracytic type. On the abaxial surface of the leaf, epidermal cells are not clearly visible. Abaxial epidermal cells have sinuous outlines and spread projections above the mesophyll, with sinuous outlines and elongated projections in the region of the midvein. The surface relief is colloquially ostiate (Fig. 4). The wax is represented by wax flakes.

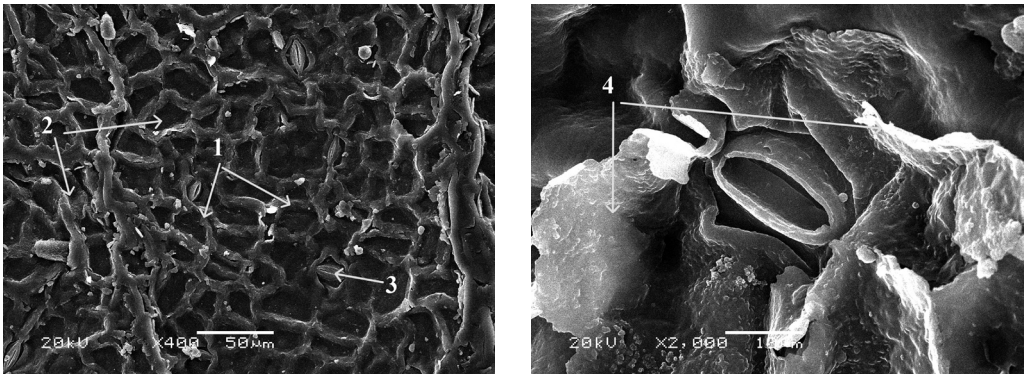


Fig. 3. Ultrastructure of the adaxial epidermis of the leaf blade of *P. nigra* cv. Italica: 1 – anticlinal walls of epidermal cells, 2 – periclinal walls of epidermal cells, 3 – stomata, 4 – epicuticular wax.

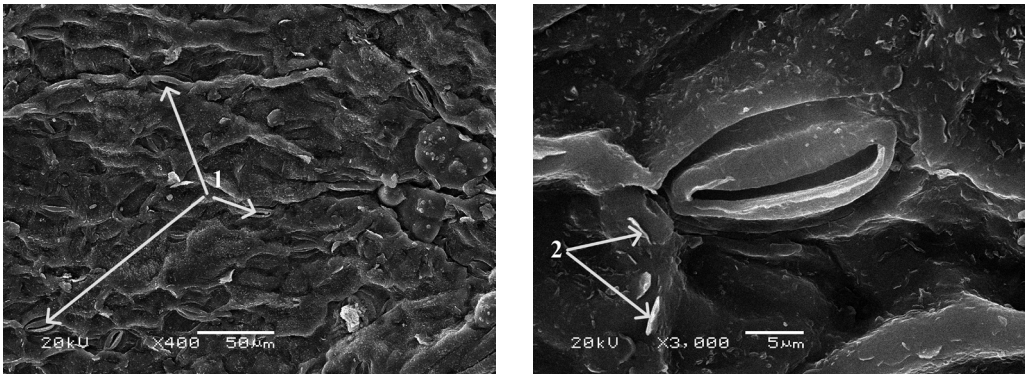


Fig. 4. Ultrastructure of the abaxial epidermis of the leaf blade of *P. nigra* cv. Italica: 1 – stomata, 2 – wax.

Leaf of *P. suaveolens* is hypostomatic, with paracytic stomata evenly distributed on the abaxial surface of the leaf blade, at the same level as the main epidermal cells. The adaxial surface of the leaf blade of the studied species is collicular. Cell boundaries are clear (Fig. 5).

Projections and outlines of epidermal cells vary: in the area of vascular bundles, cells with elongated projections and straight outlines are observed, while above the moesophyll, cells are angular (triangular, quadrangular) with straight, non-thickened anticlinal walls. External periclinal walls are convex, thin, characterized by smooth texture. The cuticle is well-developed. Epicuticular wax is represented by wax plates.

In *P. suaveolens*, abaxial surface of the leaf differs from the adaxial one. Cells of the abaxial epidermis are characterized by winding outlines and spread projections over the moesophyll, while in the area of the midrib, they have winding outlines and elongated projections. Stomata are of the paracytic type. Closing cells of stomata are characterized by a distinctly striate cuticle, whereas the periclinal walls of the main epidermal cells are characterized by a smooth cuticle (Fig. 6). The relief

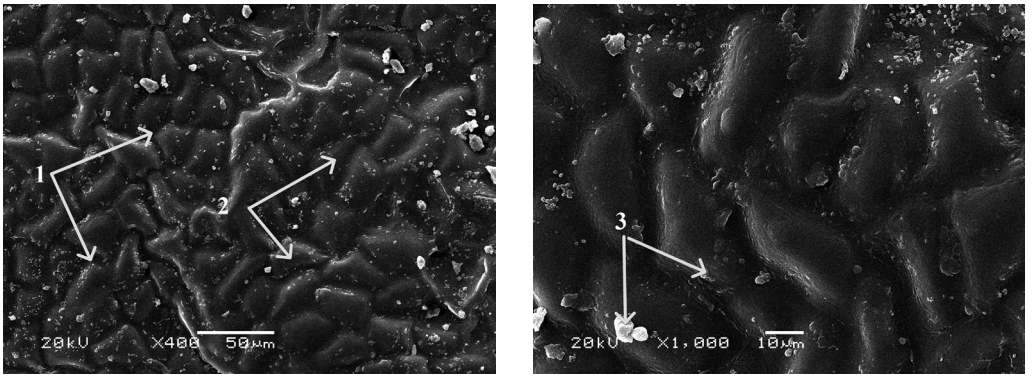


Fig. 5. Ultrastructure of the adaxial epidermis of the leaf blade of *P. suaveolens*: 1 – anticlinal walls of epidermal cells, 2 – periclinal walls of epidermal cells, 3 – epicuticular wax.

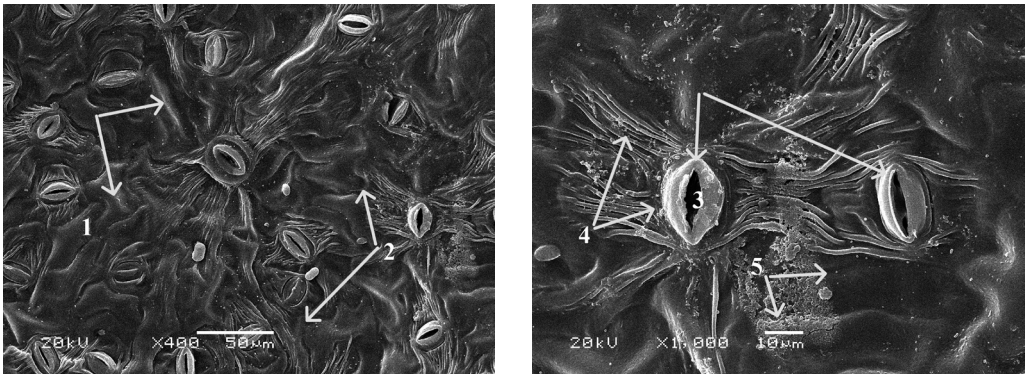


Fig. 6. Ultrastructure of the abaxial epidermis of the leaf blade of *P. suaveolens*: 1 – anticlinal walls of epidermal cells, 2 – periclinal walls of epidermal cells, 3 – stomata, 4 – cuticle, 5 – wax.

of the surface is colloquial. The periclinal walls of the cells are characterized by a smooth texture. Epicuticular wax is represented by wax granules and wax plates.

The leaf of *P. trichocarpa* is hypostomatic, with paracytic stomata (sociovate-like according to Aneli 1975), evenly distributed on the abaxial surface of the leaf blade, at the same level as the main epidermal cells. The adaxial surface of the leaf blade of this species is collicular. Cell boundaries are clear (Fig. 7). Projections and outlines of epidermal cells vary: in the region of vascular bundles, there are cells with elongated projections and straight outlines, while above the moesophyll, cells are angular (triangular, quadrangular) with straight, non-thickened anticlinal walls.

The external periclinal walls of *P. trichocarpa* cells are convex, thin and characterized by a smooth texture. The cuticle is well-developed. The relief is collicular. The periclinal walls of epidermal cells have a smooth texture, and the anticlinal walls are not raised or thickened. The epicuticular

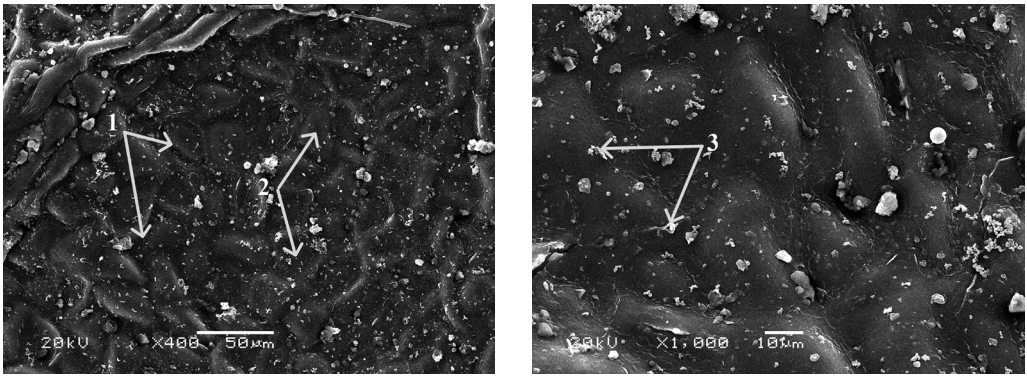


Fig. 7. Ultrastructure of the adaxial epidermis of the leaf blade of *P. trichocarpa*: 1 – anticlinal walls of epidermal cells, 2 – periclinal walls of epidermal cells, 3 – epicuticular wax.

wax is represented by wax granules.

In *P. trichocarpa*, the abaxial surface differs from the adaxial one. The cells of the abaxial epidermis are characterized by wavy outlines and projections spread over the moesophyll, with wavy outlines and elongated projections in the region of the midvein (Fig. 8).

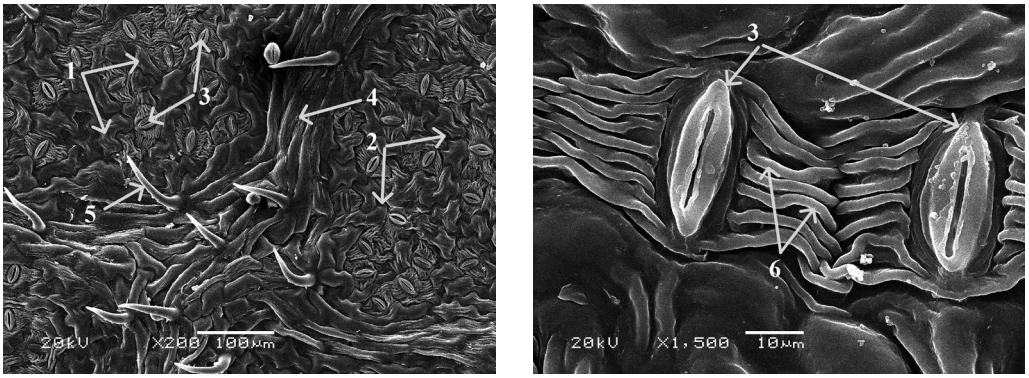


Fig. 8. Ultrastructure of the abaxial epidermis of the leaf blade of *P. trichocarpa*: 1 – anticlinal walls of epidermal cells, 2 – periclinal walls of epidermal cells, 3 – stomata, 4 – epidermal cells in the area of the central vein, 5 – trichomes, 6 – cuticle.

The stomata in *P. trichocarpa* are of the paracytic type. The closing cells of the stomata are characterized by a distinctly striate cuticle, while the periclinal walls of the main epidermal cells are characterized by a smooth cuticle. Leaf veins are covered with trichomes. The “hooks” are two-celled, formed by an isodiametric basal cell and a long distal cell. The surface relief is collicular, and the periclinal walls of the cells are characterized by a smooth texture.

Thus, the ultrastructure of the adaxial surface in *P. suaveolens* and *P. trichocarpa* is of the collicular type, while in *P. deltoides* and *P. nigra* cv. Italica, it is of the reticulate type (Table 1).

Table 1. Characteristics of the ultrastructure of the leaf surface of species and hybrids of the genus *Populus*.

Species	The type or subtype of the ultrastructure of the surface	Cell shape	Anticlinal walls		Periclinal walls	
			nature of thickening	level	level	ultrasculpture
Adaxial epidermis						
P. deltoides	reticulate type reticulate-faveolus subtype	polygonal	uniformly thickened	considerably elevated	concave	granular
P. nigra cv. Italica	reticulate-faveolus	angular	uniformly thickened	raised	deeply concave	granular
P. suaveolens	collenchymatous	spreading	uniformly thickened	below periclinal walls	convex	granular
P. trichocarpa	collenchymatous	angular	not thickened	below periclinal walls	convex	smooth

Species	The type or subtype of the ultrastructure of the surface	Cell shape	Anticlinal walls		Periclinal walls	
			nature of thickening	level	level	ultrasculpture
Abaxial epidermis						
P. deltoides	reticulate type reticulate- faveolus subtype	polygonal	uniformly thickened	considerably elevated	concave	granular
P. nigra cv. Italica	collenchymatous-coriaceous	elongated-spreading	uniformly thickened	below periclinal walls	convex	granular
P. suaveolens	collenchymatous	spreading	uniformly thickened	below periclinal walls	convex	smooth, streamwise-wrinkled
P. trichocarpa	collenchymatous	spreading	not thickened	below periclinal walls	convex	streamwise-wrinkled, smooth

Morphometric characteristics of the ultrastructure of leaf surfaces in species and hybrids of Populus indicate a higher density of adaxial epidermal cells in *P. nigra* cv. Italica, *P. suaveolens*, *P. trichocarpa* compared to the abaxial surface (Table 2). The stomatal index values in *P. deltoides* and *P. nigra* cv. Italica, with an amphistomatous leaf type, indicate that the number of stomata on the adaxial surface is less than on the abaxial surface.

Table 2. Morphometric characteristics of the ultrastructure of leaf surfaces in species and hybrids of the genus *Populus*.

Species, hybrid	Adaxial epidermis		Abaxial epidermis		Stomatal index, %	
	number of cells per 1 mm²	number of stomata per 1 mm²	number of cells per 1 mm²	number of stomata per 1 mm²	adaxial epidermis	abaxial epidermis
P. deltoides	1561.1 ±11.8	109.1 ±0.45	1918.1 ±21.42	191.8 ±0.65	12.3	16.7
P. nigra cv. Italica	2123.0 ±23.1	68.5 ±0.65	1850.2 ±13.2	219.0 ±0.54	6.1	19.14
P. suaveolens	1438.0 ±0.74	-	1023.0 ±4.8	167.0 ±0.48	-	24.61
P. trichocarpa	1315.0 ±2.78	-	1000.0 ±1.43	100.0 ±0.46	-	16.7

Note: Columns 2–5 represents mean ±standard error.

The adaxial surface of the leaves of *P. deltoides*, *P. suaveolens* and *P. trichocarpa* is characterized by cells of medium size, while for *P. nigra* cv. Italica small cells are typical (Table 3). On the abaxial surface, large cells are characteristic for the leaves of *P. suaveolens* and *P. trichocarpa*, and medium-sized cells are typical for *P. deltoides* and *P. nigra* cv. Italica.

Discussion

The results of the ultrastructural studies of the leaves of *P. deltoides*, *P. nigra* cv. Italica, *P. suaveolens* and *P. trichocarpa* show that, overall, they are characterized by plasticity. This is supported by studies on the ultrastructure of *P. alba* L. leaves, where parenchymal cells were elongated

Table 3. Morphometric characteristics (mean ±standard error) of epidermal cells and stomata of leaves of *Populus* species and hybrids, μm.

Species, hybrid	Epidermis		Stomata	
	cell length	cell width	stomatal length	stomatal width
	Adaxial epidermis			
P. deltoides	34.2 ±1.3	30.1 ±2.5	28.5 ±0.62	30.85 ±0.85
P. nigra cv. Italica	42.55 ±2.25	36.42 ±0.26	24.83 ±0.7	20.11 ±0.22
P. suaveolens	48.75 ±2.45	25.67 ±0.65	-	-
P. trichocarpa	52.65 ±1.25	31.75 ±0.88	-	-
	Abaxial epidermis			
P. deltoides	26.2 ±3.1	21.3 ±1.1	37.5 ±1.15	28.65 ±1.12
P. nigra cv. Italica	28 ±1.15	25.15 ±0.50	48.35 ±2.08	36.85 ±0.45
P. suaveolens	36.42 ±0.75	19.45 ±0.42	24.0 ±0.925	20.15 ±0.75
P. trichocarpa	40.44 ±0.92	15.67 ±0.66	21.45 ±0.35	18.23 ±0.38

in plants taken from field conditions, enhancing intercellular CO_2 exchange and increasing photosynthetic capacity compared to leaves taken from an artificial phytotron (Lin et al. 2022). The plasticity of leaves is also supported by the conclusions of Redko (1966), who, based on moisture requirements, classified all species of genus *Populus* growing in Ukraine into three groups: xeromoesophytes (*P. alba*, *P.* × *cannescens*, *P. suaveolens*, *P. tremula*, *P. trichocarpa*), moesophytes (*P. nigra* cv. Italica, *P. bolleana*, *P. balsamifera*, P. × *euramericana* cv. 'Serotina'), moesohygrophites (all other Euro-American hybrids).

For *P. suaveolens* and *P. trichocarpa*, hypostomatous leaf type is characteristic, while for *P. deltoides* and *P. nigra* cv. Italica it is amphistomatous. The exclusive presence of stomata on the adaxial surface of the leaf might suggest adaptation to growth in arid habitats. Nitrogen-enriched anatomical changes in the leaves and adjustments of stomatal behaviour during drought stress in *Populus* species lead to reduced water loss and improved plant growth during dry periods (Lu et al. 2019). Positive correlations between biomass production and abaxial stomatal density were observed in the leaves during the third growing season of the second rotation of high-density *P. deltoides* and *P. nigra* coppice (Al Afas et al. 2007). Researchers also note that in *P. deltoides* and *P. nigra* plants, the spongy parenchyma layer was thinner than the palisade layer, indicating their resilience to drought. Regarding stomatal density on the abaxial surface of the leaf epidermis, there is a pattern where species with a more southern origin tend to have fewer stomata per unit area of leaf epidermis. According to the stomatal density scale on the adaxial surface of leaves in *P. nigra* cv. Italica has low stomatal density, while *P. deltoides* has medium stomatal density. On the abaxial surface of the leaves in *P. trichocarpa*, the density of stomata is low, while the rest of the studied species have an average density of stomata. Studying the anatomical structure of *P. deltoides* hybrids in the southern mountainous regions of China, scientists found that the stomatal density of maternal and parental individuals in the upper and lower parts of the leaf epidermis varied in proportions ranging from 0.08 to 0.55 (Liu et al. 2018). Our studies on leaves of the parental individual *P. deltoides* showed a stomatal den-

sity of 0.12 on the adaxial side and 0.16 on the abaxial side, which coincides with research conducted in China. Analysis of quantitative characters of leaf surface ultrastructure suggests that species originating from a warmer climate (*P. trichocarpa*, *P. suaveolens*, *P. nigra* cv. Italica) exhibit higher density of adaxial epidermal cells compared to the abaxial ones.

All these patterns, in our opinion, indicate the adaptation of species of more southern origin (*P. nigra* cv. Italica, *P. suaveolens* and *P. trichocarpa*) to reduce transpiration, enhancing their drought resistance. At the same time, species like *P. deltoides* and *P. nigra* cv. Italica, with an amphistomatous leaf type, appear to be more environmentally flexible and occupy a much broader range, both in nature and in cultivation in Ukraine.

Conclusions

Leaves of Populus species are morphologically very similar and, therefore, it is quite difficult to identify them. It has been observed that *P. nigra* cv. Italica and *P. deltoides* exhibit an amphistomatous leaf type, while *P. trichocarpa* and *P. suaveolens* have a hypostomatous leaf type. The ultrastructural type is collicular in *P. suaveolens* and *P. trichocarpa*, while it is reticulate-complex in *P. nigra* cv. Italica and *P. deltoides*. The shape of cells on the adaxial surface is similar in *P. trichocarpa* and *P. nigra* cv. Italica. Periclinal walls of leaf cells in *P. nigra* cv. Italica, *P. suaveolens* and *P. deltoides* on the abaxial surface are granular, while in *P. trichocarpa* they are smooth. Trichomes are characteristic only for the veins of *P. trichocarpa* leaves on the abaxial surface, in the rest of the studied species, trichomes are absent on both leaf surfaces.

In all examined samples, except for *P. trichocarpa*, the epidermal cells of the adaxial surface of the leaf and, in the case of *P. nigra* cv. Italica and *P. deltoides*, the abaxial surface of the leaf, are of medium size. Medium-sized epidermal cells are characteristic of the adaxial surface of *P. trichocarpa*. Large epidermal cells are typical for *P. suaveolens* and *P. trichocarpa*.

The structural organization of elements, including number of cells, their sizes, number and arrangement of stomata and covering tissues of the leaves of *P. deltoides*, *P. nigra* cv. Italica, *P. suaveolens* and *P. trichocarpa*, helps identify these species based on morphometric features. It demonstrates their wide ecological plasticity and ability to adapt to various changing environmental conditions, including those encountered during introduction or cultivation.

References

Al Afas N., Marron N., Ceulemans R. 2007. Variability in *Populus* leaf anatomy and morphology in relation to canopy position, biomass production, and varietal taxon. Annals of Forest Science 64(5): 521–532. https://doi.org/10.1051/forest:2007029

Aneli N.A. 1975. Atlas of leaf epidermis. Mecniereba publishing house, Tbilisi. 109 p. (in Georgian).

Barthlott W., Neinhuis C., Cutler D., Ditsch F., Meusel I., Theisen I., Wilhelmi H. 1998. Classification and terminology of plant epicuticular waxes. Botanical Journal of the Linnean Society 126(3): 237–260.

Barthlott W., Wollenweber E. 1981. Zur Feinstruktur, Chemie und taxonomischen Signifikanz epicuticularer Wachse und ähnlicher Sekrete. Tropische und Subtropische Pflanzenwelt 32. 67 p.

Brailko V.A. 2014. Characteristics of leaf anatomy in some species genus *Lonicera* L., cultivated in the Southern Coast

of Crimea. Plant Introduction 3: 61–65 (in Ukrainian).

Carolin R.C. 1980. Pattern of seed surface of *Goodenia* and related genera. Australian Journal of Botany 28(1): 123–137. https://doi.org/10.1071/BT9800123

Chakrabarty C., Mukherjee P.K. 1986. Studies on *Bupleurum* L. (Umbelliferae) in India II. SEM observations of leaf surfaces. Feddes Repert 97(7–8): 489–496.

Chen J.-H., Sun H., Yang Y.-P. 2008. Comparative morphology of leaf epidermis of *Salix* (Salicaceae) with special emphasis on sections Lindleyanae and Retusae. The Linnean Society of London, Botanical Journal of the Linnean Society 157(2): 311–322. https://doi.org/10.1111/j.1095-8339.2008.00809.x

Chuan Q. 2010. Comparison of photosynthetic characteristics and leaf anatomy structure of different ploidy *Populus ussuriensis* Kom. Plant Physiology Communications 46(9): 917–922. https://api.semanticscholar.org/CorpusID:87072039

Ghahremaninejad F., Khalili Z., Maassoumi A.A., Mirzaie-Nodoushan H., Riahi M. 2012. Leaf epidermal features of *Salix* species (Salicaceae) and their systematic significance. American Journal of Botany 99(4): 769–777. http://www.jstor.org/stable/41415617

Gorlacheva Z.S. 2010. Anatomic-morphological leaf of different *Monarda* × *hybrida* Hort. Industrial Botany. Collection of Scientific Work 10: 148–151 (in Ukrainian).

Ishchuk L.P. 2016. The effect of drought resistance on the chorology of species of the genus *Salix* in Ukraine. Autochthonous and introduced plants 12: 81–85 (in Ukrainian).

Ishchuk L.P. 2017. Water-holding capacity of leaves of species of the genus *Salix* L. Formation of Urban Geen Areas 1(14): 93–98 (in Lithuanian).

Ishchuk L.P. 2019. *Salicaceae* Mirbel. family: biology, adaptation potential, conservation and use in Ukraine. Thesis for the degree of Doctor of Biological Sciences in the specialty 03.00.05 Botany. Botanical Garden after M.M. Gryshkj of NAS of Ukraine, Kyiv. 47 p. (in Ukrainian).

Ishchuk L.P., Ishchuk H.P. 2018. Study of the content of pigments in the leaves of some species and cultivars of the genus *Salix* L. Paper presented at the Proceedings of the International scientific and practical conference dedicated to the 100th anniversary of the National Academy of Sciences of Ukraine, 9–11 October, Kyiv, Ukraine: 200–201 (in Ukrainian).

Ishchuk L.P., Ishchuk H.P. 2019. Drought resistance of species of the genus *Salix* L. Paper presented at the Proceedings of the International scientific conference dedicated to the 90th anniversary of the birth of the member of the Cor. NAS of Ukraine, professor Tetiana Mykhailivna Cherevchenko DSc, 25–27 February, Kyiv, Ukraine: 216–218 (in Ukrainian).

Ishchuk L.P., Ishchuk H.P. 2020. Analysis of the pigment apparatus of leaves of some species and cultivars of the family Salicaceae Mirb. in connection with air pollution in Bila Tserkva. Environmental Sciences 32(5): 91–95 (in Ukrainian).

Ishchuk L.P., Krupa N.M., Priadkina G.O. 2018. Characterization of pigment apparatus in leaves of Salicaceae Mirbel species. Ukrainian Journal of Ecology 8(1): 426–431 (in Ukrainian). doi: 10.15421/2018_231

Juniper B.E. 1959. The surface of plants. Endeavour 18(69): 20–25.

Lin X.Y., Wang X.X., Zeng Q.Y., Yang Q. 2022. Leaf structure and photosynthesis in *Populus alba* under naturally fluctuating environments. Photosynthetica 60(2): 240–250. doi: 10.32615/ps.2022.012

Liu J.-H., Liu X.-S., Jin H., Huang P., Fu X.-X., Fang S.-Z., Tian Y. 2018. Leaf angle change and anatomical structure of *Populus deltoides*, *P. cathayana* and their hybrid F1[J]. Journal of Beijing Forestry University 40(2): 11–21. doi: 10.13332/j.1000-1522.20170317

Lu M., Chen M., Song J., Wang Y., Pan Y., Wang Ch., Pang J., Fan J., Zhang Y. 2019. Anatomy and transcriptome analysis in leaves revealed how nitrogen (N) availability influence drought acclimation of *Populus*. Trees 33: 1003–1014. https://doi.

org/10.1007/s00468-019-01834-5

Metcalfe C.R., Chalk L. 1950. Anatomy of the dicotyledons. Oxford, University Press 1–2. 1500 p.

Mytyna L.V. 2007. Features of the structure of the epidermis of leaves of *Berberis vulgaris* L. in different regions of Ukraine. Industrial Botany 7: 226–229 (in Ukrainian).

Redko H.I. 1966. Dendrological characteristics of poplars cultivated in Ukraine. Kyiv. 74 p. (in Ukrainian).

Russin W.A., Evert R.F. 1984, Studies on the leaf of *Populus deltoides* (Salicaceae): morphology and anatomy. American Journal of Botany 71(10): 1398–1415. https://doi.org/10.1002/j.1537-2197.1984.tb11997.x

Shetler S.G., Morin N.R. 1986. Seed morphology in North American *Campanulaceae*. Annals of the Missouri Botanical Garden 73(4): 653–688. doi: 10.2307/2399199

Stern W.L., Morris M.W. 1992. Vegetative anatomy of *Stanhopea* (Orchidaceae) with special reference to pseudobulb water-storage cells. Lindleyana 7(1): 34–53.

Su H., Li Y., Lan Z., Xu H., Wang B., Biswas D.K., Jiang G. 2009. Leaf-level plasticity of *Salix gordejevii* in fixed dunes compared with lowlands in Hunshandake Sandland, North China. Journal of Plant Research 122: 611–622. https://doi.org/10.1007/s10265-009-0249-1

FORESTRY IDEAS, 2024, vol. 30, No 1 (67): 173–182

Assessment of aboveground litterfall under the beech forest canopy in Vitinya permanent sample plot

Kameliya Petrova

Faculty of Forestry, University of Forestry, 10 Kliment Ohridski Blvd., 1797 Sofia, Bulgaria.
E-mail: kpetrova@ltu.bg

Received: 12 March 2024 / Accepted: 07 May 2024 / Available online: 14 May 2024

Open Access: This article is licensed under a Creative Commons Attribution 4.0 International License.

Abstract

Aboveground litterfall plays a key role in carbon and nutrient cycling in forest ecosystems. In this study, data are obtained about basic aboveground litterfall parameters and quantity of common beech (*Fagus sylvatica* L.) in Vitinya permanent sample plot for intensive monitoring. The litterfall was sampled and assessed in three individual fractions – foliar fraction (*F*), wood fraction (*W*) and fruits and seeds fraction (*FS*). It was established that annual total biomass of aboveground litterfall varies in wide range from 390 up to 787 $g \cdot m^{-2}$. The most dynamic fluctuations in the quantity are found in the *F* fraction of total biomass that falls annually on the soil surface. For 2022, the average amount of *F* fraction was 363 $g \cdot m^{-2}$, which represents 59 % of the total biomass of litterfall. The reaction of litterfall in the studied fractions for the observed period remains in the acidic spectrum. In the individual fraction's concentrations of basic cations, such as calcium and magnesium, are assessed as low. The obtained data show increasing trend of trace elements, such as iron, manganese, copper, and cadmium in *F* fraction. Very high concentrations of manganese and cadmium were found in all fractions of the aboveground litterfall. For manganese the average value in *F* fraction was 4373 $\mu g \cdot g^{-1}$ and for cadmium in *FS* fraction – 388 $ng \cdot g^{-1}$. Both obtained concentrations exceed the upper limit of these elements specified in the ICP Forests Manual for common beech litterfall fractions.

Key words: beech litterfall, intensive monitoring, litterfall fractions, litterfall pH, nutrients, trace elements.

Introduction

Litterfall is a key parameter linking trees to water transfer and soils in the biogeochemical cycle of terrestrial ecosystems (Pitman 2013, ICP Forests Manual 2020). The aboveground litterfall introduces most of soil organic carbon content into the soil (Sayer 2006), which allows forecasting the retention of org. C in the soils (Liski et al. 2005). According to Schleppi et al. (2007), the total mass and chemical composition of the litterfall are important for assessing the nutrients in forest soils. The magnitude of litterfall production is a crucial estimate for predicting the terrestrial carbon budget (Li et al. 2019).

Litterfall in forest ecosystems is the most important resource of soil organic matter and soil nutrients (Gairola et al.

2009) and therefore its quantity maintains the soil fertility (Meier et al. 2005, Zhang et al. 2014). It is estimated that in forests, litterfall can introduce approximately 18 Pg C per year to the soil surface. That amount of org. C is about one-third of the annual C uptake (Zhao and Running 2010, Malhi et al. 2011). The quality and quantity of litterfall production in temperate forests significantly affect the carbon and nutrient cycling (Xu et al. 2004, Roig et al. 2005, Neumann et al. 2018). Litter decomposition rate can determine the amount of organic matter input to forest soils (Vesterdal et al. 2008). In addition, soil's physical and chemical properties, microbial activity and diversity of soil microorganisms are directly and indirectly influenced by the litterfall (Wang et al. 2008, Farooq et al. 2022).

Long-term observations on aboveground litterfall can help to understand its impact on different ecosystem processes and how forest tree species are adapting to these changes. (Bhatti and Jassal 2014). The annual quantification of the different litter fractions can indicate the stand reaction to short and long-term weather fluxes (Broadmeadow 2002). Assessing aboveground litterfall and its basic parameters can help in modelling and predicting terrestrial ecosystem dynamics (Liski et al. 2005). It is important to note that for deciduous species, litterfall collection throughout one year and sorting it is probably the most accurate way of measuring total leaf area produced (Bréda 2003).

One of the world's largest biomonitoring networks, which provide information on forest condition, air pollution, climate change and biodiversity over the last 30 years, is International Co-operative Programme on Assessment and Monitoring of Air Pollution Effects on Forests (also known as ICP Forests). The observations of forest conditions are carried out on 2 levels. Level I (large-scale representative monitoring on a systematic network) aim to provide a periodic overview of the spatial and temporal variation of forest condition in relation to anthropogenic and natural stress factors (in particular air pollution). Level II (intensive monitoring on a number of selected permanent observation plots) aim to gain a better understanding of the cause-effect relationships between the condition of forest ecosystems and anthropogenic, as well as natural stress factors (in particular air pollution).

In Bulgaria, as part of the European Forest Ecosystem Monitoring Network, the parameters of aboveground litterfall and soil solution sampled by tension lysimeters are measured at 3 permanent sample plots (Level II) for intensive monitoring – 'Vitinya', 'Yundola' and 'Staro Oryahovo' (Kolarov et al. 1999–2002, Malinova et al. 2003). The surveys on intensive monitoring in the country until 2019 are carried out in accordance with instructions of ICP Forests (1986–2016). Since 2020 update in Part XIII Sampling and Analysis of Litterfall, new rules are applied in assessing the aboveground litterfall (ICP Forests Manual 2020).

The aim of the study is to quantify aboveground litterfall production by fractions and its chemical composition in Vitinya permanent sample plot for intensive monitoring of common beech (*Fagus sylvatica* L.) forest ecosystems. The basic parameters of litterfall and their annual dynamics were observed and assessed for the period 2011–2022.

Subject and Method

Vitinya permanent sample plot is set in the Western Balkan Range, on the terri-

tory of Vitinya State Hunting Enterprise (42°46'12" N and 23°45'36" E). The permanent sample plot is located in the middle mountain subarea (Koleva-Lizama 2002), which is characterized by a mountain climate.

It was selected as representative for the common beech forests in Bulgaria (Kolarov et al. 2002) at an altitude 1145 m a.s.l. The soil is developed on metamorphic bedrock – gneiss. It is well-known fact that gneiss tends to lead to acidic, poorly developed soils and the soil unit in Vitinya permanent sample plot area is classified as *Dystric* Cambisols.

Aboveground litterfall was collected in 5 traps, set under the beech forest canopy, each with an area of 1 m^2. The biomass in the litterfall traps was collected every two weeks. The litterfall was sorted into three different fractions – foliar fraction (*F*), wood fraction (W) composed of bark, branches and twigs and fruits and seeds fraction (*FS*).

Sampling and laboratory analyses of the observed parameters were carried out by the Executive Agency for the Environment at the Bulgarian Ministry of Environment and Waters. The survey of aboveground litterfall is carried out in connection with the implementation of 'The International Co-operative Programme on Assessment and Monitoring of Air Pollution Effects on Forests under the Convention on Long-range Transboundary Air Pollution of the United Nations Economic Commission for Europe' (Level II).

The obtained data in Vitinya permanent sample plot are compared to the indicated minimum and maximum values for the different parameters of litterfall according to ICP Forests Manual (2020).

Results and Discussion

The aboveground litterfall in the forest ecosystems is composed mainly of different amounts of foliage, branches, bark and reproductive organs. Usually, foliage litterfall occupies a major fraction of total litterfall (Liu et al. 2003). In Vitinya permanent sample plot for intensive monitoring of *Fagus sylvatica* ecosystem the total mass of aboveground litterfall has been observed for the period 2011–2022 (Fig. 1). The re-

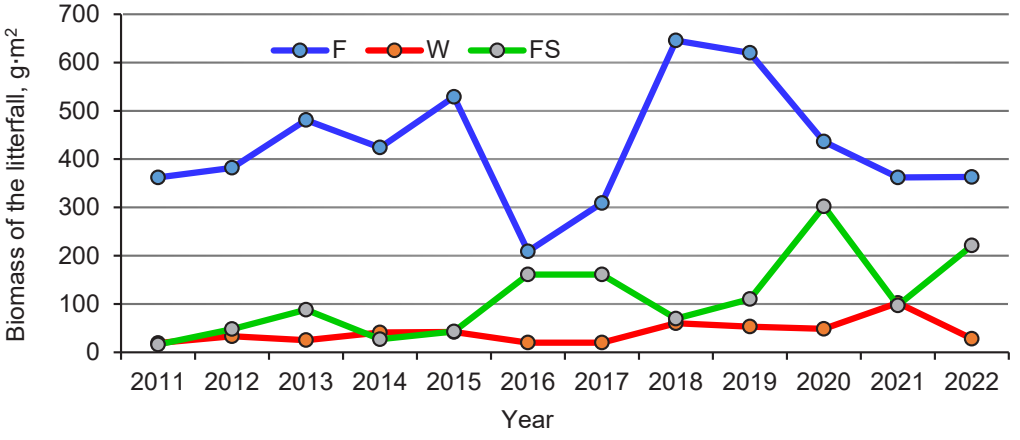


Fig. 1. Biomass of the aboveground litterfall by fractions for the period 2011–2022.
Note: *F* – foliar fraction, *W* – wood fraction, *FS* – fruits and seeds.

sults showed that annual total biomass of aboveground litterfall varies widely between 390 and 787 g·m^{-2}. The quantity of the individual aboveground litterfall fractions determines the annual dynamics of the total biomass.

In Vitinya permanent sample plot the annual foliar fraction of the aboveground litterfall comprised 54–91 % of the total biomass of the litterfall. This considerable variation in the percentage content of the foliar fraction of the total amount of litterfall could be explained by microclimatic conditions in the stand. Park et al. (2020) pointed out a narrower range of variation in deciduous stands for foliar fraction, which comprised 60 % up to 69 % of the total litterfall, while Petritan et al. (2020) reported that 66 % of the litterfall was composed of beech leaves. Fruit and seeds fraction (*FS*) also varies considerably between 4 % and 41 % of the total biomass of the litterfall that fall into the litter traps every year. The amount of wood fraction (*W*) varies within narrower limits (4–18 %) depending on the season and was the least abundant in the litterfall. The maxima of aboveground litterfall for the deciduous trees varies in wide range according to tree species from early fall to early winter. For *Fagus sylvatica* the main peaks are due to leaf fall and usually occur in October or November (Bou et al. 2015). In 2022, for Vitinya permanent sample plot the maximum of total biomass of litterfall and foliar fraction was recorded within 1 month. It was in October, in contrast to the previous two years, when the maximum was recorded in November. Fractions *W* and *FS* are traditionally poorly represented in the total biomass of the litterfall. Regarding their distribution by months, these fractions have more significant amounts in the late spring and autumn.

The data show that wood fraction was in high amounts at the beginning of the vegetation season – April and in the end – September. The largest amount of fruits and seeds fraction was established in September–October.

Table 1 presents the chemical characteristics of the aboveground litterfall by fractions in 2022.

The data in Table 1 show that pH_{H2O} by fractions for 2022 remain in strongly acidic spectrum. In general, it should be noted that the pH values indicate stability (Fig. 2) over time. The pH of *F* fraction changes very slightly. For this fraction, similar values were obtained in 2022 but lower than in the previous years. The reaction is more acidic compared to the one in 2021. The same applies to the *FS* fraction. In 2019, the lowest pH values for *FS* fraction were obtained, but it should be considered as random event. For *W*, the values are higher compared to 2021. For this fraction, high average values were obtained in 2016 and 2017, which can be accepted as accidental.

The reaction of the *FS* fraction showed a wider range of variation but is in the acidic spectrum throughout the observed period.

In 2022, the nitrogen content in the *F* fraction is assessed as low and close to the minimum values specified in the ICP Forests Manual (2020) for common beech litterfall (Table 1). For the period 2011–2022, it varies within the limits of the minimum and maximum values specified in manual and this is an indicator of good nitrogen uptake. The same applies to the amount of sulphur, which are low in all three fractions.

The nitrogen content of the aboveground litterfall for 2022 was assessed as average – it was in the range between the lower and upper limits specified in the manual for common beech lit-

Table 1. Concentrations of macronutrients and trace elements in aboveground litterfall from Vitinya permanent sample plot – 2022.

Litter traps No	Fraction	pH_{H2O}	Org. C, g per 100g	N	S	P	Ca	Mg	K	Zn	Mn	Fe	Cu	Pb	Cd
				mg·g^{-1}						µg·g^{-1}					ng·g^{-1}
1	Foliar fraction	5.1	52.6	9.3	0.8	0.4	7.3	0.9	6.0	47	4643	200	9.4	1.6	<30
2		5.0	52.0	10.0	0.8	0.5	4.0	1.0	6.4	26	4143	207	10.8	1.6	215
3		5.1	52.2	9.3	0.8	0.5	4.0	0.9	5.4	27	4087	172	10.8	1.4	219
4		5.1	54.2	9.7	1.2	0.5	4.3	1.1	5.8	35	4574	198	10.8	1.4	215
5		5.0	51.9	10.4	1.0	0.6	4.2	1.0	4.7	38	4419	229	10.1	1.7	216
Mean		**5.1**	**52.6**	**9.8**	**0.9**	**0.5**	**4.7**	**1.0**	**5.6**	**35**	**4373**	**201**	**10.4**	**1.6**	**216**
St. dev.		0.1	1.0	0.5	0.2	0.1	1.4	0.1	0.6	9	250	20	0.7	0.1	1.8
1	Wood fraction	5.5	53.5	13.8	0.9	1.2	<3.0	0.9	8.8	2	1413	91	16.7	10.5	106
2		5.4	53.1	8.9	0.9	0.9	<3.0	0.7	8.1	8	1204	95	10.7	0.7	108
3		5.6	53.6	12.4	0.8	1.0	<3.0	1.0	8.4	20	1564	106	13.8	1.3	108
4		5.5	55.2	13.7	0.9	1.3	<3.0	1.1	9.0	23	1644	121	13.9	0.6	107
5		5.3	52.7	9.2	0.8	0.9	<3.0	0.7	8.4	14	1251	104	10.7	0.8	108
Mean		**5.5**	**53.6**	**11.6**	**0.9**	**1.1**		**0.9**	**8.5**	**13**	**1415**	**103**	**13.1**	**2.8**	**107**
St. dev.		0.1	0.9	2.4	0.0	0.2		0.2	0.4	9	191	12	2.5	4.3	0.8
1	Fruits and seeds fraction	5.2	55.3	6.1	0.8	0.2	7.2	0.4	2.1	60	1288	120	15.3	4.3	321
2		5.3	54.5	9.1	0.8	0.5	9.6	0.5	1.9	62	1661	218	20.7	6.5	432
3		5.3	54.3	8.7	0.8	0.5	7.0	0.4	1.8	40	1207	165	16.6	5.4	324
4		5.2	54.3	8.4	1.2	0.5	9.2	0.5	1.9	59	1375	195	18.5	7.7	432
5		5.2	55.5	7.8	0.9	0.3	8.0	0.4	1.5	111	1307	252	18.1	6.3	429
Mean		**5.2**	**54.8**	**8.0**	**0.9**	**0.4**	**8.2**	**0.4**	**1.8**	**66**	**1367**	**190**	**17.9**	**6.0**	**388**
St. dev.		0.1	0.6	1.2	0.2	0.1	1.1	0.1	0.2	26	174	51	2.0	1.3	59

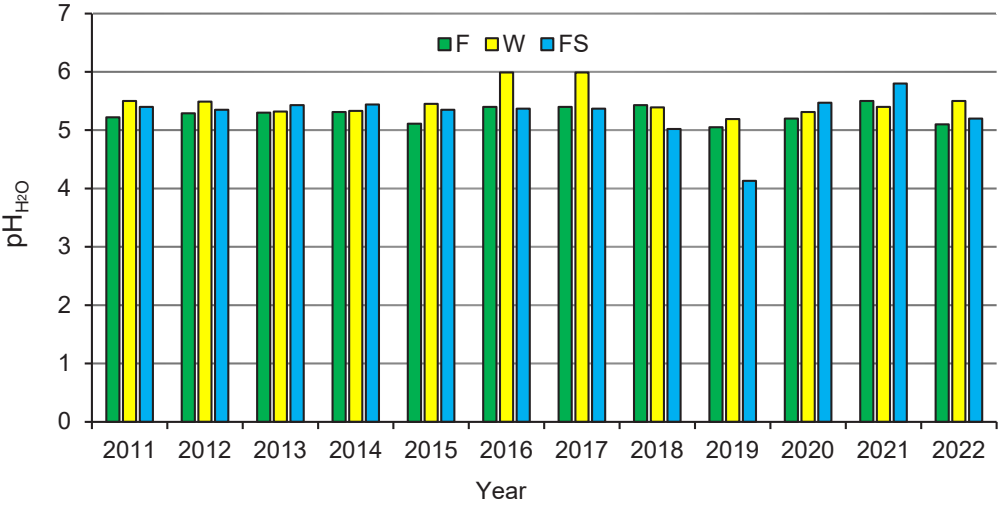


Fig. 2. Reaction (pH_{H2O}) of the aboveground litterfall fractions for the period of 2011–2022.
Note: *F* – foliar fraction, *W* – wood fraction, *FS* – fruits and seeds.

terfall (Table 1). Its quantity differs in the individual fractions throughout the study period (Fig. 3). It should be noted that most significantly total nitrogen differs in *FS* fraction, followed by *F* fraction and most stable it is in *W*.

The mean org. C/N ratio also differed in wide range in the studied fractions. The highest mean value was obtained in *W* – 70, which corresponds to the slow decomposition of organic matter. It was also high in fraction *F* – 52. FS fraction was with the fastest decomposition rate – org. C/N = 48.

Due to increased air pollution in the late 20th century, the sulphur concentra-

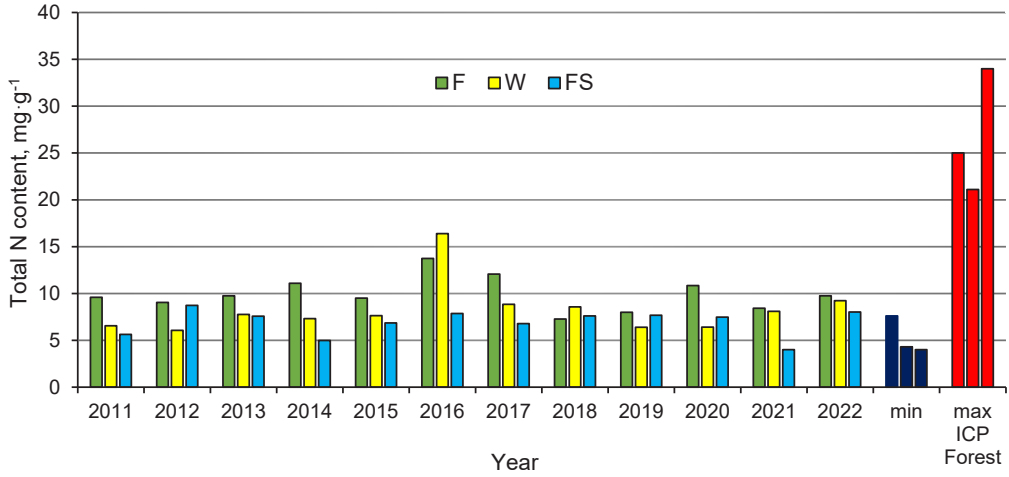


Fig. 3. Total nitrogen content in aboveground litterfall fractions for the period of 2011–2022 and ICP Forests criteria.
Note: *F* – foliar fraction, *W* – wood fraction, *FS* – fruits and seeds.

tions in deciduous litterfall are monitored in the forest monitoring system.

According to several authors (Koptsik et al. 1998, Michel and Seidling 2017), the high concentrations of sulphur in the litterfall are associated with more intensive acidic atmospheric depositions.

The obtained data showed that the sulphur concentration in the aboveground litterfall from Vitinya permanent sample plot for the observed period was between the minimum and maximum limits (Fig. 4). A decreasing trend of sulphur concentrations in *F* fraction is observed since 2011. The obtained data for 2022 (Table 1) shows that sulphur concentrations are low and very close to the minimum concentrations specified in the ICP Forests Manual (2020).

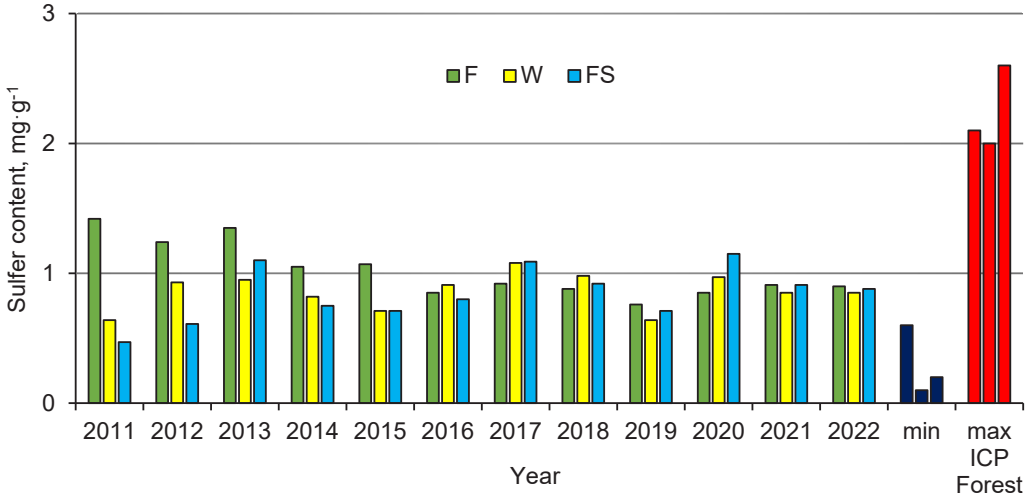


Fig. 4. Sulphur concentration in aboveground litterfall fractions for the period of 2011–2022 and ICP Forests criteria.

Note: *F* – foliar fraction, *W* – wood fraction, *FS* – fruits and seeds.

The quantity of macronutrients in litterfall play a crucial role in their re-entry on the soil surface. The content of phosphorus and calcium in *F* fraction is low, as in the previous 3 years, with values close to the minimum. They vary slightly around the lower limit for these elements. In *W*, phosphorus and calcium are even in lower concentrations – for phosphorus they vary around 1.0, and for calcium – below the limit of determination of the method (less than 3.0 $mg \cdot g^{-1}$). The results obtained in 2022 confirm that calcium shows a clear tendency to accumulate in the *FS* fraction. In all studied fractions the concentrations of magnesium are assessed as low. It should be noted that potassium concentrations vary widely from low to high. The low amounts of the main macro elements, such as calcium and magnesium in the litterfall is a prerequisite for low amounts in the mineral part of the soil as well. That can lead to more intensive process of soil impoverishment.

As for the trace elements, such as iron, manganese, copper and cadmium, the negative trend from previous years is maintained - their concentrations have increased in the *F* fraction. This is most pronounced for the more mobile elements,

especially for manganese, which has very high values in *F* fraction, exceeding the maximum values. The concentration of cadmium in the *F* and *W* fractions is very high. The accumulation of cadmium in the *FS* fraction exceeds the indicated upper limit of concentration for this element. Copper concentrations are high in *F* and *W* fractions. It should be noted that *FS* fraction accumulates very high concentrations of copper and lead. Their values are close to the maximum specified in ICP Forests Manual (2020). The accumulation of trace elements in *W* and *FS* fractions of the beech litterfall indicates their increased concentration and mobility in the soil solution, as well.

Conclusions

In 2022, the reaction of the aboveground litterfall in the individual fractions remain in the acidic spectrum. For the observed period it should be noted that the concentrations of phosphorus and calcium remain low. Higher uptake and accumulation of trace elements with acidic functions in the aboveground litterfall and the higher acidity obtained in all fractions indicate ongoing acidification process of the soil solution and vice versa. The decreasing trend of sulphur concentrations in foliar fraction continues. More concern are the higher concentrations of manganese in *F* fraction and cadmium in *FS* fraction, which exceeds the maximum values specified in the ICP Forests Manual (2020). To determine whether there is a contamination with these heavy metals, their concentrations must also be traced in the soil depth.

Acknowledgements

The study was supported by the Bulgarian Executive Environment Agency – Ministry of Environment and Waters.

References

Bhatti J.S., Jassal R.S. 2014. Long Term Aboveground Litterfall Production in Boreal Jack Pine (*Pinus banksiana*) and Black Spruce (*Picea mariana*) Stands along the Boreal Forest Transect Case Study in Western Central Canada. Ecoscience 21(3–4): 301–314. https://doi.org/10.2980/21-(3-4)-3699

Bou J., Caritat A., Vilar L. 2015. Litterfall and growth dynamics relationship with the meteorological variability in three forests in the Montseny natural park. Folia Forestalia Polonica. Series A 57(3): 145–159. https://doi.org/10.1515/ffp-2015-0015

Bréda N.J.J. 2003. Ground-based measurements of leaf area index: a review of methods, instruments and current controversies. Journal of Experimental Botany 54(392): 2403–2417. https://doi.org/10.1093/jxb/erg263

Broadmeadow M.S.J. 2002. Climate change: impacts on UK forests. In: Forestry Commission Bulletin, vol. 125. Forestry Commission, Edinburgh. 31 p.

Farooq T.H., Li Z., Yan W., Shakoor A., Kumar U., Shabbir R., Peng Y., Gayathiri E., Alotaibi S.S., Wróbel J., Kalaji H.M., Chen X. 2022. Variations in litterfall dynamics, C:N:P stoichiometry and associated nutrient return in pure and mixed stands of camphor tree and Masson pine forests. Frontiers in Environmental Science 10, 903039. 10 p. https://doi.org/10.3389/fenvs.2022.903039

Gairola S., Rawal R.S., Dhar U. 2009. Patterns of litterfall and return of nutri-

ents across anthropogenic disturbance gradients in three subalpine forests of west Himalaya, India. Journal of Forestry Research 14(2): 73–80. https://doi.org/10.1007/s10310-008-0104-6

ICP Forests 1986–2016. The International Co-operative Programme on Assessment and Monitoring of Air Pollution Effects on Forests under the Convention on Long-range Transboundary Air Pollution of the United Nations Economic Commission for Europe. http://icp-forests.net/page/icp-forests-manual

ICP Forests Manual 2020. Sampling and Analysis of Litterfall. In: Manual on methods and criteria for harmonized sampling, assessment, monitoring and analysis of the effects of air pollution on forests. UNECE – CLRTAP. Part XIII Sampling and Analysis of Litterfall, Version 2020-1. 19 p. http://icp-forests.net/page/icp-forests-manual

Kolarov D., Pavlova E., Bezlova D., Pavlov D., Doncheva M., Nikolova M., Tsvetkova N., Malinova L., Bencheva S., Antonov L. 1999–2002. Bulgarian-Swiss project No 2 'Monitoring of forest ecosystems'. University of Forestry, project No 615. 210 p. (in Bulgarian).

Kolarov D., Pavlova E., Pavlov D., Malinova L., Doncheva M., Bencheva S. 2002. Intensive monitoring of forest ecosystems in Bulgaria. Publishing House of the University of Forestry. 160 p. (in Bulgarian).

Koleva-Lizama I. 2002. Meteorological parameters. In: Intensive monitoring of forest ecosystems in Bulgaria. Publishing House of the University of Forestry: 63–66 (in Bulgarian).

Koptsik G.N., Makarov M.I., Kiseleva V.V. 1998. Principles and methods of assessment of soil sustainability to atmospheric acid deposition. Moscow University Publishing House. 96 p. (in Russian).

Li S., Yuan W., Ciais P., Viovy N., Ito A., Jia B. R., Zhu D. 2019. Benchmark estimates for aboveground litterfall data derived from ecosystem models. Environmental Research Letters 14(8), 084020. https://doi.org/10.1088/1748-9326/ab2ee4

Liu C., Ilvesniemi H., Berg B., Kutsch W., Yang Y., Ma X., Westman C. 2003. Aboveground litterfall in Eurasian Forest. Journal of Forestry Research 14(1): 27–34. https://doi.org/10.1007/BF02856758

Liski J., Peltoniemi T., Sievanen M. 2005. Carbon and decomposition model Yasso for forest soils. Ecological Modeling 189(1–2): 168–182. https://doi.org/10.1016/j.ecolmodel.2005.03.005

Malhi Y., Doughty C., Galbraith D. 2011. The allocation of ecosystem net primary productivity in tropical forests. Philosophical Transactions of the Royal Society B (Biological Sciences) 366(1582): 3225–3245. https://doi.org/10.1098/rstb.2011.0062

Malinova L., Pavlova E., Pavlov D., Nikolova M., Doncheva M. 2003. Methodical guide for implementation of intensive monitoring of forest ecosystems in Bulgaria. Executive Agency for Environment – Ministry of Environment and Water. 98 p. (in Bulgarian).

Meier I.C., Leuschner C., Hertel D. 2005. Nutrient return with leaf litter fall in *Fagus sylvatica* forests across a soil fertility gradient. Plant Ecology 177: 99–112. https://doi.org/10.1007/s11258-005-2221-z

Michel A., Seidling W. 2017. Forest Condition in Europe: 2017. Technical Report of ICP Forests. Report under the UNECE Convention on Long-Range Transboundary Air Pollution (CLRTAP). BFW-Dokumentation 24/2017. Vienna: BFW Austrian Research Centre for Forests. 128 p.

Neumann M., Ukonmaanaho L., Johnson J., Benham S., Vesterdal L., Novotný R., Verstraeten A., Lundin L., Thimonier A., Michopoulos P., Hasenauer H. 2018. Quantifying carbon and nutrient input from litterfall in European forests using field observations and modeling. Global Biogeochemical Cycles 32(6): 784–798. https://doi. org/ 10. 1029/ 2017G B0058 25

Park B.B., Rahman A., Han S.H., Youn W.B., Hyun H.J., Hernandez J., An J.Y. 2020. Carbon and Nutrient Inputs by Litterfall in Evergreen and Deciduous Forests in Korea. Forests 11(2), 143. 15 p. https://doi.org/10.3390/f11020143

Petritan I.C., Mihăilă V.V., Bragă C.I., Boura M., Vasile D., Petritan A.M. 2020.

Litterfall production and leaf area index in a virgin European beech (*Fagus sylvatica* L.) – Silver fir (*Abies alba* Mill.) forest. Dendrobiology 83: 75–84. http://dx.doi.org/10.12657/denbio.083.008

Pitman R. 2013. Litterfall – Biomass, Chemistry, Leaf Area, and Links with Wider Ecosystem Functioning. Developments in Environmental Science 12: 251–264. http://dx.doi.org/10.1016/B978-0-08-098222-9.00014-5

Roig S., del Río M., Cañellas I., Montero G. 2005. Litter fall in Mediterranean *Pinus pinaster* Ait. stands under different thinning regimes. Forest Ecology and Management 206(1–3): 179–190. https://doi.org/10.1016/j.foreco.2004.10.068

Sayer G. 2006. Using experimental manipulation to assess the roles of leaflitter in functioning of forest ecosystems. Biological Reviews 81(1): 1–31. https://doi.org/10.1017/S1464793105006846

Schleppi P., Conedera M., Sedivy I., Thimonier A. 2007. Correcting non-linearity and slope effects in the estimation of the leaf area index of forests from hemispherical photographs. Agricultural and Forest Meteorology 144(3–4): 236–242. https://doi.org/10.1016/j.agrformet.2007.02.004

Vesterdal L., Schmidt I.K., Calleson I., Nilsson L.O., Gundersen P. 2008. Carbon and nitrogen in forest floor and mineral soil under six common European species. Forest Ecology and Management 255(1): 35–48. https://doi.org/10.1016/j.foreco.2007.08.015

Wang Q., Wang S., Huang Y. 2008. Comparisons of Litterfall, Litter Decomposition and Nutrient Return in a Monoculture *Cunninghamia Lanceolata* and a Mixed Stand in Southern China. Forest Ecology and Management 255(3–4): 1210–1218. https://doi.org/10.1016/j.foreco.2007.10.026

Xu X., Hirata E., Shibata H. 2004. Effect of typhoon disturbance on fine litterfall and related nutrient input in a subtropical forest on Okinawa Island, Japan. Basic Applied Ecology 5(3): 271–282. https://doi.org/10.1016/j.baae.2004.01.001

Zhao M., Running S.W. 2010. Drought-Induced Reduction in Global Terrestrial Net Primary Production from 2000 through 2009. Science 329(5994): 940–943. https://doi.org/10.1126/science.1192666

Zhang H., Yuan W., Dong W., Liu S. 2014. Seasonal patterns of litterfall in forest ecosystem worldwide. Ecological Complexity 20: 240–247. https://doi.org/10.1016/j.ecocom.2014.01.003

FORESTRY IDEAS, 2024, vol. 30, No 1 (67): 183–196

Record of root endophytic fungi associated with Pteridophytes from Gunung Tukung Gede Nature Reserve, Indonesia

Rida Oktorida Khastini[1,2*], Iing Dwi Lestari[1], Indah Juwita Sari[1], and Fajrin Indah Nurunnisa[1]

[1]Department of Biology Education, Faculty of Teacher Training and Education, Sultan Ageng Tirtayasa University, Serang 42117, Indonesia.
[2]Center of Excellence Local Food Innovation, Sultan Ageng Tirtayasa University, Serang 42124, Indonesia. E-mail: rida.khastini@untirta.ac.id

Received: 10 November 2023 / Accepted: 05 June 2024 / Available online: 11 June 2024

Open Access: This article is licensed under a Creative Commons Attribution 4.0 International License.

Abstract

The root endophytic fungi coexist in a mutualistic relationship within their host plants. This study aimed to analyse the complex relationships between these plants and their fungi, revealing insight into the abundance of microbial communities living in the root systems of distinct Pteridophyte species inside this protected environment in the Gunung Tukung Gede Nature Reserve, Indonesia, and explore the potential functional roles of these fungal communities in the ecosystem. The research was carried out between July 2022 and January 2023. The roots of Pteridophyta were sampled randomly from three stations. The environmental variables examined were temperature, soil pH, moisture, and light intensity. The fungi were isolated and cultured in the PDA medium, which could then be identified. There were eight genera of root endophytic fungi: *Aspergillus* sp., *Trichoderma* sp., *Phoma* sp., *Phialophora* sp., *Penicillium* sp., *Paecilomyces* sp., *Humicola* sp., and *Fusarium* sp. In the designated conservation zones, this mutualistic connection contributes to the preservation of ecosystem health and biodiversity by being essential to Pteridophyta's resilience and intake of nutrients.

Keywords: conservation zone, diversity, ecosystem, mutualistic.

Introduction

Pteridophytes are essential to the ecology and growth of terrestrial ecosystems. The plants are seedless taxa having a vascular system, megaphylls, and spore dissemination as their reproductive mechanism (Aros-Mualin et al. 2021). Particularly in areas with high humidity, like tropical rainforests, Pteridophytes are frequently seen in Indonesian woods. These ancient plants significantly impact biodiversity and ecological stability due to their unique reproductive strategies and widespread.

Gunung Tukung Gede Nature Reserve (GTGNR) is a forest area with an altitude

of 125–750 m with climate type A (tropical) and an average rainfall of ±2151 mm·yr^{-1} (Sunarti 2011). Many Pteridophyte plants are found in the area. Information on biodiversity in the ecosystem at GTGNR that has been inventoried, such as flora diversity, as in the research of Djarwaningsih (2011), who managed to find 167 species of plants and fauna diversity, including mammals, birds, and reptilians. Khastini et al. (2021) reported on the diversity of entomopathogenic fungi from this area, but information on the diversity of root endophytic fungi is still lacking.

Various symbiotic microorganisms, known as root endophytic fungi, have attracted increasing attention in recent years as one of the many variables affecting the health and adaptation of Pteridophytes. These fungi serve essential ecological functions within forest ecosystems and act as a source of germplasm with potential applications in food and medicine (Suraida et al. 2013). Root endophytic fungi can colonise plant root tissues but do not inhibit the growth and development of their host plants (Sun et al. 2022). They can increase the growth of their host plants by optimising the absorption of nutrients through the structures they form or by producing growth-regulating hormones (Khastini 2018). They can produce secondary metabolite compounds that can be isolated into antimicrobial compounds and kill or inhibit pathogens (Harahap et al. 2017). Root endophytic fungi live in the roots and have the potential to influence plant communities (Rillig et al. 2014). Sporophytes and gametophytes of Pteridophytes form symbiotic associations with them (Muthukumar and Prabha 2012). This mutualistic symbiosis is essential for plant establishment, survival, and health. The host plant obtains nutrients from the fungi and provides a carbon supply to them (Muthukumar et al. 2014). One of the advantages that fungal colonisation confers upon the host plant is the enzymatic degradation of organic nutrient sources in the soils and the subsequent transfer of the resulting products to plants. This is because root endophytic fungi are widely distributed in the rhizosphere or rhizoplane of plants growing in soils. They can increase drought tolerance resistance to soil pathogens, increase soil aggregate stability, and increase plant growth and yield so that it can be developed as a biological fertilizer (Watts et al 2023). Their role is quite important, so information on the diversity of microorganisms is needed.

Microhabitats play a critical role in creating the ecology of Pteridophyte communities in GTGNR. A complex interaction of variables, such as differences in the species mix of plants, the texture of the soil, and the presence of nearby flora, distinguishes these microenvironments. Pteridophytes flourish in these varied and dynamic environments, exhibiting extraordinary resilience and ecological value. Notably, they play a crucial role in preserving the stability of the ecosystem inside the reserve due to their capacity to reduce water loss, primarily through the activity of their sporophytes. Numerous adaptive traits have developed in these plants, including waxy cuticles on fronds that ward off water vapor, sensitive stomata that respond to variations in soil and air temperatures, and leaf water potentials that are influenced (Krieg and Chambers 2022). In contrast, gametophytes rely on their capacity to endure and recover from water fluctuation since they lack xylem, effective waxy cuticles, or stomata.

This study explores the variety of root endophytic fungi in Pteridophytes to uncover what is beneath the forest floor of

Gunung Tukung Gede Nature Reserve. It aims to analyse the complex relationships between these plants and their fungi, revealing insight into the abundance of microbial communities living in the root systems of distinct Pteridophyte species inside this protected environment. This study adds to the growing knowledge on plant-fungus interactions by concentrating on a particular and comparatively unexplored ecological niche of the Pteridophytes root endosphere in a biodiverse hotspot.

Object and Method

The object of the study

Root endophytic fungi were isolated from the Pteridophyta plant roots in GTGNR as illustrated in Figure 1. The sampling location was divided into three research stations, I and II in the eastern area while Station III was in the western area. It represents distinct conditions: open vegetation, closed vegetation, and near settlements condition. Samples were collected using random sampling in the plot. Plots were determined based on a plot size of 5×5 m.

Based on observation, Station I (Fig. 2A) is a typical open vegetation area, was dominated by *Pleocnemia irregularis* (C. Presl) Holttum with medium density. There are also three other species of Pterydophyta found in the station, e.g., *Davallia denticulate* (Burm. f.) Kuhn, *Cyclosorus terminans* (Wall. ex Hook.) Shing, *Christella* sp. The soil texture is loamy sand. *Gnetum gnemon* L. trees planted by residents surround this station but are not intertwined, so the Pteridophytes underneath get high sunlight.

Station II, with closed vegetation (Fig. 2B), is dominated by *Stenochlaena palustris* (Burm. f.) Bedd. plants with a high density. *Pleocnemia irregularis* (C. Presl) Holtt. and *Adiantum tenerum* Sw. are two other species found in this station. The soil texture is clayey loam. This station is surrounded by *Pterospermum javanicum* Jungh., which is intertwined so that the Pteridophyte below are blocked from sunlight.

Station III is located near residential areas (Fig. 2C) dominated by *Christella dentata* (Forssk.) Brownsey & Jermy plants with moderate density. The soil texture is sandy loam. This station is surrounded by *Shorea* sp. that is not intertwined so that the Pteridophytes underneath are blocked from sunlight.

Environmental factors

Environmental parameters such as temperature, relative humidity and light intensity at the sampling sites are measured and documented using Fluke 971 Temperature Humidity Meter and Digital Lux Meter Photometer Smart Sensor AS823. The environmental parameters can be viewed in Table 1.

The average temperature of the coldest month in the GTGNR is typically around 15 °C, while the average temperature of the hottest month is around 25 °C. The absolute minimum temperature recorded in the area is 10 °C, and the absolute maximum temperature is 30 °C. The average annual temperature is approximately 20 °C. Regarding precipitation, the average monthly precipitation varies throughout the year. The highest monthly average precipitation is typically around 300 mm, while the lowest monthly average precipitation is around 50 mm. The total annual precipitation is approximately 1500 mm.

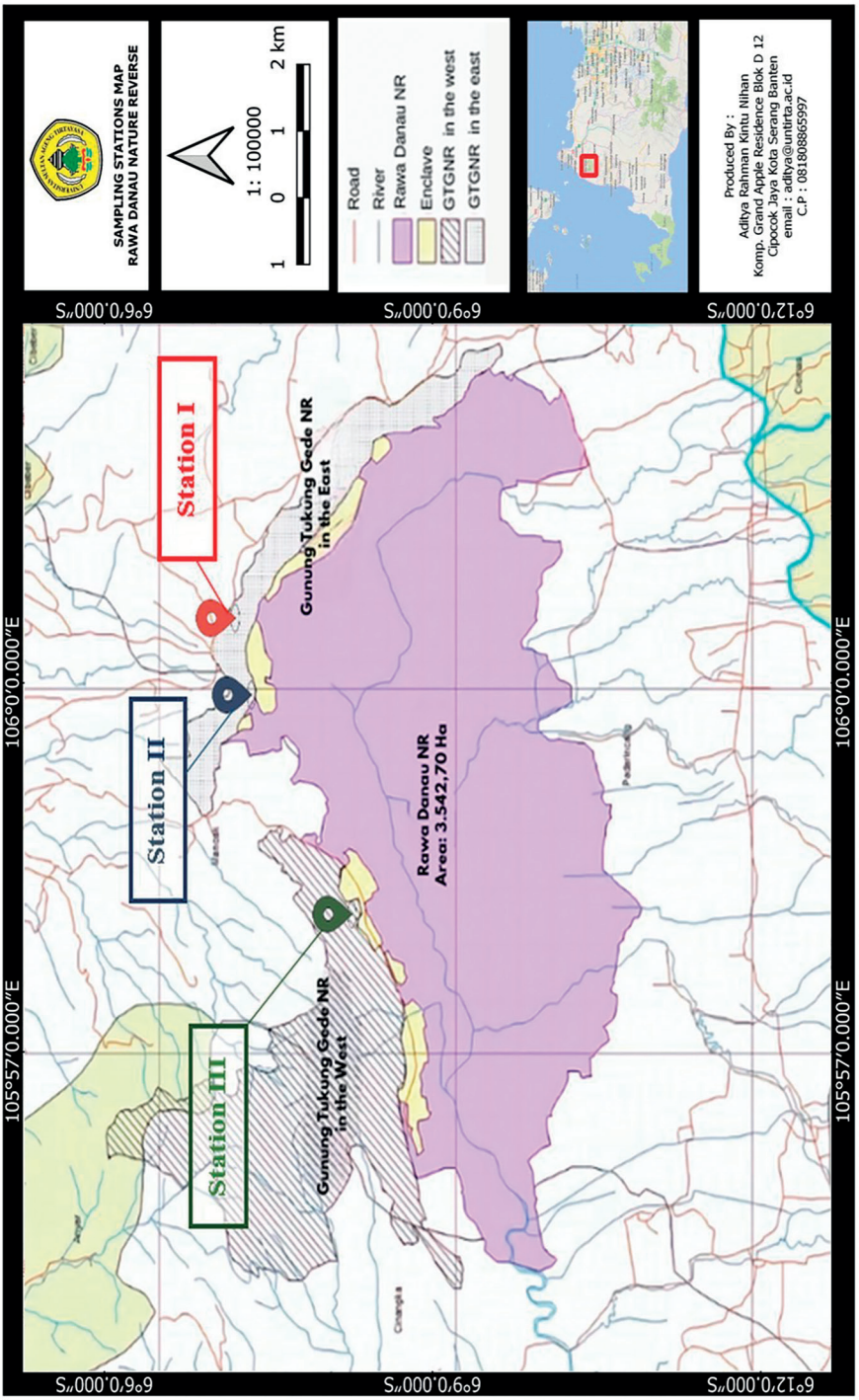


Fig. 1. Sampling location in the GTGNR.



Fig. 2. Sampling site condition: A – Station I, B – Station II, C – Station III.

Table 1. Condition of environmental factor of the sampling station.

Station	GPS coordinates	Temperature, °C	Relative humidity, %	Light intensity, lux	Soil type	Soil pH
I	6°8'17.16" S, 106°0'18.84" E	28	51	$809.6 \cdot 10^2$	Ultisol	3.94
II	6°8'8.22" S, 106°0'36.48" E	26	58	$10.6 \cdot 10^2$	Ultisol	3.92
III	6°8'38.4" S, 105°58'52.32" E	27	48	$29.8 \cdot 10^2$	Latosol	6

Isolation and colonisation process of root endophytic fungi in Pteridophyta plant

Isolation of root endophytic fungi was carried out using a modification of the surface sterilisation method of Khastini et al. (2022). About 30 root samples of Pteridophyte were collected in each of the stations. They were washed with tap water to remove debris and then cut into approximately 1 cm. The segment root samples were washed with 70% alcohol for 1 min, followed by a solution of NaOCl 0.1% for 15 min, and rinsed three times using sterile water using a vortex mixer. The sterile root segments were air-dried overnight and then planted into PDA, pH 6.0. If mycelia growth was observed on PDA, they were then transferred to a new PDA. Single spore isolation is commonly performed to obtain a pure culture of the fungal isolate.

The pure isolates obtained were observed for their morphological characteristics macroscopically and microscopically using a compound microscope (Leica DM500). Macroscopic observations were based on colony colour, colony dorsal colour, colony surface, fungal colony growth diameter, and concentric circles. Microscopic observations can be seen from the presence or absence of septa on hyphae, hyphal pigmentation, spore shape and ornamentation, and spore stalk shape and ornamentation (Khastini 2016). All isolates were identified based on their morphological characteristics (Barnett and Hunter 1998, Seifert and Gams 2011) as well as compared with well-identified living cultures from the collection of Biology Education Laboratory, UNTIRTA.

A methodical approach was used to investigate fungal growth within the root, followed Khastini et al. (2012). Pteridophyte's root system was carefully removed from the shoot. To get rid of any unnecessary items such as soil particles attached to it, it was first cleaned. After 20 min of clearing in 10% KOH at 80 °C, the roots were neutralised in 1% HCl for a further 20 min at the same temperature. The roots were dyed with a solution of 0.05% cotton blue in 50% acetic vinegar to aid in the visibility of fungal structures. To conduct further investigation, the roots were sectioned

by a freezing microtome to a thickness of 10–25 µm mounted in phenol glycerin jelly, carefully placed on slides and examined under a light microscope (Leica DM 2500) for microscopic details.

Result and Discussion

Isolation of root endophytic fungi associated with Pteridophyta plants

The results of the identification of root endophytic fungi obtained as many as 21 isolates with 8 different genera of root endophytic fungi, these are *Aspergillus*, *Trichoderma*, *Phoma*, *Phialophora*, *Penicillium*, *Paecilomyces*, *Humicola*, and *Fusarium* (Table 2).

The composition of root endophytic fungi identified at each research station varies. *Penicillium* sp. and *Paecilomyces* sp. fungi were only found at Station I. *Phialophora* sp. and *Phoma* sp. fungi were only found at Station II. *Humicola* sp., *Trichoderma* sp. and *Aspergillus niger* Tiegh. were only found at Station III. Some of these fungi were only found at one station, while others were at more than one. *Aspergillus oryzae* was found at stations I and II, and *Aspergillus fumigatus* Fresenius at stations I and III. The difference in

Table 2. Identification results of root endophytic fungi species in Pteridophytes.

Station	Species Pteridophytes	Local name	Identification of root endophytic fungi	Isolate code
I	*Pleocnemia irregularis*	Paku andam/ Paku kapal	*Aspergillus oryzae* (Ahlburg) E. Cohn	APi1
			Aspergillus fumigatus Fresenius.	APi2
			Paecilomyces sp.	APi3
			Fusarium sp.	APi4
	Davalia denticulate (Burm. f.) Kuhn	Paku tertutup	*Aspergillus oryzae*	ADd1
			Fusarium sp.	ADd2
	Cyclosorus terminans	-	*Penicillium* sp.	ACt1
	Christella sp.	-	*Aspergillus oryzae*	AC1
			Fusarium sp.	AC1
II	*Stenochlaena palusatris*	Paku kalakai	*Fusarium* sp.	BSp1
			Aspergillus oryzae	BSp2
			Phialophora sp.	BSp3
			Phoma sp.	BSp4
	Pleocnemia irregularis	Paku andam/ Paku kapal	*Fusarium* sp.	BPi1
	Adiantum tenerum	Paku suplir	*Fusarium* sp.	Bat1
III	*Christella dentata*	-	*Aspergillus niger* Tiegh.	CCd1
			Aspergillus fumigatus Fresenius	CCd2
	Christella sp.	-	*Trichoderma* sp.	CC1
	Lygodium scandens L. Sw.	Paku hata/Paku ribu-ribu	*Humicola* sp.	CLs1
	Pteris multifida Poir.	-	*Aspergillus niger*	CPm1

composition is due to differences in habitat and vegetation type. The noted variations in endophytic fungal composition are caused mainly by environmental variables. The interactions between soil fertility and the ecological environment shape endophytic fungal composition. According to studies by Min et al. (2016), this impact indirectly affects the structure and composition of the endophytic fungus population.

Environmental factors can influence differences in the composition of endophytic fungi. According to Table 2, Stations I and II have the highest number of isolates, but it is higher at Station I because it has a low pH of 3.94. Station III is stated to have low diversity in fungal isolates. The condition is due to two main factors, namely low humidity and high pH compared to other stations. Low humidity at Station III can affect the diversity of endophytic fungi that can grow in the area. Many fungi, including endophytic, have specific pH ranges within which they can grow optimally. When the pH level exceeds these optimal ranges, it can inhibit their growth, leading to a lower diversity and abundance of these species in the environment. This phenomenon is well-documented in Geisen et al. (2021), where it is observed that fungi with acidic growth preferences may be less abundant in environments with high pH levels.

Humid weather plays an important role in the growth of endophytic fungi. Its ability to facilitate the spread of fungal spores through rain splashes and wind affects the diversity of endophytic fungi that can grow. In addition, comparisons between Station III and other stations show that the low humidity and high pH at Station III contribute to the low diversity in the area. Manurung et al (2022) stated that humid weather influences the growth of endophytic fungi. Pteridophyte growth is significantly influenced by temperature. Different species of these plants thrive temperature ranges of 26–28 °C because they are susceptible to temperature changes. Most Pteridophytes grow better in moderate temperatures, while some can adapt to colder climates, while others perform better in warmer climates. Temperature has a crucial role in the growth and spread of Pteridophytes because it influences the rate of photosynthesis, the activity of enzymes, and the total metabolic activities.

The pH of the soil and its surroundings significantly affects the development of Pteridophytes. Different species have varying pH requirements, with many preferring slightly acidic to neutral soils. This preference is due to the enzymatic activities of Pteridophytes, which are often optimised under these pH conditions. For example, enzymes involved in nutrient uptake and metabolic processes are more active in slightly acidic to neutral soils, facilitating the growth and development of Pteridophytes (Mishra et al 2021). It can be seen that the pH levels at each research station varied, with Station I having a low pH of 3.94, which is likely to support a higher diversity of fungi due to its optimal pH conditions for the growth of the isolated endophytes. In contrast, Station III, which is stated to have low diversity on fungal isolates, may have a higher pH level of 6, making it less favourable for the growth of certain endophytic fungi. This observation aligns with the general understanding that pH plays a crucial role in determining the growth and dominance of these fungi.

One important aspect controlling the growth of Pteridophytes is light intensity. Although variety may not be directly impacted, it has a major impact on plant development, with Station I showing the highest plant growth due to its highest light intensity $809.6 \cdot 10^2$ lux. According to

Behera and Biswal (1990), the Pteridophyta plant is a shade plant, Pteridophyta responds to various light intensities in a somewhat complicated way. These plants can tolerate various lighting situations; however, many prefer shaded or partially shaded settings. Desiccation may result from exposure to too much light, whereas photosynthesis and general development may be hampered by inadequate light. Pteridophytes frequently flourish in the woodland understory, where plants get filtered or dappled sunlight.

Soil moisture levels significantly influence Pteridophyte development and dispersion. A somewhat regular range of soil moisture content is revealed by the soil moisture levels at stations I, II, and III, which vary from around 48 % to 58 %. Since they lack the drought-resistant characteristics in certain higher plants, most Pteridophytes depend on regular soil moisture to survive. The amount of water in the soil impacts the plant's capacity to absorb nutrients, exert turgor pressure, and stay well hydrated. For the growth of fern sporophytes, which depend on water to distribute their reproductive spores, adequate soil moisture is essential. It is supported by Qian et al. (2022) that the Pteridophytes cannot effectively manage transpiratory water loss.

The study's findings should be understood in the context of the complex interactions between pH, temperature, and other environmental factors that influence the growth and distribution of fungi in GTGNR. It is well recognised that environmental elements, including soil moisture, nutrient availability, and habitat heterogeneity, significantly impact fungal diversity in addition to pH and temperature. For instance, research conducted in cross coastal and inland Santa Barbara County, California by Mordecai et al. (2012) discovered that soil moisture significantly impacted the fungus population's makeup. Similarly, Naranjo-Ortiz and Gabaldón (2019) discovered that in a temperate forest environment, the availability of nutrients and habitat heterogeneity had a significant role in determining the makeup of the fungal population. In order to fully understand the study's conclusions, it is essential to consider the holistic interactions between pH, temperature, and other environmental variables. Comprehending these intricate interplays is crucial in clarifying the factors that influence the fungal composition of the reserve and influencing conservation and management tactics meant to maintain its fungal biodiversity. We may obtain a more comprehensive picture of the ecological processes influencing fungal communities in GTGNR by incorporating a variety of environmental characteristics into our research.

Among the isolated endophytic fungi, a variety of colony morphologies have been reported (Fig. 3), ranging from *Aspergillus*'s fluffy, cotton-like texture to *Penicillium*'s unique powdery look. Initial insights into the possible functional variety and ecological functions of the detected endophytic fungus linked with the Pteridophyte can be gained from these apparent differences in colony formation. The physical variations point to adaptations to different ecological niches and substrate preferences, which raises the possibility of a variety of roles these fungi may play in the endosphere of the plant.

The isolation of endophytic fungus from Pteridophyta plant roots has revealed an interesting variety, particularly the existence of three different species of *Aspergillus*, e.g *A. oryzae*, *A. niger*, *A. fumigatus* Fresenius (Fig. 3A-C). Comprehending the different characteristics of various *Aspergillus* species is crucial for

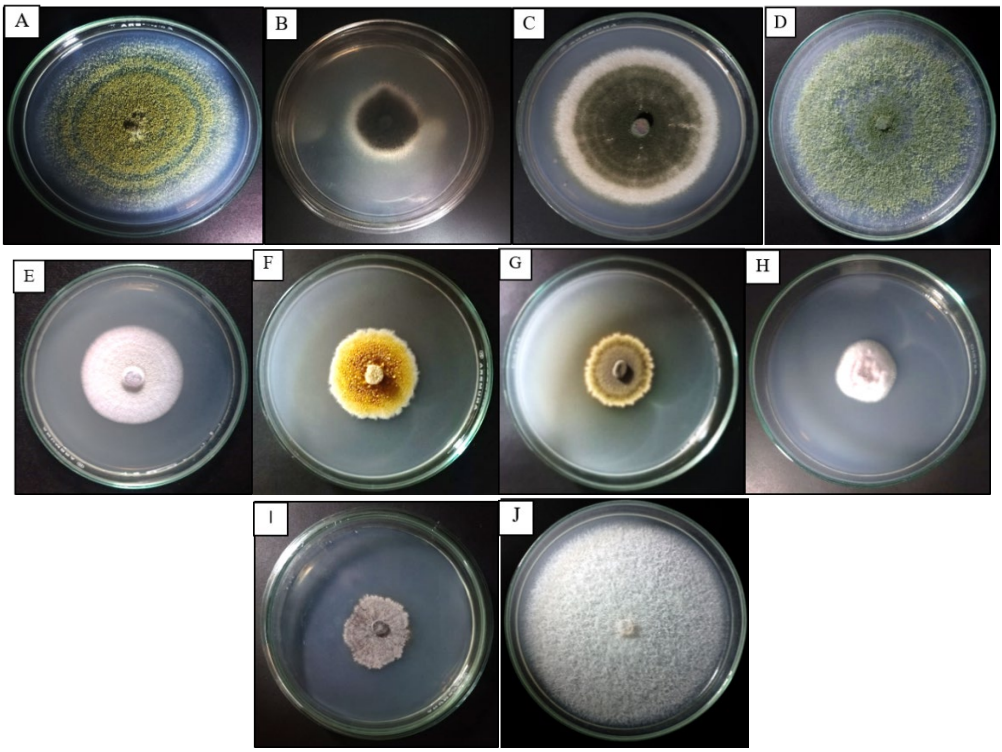


Fig. 3. Macroscopic picture of root endophytic fungi: A – *Aspergillus oryzae*, B – *A. niger*, C – *A. fumigatus*, D – *Trichoderma* sp., E – *Phoma* sp., F – *Paecilomyces* sp., G – *Penicillium* sp., H – *Phialophora* sp., I – *Humicola* sp., J – *Fusarium* sp.

the objective of biodiversity analysis and possible agricultural applications. *A. oryzae* is one strain of *Aspergillus* that has been shown to have beneficial impacts on plant growth and protection. This is consistent with the results of Wen et al. (2022), who found and effectively isolated *A. oryzae* from the *Paris polyphylla* Sm. rhizome in Dali. Furthermore, Galeano et al. (2021) revealed that the endophytic fungus *A. niger* 9-P showed activity associated with the development of plant growth-promoting (PGP) features when it was isolated from native fodder grass in the Pantanal of Nhecolândia area. Study conducted by Jiang et al. (2022) which revealed the presence of the endophytic fungus *A. fumigatus*, is another important addition in providing evidence of possible symbiotic connections.

As for the *Trichoderma* (Fig. 3D) the green colonies with a glanular surface, concentric circles, no exudate drops, and yellowish green colony back colour. These colonies grow rapidly, first white, and then greenish. According to Tseng et al. (2020), *Trichoderma* sp. endophytic strain enhances host growth and protects against pathogen attack. Our comprehensive research shows a noteworthy correlation between Pteridophyta plants and these fungi, adding to the growing information about endophytic fungi.

Furthermore, the complex relationship that exists between Pteridophyta plants and the fungal communities that are as-

sociated with them is strengthened by the presence of a variety of filamentous ascomycetes in the roots of these plants, such as *Paecilomyces* sp., *Penicillium* sp., *Phialophora* sp., *Humicola* sp., and different species of *Fusarium*. Tseng et al. (2020) highlight the dynamic character of interactions between fungal species and Pteridophyta plants, suggesting that the two may have a mutualistic connection. Nejad et al.'s (2022) finding of *Phoma* sp. in vascular tissue adds to our knowledge by illuminating other connections between *Phoma* and Pteridophyta species.

All of these study results make a substantial contribution to understanding the intricate connections that exist between endophytic fungus and Pteridophyta plants. There are developing practical uses for this information, which goes beyond taxonomic considerations. As Musa et al. (2023) have shown, *Paecilomyces lilacinus*, for example, may reduce heavy metal stress, giving host plants a useful benefit in harsh environmental settings. According to Toghueo and Boyom (2020), endophytic *Penicillium* sp. is highly adaptable, as evidenced by its capacity to flourish in a various ecological niche and protect host plants from a range of stressors. Furthermore, as shown by Almeida et al. (2020), ecological activities of *Phialophora* sp. are increased by its potential as a bio-control agent against fungi linked to plant illnesses. Together, these many discoveries deepen our comprehension of the complex.

Colonisation process of root endophytic fungi associated with Pteridophyta plants

Based on the root section, it can be seen than the endophytic fungi will colonise the root cortex area and develop the fungal structure inside. Based on observation, several identified endophytic fungal structures, including conidiophores, vesicles, conidia, and microsclerotium, are presented in Figure 4. Colonising root endophytic fungi in the cortical area of plant roots involves several stages, including recognition, attraction, penetration, and the emergence of a mutualistic relationship. This symbiotic relationship benefits both the fungus and the plant; the fungus aids in nutrient uptake and stress tolerance, and the plant provides sugars and

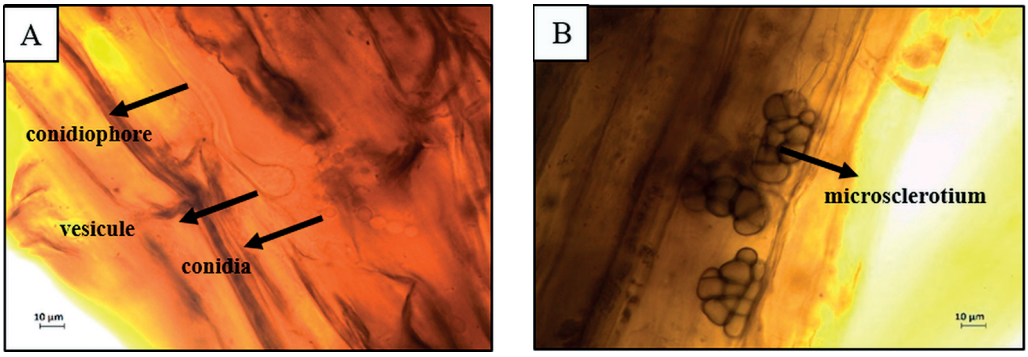


Fig. 4. The colonisation structure of endophytic fungi in the Pteridophyta root: A – asexual reproduction structure, B – microsclerotium as a spesialised structure within the root cell (photo by F. I. Nurunnisa).

organic molecules (Alam et al. 2021). This intricate interaction is necessary for the environment's long-term viability and the health of plants.

Various fungi, such as arbuscular mycorrhizae, epiphytic lichens and microfungi, pathogens, saprotrophs, and pathogens are reported to be associated with the Pteridophyte (Del Olmo-Ruiz and Arnold 2014). The colonisation of Pteridophyte roots by endophytic fungi is closely related to the development of these organisms. The Pteridophytes and the root endophytic fungus have a favorable connection. The fungus colonised the plant's root tissues in this symbiotic relationship, expanding their hyphae into the surrounding soil. This colonisation significantly impacts Pteridophyte development in many ways.

Pteridophytes play a critical role in maintaining biodiversity and sustaining various ecosystems, as demonstrated by these environmentally relevant interactions between Pteridophyta plants and root-endophytic fungus, especially in protected areas. By assisting in nutrient absorption, particularly for phosphorus and micronutrients, which are frequently in short supply, the association helps Pteridophyte adapt to various environmental circumstances. By making it easier for Pteridophyta species to get nutrients, fungi aid in their recovery from disturbances and promote their growth in nutrient-poor soils. It becomes essential to maintain this mutualistic connection in conservation zones to preserve the general health and ecological balance of these crucial ecosystems and the survival and vigor of Pteridophyte populations. Conservation initiatives aimed at protecting Pteridophyta and their fungal partners are essential for these plants' well-being and preserving biodiversity in these unique environments.

Conclusion

We conclude that the important role of the relationship between Pteridophyta and root-endophytic fungi is very closely related to environmental factors in the Gunung Tukung Gede Nature Reserve. Pteridophytes serve an important role, highlighting ecological significance and adaptable features. In conclusion, research on endophytic fungi isolated from Pteridophyta plant roots has given us a thorough understanding of the complex interactions within these ecosystems. Different *Aspergillus* species have been identified, and the presence of filamentous ascomycetes such as *Paecilomyces* sp., *Penicillium* sp., *Phialophora* sp., *Humicola* sp., and different *Fusarium* species highlights how dynamic and intricate the relationships between fungus and Pteridophyta plants are. These discoveries deepen the knowledge of the complex relationships among endophytic fungal communities. Those endophytic fungi also provide insights into ecological dynamics and have potential implications in plant resilience and environmental management, extending beyond the field of taxonomy.

References

Alam B., Lǐ J., Gě Q., Khan M.A., Gōng J., Mehmood S., Yuán Y., Gǒng W. 2021. Endophytic Fungi: From Symbiosis to Secondary Metabolite Communications or Vice Versa? Frontiers in plant science 12, 791033. 24 p. https://doi.org/10.3389/fpls.2021.791033

Almeida A.B., Concas J., Campos M.D., Materatski P., Varanda C., Patanita M., Murolo S., Romanazzi G., Félix M.D.R. 2020. Endophytic Fungi as Potential Biological Control Agents against Grapevine Trunk Diseases in Alentejo Region. Biology

9(12), 420. 23 p. https://doi.org/10.3390/biology9120420

Aros-Mualin D., Noben S., Karger D.N., Carvajal-Hernández C.I., Salazar L., Hernández-Rojas A., Kluge J., Sundue M.A., Lehnert M., Quandt D., Kessler M. 2021. Functional Diversity in Ferns is Driven by Species Richness Rather Than by Environmental Constraints. Frontiers in plant science 11, 615723. 11 p. https://doi.org/10.3389/fpls.2020.615723

Barnett H.L., Hunter B.B. 1998. Illustrated Genera of Imperfect Fungi. 4th ed. USA: Prentice-Hall Inc. 218 p.

Behera Y.N., Biswal B. 1990. Leaf senescence in fern: effect of duration, intensity and quality of light. Environmental and experimental botany 30(2): 181–186. https://doi.org/10.1016/0098-8472(90)90063-A

Del Olmo-Ruiz M., Arnold A.E. 2014. Interannual variation and host affiliations of endophytic fungi associated with ferns at La Selva, Costa Rica. Mycologia 106(1): 8–21. https://doi.org/10.3852/13-098

Djarwaningsih T. 2011. Flora diversity in the Cikolelet village area – Tukung Gede mountain natural reserve, Serang – Banten [Keragaman flora di wilayah desa Cikolelet – Cagar Alam Gunung Tukung Gede, Serang – Banten]. Special Edition of the Biological Research Periodical [Berk. Penel. Hayati Edisi Khusus] 5A: 15–20 (in Indonesian). https://berkalahayati.org/files/journals/1/articles/251/submission/251-785-1-SM.pdf

Galeano R.M.S., Franco D.G., Chaves P.O., Giannesi G.C., Masui D.C., Ruller R., Corrêa B.O., Brasil M.D.S, Zanoelo F.F. 2021. Plant growth promoting potential of endophytic Aspergillus niger 9-p isolated from native forage grass in Pantanal of Nhecolândia region, Brazil. Rhizosphere 18, 100332. https://doi.org/10.1016/j.rhisph.2021.100332

Geisen S., Hooven F.C., Kostenko O., Snoek L.B., Putten W.H. 2021. Fungal Root Endophytes Influence Plants in a Species-specific Manner that depends on Plant's Growth Stage. Journal of Ecology 109(4): 1618–1632. https://doi.org/10.1111/1365-2745.13584

Harahap I., Elsie, Aulia R. Rahmi R.A. 2017. Isolation of Endophytic Fungi from Vetiver Root Plants (*Vetiveria zizanioides* L.) and Antifungal Activity Test against *Candida albicans* [Isolasi Cendawan Endofit dari Tanaman Akar Wangi (*Vetiveria zizanioides* L.) dan Uji Aktivitas Antifungi terhadap *Candida albicans*]. Prosiding 2nd CELSciTech UNRI, vol. 2: 36–42 (in Indonesian). https://ejurnal.umri.ac.id/index.php/PCST/article/view/265/166

Jiang Y., Wu J., Kawagishi H., Jiang C., Zhou Q., Tong Z., Tong Y., Wang P. 2022. Study on Secondary Metabolites of Endophytic Fungus, *Aspergillus fumigatus*, from *Crocus sativus* L. Guided by UHPLC-HRMS/MS-Based Molecular Network. International Journal of Analytical Chemistry 2022, 7067665. 11 p. https://doi.org/10.1155/2022/7067665

Khastini R.O., Ohta H., Narisawa K. 2012. The role of a dark septate endophytic fungus, *Veronaeopsis simplex* Y34, in *Fusarium* disease suppression in Chinese cabbage. Journal of Microbiology 50(4): 618–624. https://doi.org/10.1007/s12275-012-2105-6

Khastini R.O. 2016. Dark Septate Root Endophytic Fungi in the Root System of *Avicennia* sp. Origin of the Pulau Dua Banten Nature Reserve and its Potential as a Producer of Antibacterial Compounds [Cendawan Endofit Akar Bersepta Gelap Pada Sistem Perakaran *Avicennia* sp. Asal Cagar Alam Pulau Dua Banten dan Potensinya sebagai Penghasil Senyawa Antibakteri]. Prosiding Seminar Nasional from Basic Science to Comprehensive Education Makassar, 26 Agustus 2016, 1992: 167–173 (in Indonesian).

Khastini R.O. 2018. Isolation and Screening of Root Endophytic Fungi from the Rhizosphere of Talas Beneng [Isolasi, dan Penapisan Cendawan Endofit Akar Asal Rhizosfer Talas Beneng]. Jurnal Biotek 6(2): 25–36 (in Indonesian). https://doi.org/10.24252/jb.v6i2.6823

Khastini R.O., Maryani N., Lestari I.D., Rifqiawati I., Millah N.U. 2021. Diver-

sity of Entomopathogenic Fungi from Gunung Tukung Gede Nature Reserve. Bioeduscience 5(2): 116–121. https://doi.org/10.22236/j.bes/526004

Khastini R.O., Sukarno N., Suharsono U.W., Hashidoko Y. 2022. Isolation and Growth Response of Root Mutualistic Fungi on Several Agriculture and Forestry Plants [Isolasi dan Respons Tumbuh Cendawan Mutualistik Akar pada Beberapa Tanaman Pangan dan Kehutanan]. Indonesian Journal of Agricultural Sciences [Jurnal Ilmu Pertanian Indonesia] 27(1): 85–94 (in Indonesian). https://doi.org/10.18343/jipi.27.1.85

Krieg C.P., Chambers S.M. 2022. The ecology and physiology of fern gametophytes: A methodological synthesis. Applications in Plant Sciences 10(2), e11464. 13 p. https://doi.org/10.1002/aps3.11464

Manurung P.L., Rahmawati R., Kurniatuhadi R. 2022. Inventaritation of Endophyte Fungi from Avicennia Marina Leaves in Mempawah Mangrove Center, Pasir Village, Mempawah, West Borneo. LenteraBio: Berkala Ilmiah Biologi 11(3): 378–384 (in Indonesian). https://doi.org/10.26740/lenterabio.v11n3.p378-384

Min J., Chen L., Xin H.-L., Zheng C.-J., Rahman K., Han T., Qin L.-P. 2016. A friendly relationship between endophytic fungi and medicinal plants: a systematic review. Frontiers in Microbiology 7, 906. 14 p. https://doi.org/10.3389/fmicb.2016.00906

Mishra A., Gond S.K., Kumar A., Sharma V.K., Verma S.K., Kharwar R.N. 2012. Sourcing the Fungal Endophytes: A Beneficial Transaction of Biodiversity, Bioactive Natural Products, Plant Protection and Nanotechnology. In: Satyanarayana T., Johri B. (Eds), Microorganisms in Sustainable Agriculture and Biotechnology. Springer, Dordrecht: 581–612. https://doi.org/10.1007/978-94-007-2214-9_26

Mordecai E.A. 2012. Soil moisture and fungi affect seed survival in California grassland annual plants. PloS one 7(6), e39083. 8 p. https://doi.org/10.1371/journal.pone.0039083

Musa M., Jan F.G., Hamayun M., Jan G., Khan S.A., Rehman G., Ali S., Lee I.J. 2023. An Endophytic Fungal Isolate *Paecilomyces lilacinus* Produces Bioactive Secondary Metabolites and Promotes Growth of *Solanum lycopersicum* under Heavy Metal Stress. Agronomy 13(3), 883. 17 p. http://dx.doi.org/10.3390/agronomy13030883

Muthukumar T., Prabha K. 2012. Fungal associations in gametophytes and young sporophytic roots of the fern *Nephrolepis exaltata*. Acta Botanica Croatica 71(1): 139–146. https://doi.org/10.2478/v10184-011-0056-3

Muthukumar T., Sathiyaraj G., Priyadharsini P., Uma E., Sathiyadash K. 2014. Arbuscular mycorrhizal and dark septate endophyte fungal associations in ferns and lycophytes of Palni Hills, Western Ghats, southern India. Revista Brasileira de Botanica 37(4): 561–581. https://doi.org/10.1007/s40415-014-0085-y

Naranjo-Ortiz M.A., Gabaldón T. 2019. Fungal evolution: major ecological adaptations and evolutionary transitions. Biological reviews of the Cambridge Philosophical Society 94(4): 1443–1476. https://doi.org/10.1111/brv.12510

Nejad M.S., Najafabadi N.S., Aghighi S., Pakina E., Zargar M. 2022. Evaluation of *Phoma* sp. Biomass as an Endophytic Fungus for Synthesis of Extracellular Gold Nanoparticles with Antibacterial and Antifungal Properties. Molecules (Basel, Switzerland) 27(4), 1181. 15 p. https://doi.org/10.3390/molecules27041181

Qian H., Kessler M., Vetaas O.R. 2022. Pteridophyte species richness in the central Himalaya is limited by cold climate extremes at high elevations and rainfall seasonality at low elevations. Ecology and Evolution 12(5), e8958. 14 p. https://doi.org/10.1002/ece3.8958

Rillig M.C., Wendt S., Antonovics J., Hempel S., Kohler J., Wehner J., Caruso T. 2014. Interactive effects of root endophytes and arbuscular mycorrhizal fungi on an experimental plant community. Oecologia 174: 263–270. https://doi.org/10.1007/s00442-013-2759-8

Seifert K.A., Gams W. 2011. The Genera of

Hyphomycetes, CBS biodiversity series No.9. Utrecht, The Netherlands: CBS-KNAW Fungal Biodiversity Center. Persoonia – Molecular Phylogeny and Evolution of Fungi 27(11): 119–129. 11 p. https://doi.org/10.3767/003158511X617435

Sun R.-T., Feng X.-C., Zhang Z.-Z., Zhou N., Feng H.-D., Liu Y.-M., Hashem A., Al-Arjani A.-B.F., Abd Allah E.F., Wu Q.-S. 2022. Root Endophytic Fungi Regulate Changes in Sugar and Medicinal Compositions of *Polygonum cuspidatum*. Frontiers in Plant Science 13, 818909. 11 p. https://doi.org/10.3389/fpls.2022.818909

Sunarti S. 2011. Research on Forest Vegetation in the Gantung Rock and Pagar Rock Areas, Mount Tukung Gede Nature Reserve, Serang [Penelitian Vegetasi Hutan di Wilayah Cadas Gantung dan Cadas Pagar, Cagar Alam Gunung Tukung Gede, Serang]. [Berk. Penel. Hayati Edisi Khusus] 5A: 109–119 (in Indonesian). https://berkalahayati.org/files/journals/1/articles/266/submission/266-842-1-SM.pdf

Suraida S., Susanti T., Amriyanto R. 2013. Diversity of Ferns (Pteridophyta) in the Recognize Forest Park, Jambi City [Keanekaragaman Tumbuhan Paku (Pteridophyta) di Taman Hutan Kenali Kota Jambi]. Prosiding Semirata FMIPA, Universitas Lampung: 387–392 (in Indonesian). https://jurnal.fmipa.unila.ac.id/semirata/article/view/640

Toghueo R.M.K., Boyom F.F. 2020. Endophytic *Penicillium* species and their agricultural, biotechnological, and pharmaceutical applications. Biotech 10(3), 107. https://doi.org/10.1007/s13205-020-2081-1

Tseng Y.-H., Rouina H., Groten K., Rajani P., Furch A.C.U., Reichelt M., Baldwin I.T., Nataraja K.N., Shaanker R.U., Oelmüller R. 2020. An Endophytic Trichoderma Strain Promotes Growth of Its Hosts and Defends Against Pathogen Attack. Frontiers in plant science 11, 573670. 16 p. https://doi.org/10.3389/fpls.2020.573670

Watts D., Palombo E.A., Castillo A.J., Zaferanloo B. 2023. Endophytes in Agriculture: Potential to Improve Yields and Tolerances of Agricultural Crops. Microorganisms 11(5), 1276. 29 p. https://doi.org/10.3390/microorganisms11051276

Wen J., Okyere S.K., Wang S., Wang J., Xie L., Ran Y., Hu Y. 2022. Endophytic Fungi: An Effective Alternative Source of Plant-Derived Bioactive Compounds for Pharmacological Studies. Journal of fungi (Basel, Switzerland) 8(2), 205. 45 p. https://doi.org/10.3390/jof8020205

FORESTRY IDEAS, 2024, vol. 30, No 1 (67): 197–207

Oleoresin *Baeckea frutescens* L. activity against *Pleurotus ostreatus* (Jacq. ex Fr.) P.Kumm.

Renhart Jemi*, Nuwa, and Lamboris Rianto Sitorus

Department of Forestry, Faculty of Agriculture, University of Palangka Raya, Central Kalimantan 27111, Indonesia. *E-mal: jemi@for.upr.ac.id

Received: 30 January 2024 / Accepted: 06 June 2024 / Available online: 13 June 2024

Open Access: This article is licensed under a Creative Commons Attribution 4.0 International License.

Abstract

This study aims to determine the oleoresin activity of *Baeckea frutescens* L. against the fungus *Pleurotus ostreatus* (Jacq. ex Fr.) P.Kumm. and to analyse its most active component. The research method used was ethanol solvent maceration extraction, and then fractionation was carried out using successive solvents, namely *n*-hexane, chloroform, and ethyl acetate. Then the *P. ostreatus* antifungal test, and analysis of the most active compound components using Gas Chromatography-Mass Spectrometry were applied. The results showed that *B. frutescens* oleoresin produced a yield of 11.41 % in ethanol extract. The most active antifungal activity was found in ethanol oleoresin soluble oleoresin with $IC_{(50)}$ = 177 ±02 mg·L^{-1}. It contains 21 bioactive compounds consisting of 4 antifungal components, namely quinic acid, α-terpineol, linalool, and 2-cyclohexen-1-one.

Key words: antifungal, bioactive, extract, GC-MS, quinic acid.

Introduction

Indonesia has 4000 types of wood, and 80–85 % of them fall into durable classes III and IV. Types of wood that have a low durability class tend to be easily attacked by wood-destroying organisms. Those that most commonly attack tropical areas are wood rotting fungi. As a result of fungal attacks, the strength of the wood decreases because the cell wall components that strengthen the wood have been damaged. One of the wood rot fungi is *Pleurotus ostreatus* (Jacq.ex Fr.) P. Kumm. According to Singh and Singh (2014) the fungus *P. ostreatus* attacks softwood. Overcoming attacks by wood-destroying fungi means preserving forests.

Overcoming wood damage by *P. ostreatus* can be done by using preservatives. Most of the preservatives used today are synthetic so they can cause environmental pollution. To prevent this, alternative materials are needed using biodegradable preservatives. The materials are easy to obtain and can be renewed. One of them is extractive substances contained in plants which have bioactive prop-

erties and are able to kill wood-destroying organisms (Setiawan et al. 2019). Extractive substances are secondary metabolic products of compounds that function ecologically and can be obtained from various types of plants. One of them is *Baeckea frutescens* L. which is a needle-leaved shrub from the Myrtaceae family (Supandi et al. 2019, Huong et al. 2023) which has the potential to be used for its leaves. They produce extractive substances in the form of essential oil. Previous research results stated that the leaves and twigs of *B. frutescens* produce essential oil which has anti-inflammatory, anti-oxidant, anti-bacterial, anti-fungal, anti-microbial and cytotoxic activity (Razmavar et al. 2014, Navanesan et al. 2015, Irma 2016, Nisa et al. 2017, Shahruzaman et al. 2019).

So far there have been no research reports regarding the activity of *B. frutescens* oleoresin against the fungus *P. ostreatus*. The results of research on oleoresin from frutescens are predominantly *Capsicum frutescens* L. (Do et al. 2021). It is a semi-solid extract consisting of resin and essential oils, obtained from extraction using organic solvents. Based on this background, research was carried out on the extraction of oleoresin from *B. frutescens* leaves, then its activity was tested on the fungus *P. ostreatus*, and the chemical content of the oleoresin was analysed. The aim of the research was to determine the activity of *P. ostreatus* and the oleoresin content of *B. frutescens*.

Material and Methods

Taking *B. frutescens* leaves and preparing leaf samples

B. frutescens leaves were obtained from forest areas in Kereng Bangkirai, Sebangau District, Palangka Raya City, Central Kalimantan (located at 2°16'14.595″ to 2°06'18.8" S and 113°50'35.255″ to 113°45'06.3″ E). The leaves were harvested and then dried in the open. Drying until the leaf moisture content is 10–15 % (Zahra et al. 2019). The dried leaves were blended, then filtered by passing 40 mesh particles and held in 60 mesh. The leaf powder needed was 500 g.

Maceration

B. frutescens leaves with a dry weight of 250 g were macerated in ethanol at room temperature with a pressure of 1 atm for 24 h while stirring. The ratio of simplicia to solvent is 1:5 (v/v). The maceration process was repeated with stirring every three hours, for 15 min until a clear filtrate was obtained. The ethanol extract solution obtained was evaporated with a rotary evaporator at a temperature of 45–50 °C until the solvent was concentrated. The evaporated extract solution was placed in a 1000 mL glass above a batch of water at a temperature of 45–50 °C to evaporate the remaining solvent in the extract and obtain a thick extract (Setiawan et al. 2019).

Stratified fractionation of ethanol extract

50 mL of ethanol extract from *B. frutescens* leaf powder was put into a funnel separator for multilevel fractionation. Fractionation in stages, using the first solvent *n*-hexane 100 mL. This mixture was shaken for 10–15 min and left until separation occurred between the ethanol and *n*-hexane solvents. Fractionation of the *n*-hexane obtained. Next, the residue obtained was mixed with chloroform solvent. In the same way, separation is carried out and the chloroform and residue

fractions are produced. In the final stage, the resulting residue is mixed with ethyl acetate solvent. The multistage fractionation process is shown in Figure 1. The extract from each fraction was concentrated using a rotary evaporator to evaporate the remaining solvent and produce a thick extract (Setiawan et al. 2019).

The ethanol extract of 100 mL was subjected to multilevel fractionation with different solvents sequentially *n*-hexane, chloroform, and ethyl acetate. The fractionation process consists of a mixture of crude extract, solvent, and distilled water in a ratio of 1:2:2. The crude extract mixture was shaken in a separatory funnel for 10–15 min and then left until synchronisation occurred between the dissolved extract and the crude extract which dissolved in ethanol. Each filtrate fraction obtained was evaporated using a rotary evaporator to evaporate the remaining solvent and produce a thick extract (Setiawan et al. 2019).

Cultivation of the fungus

The fungus used was *P. osteratus* which belongs to the group of wood-decaying fungi (Nakazawa et al. 2017). It was first

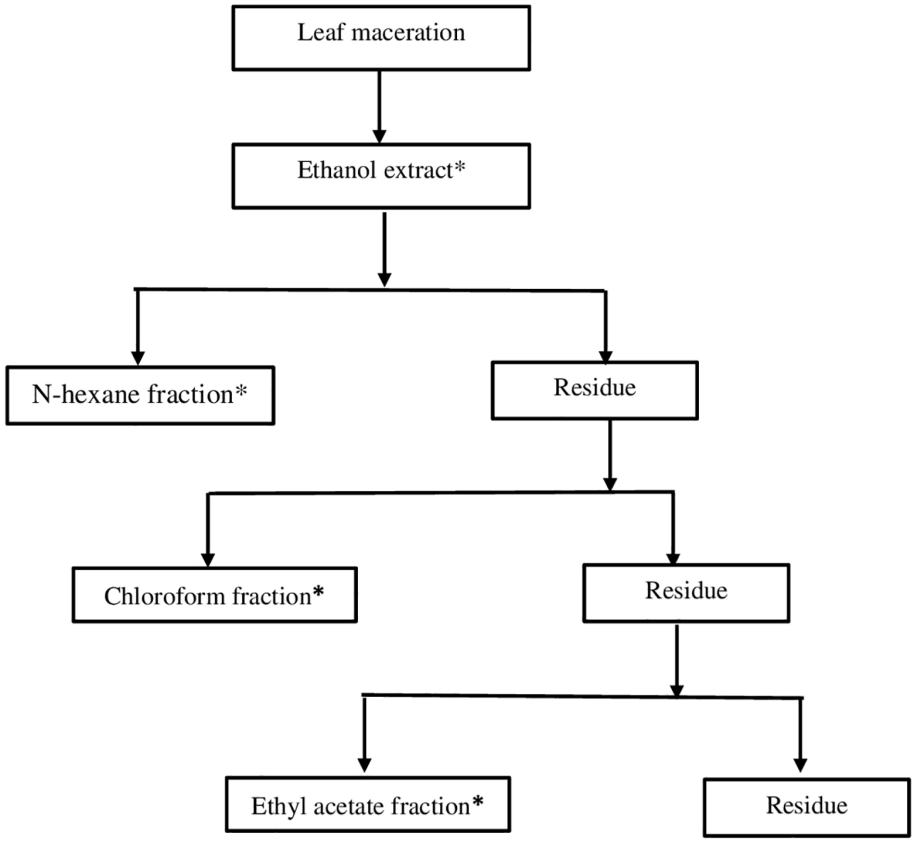


Fig. 1. Scheme of multistage oleoresin extraction using 4 solvents.
Note: * tested for fungus *P. ostreatus*.

cultured on potato dextrose agar (PDA) growth medium for 7 days. The composition of the growth medium is as follows: 1 L contains 50 g glucose, 120 g onion extract, 50 g glucose, 0.3 g K_2HPO_4, 0.2 g $MgSO_4.7H_2O$, 5 g polyptone and 30 g agar powder at pH 6.0.

Anti-fungal activity testing

Testing of all oleoresins, which were obtained from maceration and fractionation was realised. The treatments were variations in the concentration of extractive substances as follows: 0, 50, 100, 250, 500, and 1000 mg·L^{-1}. Previously the Petri dish was autoclaved for 15 min at a temperature of ±120 °C with a pressure of 1 atm. Poured with media and oleoresin according to the treatment, each treatment was repeated 3 times and planted with *P. osteratus* mushrooms. Next, it was incubated at 25 °C for 7 days in a dark room. The inhibitory activity of fungal growth by extractive substances was carried out at the end of the incubation period, by measuring the growth diameter and comparing it with the growth of control mycelium. The basis for determining anti-fungal activity uses the formula (1) (Kamaruzzaman et al. 2021).

$$\text{Percent inhibition} = (C\text{-}T)\cdot C^{-1}\cdot 100, \quad (1)$$

where: T is the area of mycelium in the treatment petri dish, and C is the area of mycelium in the control Petri dish.

Data analysis

Data on the percentage of inhibition of fungal growth were analysed with probit to determine the value of $IC_{(50)}$. Calculations using the SPSS 17.0 program. A compound was declared active if it had an $IC_{(50)}$ value <1000 mg·L^{-1} and inactive if it had an $IC_{(50)}$ value >1000 mg·L^{-1} (Meyer et al. 1982).

Gas chromatography-mass spectrometry (GC-MS) analysis

A total of 0.5 mg of oleoresin *B. frutescens* which had the highest inhibition was carried out by the GC-MS test. The results were analysed and adjusted using the WILLEY7.LIB database. GC-MS brand is Shimadzu; Type: GCMS QP2010 Plus. The analysis was carried out at the Commodity and Environmental Testing Laboratory, Center for Industrial Research and Standardisation. Banjarbaru South Kalimantan Indonesia.

Results and Discussion

Oleoresin antifungal *B. frutescens*

As a result of maceration of the leaves of *B. frutescens* with ethanol solvent it was obtained 11.41 % oleoresin, 2.55 % *n*-hexane, 2.01 % chloroform, and 0.50 % ethyl acetate. The differences in yields produced were due to differences in the polarity of each solvent. *B. frutescens* oleoresin which is soluble in several solvents was then tested for the activity of the *P. ostreatus* fungus. The results of the fungal growth inhibition test are shown in Table 1 and the growth of fungal mycelium at several oleoresin concentrations is shown in Figure 2.

Table 1. $IC_{(50)}$ value of *B. frutescens* oleoresin against *P. ostreatus* fungus.

No	Soluble oleoresin	$IC_{(50)}$, mg·L^{-1}	Classification*
1	Ethanol	177 ±*0*.21	Active
2	*n*-hexane fraction	242 ±*0*.15	Active
3	Chloroform fraction	233 ±*0*.61	Active
4	Ethyl acetate fraction	270 ±*0*.14	Active

Note: * Classification is according to Meyer et al. (1982).

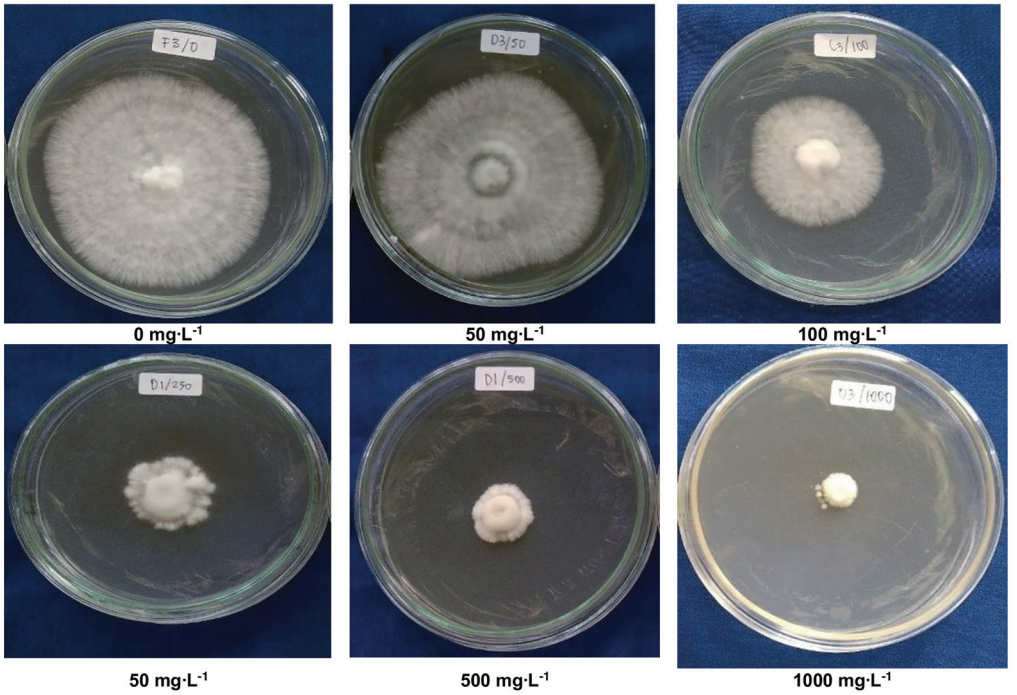


Fig. 2. Effect of *B. frutescens* oleoresin concentration on the growth of *P. ostreatus* mycelium (photo by L. R. Sitorus).

Table 1 displays the results of *B. frutescens* oleoresin activation test on the growth of *P. ostreatus* mycelium with $IC_{(50)}$ = 177 ±0.2 to 270 ±0.14 mg·L^{-1}. As well as the anti-fungal activation of *B. frutescens* oleoresin, all of them are classified as active because $IC_{(50)}$ ≤ 1000 mg·L^{-1} (Meyer et al. 1982). However, the ethanol soluble oleoresin extract was the most active of the four. This is because the ethanol soluble oleoresin extract has the lowest $IC_{(50)}$ = 177 ±0.2 mg·L^{-1} and was able to inhibit the mycelium of *P. ostreatus* fungus compared to the four oleoserin extracts. The research results of Wu et al. (2021) stated that the ethanol extract of *Fagus crenata* Blume wood was able to inhibit the delignification process and hydrolytic enzyme reactions of *P. ostretaus.* The research results of Fakhrudin et al. (2015), Hastuti et al. (2018), Dewi et al. (2019). stated oleoresin from *Ginger* rhizomes and *Polygonum minus* Huds. is with a higher phenol content, so it can inhibit the growth of *Trichophyton rubrum* Sabour.

Content of oleoresin compound *B. frutescens* which dissolves in ethanol

B. frutescens oleoresin in ethanol extract had the most active *P. ostreatus* growth inhibition activity than the *n*-hexane fraction, chloroform fraction, and ethyl acetate fraction. So, the selection was made to remove the content of the oleoresin compound using GC-MS analysis which is presented in Figure 3.

Analysis of the components of the oleoresin compound *B. frutescenes* in the ethanol extract showed 21 compounds and the literature review which are presented in Table 2.

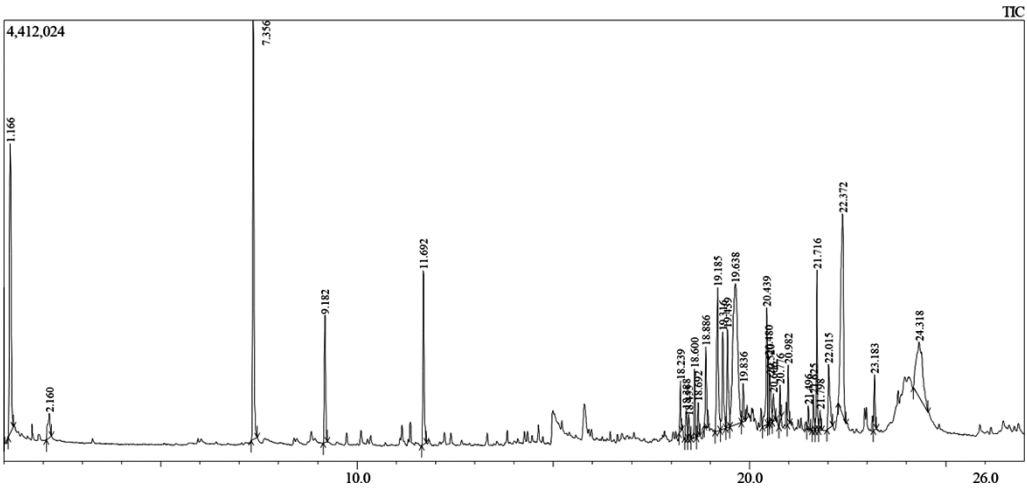


Fig. 3. Chromatogram of *B. frutescens* oleoresin in ethanol extract.

Note: Retention time (RT) 2.160 = propanoic acid; RT 7.356 = 1,8-cineole; RT 9.182 = linalool; RT 11.692 = α-terpineol; RT 18.239 = (-)-caryophyllene oxide; RT 18.388 = quinic acid; RT 18.451 = β-selinene; RT 18.691 = 3,4-dimethoxyphenyl propionamide; RT 19.188 = 3-methoxymethyl-2,5,5,8a-tetramethyl-6,7,8,8a-tetrahydro-5h-chromene; RT 19.440 = 2-cyclohexen-1-one; RT 20.519 = anthracene, 9-trimethylsilyl; RT 20.604 = pluchidiol; RT 20.775 = (R)-2-benzyl proline methylamide; RT 20.98 = ergostane-3,5,6,12,25-pentol, 25-acetate; RT 21.497 = 4-methoxy-3-(methoxymethyl)phenol; RT 21.624 = 4,4,8-trimethyl-tricyclo [6.3.1.0 1,5] dodecane-2,9-diol; RT 21.797 = 2-propenoic acid; RT 22.009 = phi-aspidinol; RT 22.372 = 1-butanone; RT 23.183 = Methan; RT 24.317 = Urs-12-en-28-al.

Table 2. GC-MS of *B. frutescenes* oleoresin in ethanol extract.

Compound	SI	Content, %	Compound formula	Bioaactive (references)
Propanoic acid	-	2.274	$C_3H_6O_2$	Antimicrobial (Zhang et al. 2011)
1,8-cineole	90	5.499	$C_{10}H_{18}O$	Antiinflammatory (Santos and Rao 2000)
Linalool	82	1.912	$C_{10}H_{18}O$	Antifungal (Dias et al. 2018)
α-terpineol	86	3.047	$C_{10}H18O$	Antifungal (An et al. 2019)
(-)-caryophyllene oxide	80	0.822	$C_{15}H_{24}O$	Anticancer and analgesic (Fidyt et al. 2016)
Quinic acid		0.214	$C_7H_{12}O_6$	Antifungal (Ma and Ma 2015)
β-selinene		0.224	$C_{15}H_{24}$	Antioxidant (Chandra et al. 2017)
3,4-dimethoxyphenyl propionamide		0.825	$C_{10}H_{15}NO_2$	Antibodies (Fernández-Martínez et al. 2001)
3-methoxymethyl-2,5,5,8a-tetramethyl-6,7,8,8a-tetrahydro-5h-chromene		14.564	$C_{15}H_{24}O_2$	
2-cyclohexen-1-one		0.842	C_6H_8O	Antifungal (Shakil et al. 2013)

Compound	SI	Content, %	Compound formula	Bioaactive (references)
Anthracene, 9-trimethylsilyl		1.082	$C_{15}H_{11}Cl$	Antracene (Sirimanne et al. 1991)
Pluchidiol		0.845	$C_5H_{12}ClNO_2$	
(R)-2-benzyl proline methyl-amide		0.635	$C_{12}H_{15}NO_2$	
Ergostane-3,5,6,12,25-pentol, 25-acetate		0.272	$C_{30}H_{52}O_6$	
4-methoxy-3-(methoxymethyl) phenol		0.383	$C_9H_{12}O_3$	Antimicrobial and antiinflammatory (Manivannan and Shopna 2017)
4,4,8-trimethyl-tricyclo [6.3.1.0 1,5] dodecane-2,9-diol		0.175	$C_{10}H_{19}NO$	
2-propenoic acid		0.195	$C_3H_4O_2$	Antimicrobial (Murdoch et al. 2007)
phi-aspidinol		2.179	$C_{12}H_{16}O_4$	
1-butanone		33.435	C_4H_8O	
Methan		1.754	CH_4	Antimicrobial (Rawat and Singh 2019)
Urs-12-en-28-al		1.589	$C_{30}H_{48}O$	

Note: SI is similarity index.

Table 2 explains the components of the dominant *B. frutescens* oleoresin compound, namely 1,8-cineole, 3-methoxymethyl-2,5,5,8a-tetramethyl-6,7,8,8a-tetrahydro-5h-chromene and 1-butanone. The 1,8-cineeole gives the characteristic aroma of fresh camphor, and spicy and anti-fungal properties to the oleoresin of *B. frutescens* (Tadtong et al. 2015, Kim et al. 2018). In the ethanol extract, 4 active antifungal compound components were obtained, namely α-terpineol, linalool, 2-cyclohexen-1-one and quinic acid (Shakil et al. 2013, Ma and Ma 2015, Kong et al. 2019, Li et al. 2022). The dominant compounds contained were from the terpenoid group. The most abundant terpenoids are monoterpenes and sesquiterpenes with amounts of C10 and C15. The two types of terpenoids had differences in boiling points which can affect gas chromatography, compounds with low boiling points will come out first into the detector. This is possible because a lower boiling point causes the compound to evaporate more easily so the retention time is faster. The retention time of each compound component is determined by the boiling point of the compound component (Harianingsih et al. 2017). Due to the low similarity index (SI) of standard mass spectra from the NIST12, NIST62 and WILEY229 tool libraries cannot be used. Supporting data through searching mass spectra from previous research results were found as well. So further SI analysis was carried out with a literature study of fragmentation patterns. The compounds 1,8-cineole, linalool, α-terpineol, (-)-caryophyllene oxide resulted from GC-MS analysis in Table 2. According to the similarity index value with the results of GC-MS analysis of *B. frutescenes* essential oil it is the same as the similarity index value resulting

from research using essential oils from *B. frutescenes* leaves from research by Saad et al. (2021), Jemi et al. (2021) and Tam et al. (2004). The SI of a compound showed that it is close to 100 %, indicating that it is getting closer to the compound standard (Fitriani et al. 2020).

Based on the results of GC-MS analysis and literature searches, the four compounds are anti-fungal. Of them, the more dominant is quinic acid based on the number of -OH functional groups. Because the -OH groups are reactive and capable of damaging fungal cell walls and cannot be eliminated by fungal enzymatic reactions. So, the non-functioning of lignolytic enzymes results in disrupted fungal growth and ultimately death (Shakil et al. 2013, Ma and Ma 2015, Kong et al. 2019, Broda 2020, Li et al. 2022).

Conclusion

B. frutescens oleoresin produced the highest yield in ethanol extract, followed by the *n*-hexane, chloroform, and ethyl acetate fractions. Ethanol-soluble oleresin was the most active in inhibiting the growth of *P. ostreatus*. It also contains anti-fungal compounds, namely quinic acid, α-terpineol, linalool and 2-cyclohex-en-1-one.

The research results recommend that *B. frutescens* oleoresin can be processed and used as an environmentally friendly wood preservative, especially against attacks by the fungus *P. ostreatus*. This can reduce the use of synthetic preservatives.

References

An P., Yang X., Yu J., Qi J., Ren X., Kong Q. 2019. α-terpineol and terpene-4-ol, the critical components of tea tree oil, exert antifungal activities *in vitro* and *in vivo* against *Aspergillus niger* in grapes by inducing morphous damage and metabolic changes of fungus. Food control 98: 42–53. https://doi.org/10.1016/j.foodcont.2018.11.013

Broda M. 2020. Natural compounds for wood protection against fungi – A review. Molecules 25(15), 3538. 24 p. https://doi.org/10.3390/molecules25153538

Chandra M., Prakash O., Kumar R., Bachheti R.K., Bhushan B., Kumar M., Pant A.K. 2017. *β*-selinene-rich essential oils from the parts of Callicarpa macrophylla and their antioxidant and pharmacological activities. Medicines 4(3), 52. 17 p. doi: 10.3390/medicines4030052

Dewi S., Asseggaf S.N.Y.R.S., Natalia D., Mahyarudin M. 2019. Efek Ekstrak Etanol Daun Kesum (*Polygonum minus* Huds.) sebagai Antifungi terhadap *Trichophyton rubrum*. Jurnal Kesehatan Andalas 8(2): 198–203. https://doi.org/10.25077/jka.v8i2.992

Dias I.J., Trajano E.R.I.S., Castro R.D., Ferreira G.L.S., Medeiros H.C.M., Gomes D.Q.C. 2018. Antifungal activity of linalool in cases of *Candida* spp. isolated from individuals with oral candidiasis. Brazilian Journal of Biology 78(2): 368–374. https://doi.org/10.1590/1519-6984.171054

Do H.M.V., Vo M.T., Huynh B.T., Nguyen D.T.D., Thi T.A.N., Truong C.T., Nguyen D.H. 2021. Preparation and analgesic activity test of *Capsicum frutescens* oleoresin. Vietnam Journal of Science and Technology 59(2): 149–157. https://doi.org/10.15625/2525-2518/59/2/15408

Fakhrudin M.I., Anam C., Andriani M.A.M. 2015. Characteristics of ginger oleoresin based on size and soaking time of ginger powder in ethanol [Karakteristik oleoresin jahe berdasarkan ukuran dan lama perendaman serbuk jahe dalam etanol]. Asian Journal of Natural Product Biochemistry 13(1): 25–33 (in Indonesian).

Fernández-Martínez E., Morales-Ríos M.S., Pérez-Álvarez V., Muriel P. 2001. Effects of thalidomide and 3-phthalimido-3-(3, 4-dimethoxyphenyl)-propanamide

on bile duct obstruction-induced cirrhosis in the rat. Drug Development Research 54(4): 209–218. https://doi.org/10.1002/ddr.10022

Fidyt K., Fiedorowicz A., Strządała L., Szumny A. 2016. *β*-caryophyllene and *β*-caryophyllene oxide-natural compounds of anticancer and analgesic properties. Cancer Medicine 5(10): 3007–3017. doi: 10.1002/cam4.816

Fitriani R., Rosyidah K., Rohman T. 2020. Antioxidant activity test and Gas Chromatography-Mass Spectrometry (GC-MS) analysis of the ethyl acetate fraction of purun tikus (*Eleocharis dulcis*) leaves [Uji Aktivitas antioksidan dan Analisis Gas Chromatography-Mass Spectrometry (GC-MS) fraksi etil asetat daun purun tikus (*Eleocharis dulcis*)]. Chimica et Natura Acta 8(3): 104–108 (in Indonesian). https://doi.org/10.24198/cna.v8.n3.32204

Harianingsih H., Wulandari R., Harliyanto C., Andiani C.N. 2017. Identification of GC-MS Essential Oils Extract from Citronella (*Cymbopogon winterianus*) Using Metanol Solvent [Identifikasi GC-MS Ekstrak Minyak Atsiri dari Sereh Wangi (*Cymbopogon winterianus*) Menggunakan Pelarut Metanol]. Techno Jurnal Fakultas Teknik, Universitas Muhammadiyah Purwokerto 18(1): 23–27 (in Indonesian). doi: 10.30595/techno.v18i1.1445

Hastuti D., Rohadi R., Putri A.S. 2018. The Ratio of *n*-hexane-ethanol To Physical and Chemical Characteristics of Oleoresin Press Cage Ginger (*Zingiber majus* Rumph) Variety Emprit [Rasio *N*-Heksana-Etanol Terhadap Karakteristik Fisik Dan Kimia Oleoresin Ampas Jahe (*Zingiber majus* Rumph) Varietas Emprit]. Jurnal Teknologi Pangan dan Hasil Pertanian 13(1): 41–56 (in Indonesian). http://dx.doi.org/10.26623/jtphp.v13i1.2374

Huong D.T.L., Duc D.X., Son N.T. 2023. *Baeckea frutescens* L.: A Review on Phytochemistry, Biosynthesis, Synthesis, and Pharmacology. Natural Product Communications 18(7): 1–22. https://doi.org/10.1177/1934578X231189143

Irma A. 2016. Antifungal Activity of Essential Oil of Roof End Leaves (*Baeckea frutescens* L.) [Aktivitas Antijamur Minyak Atsiri Daun Ujung Atap (*Baeckea frutescens* L.)]. Universitas Palangka Raya. Palangka Raya. 75 p. (in Indonesian).

Jemi R., Simanullang S., Sarinah, Nuwa, Luhan G., Koroh D.N. 2021. *Baeckea frutescen* L. essential oil was tested with *Aedes aegypti* larvae at various concentration levels. In: IOP Conference Series: Materials Science and Engineering, vol. 1011, No. 1, 012002. 10 p. IOP Publishing. doi: 10.1088/1757-899X/1011/1/012002

Kamaruzzaman M., Islam M.S., Mahmud S., Polash S.A., Sultana R., Hasan M.A., Wang C., Jiang C. 2021. *In vitro* and *in silico* approach of fungal growth inhibition by *Trichoderma asperellum* HbGT6-07 derived volatile organic compounds. Arabian Journal of Chemistry 14(9), 103290. 21 p. https://doi.org/10.1016/j.arabjc.2021.103290

Kim H.M., Kwon H., Kim K., Lee S. E. 2018. Antifungal and Antiaflatoxigenic Activities of 1, 8-Cineole and t-Cinnamaldehyde on *Aspergillus flavus*. Applied Sciences 8(9), 1655. 9 p. https://doi.org/10.3390/app8091655

Kong Q., Zhang L., An P., Qi J., Yu X., Lu J., Ren X. 2019. Antifungal mechanisms of α-terpineol and terpene-4-alcohol as the critical components of *Melaleuca alternifolia* oil in the inhibition of rot disease caused by *Aspergillus ochraceus* in postharvest grapes. Journal of applied microbiology 126(4): 1161–1174. https://doi.org/10.1111/jam.14193

Li X., Wang Q., Li H., Wang X., Zhang R., Yang X., Shi Q. 2022. Revealing the mechanisms for linalool antifungal activity against *Fusarium oxysporum* and its efficient control of Fusarium Wilt in tomato plants. International Journal of Molecular Sciences 24(1), 458. https://doi.org/10.3390/ijms24010458

Ma J.-N., Ma C.-M. 2015. Antifungal inhibitory activities of caffeic and quinic acid derivatives. In: Preedy V.R. (Ed.), Coffee in Health and Disease Prevention. Academic Press, Chapter 71: 635–641. https://doi.

org/10.1016/B978-0-12-409517-5.00071-1

Manivannan R., Shopna R. 2017. Anti-microbial and Anti-inflammatory Activity of New 4-methoxy-3-(methoxymethyl) Phenol and (E)-N'-(5-bromo-2-methoxybenzylidene)-4-methoxy Benzohydrazide Isolated from Calotropis gigantean white. Natural Product Sciences 23(1): 69–74. https://doi.org/10.20307/nps.2017.23.1.69

Meyer B.N., Ferrigni N.R., Putnam J.E., Jacobsen L.B., Nichols D.E., McLaughlin J.L. 1982. Brine Shrimp: a Convenient General Bioassay for Active Plant Constituents. Planta med 45(5): 31–34. doi: 10.1055/s-2007-971236

Murdoch A.I., McCauley R.D., Hampson D.J. 2007. Review of the Efficacy and Safety of Poly (2-propenal, 2-propenoic acid): a Novel Antimicrobial Polymer. The Thai Journal of Veterinary Medicine 37(4): 9–17. https://he01.tci-thaijo.org/index.php/tjvm/article/view/36132

Nakazawa T., Izuno A., Horii M., Kodera R., Nishimura H., Hirayama Y., Tsunematsu Y., Miyazaki Y., Awano T., Muraguchi H., Watanabe K., Sakamoto M., Takabe K., Watanabe T., Isagi Y., Honda Y. 2017. Effects of *pex1* disruption on wood lignin biodegradation, fruiting development and the utilization of carbon sources in the white-rot Agaricomycete *Pleurotus ostreatus* and non-wood decaying *Coprinopsis cinerea*. Fungal Genetics and Biology 109: 7–15. https://doi.org/10.1016/j.fgb.2017.10.002

Navanesan S., Wahab N.A., Manickam S., Sim K.S. 2015. Evaluation of Selected Biological Capacities of *Baeckea frutescens*. BMC complementary and Alternative Medicine 15(1), 186. 8 p. https://doi.org/10.1186/s12906-015-0712-6

Nisa K., Nurhayati S., Apriyana W., Indrianingsih A.W. 2017. Investigation of total phenolic and flavonoid contents, and evaluation of antimicrobial and antioxidant activities from *Baeckea frutescens* extracts. In: IOP Conference Series: Earth and Environmental Science 101(1), 012002. doi: 10.1088/1755-1315/101/1/012002

Rawat P., Singh R.N. 2019. Synthesis, spectral analysis and study of antimicrobial activity of 2,5-diformyl-1*H*-pyrrole bis (methan-1-yl-1-ylidene) dimalonohydrazone. Arabian Journal of Chemistry 12(7): 1219–1233. https://doi.org/10.1016/j.arabjc.2014.10.050

Razmavar S., Abdulla M.A., Ismail S.B., Hassandarvish P. 2014. Antibacterial Activity of Leaf Extracts of *Baeckea frutescens* Against Methicillin-Resistant *Staphylococcus aureus*. BioMed Research International, Article ID 521287, 5 p. https://doi.org/10.1155/2014/521287

Saad H.M., Rahman S.N.S.A., Navanesan S., Tan C.H., Manickam S., Abd Malek S.N., Sim K.S. 2021. Evaluation of antioxidant activity and phytochemical composition of *Baeckea frutescens* and *Leptospermum javanicum* essential oils. South African Journal of Botany 141: 474–479. https://doi.org/10.1016/j.sajb.2021.06.005

Santos F.A., Rao V.S. 2000. Antiinflammatory and antinociceptive effects of 1,8-cineole a terpenoid oxide present in many plant essential oils. Phytotherapy Research 14(4): 240–244. https://doi.org/10.1002/1099-1573(200006)14:4<240::AID-PTR573>3.0.CO;2-X

Setiawan A., Farah D., Evy W. 2019. Antifungal Activity Test of Api-api Leaf Extract (*Avicennia maria* Vierh) to Inhibit the Growth of *Schizophyllum commune* Fries Fungus [Uji Aktivitas Antijamur Ekstrak Daun Api-api (*Avicennia maria* Vierh) untuk Menghambat Pertumbuhan Jamur *Schizophyllum commune* Fries]. Jurnal Hutan Lestari 7(1): 517–524 (in Indonesian). http://dx.doi.org/10.26418/jhl.v7i1.32376

Shahruzaman S.H., Mustafa M.F., Ramli S., Fakurazi S., Maniam S. 2019. The cytotoxic properties of *Baeckea frutescens* branches extracts in eliminating breast Cancer cells. Evidence-Based Complementary and Alternative Medicine, Article ID 9607590. 9 p. https://doi.org/10.1155/2019/9607590

Shakil N.A., Singh M.K., Sathiyendiran M., Kumar J., Padaria J.C. 2013. Microwave synthesis, characterization and bio-efficacy evaluation of novel chalcone based 6-carbethoxy-2-cyclohexen-1-one and 2H-indazol-3-ol derivatives. European Journal

of Medicinal Chemistry 59: 120–131. doi: 10.1016/j.ejmech.2012.10.038

Singh A.P., Singh T. 2014. Biotechnological applications of wood-rotting fungi: A review. Biomass and Bioenergy 62: 198–206. https://doi.org/10.1016/j.biombioe.2013.12.013

Sirimanne S.R., Li Z., VanderVeer D.R., Tolbert L.M. 1991. One-electron oxidation of 9-methylanthracene and 9-[(trimethylsilyl) methyl] anthracene: reversal of radical-cation selectivity by the trimethylsilyl group. Journal of the American Chemical Society 113(5): 1766–1769. https://doi.org/10.1021/ja00005a047

Supandi M., Wibowo M.A., Zahara T.A. 2019. Characteristics of Rooftop Leaf Essential Oil (*Baeckea frutescens* L) from the Forest of Sungai Manjung Village, Ketapangan Regency, West Kalimantan [Karakteristik Minyak Atsiri Daun Ujung Atap (*Baeckea frutescens* L) Dari Hutan Desa Sungai Manjung Kabupaten Ketapangan Kalbar]. Indonesian Journal of Pure and Applied Chemistry 2(2): 74–83 (in Indonesian).

Tadtong S., Kamkaen N., Watthanachaiyingcharoen R., Ruangrungsi N. 2015. Chemical components of four essential oils in aromatherapy recipe. Natural Product Communications 10(6): 1091–1092. doi: 10.1177/1934578X1501000673

Tam N.G.T., Thuam D.T., Bighelli A., Castola V., Muselli A., Richomme P., Casanova J. 2004. *Baeckea frutescens* leaf oil from Vietnam: composition and chemical variability. Flavour and fragrance journal 19(3): 217–220. https://doi.org/10.1002/ffj.1281

Wu H., Nakazawa T., Morimoto R., Sakamoto M., Honda Y. 2021. Targeted disruption of *hir1* alters the transcriptional expression pattern of putative lignocellulolytic genes in the white-rot fungus *Pleurotus ostreatus*. Fungal Genetics and Biology 147, 103507. 11 p. https://doi.org/10.1016/j.fgb.2020.103507

Zahra A.M., Budiastra I.W., Sugiyono S., Mardjan S.S. 2019. Physicochemical properties of nutmeg mace oleoresin obtained by ultrasound-assisted extraction on different drying methods [Sifat Fisikokimia Oleoresin Fuli Pala Hasil Ekstraksi Berbantu Ultrasonik Pada Metode Pengeringan yang Berbeda]. Warta Industri Hasil Pertanian 36(1): 1–10. http://dx.doi.org/10.32765/warta%20ihp.v36i1.4722

Zhang W., Liu W., Jiang X., Jiang F., Zhuang H., Fu L. 2011. Design, synthesis and antimicrobial activity of chiral 2-(substituted-hydroxyl)-3-(benzo [d] oxazol-5-yl) propanoic acid derivatives. European journal of medicinal chemistry 46(9): 3639–3650. https://doi.org/10.1016/j.ejmech.2011.05.028